An investigation into the mechanisms of lipotoxicity in rodent and human-derived β-cell lines

Submitted by Patricia Maloney to the University of Exeter as a thesis for the degree of Doctor of Philosophy in Medical Studies, June 2019

I certify that all material in this thesis which is not my own work has been identified and that any material that has previously been submitted and approved for the award of a degree by this or any University has been acknowledged.

Signed…….

Acknowledgements

I would like to thank the people who have helped me throughout my PhD:

- To my parents, Jennifer and Mark Thomas who's never-ending love and support have got me to where I am today. Further, to my family, whose belief in me has been a constant source of strength.
- To my supervisors Professor Noel Morgan and Dr Hannah Welters who gave me this opportunity and whose guidance has been invaluable throughout my PhD. I could not have asked for better supervisors than Noel and Hannah. They have been an inspirational example of how to conduct yourself in academia with grace, integrity and kindness and who I will forever aspire to be like in my future career.
- To Nikki-Anne Archer whose friendship has kept be going (dare I say alive) in the past 3 years. Also, to my wonderful friends that I have made during my time in Exeter.
- Finally:

'I will give thanks to you, LORD, with all my heart; I will tell of your great deeds'

Psalm 9:1 (GNTA)

Abstract

Background and aims: In vitro studies with rodent beta cells suggest that individual free fatty acids (FFA) can exert differential effects such that long-chain saturated fatty acids (LC-SFA) promote toxicity while their monounsaturated counterparts (e.g. C18:1) are benign. This is potentially important, if also true in humans, because patients with type 2 diabetes often display elevated circulating FFA. Furthermore, elevated levels of odd chain SFA (C15:0, C17:0) have been associated with a reduced prevalence of diabetes, but their impact on beta cell viability has not been assessed. The investigations detailed within this thesis have characterised the effects of various FFA on beta cell viability. Further, the subcellular distribution of long-chain fatty acids (LC-FFA) has been characterised to elucidate the underlying mechanisms of lipotoxicity in the human EndoC-βH1 and the rat INS-1 beta cell lines.

Methods: Cells were exposed to a range of LC-FFA for increasing periods and viability was subsequently assessed using either vital dye staining or flow cytometry. The distribution of LC-FFA within cells was studied using a fluorescent palmitate analogue, BODIPY FL C_{16}, and Transmission Electron Microscopy (TEM). Golgi co-localisation was determined with the aid of Golgi-RFP. The oxygen consumption rate (OCR) of cells was measured using a Seahorse XF96^{e} analyser.

Results: Exposure of INS-1 cells to C15:0, C16:0, C17:0 and C18:0 caused a dose-dependent loss of viability over 24h, which was completely attenuated with the co-incubation of C18:1. Conversely, exposure of EndoC-βH1 cells to C15:0, C16:0, C17:0 and C18:0 did *not* cause a loss in viability, even at concentrations up to 1mM, and for exposure periods of 72hrs. Furthermore, EndoC-βH1 cells were resistant to the cytotoxic effects of C16:0 (0.5mM) and glucose (20mM) combined, a phenomenon previously observed in rodent beta cells. Interestingly, the stearoyl-CoA desaturase

(SCD-1) inhibitor 10,12-CLA, and the V-ATPase inhibitor, bafilomycin, both caused EndoC-βH1 cell death. The long-chain monounsaturated fatty acid (LC-MUFA) C18:1 also caused a modest increase in EndoC-βH1 cell death relative to control, although cell death was not observed in those cells treated with C16:1.

In the INS-1 cell line, exposing cells to both C16:0, C18:1 and the fluorescent tracer BODIPY FL C_{16}, caused C16:0 to become distributed in a punctate manner throughout the cytosol, a feature not observed when INS-1 cells were solely treated with C16:0 and BODIPY FL C_{16}. Treating INS-1 cells with unlabelled C16:0 caused the ER to appear dilated. Moreover, C16:0 was found to accumulate at the Golgi apparatus. In contrast, C18:1 did not cause swelling of the Golgi apparatus; it did not cause alterations to ER morphology and C18:1 was routed to the mitochondria for oxidation. To what extent C18:1 is oxidised in INS-1 cells, however, remains unclear. Strikingly, C16:0-induced ER dilation and swelling of the Golgi apparatus was not observed in the presence of C18:1.

In the EndoC-βH1 cell line, similarly to the INS-1 cell line when treated with C18:1, C16:0 did not localise to the Golgi, was distributed in a punctate manner throughout the cytosol, and did not cause the ER to become dilated. Furthermore, cytosolic puncta were observed in EndoC-βH1 cells treated with C16:0 and BODIPY FL C_{16} in combination with C17:0, C19:0, and C18:1.

Conclusion: Differences observed in the viability profile of LC-FFA in human compared to rodent β-cells may be due to differential routing of lipids. Further research is required to determine whether lipotoxicity occurs in human pancreatic β-cells in the pathophysiology of T2D.

Contents **Page no.**

List of figures

List of Tables

Abbreviations

$^{\bullet}HO$	Hydroxyl radicals
4-PBA	4-phenylbutyrate
9,11-CLA	Cis-9, trans-11-conjugated linoleic acid
10,12-CLA	Cis-10,12-conjugated linoleic acid
ADS	Antibody diluting solution
ATF4	Activating transcription factor 4
ATF6α	Activating transcription factor 6α
ATP	Adenosine triphosphate
BiP	Binding immunoglobulin protein
BMI	Body mass index
BODIPY	Boron-dipyrromethene
BSA	Bovine serum albumin
CAT	Catalase
CHOP	C/EBP-homologous protein
CoA	Coenzyme A
CPT-1	Carnitine acyltransferase I
DAG	Diacylglycerol

DAG	Diacylglycerol
DNL	De novo lipogenesis
ECAR	Extracellular acidification rate
EFA	Extracellular Flux Analyser
eIF2α	Eukaryotic translation initiation factor 2α phosphorylation
ER	Endoplasmic reticulum
ERK	Extracellular signal-regulated kinase
EtOH	Ethanol
FACS	Fluorescence activated cell sorting
FCCP	Carbonyl cyanide-4-(trifluoromethoxy)phenylhydrazone
FFA	Free fatty acids
FFAR1	Free fatty acid receptor 1
FIA	Fluorescent intensity analysis
GAD65	Glutamate decarboxylase 65
GLUT2	Glucose transporter 2
GPR	G protein-coupled receptor
GSIS	Glucose-stimulated insulin secretion
GWAS	Genome-wide association studies
H_2O_2	Hydrogen peroxide
hOGG1	Human 8-oxoguanine DNA glycosylase/apurinic lyase
HSL	Hormone-sensitive lipase
IBMX	3-isobutyl-1-methylxanthine
IL-6	Interleukin-6
IRE1	Inositol-requiring enzyme 1α

JNK	c-Jun N-terminal kinase
KCl	Potassium chloride
LAMP2	Lysosome-associated membrane protein 2
LC-CoA	Long chain coenzyme A
LC-FFA	Long-chain free fatty acids
LC-MUFA	Long-chain monounsaturated fatty acids
LC-SFA	Long-chain saturated fatty acid
LDL	Low-density lipoproteins
LPL	Lipoprotein lipase
MAPK	Mitogen-activated protein kinase
MODY	Maturity-onset diabetes of the young
MPT	Mitochondrial permeability transition
MRS	Magnetic resonance spectroscopy
$O^{2-\bullet}$	Superoxide
OCR	Oxygen consumption rate
PBS	Phosphate-buffered saline
PEG	Polyethylene glycerol
PERK	Protein kinase-like eukaryotic initiation factor 2α kinase
PFA	Paraformaldehyde
PI	Propidium iodide
PTEC	Proximal tubular epithelial cells
PKC-δ	Protein kinase C delta type
PP	Pancreatic polypeptide
PPAR	Peroxisome proliferator-activated receptors

R/A	Rotenone/antimycin
ROI	Region of interest
ROS	Reactive oxygen species
SCD-1	Stearoyl-CoA desaturase
SEM	Standard error of the mean
SERCA	Sarcoendoplasmic-reticulum pump Ca^{2+}-ATPase
SNP	Single nucleotide polymorphism
SOD	Superoxide dismutase
SPT	Serine palmitoyl-transferase
T1D	Type 1 diabetes
T2D	Type 2 diabetes
TCA	Tricarboxylic acid cycle
TEM	Transmission electron microscopy
TNF-α	Tumour necrosis factor-α
TUDCA	Tauroursodeoxycholic acid
UCP2	Uncoupling protein-2
UPR	Unfolded protein response
V-ATPase	Vacuolar H^+-ATPase
VSVG	Vesicular stomatitis virus G protein
ZDF	Zucker diabetic fatty

Chapter 1.

Introduction

1.1 Diabetes mellitus

Diabetes is the most prevalent endocrine disorder globally, with >422 million individuals living with the disease worldwide (WHO, 2016). It is a lifelong condition characterised by elevated blood glucose (hyperglycaemia). The two main forms of diabetes are type 1 (T1D) and type 2 diabetes (T2D); with less prevalent forms including gestational, neonatal and maturity-onset diabetes of the young (MODY). T1D was traditionally considered a disease of children and adolescents although, it is now recognised that the onset of T1D can occur in adulthood (Thomas et al. 2018) with equal frequency. T1D is an autoimmune disease where β-cells of the pancreas are destroyed leading to insulin deficiency. Subsequently, individuals with T1D are fully reliant on exogenous insulin. In T2D however, cells of the body become resistant to the effects of insulin, and pancreatic β-cells may become dysfunctional and die (as reviewed by Blair, 2016). The causes of T2D, however, remains unclear, although it is thought to be a polygenic disorder triggered by environmental factors including, most notably obesity and sedentary lifestyle (figure 1.1) (Ali et al. 2013).

1.2 Type 2 diabetes mellitus

Long considered a disease of adulthood (>40 years old), T2D is now being diagnosed in increasing numbers of children and younger people (<40 years old) (WHO, 2006; Dabelea et al. 2014). T2D (and other forms of diabetes) is diagnosed by measuring the concentration of glucose present in the blood, as individuals with T2D have elevated circulating glucose (hyperglycaemia) (WHO, 2006; Kumar et al. 2010). The development of hyperglycaemia is often preceded by insulin resistance which can occur with ageing or following an increase in bodyweight and fat mass (as reviewed by Barzilai et al. 2012). Insulin resistance is an increasing insensitivity to the actions

of insulin in target tissues (such as the liver, skeletal muscles, and adipose tissue; reviewed by Blair, 2016). Subsequently, blood glucose concentrations rise, with pancreatic β-cells adapting to hyperglycaemia by increasing their secretion of insulin. T2D develops when β-cells fail to secrete sufficient amounts of insulin to compensate for the rising insulin resistance, and ultimately, they may undergo cell death (as discussed by Prentki et al. 2002). However, recently it has been proposed that pancreatic β-cells do not undergo cell death in T2D but instead dedifferentiate, losing their function and identity as a β-cell due to a decrease in the expression of β-cell specific markers (Diedisheim et al. 2018). However, the concept of β-cell dedifferentiation in T2D is still a subject under investigation.

Treatment of T2D aims to maintain blood glucose levels as close to the normal range (4-7mmol/L before eating) as possible to minimise the risk of developing microvascular (such as retinopathy and nephropathy) and macrovascular (cardiovascular disease and stroke) complications (as reviewed by Rask-Maden & King, 2013). At diagnosis, hyperglycaemia is often managed mainly with lifestyle interventions such as dietary modifications and increased physical activity. If hyperglycaemia cannot be managed by lifestyle interventions alone, medications such as metformin are prescribed. The biguanide metformin acts to target insulin resistance, whereas other drugs, such as sulphonylureas, act to stimulate insulin secretion from pancreatic β-cells (Arner et al. 2018; Bailey et al. 2016). Later stages of treatment may, however, require the introduction of insulin therapy (Bastaki, 2005; NICE, 2015).

T2D accounts for approximately 90% of all diabetes cases, with >380 million individuals worldwide living with the condition (WHO, 2016). Since 1985 there has been a 10-fold increase in the number of people living with T2D and this figure is set to continue to rise. By 2030 it is predicted that more than 552 million people worldwide

will have T2D (Murea et al. 2012). Out of the 380 million individuals currently living with T2D, 3.7 million reside in the UK, with an estimated 1 million additional UK residents having T2D that has not been diagnosed (DiabetesUK, 2017). T2D and its complications cost the NHS more than £6 billion each year in patient care (NHS England, 2018). Consequently, T2D poses a serious financial and clinical challenge to the NHS. The majority of therapies currently available for T2D aim to manage hyperglycaemia, thereby preventing or reducing the complications of T2D (as reviewed by Upadhyay et al. 2017). Few drugs promote β-cell viability directly, and it is of paramount importance that mechanisms involved in regulating β-cell death and viability are elucidated. This will then facilitate the development of new approaches to therapy which complement the existing agents and their targets.

1.3 Type 2 diabetes and obesity

The risk that a person may develop T2D depends on both their inherent genetic makeup and certain lifestyle factors, including sedentary behaviour and poor diet which can lead to obesity (figure 1.1). There is a strong association between obesity and T2D, with more than half of those individuals with T2D being obese in the UK (Holman et al. 2011). In the UK it has been observed that subjects with obesity are seven times more likely to be diagnosed with T2D compared to those who are not obese (Abdullah et al. 2010). Just as the incidence of obesity has risen so has that of T2D, suggesting a firm correlation between the two conditions. Since 1993 the rates of obesity have almost doubled, and it is predicted that by 2050 60% of men and 50% of women in the UK will be obese (Health Survey for England 1993-2012).

Public Health England classifies obesity as having a body mass index (BMI) of 30kg/m^2 or over (NIHC, 2014). The primary cause of obesity is an energy imbalance,

where more energy is consumed than the body requires. The surplus energy is stored as fat which can lead to obesity if the energy imbalance remains unaddressed (Eckel et al. 2011). The precise mechanisms which link obesity and T2D, however, remain unclear, as does our understanding of inter-individual differences, since many obese subjects never develop T2D and conversely, many lean individuals do develop T2D.

1.3.1 Genetics of T2D and obesity

Epidemiological studies support the principle of inherited genetic susceptibility as a major risk factor for developing T2D. Population-based studies have observed that when one parent has T2D, there is a 40% risk of the offspring developing T2D, whereas if both parents have the disease, there is a 70% risk. Furthermore, first degree relatives of those subjects with T2D are three times more likely to develop the disease compared to those with no family history (Meigs et al. 2000).

Recent advances in genome-wide association studies (GWAS) have facilitated the identification of >128 common genetic risk variants associated with T2D, supporting the theory that T2D is a polygenetic condition (Xue et al. 2018; Scott et al. 2017; Mahajan et al. 2018). Many of the T2D genes identified by GWAS are associated with β-cell dysfunction, such as *KCNJ11* where a single nucleotide polymorphism (SNP) in this gene causes impaired insulin secretion (Laukkanen et al. 2004). Genetic polymorphisms are thought to contribute towards sustained β-cell dysfunction, contributing towards β-cell death and subsequently overt T2D (Ali, 2013).

Advances in GWAS have also enabled a genetic link between obesity and T2D to be investigated. In 2007, Frayling *et al.* conducted a genome-wide search for T2D-susceptibility genes, in UK individuals with T2D and their age-matched controls. The

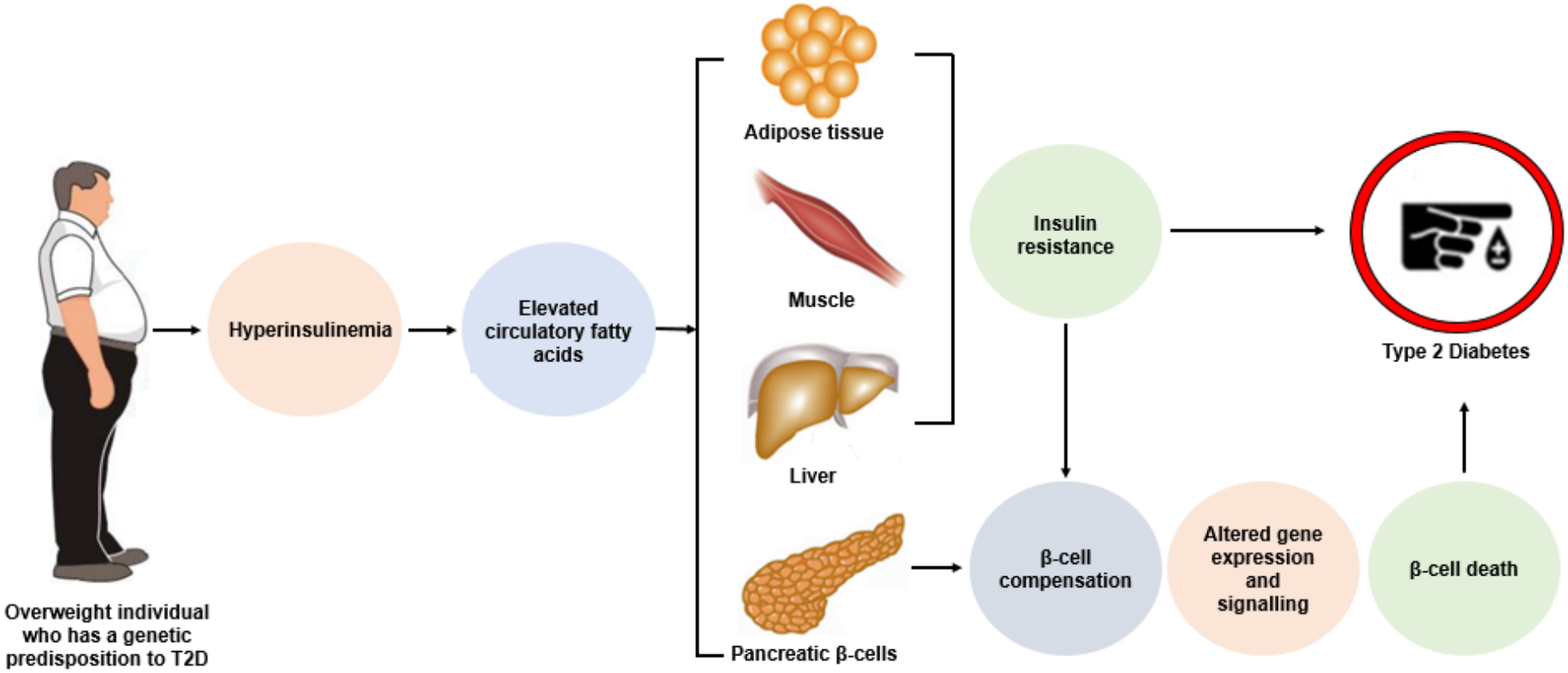

Figure 1.1 Pathogenesis of T2D triggered by obesity. Excess consumption of fats and carbohydrates can lead to hyperinsulinemia and elevated circulatory fatty acid concentrations. In turn, this can lead to insulin resistance which, in genetically susceptible subjects, can contribute towards pancreatic β-cell death, ultimately leading to overt T2D (Prentki, 2002).

researchers identified a common variant in the *FTO* (fat mass and obesity associated gene) which was confirmed to predispose to T2D through an increase in body mass index (BMI). It was observed that those individuals who were homozygous for the risk allele weighed approximately 3kg more than those without the *FTO* risk allele, and had a 1.67-fold increase in the odds ratio for development of obesity (Frayling et al. 2007). The risk variants in the *FTO* gene are seemingly the only genetic variants which link obesity and T2D. The full genetic architecture of T2D and obesity is however not known, so GWAS may yet identify additional genes which link T2D and obesity in the future.

1.3.2 Fat storage and T2D

Ectopic fat storage is thought to be a contributing factor in the pathogenesis of T2D (as reviewed by Lewis et al. 2002). Adipose tissue is the main site of fat storage in the body. It is the largest endocrine tissue in humans, secreting a range of biologically active compounds including free fatty acids (FFA), numerous hormones (for example leptin and adiponectin) and inflammatory mediators (such as tumour necrosis factor-α (TNF-α) and interleukin-6 (IL-6)). In obesity, however, the secretion of these compounds by adipose tissue becomes deranged (Eckel et al. 2011; Trayhurn & Wood, 2004). In subjects with obesity, excess adipose tissue releases elevated concentrations of pro-inflammatory cytokines (predominantly TNF-α and IL-6), whereas anti-inflammatory cytokine production (for example IL-10) is suppressed (Schmidt et al. 2015). Pro-inflammatory cytokines have the potential to cause pancreatic β-cell death, contributing to the development of T2D (as reviewed by Donath et al. 2003). Moreover, the increase in circulating FFA from adipose tissue (specifically the long-chain saturated fatty acid (LC-SFA) palmitate) can induce

chemokine and cytokine expression in human islets, which further contribute towards islet inflammation and subsequently β-cell death in T2D (Igoille-Esteve et al. 2010).

Adiponectin, the most abundant secretory protein released from adipocytes, is decreased in obesity. When administered systemically to obese rodent models, adiponectin increases the rates of fatty acid oxidation and causes a decrease in fatty acid accumulation in the muscle (Shetty et al. 2004). Adiponectin is also associated with the profile of circulatory FFA. With a decrease in adiponectin concentrations, there is a significant increase in the LC-SFA palmitic acid (C16:0), observed in both rodents and humans, which can be toxic to pancreatic β-cells during chronic exposure (Welters et al. 2004). With elevated adiponectin, however, there is an elevation in the LC-MUFA oleic acid (C18:1), which may play a protective role against LC-SFA induced β-cell death (see section 1.8) (Heredia et al. 2009; Fernandez-Real et al. 2005; Welters et al. 2004). Elevated adiponectin is associated with a lower incidence of T2D. This may, in part be due to adiponectin's role in regulating fatty acid metabolism, and its ability to partially rescue β-cells from fatty acid-induced toxicity (Rakatzi et al. 2004; Duncan et al. 2004).

Excess ectopic fat in the pancreas is also thought to be a feature of T2D. Ectopic fat is the deposition of triglycerides in cells that are not adipose tissue and which normally contain only small amounts of fat (as reviewed by Lettner et al. 2008). Lee et al. (1992) were first to identify fat accumulation in the pancreatic islets of T2D Zucker diabetic fatty (ZDF) rats. Subsequently, Lee and colleagues (1992) showed that triglycerides accumulate in the pancreatic islets of T2D rodent models, two weeks before β-cell apoptosis occurred, implying that pancreatic ectopic fat may contribute towards β-cell death in these models of T2D. Magnetic resonance spectroscopy (MRS) studies have shown pancreatic fat also to be elevated in human subjects with obesity, but

significantly more so in those individuals with obesity and T2D (Tushuizen et al. 2007). In a recent clinical study, pancreatic triglyceride content decreased with weight loss in subjects with T2D and obesity but not in BMI-matched controls, despite a comparable decrease in body weight (Steven et al. 2015). This implies that pancreatic ectopic fat is a feature of T2D and that the pancreatic extracellular milieu has a high concentration of fatty acids, possibly contributing to β-cell death.

1.4 Insulin resistance in T2D

It has long been recognised that insulin resistance is linked to the development of T2D (Weyer et al. 1999). Insulin resistance can be caused by elevated concentrations of circulating FFA, inactivity, overconsumption of energy-dense foods, and age (as reviewed in Peterson & Shulman, 2018). Insulin resistance is a condition whereby insulin-target cells no longer respond appropriately to circulating insulin. At a cellular level, insulin resistance occurs due to the insulin signal being disrupted (often by the degradation of insulin receptor substrate-1) which reduces the strength of the signal, causing attenuation of insulin's final actions (Pederson et al. 2001).

The main role of insulin in healthy target tissues, such as adipose, liver and muscle, is to coordinate the storage, mobilisation and utilisation of fatty acids and glucose. Insulin resistance prevents glucose uptake and its subsequent conversion to glycogen in muscle and triglycerides in adipose tissue. Glucose, therefore, remains in the blood leading to hyperglycaemia. Hyperglycaemia is further exacerbated by hepatic glucose production, as hepatocytes continue to produce glucose due to the gluconeogenic pathways not being appropriately inhibited by insulin (Cerf, 2013). Moreover, insulin resistance results in an increase in fatty acids in the blood. In healthy individuals, insulin increases the activity of lipoprotein lipase (LPL), which facilitates the clearance

of triglyceride-rich lipoproteins from the blood, and inhibits the activity of hormone-sensitive lipase (HSL) in adipose tissue, which reduces the release of FFA into circulation (Liu et al. 2005; Meijssen et al. 2001). In insulin resistance, triglycerides are not cleared from the blood, which can manifest as dyslipidaemia (abnormal fat concentrations in the blood). Insulin resistance can, therefore, cause dyslipidaemia, but conversely, lipids can also cause insulin resistance. Studies using an intravenous lipid infusion (with heparin to activate LPL) to elevate circulating fatty acids in healthy individuals have demonstrated that fatty acids cause a dose-dependent inhibition of insulin-stimulated glucose uptake by cells and an increase in hepatic gluconeogenesis (Boden et al. 1994; Roden et al. 2000).

In summary, insulin resistance causes an increase in circulating fatty acids which, in turn, exacerbates insulin resistance of peripheral tissue. Insulin resistance of the peripheral tissues subsequently causes glucose concentrations in the blood to rise. Elevated fatty acids and glucose are thought to contribute towards the death of pancreatic β-cells and T2D in genetically susceptible individuals (as reviewed by Ruan & Lodish, 2003).

1.5 Fatty acids

Fatty acids present in the body are either derived from the diet or from de novo lipogenesis (DNL) in the liver and adipose tissue, where surplus carbohydrates are converted to fats. Fatty acids are a diverse group of compounds which differ in their carbon chain length, configuration and metabolic effects (figure 1.2). They are used by cells for a range of processes including as a fuel source, a component of cellular membranes, and as precursors for a range of signalling molecules including hormones and inflammatory mediators (figure 1.3) (as reviewed by Carta et al. 2017). Fatty acids

are transported around the body either esterified, predominantly as triglycerides (three fatty acids esterified to glycerol) or in a non-esterified form (i.e. FFA). The majority of non-esterified FFA are transported in plasma bound to albumin, although a small fraction of FFA circulates unbound to albumin (Huber & Kleinfeld, 2017). Alterations in the ratio and concentrations of fatty acids in the circulation have been shown to play a significant role in the pathophysiology of T2D (Lee et al. 1994). Dyslipidaemia can be classified as elevated FFA, increased low-density lipoproteins (LDL) (which transport fats in circulation), high cholesterol, raised triglycerides and/or low levels of high-density lipoproteins (as discussed in Thompson, 2004). In the pathophysiology of insulin resistance and T2D however, an elevation in the plasma FFA pool seemingly assumes greater importance than disruption of lipoprotein levels or triglycerides (Acosta-Montano & Garcia-Gonzalez, 2018).

1.5.1 The free fatty acid plasma pool

Adipose tissue is the main source of FFA in plasma. Under normal physiological conditions, plasma FFA is tightly regulated according to the energy demands of the body (see section 1.5.2). The concentration of the plasma FFA pool is between 100μM to >1mM, although concentrations vary depending on factors such as the time of day, physiological state, and stress levels (Huber and Kleinfeld, 2017). In subjects with obesity and insulin resistance, there is an elevation in circulating FFA (Eckel et al. 2011), although the source of surplus FFA remains to be fully elucidated. Elevated FFA can, however, in part, be attributed to a reduction in FFA clearance, enlarged adipocytes releasing more FFA, and/or an increase in the activity of LPL and inhibition of HPL in adipose tissue due to insulin resistance (as reviewed by Boden, 2008).

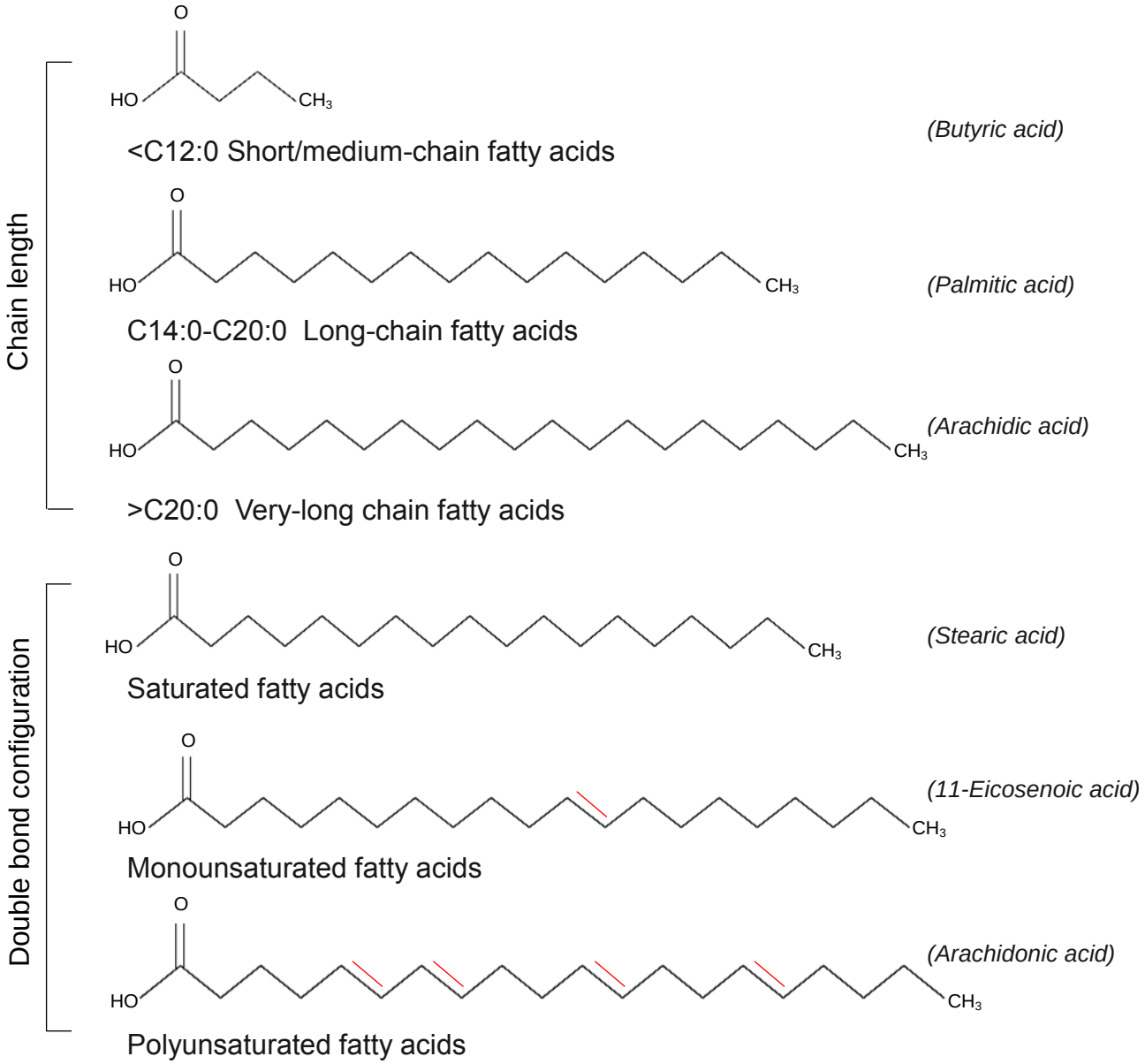

Figure 1.2 Fatty acid classification. Fatty acids are classified according to the number of carbons in their aliphatic chain or by the number of double carbon-carbon bonds. Fatty acids with <14 carbons are short to medium chain fatty acids whereas fatty acids with 14-20 carbons are LC-FFA. Those fatty acids with no double bonds in the hydrocarbon chain are the saturated fatty acids. The insertion of one double carbon bond, however, generates fatty acids referred to as monounsaturates, and those with more than one double carbon bond are polyunsaturated fatty acids (Nestle et al. 1994; Kikukawa et al. 2015; Tallima et al. 2018).

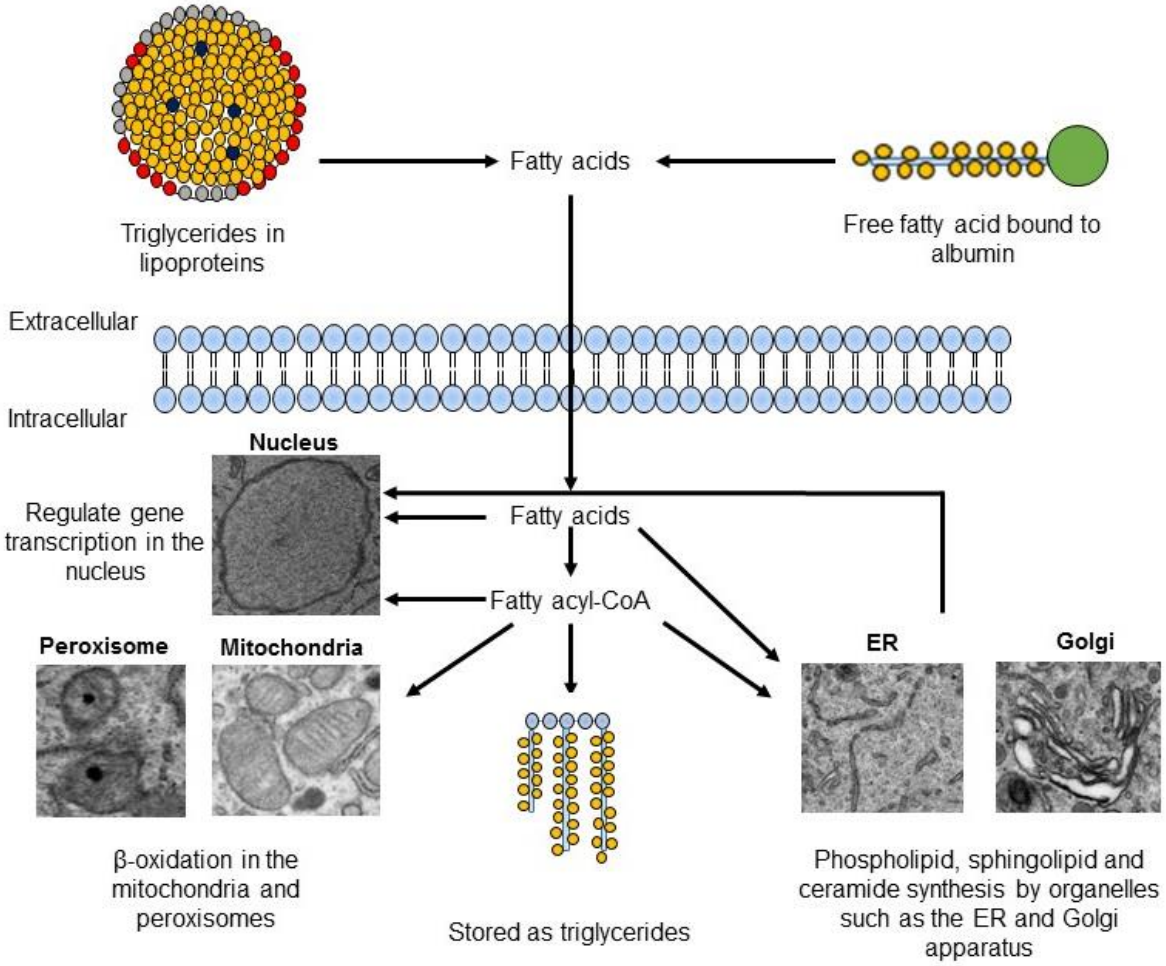

Figure 1.3 Cellular uses of FFA. FFAs are transported to the cell either bound to albumin or packed in lipoproteins, before being dissociated from their protein carriers by receptors on the outer face of the plasma membrane. The FFAs are then taken up into the cell and activated in the cytosol by the addition of a CoA (coenzyme A) group. Both FFA and fatty acyl-CoA (the activated form) can form precursors to lipid signalling molecules or can be converted to membrane lipid species (for incorporation into cellular membranes), at sites such as the ER and Golgi apparatus. Other uses of FFA, fatty acyl-CoA and fatty acid metabolites (such as ceramide) are to modulate gene expression in the nucleus or, in the case of fatty acyl CoA, to act as a source of fuel, being oxidised in the mitochondria to yield energy (in the form of adenosine triphosphate (ATP)) or converted to triglycerides for energy storage (Carta et al. 2017).

Recent advances in lipidomics have enabled the circulatory FFA profile to be characterised in both lean and obese individuals. In healthy lean individuals, the FFA plasma pool is composed of more than 40 different fatty acid species, approximately 78% of which are the long-chain free fatty acids (LC-FFAs) oleic acid (C18:1), palmitic acid (C16:0), and stearic acid (C18:0) (Quehenberger et al. 2010). In obese subjects, lipidomics has identified an elevation in the LC-SFAs C16:0 and stearic acid C18:0, whereas the LC-MUFA C18:1 is decreased (Sansone et al. 2016). C16:0 is consumed in the diet or synthesised endogenously from carbon substrates (such as carbohydrates) through the de novo lipogenesis (DNL) pathway. The homeostatic control of C16:0 in tissue is highly regulated and kept within a strict physiological range. The accumulation of C16:0 is prevented by desaturation to C16:1, and/or elongation to C18:0 with further desaturation to C18:1 (Silbernagel et al. 2012). In hyperglycaemic conditions (for example T2D), an overproduction of C16:0 by DNL has been observed to contribute towards dyslipidaemia, insulin resistance and the dysregulation of fat storage and distribution (Donnelly et al. 2005).

1.5.2 The effect of FFA on glucose metabolism

First suggested by Randle *et al.* (1963), the “glucose-FFA cycle” is a system in mammals whereby glucose and fatty acids compete to be oxidised in tissue such as muscle and adipose. It is proposed that a disruption to the glucose-FFA cycle by obesity and insulin resistance, results in high plasma concentrations of FFA (Hue, 2009). In a healthy lean individual, FFA bound to albumin is the form in which stored body fat from adipose tissue is transported to tissue. The FFA plasma pool plays an essential role in metabolic regulation during feeding and fasting, as when blood glucose concentrations are low FFA act as a major fuel source for many tissues. Based on their observations in isolated rat cardiac muscle, Randle et al. (1963) proposed that

when blood glucose levels are elevated, FFA oxidation is inhibited, thereby enhancing FFA storage, glucose oxidation and glucose storage in muscle and adipose. Conversely, when blood FFA levels are elevated, glucose oxidation is inhibited from increasing FFA oxidation (Randle, 1963). This hypothesis was later confirmed by the work of Boden et al. (1994) who demonstrated that increased FFA oxidation decreased glucose oxidation in human skeletal muscle 1h post-acute lipid infusion.

At a cellular level, Randle proposed that glucose and FFA metabolic pathways could be regulated by nutrients, depending on whether glucose or FFA was in excess. Randle proposed that an increase in FFA oxidation would ultimately lead to the inhibition of the glucose sensor, hexokinase, causing a reduction in the uptake of glucose (Randle et al. 1963). In later years, it was identified that an increase in glucose oxidation subsequently elevates malonyl-CoA production which acts to inhibit carnitine acyltransferase I (CPT-1). Inhibition of CPT-1 reroutes FFA into cytosolic esterification pathways; storing FFA as triglycerides to be used in periods when glucose concentrations are low (McGarry et al.1977).

The glucose-FFA cycle is particularly important in pancreatic β-cells. In response to elevated glucose, FFA are rerouted into esterification pathways which is vital to enable glucose-stimulated insulin secretion (GSIS) to occur (Prentki et al. 2013). The rerouting of FFA not only enables GSIS but also amplifies GSIS via the generation of lipid signalling molecules (see section 1.6.1) (Prentki et al. 2013). In T2D however, hyperglycaemia combined with excess fatty acids is thought to contribute towards β-cell death via the mass accumulation of esterified FFA in the cytoplasm (as reviewed by Kim & Yoon, 2011).

1.6 Pancreatic β-cells

Pancreatic β-cell dysfunction and death is a major feature of T2D. Beta-cells are located in the endocrine tissue of the pancreas within cell aggregates named the 'islets of Langerhans' (islets henceforth) (as reviewed by Kulkarni, 2004) (figure 1.4). The main function of the pancreatic β-cell is to secrete the hormone insulin, the primary regulator of blood glucose concentrations.

1.6.1 Insulin secretion

Pancreatic β-cells secrete insulin in response to a range of stimuli, the primary modulator being glucose. The full mechanisms by which insulin is secreted remains unclear although insulin secretion is believed to occur via K_{ATP}-dependent and K_{ATP}-independent pathways (as reviewed by Jenson et al. 2008). The canonical pathway of GSIS is the K_{ATP}-dependent pathway, where glucose is metabolised in the cytosol and mitochondria to generate ATP. The increase in ATP is sensed by ATP-sensitive K^+ channels on the plasma membrane, causing K_{ATP}-channels to close and consequently the plasma membrane to depolarise. Depolarisation of the plasma membrane opens voltage-gated Ca^{2+} channels, resulting in an influx of Ca^{2+} which leads to the exocytosis of insulin-containing secretory granules (as discussed by Fu et al. 2013).

Insulin secretion, however, is not triggered solely by glucose. Malaisse et al. (1967) were the first to observe that β-cells secrete insulin in response to FFA, with later research establishing that FFA can stimulate insulin secretion through their oxidation, or by potentiating GSIS (Prentki et al. 2013). FFA-induced insulin secretion occurs via metabolic pathways and membrane receptor activation (figure 1.5). Similarly to

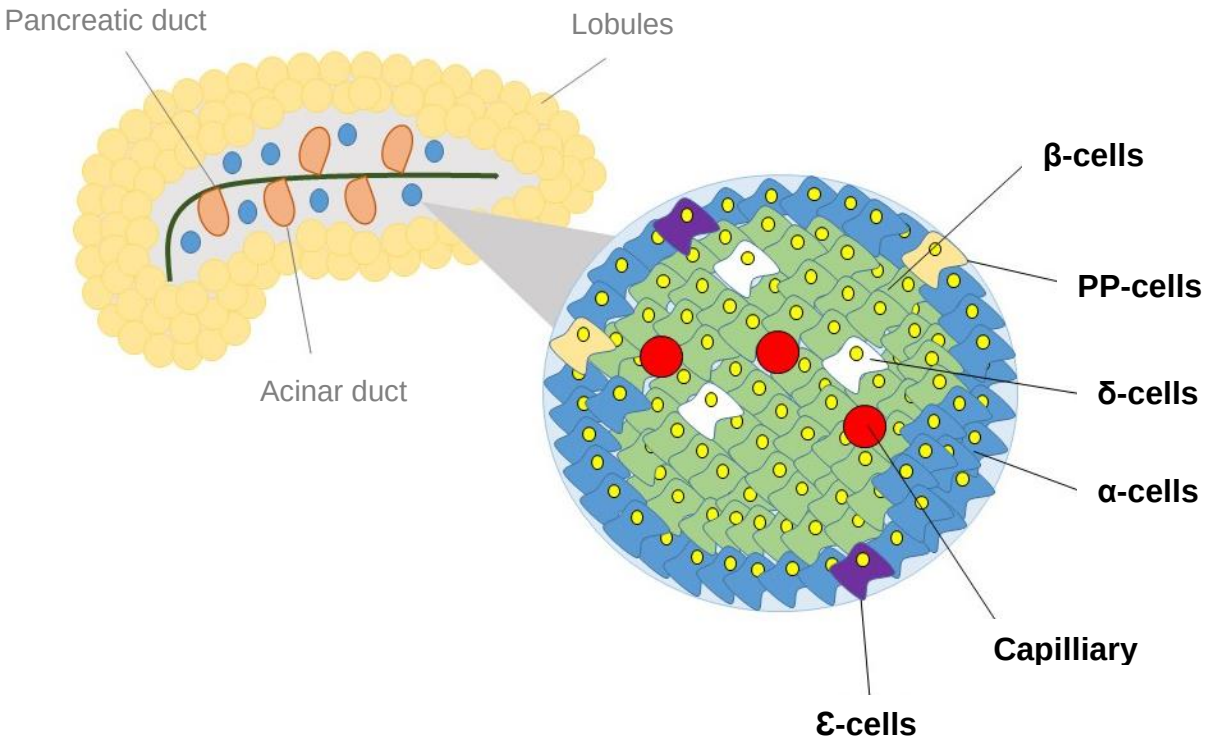

Figure 1.4: Islets of Langerhans

The β-cells are one of five cell types contained in the islets of Langerhans. β-cells secrete the hormone insulin, whereas α-cells secrete glucagon, δ-cells secrete somatostatin, Ɛ-cells secretes ghrelin, and PP-cells secrete polypeptide (Kulkarni, 2004).

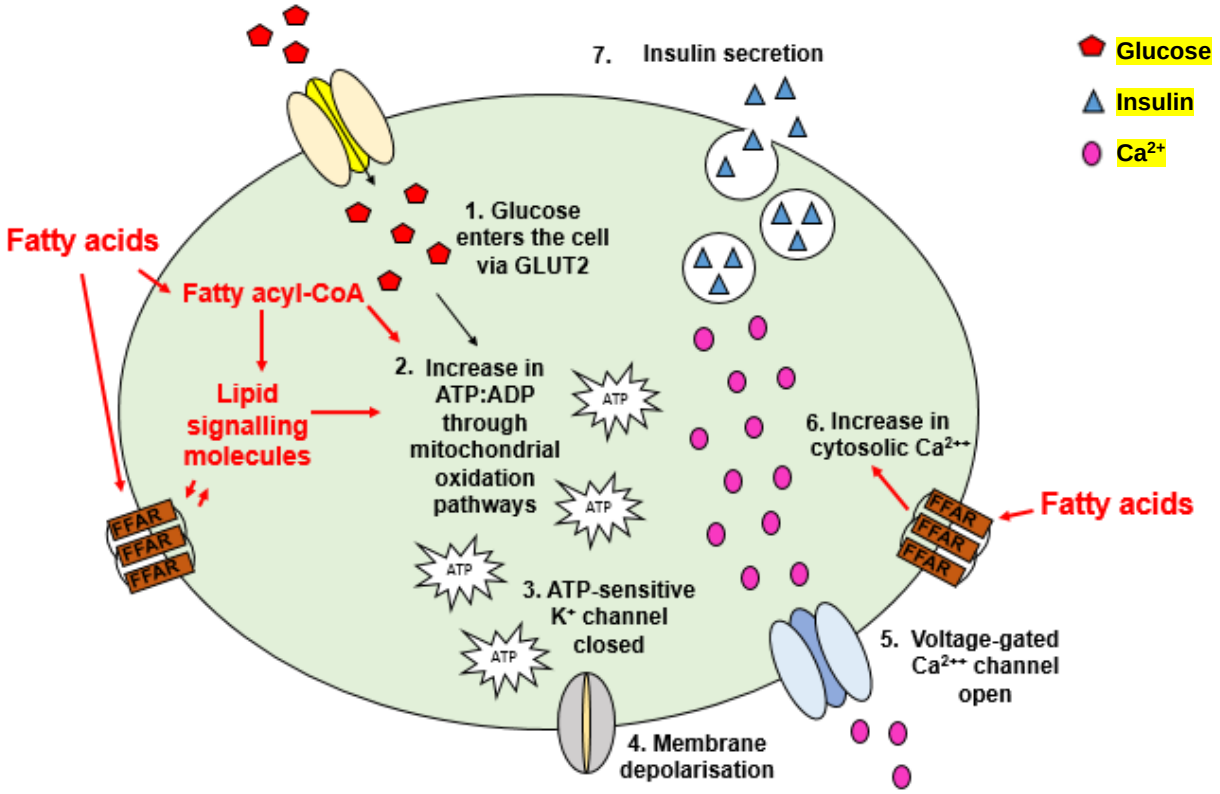

Fig. 1.5 The role of fatty acids in insulin secretion. LC-FFA can stimulate insulin secretion through: (A) their oxidation which subsequently leads to an increase in ATP production causing the K_{ATP} channels to close, voltage-gated Ca^{2+} channels to open and leading ultimately to increased insulin secretion. (B) An increase in glucose concentrations can cause malonyl-CoA concentrations to rise, which blocks CPT-1. This re-routes FFA into esterification pathways to generate lipid droplets and lipid signalling molecules (such as long chain coenzyme A (LC-CoA)) which can act as signalling molecules to amplify GSIS. Moreover, stored FFA derived from this pathway can act as autocrine signalling molecules which activate certain G protein-coupled receptors (GPR) such as free fatty acid receptor 1 (FFAR1). (B, C) FFA (specifically medium and long-chain FFA) can activate FFAR1 (also known as GPR40) which can either (C) cause the release of Ca^{2+} from the endoplasmic reticulum (ER), thereby triggering insulin secretion, or (D) generate lipid signalling molecules (such as diacylglycerol (DAG)) which potentiates insulin secretion (Prentki, 2013; Amisten, 2013).

glucose, however, the mechanisms by which FFA trigger insulin secretion are still to be fully characterised (Nolan et al. 2006).

1.6.2 FFA induced β-cell dysfunction

Prior to β-cell death, the pancreatic β-cells undergo a period of dysfunction, in which fatty acids play a contributory role (Weir & Bonner-Weir, 2004). In pre-diabetes and the early stages of T2D, β-cells increase their secretion of insulin as an adaptive response to elevated blood glucose (β-cell compensation). In rodent models, this compensation is accompanied by an increase in β-cell number (hyperplasia) and size (hypertrophy) (as reviewed by Chang- Choi et al. 2008). Whether β-cell compensation and an increase in β-cell mass occur in humans, and by what mechanisms, is however currently under investigation. Following β-cell compensation, it is thought that the β-cells begin to decompensate, and may dedifferentiate into progenitor-like endocrine cells (Talchai et al. 2012). Ultimately, severe decompensation and β-cell death ensue, in part due to functional exhaustion (as discussed by Acilli et al. 2016; Weir & Bonner-Weir, 2004), leading to a reduction in β-cell mass. Interestingly, it has been proposed that the reduction in β-cell mass may be due to dedifferentiation (Talchai et al. 2012). However, there is also a body of literature that supports β-cell apoptosis as a primary cause (Wang et al. 2014; Butler et al. 2003; Jurgens et al. 2011).

In vitro and in vivo studies have ascertained that chronic exposure to LC-SFA leads to an elevation in basal insulin secretion by β-cells and a blunted insulin secretory response to glucose (Malmgren et al. 2012). Further, fatty acids have been shown to cause β-cell compensation independently of glucose as, when fed a high-fat diet, the β-cell mass of animal models increases even when glucose is within the physiological range (Chang-Chen et al. 2008; Van Citters et al. 2002; Steil et al. 2001). The

molecular mechanisms of fatty acid-induced compensation are yet to be elucidated but rat islets cultured in FFA for 4 days exhibit enrichment in actin along their plasma membrane, an increase in DNA synthesis and a reduction in insulin content (Vernier et al. 2012). There are extensive theories as to how chronic exposure to fatty acids causes a direct decrease in insulin secretion at both the transcriptional and proteome level (reviewed in Sharma & Alonso, 2014) although it is beyond the scope of this study to discuss them in detail. Instead, the remainder of this thesis will discuss the role fatty acids play in β-cell death.

1.7 The role of FFAs in β-cell death

Elevated FFAs are believed to be a causative factor in β-cell death, a process that has been termed lipotoxicity. The mechanisms by which beta-cell lipotoxicity occur remain unclear. Lipotoxicity is dependent upon the FFA concentration, exposure duration, and strikingly the carbon chain length and degree of saturation of the FFA (Sharma & Alonso, 2014). The work of Welters et al. (2004), Diakogiannaki et al. (2007) and others such as Maedler et al. (2001) have repeatedly demonstrated that in rodent β-cells and human islets, it is the LC-SFA (such as C16:0 and C18:0) that are most toxic to pancreatic β-cells whereas short to medium chain FFA is less toxic. Moreover, the LC-MUFA (for example C18:1) do not cause β-cell death and can even exert a protective effect against their LC-SFA counterparts (Mika et al. 2016; Maedler et al. 2001; Welters et al. 2004). Furthermore, under certain circumstances, lipotoxicity can be aggravated by high concentrations of glucose (glucolipotoxicity) (as discussed by Poitout et al. 2010). In subjects with T2D, both hyperglycaemia and elevated FFA are often present in the extracellular milieu. Glucolipotoxicity is considered to contribute towards decreased insulin secretion, impaired insulin gene expression, and eventually

β-cell death in T2D (Poitout et al. 2010). This thesis, however, is principally concerned with the phenomena of lipotoxicity in pancreatic β-cells.

The mechanisms by which lipotoxicity occurs is highly debated. There is a wealth of literature which suggest that processes such as ceramide accumulation (Shimabukuro et al. 1998), ER stress (Cunha et al. 2008), oxidative stress (Elsner et al. 2011), mitochondrial dysfunction (Molina et al. 2009) and autophagy (Choi et al. 2009) mediate LC-FFA-induced β-cell death (Sharma & Alonso, 2014). Further, LC-FFA seemingly triggers β-cell death via the apoptotic pathway (Diakogiannaki et al. 2007).

1.7.1 Ceramide accumulation

Ceramide consists of a sphingosine and LC-FFA side-chain (figure 1.6) and is biosynthesised via a de novo pathway (as discussed by Hannun & Obeid, 2018). Serine palmitoyl-transferase (SPT), the enzyme which catalyses the first step of de novo ceramide synthesis, has a high affinity for its substrates l-serine and palmitoyl-CoA (the activated form of C16:0). As such, any increase in C16:0 availability can induce an aberrant production of ceramide via the de novo pathway, leading to ceramide accumulation (Veret et al. 2013).

Ceramide accumulation is one potential mechanism by which LC-FFA induce β-cell death. It has been observed that in individuals with T2D there is a marked increase in sphingolipids in the blood (Haus et al. 2009). Sphingolipids are a diverse group of lipids which act as cell signalling molecules, regulating such cellular processes as apoptosis, inflammatory responses and senescence (Hannun & Obeid, 2018). It is well documented that nearly all stress stimuli (including obesity) induce sphingolipid synthesis which can lead to the intracellular accumulation of the sphingolipid ceramide

Figure 1.6 Chemical structure of C_{16}-ceramide. A sphingoid base linked to C16:0 by an amide bond, yielding C_{16}-ceramide. The sphingoid base may be linked to fatty acids which vary in carbon chain length to form a ceramide molecule, although C16:0 has been included within this schematic (adapted from Becam et al. 2017).

in β-cells (Bikman & Summers, 2011). Yano et al. (2011) suggest that an accumulation of ceramide can affect mitochondrial membrane integrity, inducing an excessive production of reactive oxygen species (ROS) which disrupt insulin secretion and promote apoptosis in β-cells. Shimabukuro et al. (1998) were the first to identify the involvement of ceramide in FFA-induced β-cell death. Using the SPT inhibitor, fumonisin B1, to block ceramide de novo synthesis, they showed attenuation of C16:0 induced β-cell death in Zucker diabetic fatty (ZDF) rats (Shimabukuro et al. 1998). Subsequent studies identified various possible mechanisms of C16:0/ceramide induced β-cell death including impaired protein trafficking, ER stress, mitochondrial dysfunction and alterations in ion-channel activity (Boslem et al. 2011; Zhang et al. 2009; Giussani et al. 2006; Hannun & Obeid, 2018). Collectively, these studies support a role for ceramide in β-cell lipotoxicity.

It can be argued, however, that the deleterious effects of ceramide depend on the model being used. For example, Shimabukuro et al. (1998) used ZDF rats which could be considered as an extreme case of ceramide accumulation as this model has

extremely high concentrations of circulating lipids (>1mM) (Boslem et al. 2013). Conversely, only a modest increase in ceramide accumulation was observed in the β-cells of the POKO mouse, a murine model with chronic dyslipidaemia (>1mM) generated in part to investigate the effects of lipotoxicity (Medina-Gomez et al. 2007; Medina-Gomez et al. 2009). The modest increase in β-cell ceramide led Medina-Gomez et al. to speculate that β-cells may be more resistant to lipid overloading compared to other cell types (for example hepatocytes) (Medina-Gomez et al. 2007; Medina-Gomez et al. 2009). In the RINm5F β-cell line, inhibition of de novo ceramide synthesis with l-cycloserine or fumonisin B1 failed to attenuate C16:0 induced cell death (Baldwin et al. 2012). Work is ongoing to identify the role of ceramide in β-cell lipotoxicity, and with the generation of the human EndoC-βH1 cell line, this can now be determined in a human model.

1.7.2 Endoplasmic reticulum (ER) stress

Accumulating evidence links chronic ER stress to lipotoxicity in pancreatic β-cells (Han & Kaufman, 2016). The ER plays an important role in Ca^{2+} homeostasis, lipid metabolism, protein synthesis and the posttranslational modification and trafficking of proteins (as reviewed by Han & Kaufman, 2016). A disturbance of ER homeostasis by excess fatty acids or other physiological or pharmacological stressors triggers ER stress. ER stress causes unfolded or misfolded proteins to accumulate, activating ER stress sensors which trigger the unfolded protein response (UPR) signalling pathway (figure 1.7) (as reviewed by Fonseca et al. 2012). The UPR is mainly activated to restore ER function, although, it can act as a binary switch between cell survival and cell death (Tse et al. 2016). Acute ER stress induces a regulated UPR which promotes cell viability, whereas chronic ER stress causes the UPR to become hyperactivated,

leading to apoptosis through the activation of the transcription factor C/EBP-homologous protein (CHOP) (as reviewed by Fonseca, 2012).

Prolonged β-cell exposure to LC-SFA induces ER stress in vitro and in vivo, although the mechanisms are still under investigation (Boslem et al. 2013). Chronic administration of LC-SFA selectively enhances the PERK (PRKR-like endoplasmic reticulum kinase) arm of the UPR in rodent β-cells and human islets (Cunha et al. 2008). Specifically, when rodent clonal β-cells are treated for 4-72hrs with C16:0 there is an upregulation of activating transcription factor 4 (*Atf4*), eukaryotic translation initiation factor 2α phosphorylation (eIF2α), and *CHOP,* leading to apoptosis (Boslem et al. 2013; Cunha et al. 2008; Laybutt et al. 2007; Karaskov et al. 2006; Diakogiannaki et al. 2007). In those studies which reduce ER stress by exposing rodent-derived β-cells to small molecules or chemical chaperones that prevent misfolding (such as tauroursodeoxycholic acid (TUDCA)), C16:0-induced β-cell death was prevented (Chen et al. 2013; Tran et al. 2014). Conversely, when assessed directly, C16:0 did not appear to promote protein misfolding of a reporter protein (mutant vesicular stomatitis virus G protein (VSVG)), in the rodent β-cell line, MIN6 (Preston et al. 2009). Rather, it is thought that C16:0 acts to slow protein trafficking out of the ER, thereby triggering ER stress though protein overloading (Boslem et al. 2013; Preston et al. 2009). Trafficking defects have been linked to alterations in sphingolipid metabolism where a C16:0 induced loss of the sphingolipid, sphingomyelin, disrupts ER lipid rafts. ER lipid rafts are thought to be essential for packaging secretory cargo into export vesicles, and their disruption contributes towards defective protein trafficking and ER stress in rodent β-cells (Boslem et al. 2013).

A further hypothesis for the mechanism by which LC-SFA induce ER stress is by altering the activity of the Ca^{2+} pump, SERCA (sarcoendoplasmic-reticulum pump

Ca^{2+}-ATPase), which depletes ER Ca^{2+} stores thereby triggering ER stress (Cunha et al. 2008). However, the depletion of ER Ca^{2+} stores by FFA is not universally observed, with Karaskov et al. (2006) failing to identify alteration in ER Ca^{2+} concentrations in INS-1E cells exposed to C16:0 for 6hrs.

Protein palmitoylation is also believed to play a role in C16:0 induced ER-stress in β-cells. Protein palmitoylation is a major posttranslational modification where C16:0 is added to a protein to affect its function (including protein trafficking and stability) (as reviewed by Linder & Deschenes, 2007). Using the protein palmitoylation inhibitor, 2-bromopalmitate, Baldwin et al. (2012) observed an attenuation in C16:0-induced ER stress, coupled with a reduction in β-cell death. This indicated that FFA-induced β-cell death might be mediated by unregulated palmitoylation of proteins, stimulating ER stress (Baldwin et al. 2012).

Collectively, these studies indicate that ER stress and the UPR can mediate LC-SFA induced lipotoxicity in β-cells, with possible mechanisms including LC-SFA induced ER Ca^{2+} store depletion, defective ER-Golgi protein trafficking and C16:0 induced unregulated palmitoylation. Further investigations are required however to elucidate the mechanism by which LC-SFA trigger ER stress.

1.7.3 Oxidative stress and lipotoxicity

One school of thought is that β-cell lipotoxicity occurs due to enhanced ROS formation by the oxidation of FFA in the mitochondria and peroxisomes (Elsner et al. 2011). Clinical studies suggest that individuals with T2D are subject to chronic oxidative stress, with markers of oxidative damage (such as 8-OH-deoxyguanine) being present in pancreatic biopsies of patients with T2D (Sakuaba et al. 2002; Robertson et al. 2004). Oxidative stress refers to the imbalance of excess ROS and insufficient

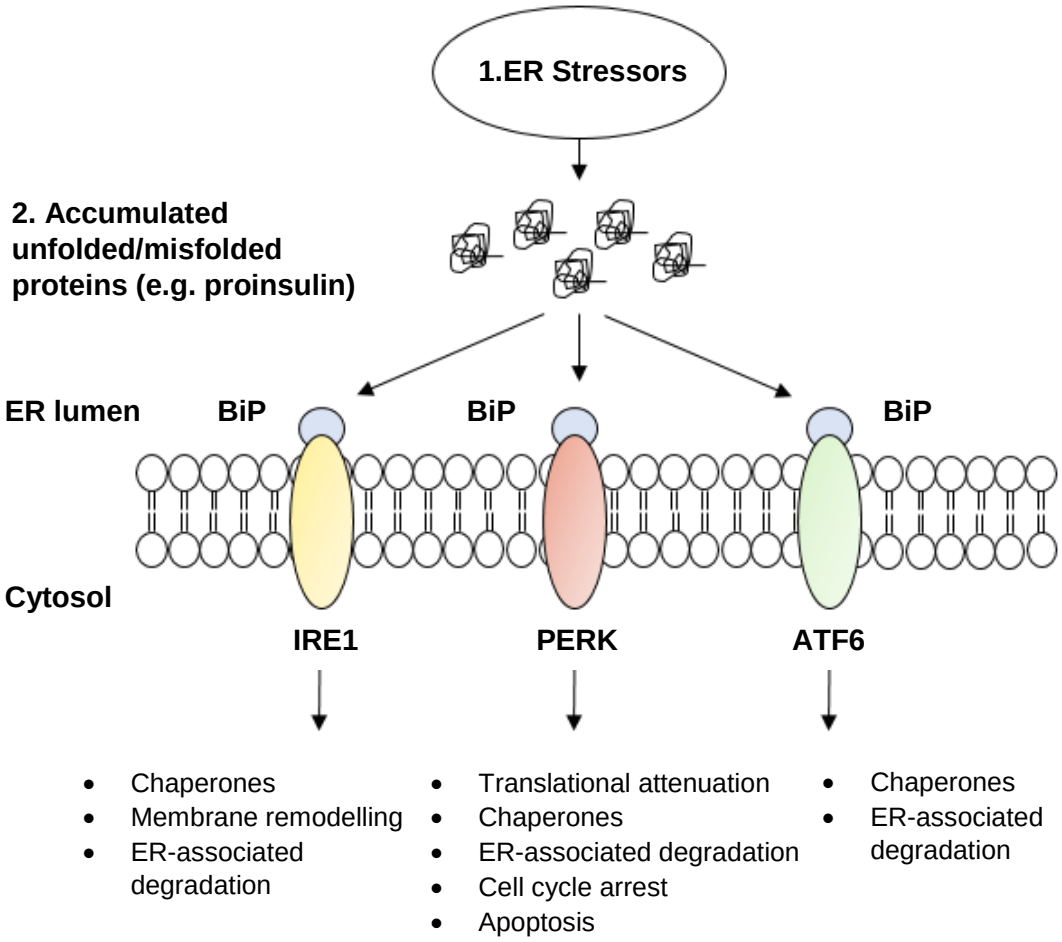

Figure 1.7 ER stress and the UPR cascade. ER stress is activated by such factors as a prolonged exposure to excess LC-SFA, leading to the accumulation of unfolded or misfolded proteins in the ER lumen. The unfolded/misfolded proteins bind to and sequester immunoglobulin heavy-chain binding protein (BiP; also known as GRP78) which triggers the activation of inositol-requiring enzyme 1α (IRE1), protein kinase-like eukaryotic initiation factor 2α kinase (PERK) and ATF6α (activating transcription factor 6α). The activation of these ER transmembrane ER stress sensors activates the UPR signalling pathway, which, downstream results in the alleviation of ER stress, restored homeostasis or apoptosis (Fonseca et al. 2012).

capacity of the cell to mount an effective antioxidant response (Ray et al. 2012). Pancreatic β-cells are highly susceptible to oxidative stress as they lack a comprehensive antioxidant system. Compared to the liver, β-cells express ~50% less of the antioxidant enzyme, superoxide dismutase (SOD), and only ~1% of the proportion of catalase (CAT) (Pi et al. 2010). It is proposed that low levels of antioxidant enzymes in β-cells enable ROS to act as metabolic signalling molecules for GSIS (Pi et al. 2010). A sustained elevation of ROS, however, causes lipid peroxidation, oxidation of proteins and DNA damage to the β-cell, which are thought to contribute significantly to β-cell death (Lenzen, 2008).

The LC-SFA C16:0 and long-chain monounsaturated fatty acids (LC-MUFA) C18:1 have both been shown to stimulate ROS production in rodent-derived pancreatic β-cells (Maestre et al. 2003). The main ROS in β-cells includes superoxide ($O^{2-\bullet}$), hydroxyl radicals ($^{\bullet}HO$), and hydrogen peroxide (H_2O_2); which are mostly derived from nutrient oxidation (as reviewed by Wojtczak, 2008). Mitochondrial oxidation of LC-FFA produces ROS via complex I and III of the electron transport chain, whereas peroxisomal oxidation produces ROS as a bi-product of β-oxidation (Elsner et al. 2011). Consequently, an increase in LC-FFA oxidation can increase ROS formation, potentially leading to oxidative stress and β-cell death.

It has been proposed that long-term overloading of LC-FFA oxidation by the mitochondria can cause increased ROS production (Koshkin et al. 2003). LC-FFA induced increases in ROS production can increase mitochondrial DNA damage in the rodent-derived INS-1 β-cell line, which ultimately leads to apoptosis (Rachek et al. 2006). Researchers, however, demonstrated that ROS-induced mitochondrial DNA damage could be overcome by transfecting INS-1 cells with a vector for the DNA repair enzyme, hOGG1 (human 8-oxoguanine DNA glycosylase/apurinic lyase). An increase

in the expression of hOGG1 successfully minimised the induction of apoptosis in LC-FFA treated INS-1 cells, reducing cytochrome c release from the mitochondria (Rachek et al. 2006; Newsholme et al. 2007). This indicates that mitochondrial DNA damage, induced by LC-FFA derived ROS, may be a component of lipotoxicity in β-cells.

It has been proposed, however, that β-cells have a protective mechanism which prevents ROS induced β-cell death due to elevated LC-FFA oxidation, namely uncoupling protein-2 (UCP2). UCP2 is located in the inner mitochondrial membrane and acts to uncouple the electron transport chain, lowering the mitochondrial membrane potential to decrease ATP production when there is a surplus of LC-FFA being oxidised. The activation of UCP2 by ROS in the mitochondrion is considered to be a cellular protective mechanism which stops ROS production and enables harmful peroxides to be exported from the mitochondrion (Poitout et al. 2010). This theory is supported by Lee et al. (2001) who observed that overexpression of UCP2 protects against ROS induced cell death in the rodent-derived INS-1 β-cell line. However, the decrease in ATP production caused by LC-FFA induced UCP2 activity may be a detrimental process to β-cells as it also attenuates insulin secretion, which if sustained can contribute to β-cell dysfunction (Fariss et al. 2005).

LC-SFA such as C16:0 and C18:0 can also initially undergo β-oxidation in the peroxisomes, before being transported to the mitochondria to complete their oxidation (Wanders et al. 2010). In contrast to the mitochondria, peroxisomal β-oxidation is not linked to ATP production but rather generates the ROS, H_2O_2. In β-cells, the antioxidant enzyme catalase is virtually absent, thereby leaving β-cells vulnerable to elevated concentrations of H_2O_2 (Lenzen et al. 1996). This has led to the theory that C16:0 induced β-cell lipotoxicity could be due to an excess of H_2O_2 arising from

peroxisomal β-oxidation (Elsner et al. 2011). Further, using the H_2O_2-sensitive fluorescent protein, HyPer, Elsner et al. (2011) showed that the peroxisomes were the major site of H_2O_2 formation in rodent β-cells, with the mitochondria being a minor site of H_2O_2 production. Subsequently, it has been proposed that peroxisomal LC-FFA β-oxidation contributes towards ROS-induced lipotoxicity more so than mitochondrial LC-FFA oxidation (Gehrmann et al. 2010).

In summary, the metabolism of LC-FFA may trigger β-cell death through oxidative stress. Although currently, the role of oxidative stress is still under investigation, especially considering that elevated ROS in response to LC-FFA is not always observed in β-cells (Moore et al. 2004).

1.7.4 Mitochondrial dysfunction and lipotoxicity

Given the central role for mitochondria in insulin secretion and the apoptotic pathway, it is unsurprising that emerging literature has identified mitochondrial aberrations in β-cell lipotoxicity (Stiles & Shirihai, 2012). Mitochondria are highly dynamic organelles which constantly fuse (fusion) and divide (fission) to form interconnecting networks in cells, evenly distributing metabolites, lipids and proteins to facilitate metabolic efficiency (as discussed by Wiederkehr & Wollheim, 2009). The disruption of mitochondrial networks (for example by LC-FFA) has, however, been shown to have a profound effect on β-cell function and can lead to apoptosis (Molina et al. 2009; Suen et al. 2008). For example, an increase in fission frequency causes a deterioration in mitochondrial signal generation and insulin secretion in β-cells, potentially leading to apoptosis (Park et al. 2008). Consequently, mitochondrial morphology is indicative of fusion/fission dynamics which is intimately linked with mitochondrial function. There is

limited evidence however for the underlying mechanisms of β-cell mitochondrial defects in the pathophysiology of T2D although LC-FFA is known to play a role.

When investigating the effects of LC-SFA directly on β-cell mitochondrial dynamics, Molina et al. (2009) reported that C16:0 caused an arrest of mitochondrial fusion activity, with the complete fragmentation of the mitochondria in INS-1 β-cells in as little as 4hrs. When inhibiting mitochondrial fission, Molina and colleagues preserved the mitochondrial morphology of INS-1 cells and prevented apoptosis (Molina et al. 2009). The complete mitochondrial fragmentation induced by C16:0, however, does not correlate with those studies which observed mitochondrial swelling in response to LC-FFA in pancreatic β-cells (Fex et al. 2007; Anello et al. 2005; Diakogiannaki et al. 2008). This discrepancy warrants further investigation.

In islets isolated post mortem from overweight individuals with T2D, β-cell mitochondrial density volume is significantly higher compared to individuals without T2D (Anello et al. 2005). Similarly, Fex et al. (2007) observed swollen mitochondria in insulin-resistant mice fed a high-fat diet. Further, Diakogiannaki et al. (2008) have identified mitochondrial enlargement accompanied by apoptosis in the rat-derived BRIN-BD11 β-cell line, treated with C16:0 for 18hrs. Mitochondrial swelling may be due to the induction of the mitochondrial permeability transition (MPT) pore (Koshkin et al. 2008). The MPT is a Ca^{2+}-dependent nonspecific pore in the mitochondrial inner membrane. In rat β-cell lines, C16:0 has been shown to promote the opening of the MPT pore causing mitochondrial swelling and the release of proteins capable of inducing apoptosis (Koshkin et al. 2008).

C16:0 is known to induce the release of the apoptogenic factor, cytochrome c, from the mitochondria of human islets (Maedler et al. 2003). Cytochrome c is anchored to

the inner mitochondrial membrane by the phospholipid cardiolipin, which may play a significant role in LC-SFA induced β-cell death. Cardiolipin contains four unsaturated fatty acid molecules in its structure, although the fatty acid species incorporated into cardiolipin during its synthesis and remodelling, will be altered by the prevailing fatty acid milieu (Wahjudi et al. 2011). If saturated fatty acid species are incorporated into cardiolipin, there will be an alteration in its binding properties, and a reduced affinity for cytochrome c. This may promote the dissociation of cytochrome c from cardiolipin which can then trigger apoptosis (Iverson & Orrenius, 2004). Incorporation of LC-MUFA into cardiolipin, however, would not exert this effect, offering a possible explanation as to why LC-MUFA are better tolerated than LC-SFA by β-cells. However, the role of cardiolipin synthesis and remodelling with saturated fatty acid species has received very little attention as a possible mediator of LC-SFA induced apoptosis in β-cells (Newsholme et al. 2007; Iverson & Orrenius, 2004).

In summary, the LC-FFA induced: disruption to mitochondrial networks, mitochondrial swelling and mitochondrial remodelling may play a pivotal role in lipotoxicity.

1.7.5 The role of fatty acid metabolism in causing lipotoxicity

The oxidation of LC-FFA is thought to play a key role in mediating LC-SFA induced toxicity in pancreatic β-cells, although research is conflicting as to how this occurs. Certain studies indicate that increased oxidation of LC-FFA is cytotoxic to β-cells (Graciano et al. 2011), whereas other results suggest that the metabolism of LC-FFA prevents the toxicity of the FFA (Lee et al. 2014). For example, supplementing β-cells with tricarboxylic acid cycle (TCA) intermediates was shown to decrease C16:0 induced β-cell death (Lee et al. 2014). Further, when LC-FFA oxidation is blocked using etomoxir, a pharmacological inhibitor of CPT-1, there is an increase in C16:0

induced cell death according to some authors (El-Assad et al. 2003; Sargsyan et al. 2011), and an attenuation according to our group (Diakogiannaki et al. 2007). The LC-MUFA, C18:1, is not toxic to β-cells (Maedler et al. 2003), despite being metabolised by the same pathways as LC-SFA, again suggesting that metabolism of LC-FFA is not directly responsible for causing cell death. This contradicts studies which suggest that metabolism of LC-FFA is cytotoxic to cells. For example, the non-oxidisable C16:0 analogues, methyl ester and bromo-C16:0, which are not transported into the mitochondria by CPT-1, do not cause cell death (Newsholme et al. 2007). Additionally, increased fatty acid oxidation also increases the production of ROS, which β-cells are ill-equipped to process as they lack a comprehensive antioxidant system; leading to β-cell death (Graciano et al. 2011).

In summary, studies are conflicting as to whether LC-FFA oxidation plays a role in β-cell lipotoxicity and consequently, further investigations are necessary to clarify the role of fatty acid metabolism in β-cell death.

1.7.6 Autophagy

Exposure of rodent β-cells and human islets to LC-FFA is widely reported to induce autophagy (Ebato et al. 2008; Oh, 2018; Las & Shirihai, 2010). Macroautophagy (hereafter named 'autophagy') is a major intracellular degradation pathway. By this mechanism, cytoplasmic material such as lipids, are sequestered in double-membrane vesicles and delivered to the lysosomes for degradation (figure 1.8) (Kurokawa & Kornbluth, 2012). Post-degradation, the material is released back into the cell in its constituent parts, producing a source of energy and new building blocks for cellular homeostasis (Singh & Cuervo, 2012; Las & Shirihai, 2010). Under basal conditions, autophagy contributes towards cellular homeostasis, whereas under cell

stress, autophagy can also act to mediate cell survival or cell death (Singh & Cuervo, 2012; Oh et al. 2018).

Autophagy is known to occur during LC-FFA induced β-cell lipotoxicity in T2D although, whether autophagy has a protective or detrimental role remains a matter of debate (Oh et al. 2018; Ebato et al. 2008; Las et al. 2010). A protective role for autophagy against C16:0-induced β-cell death was proposed by Choi et al. (2009). In the rat-derived INS-1 β-cell line, it was suggested that increasing autophagosome formation using rapamycin reduced C16:0-induced β-cell death. Conversely, decreasing autophagosome formation increased C16:0-induced β-cell death (Choi et al. 2009). Further, upon alleviating ER stress with 4-phenylbutyrate (4-PBA), a chemical chaperone which prevents protein aggregation, Choi et al. observed a reduction in C16:0-induced autophagic vesicles implying that ER stress may play a role in driving C16:0-induced autophagy (Choi et al. 2009).

The body of literature supporting a detrimental role for C16:0-induced autophagy, however, is much greater. Beta-cell death and glucose intolerance have been observed in mice deficient for β-cell *Atg7*, an essential gene for autophagosome formation (Ebato et al. 2008). The loss of autophagy in the β-cells of Atg7-deficient mice fed a high-fat diet, significantly increased oxidative stress and was coupled with the accumulation of ubiquitinated proteins and damaged organelles, which it was speculated contributed towards β-cell degeneration (Ebato et al. 2008). Further, in human islets and INS-1 β-cells, prolonged exposure to elevated concentrations of C16:0 increased the accumulation of overloaded autophagosomes, with suppression of autophagic degradation. This disruption to autophagic flux led to an impairment in insulin secretion and β-cell death (Las et al. 2011; Mir et al. 2015; Masini, 2009). A large number of overloaded autophagosomes has also been observed in the β-cells

of individuals with T2D (Masini et al. 2009). Coupled to overloaded autophagosome accumulation in post mortem β-cells and islets post LC-FFA treatment, was a reduced expression of lysosome-associated membrane protein 2 (*LAMP2)* and cathepsin B and D. *LAMP2* and cathepsin B and D are involved in protein degradation and in lysosomal fusion of the autophagic pathway (Masini et al. 2009). This suggests that an increase in overloaded autophagosomes in β-cells exposed to LC-FFA may be due to a decrease in autophagic flux because of decreased lysosome fusion and autophagosome degradation. This decrease in autophagic flux may then contribute to β-cell lipotoxicity rather than exerting protection (Las et al. 2010; Masini et al. 2009).

In summary, the majority of evidence supports C16:0-induced autophagy being detrimental to pancreatic β-cell viability. Further, the interruption to autophagic flux by C16:0 and subsequent β-cell death, support the theory that autophagy-associated death occurs as a result of a blockage of autophagic flux rather than an induction of autophagosome formation (Las et al. 2010).

1.8 Monounsaturated fatty acids and β-cell cytoprotection

As discussed earlier, the toxicity of LC-FFAs depends on their degree of saturation. The literature clearly shows LC-SFA (such as C16:0) to induce apoptosis in pancreatic β-cells, whereas the effects of LC-MUFA (for example C18:1) on β-cell viability are less clear. Certain studies have shown C18:1 to increase apoptosis in INS-1 and MIN6 cells, preceded by the induction of ER stress markers (Wrede et al. 2002; Martinez et al. 2008; Yuan et al. 2010). There is a larger body of literature however, which supports the view that C18:1 is not toxic to pancreatic β-cells and, when co-incubated with C16:0, completely attenuates C16:0-induced toxicity in rodent-derived β-cells and

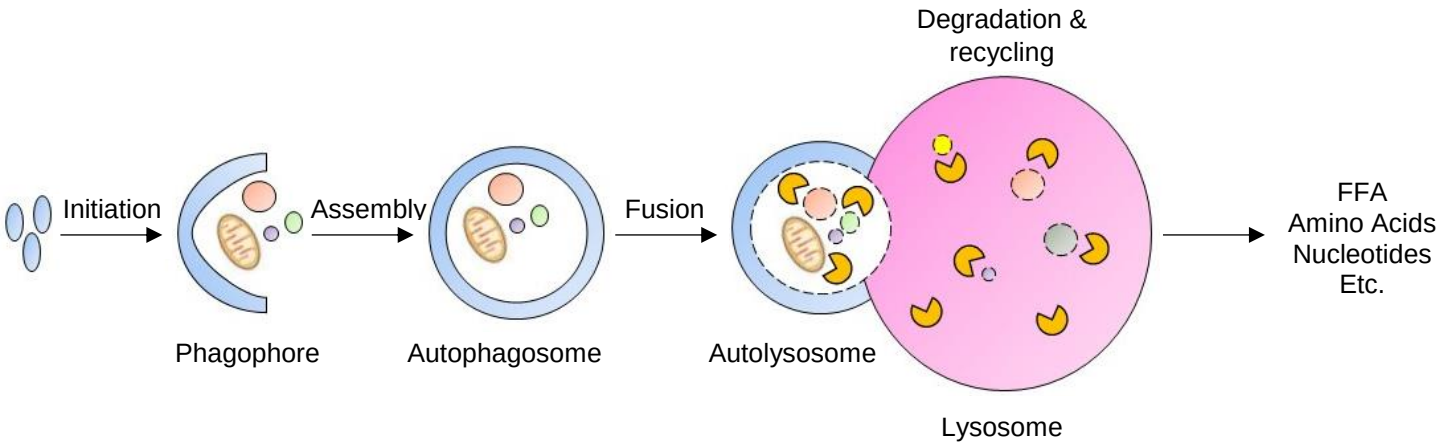

Figure 1.8 Autophagy pathway. Autophagy can be stimulated by ROS, ER stress and LC-FFA. The initiation of autophagy is the generation of an isolated membrane. The isolated membrane engulfs cytosolic proteins and organelles. Upon completion of the membrane, an autophagosome is formed which transports its cargo to lysosomes. The fusion of the autophagosome to a lysosome forms an autolysosome. Hydrolases from the lysosome subsequently break down the inner membrane and cytoplasmic contents of the autophagosome, releasing the constituent parts back into the cytoplasm for use by the cell (Hannigan &Gorski, 2009).

human islets (Welters et al. 2004; Maedler et al. 2003; Maedler et al. 2001; Nemcova-Furstova et al. 2011; Plotz et al. 2016). Further, in rodent β-cell lines, contrary to C16:0, C18:1 does not activate pro-apoptotic enzymes such as the apoptogenic kinases protein kinase C delta type (PKC-δ) and c-Jun N-terminal kinase (JNK) (Eitel et al. 2003; Cunha et al. 2008). Further, C16:0-induced caspase 3/7 activity is abolished immediately upon addition of the LC-MUFA, C16:1, promoting β-cell survival (Dhayal et al. 2008). The differential effects of C16:0 and C18:1 on β-cell viability, and the mechanisms by which C18:1 attenuates C16:0-induced β-cell death have been investigated for a number of years, and is in part the subject of this study.

Dhayal et al. 2008 have found that the anti-apoptotic protection exerted by C18:1 does not require the activation or metabolism of the LC-MUFA by pancreatic β-cells. Blocking the uptake of LC-MUFA into the mitochondria using etomoxir, which inhibits CPT-1, does not prevent C18:1 attenuating C16:0-induced β-cell death. This suggests that mitochondrial entry and subsequent mitochondrial oxidation of LC-MUFA is not a pre-requisite for the protective action of C18:1. Similarly, the non-metabolisable methyl ester C16:1 attenuates C16:0-induced β-cell death, thereby indicating that formation of acyl-CoA is not necessary for the LC-MUFA protective response, as the presence of a methyl moiety will prevent acyl-CoA formation (Dhayal et al. 2008).

C16:0 is well documented to activate ER stress and the UPR signalling pathways (figure 1.7), which can lead to apoptosis. Seemingly, C18:1 does not activate ER stress and the UPR signalling pathways in β-cells (Karaskov et al. 2006; Sommerweiss et al. 2013). Moreover, Diakogiannaki et al. (2008) have observed that C16:1 markedly suppresses the induction of ER stress markers in C16:0-treated β-cells. Attenuated ER stress markers included elf2α phosphorylation and the induction of ATF4 and CHOP. Further, in a recent proteomic analysis, when C16:0 and C18:1 were co-exposed to β-cells, there was a differential expression of proteins compared to those cells expressed in the presence of C16:0 alone. Differentially expressed proteins included those involved in the ER stress response and proteins with antioxidant activity and an anti-apoptotic function (Sargsyan et al. 2016). The expression of proteins with antioxidant activity, triggered by C18:1, may offer an explanation for the observation that C18:1 prevents C16:0-induced peroxisomal H_2O_2 production in β-cells (Gehrmann et al. 2015). Moreover, contrary to C16:0, C18:1 does not trigger peroxisomal H_2O_2 generation (Gehrmann et al. 2015). Whether this phenomenon is due to C18:1 not

being oxidised by peroxisomes or C18:1 increasing the activity of antioxidant proteins is unknown.

Emerging evidence has identified that C18:1, but not C16:0, can generate lipid droplets in rodent β-cells (Gehrmann et al. 2015; Plotz et al. 2016). When C16:0 is co-incubated with C18:1 however, lipid droplet formation increases in β-cells (Gehrmann et al. 2015; Plotz et al. 2016). It has been proposed that C18:1 rescues C16:0 induced apoptosis by channelling C16:0 into triglyceride pools and away from pathways which lead to apoptosis (Gehrmann et al. 2015). When triglyceride synthesis is impaired, C18:1 has been shown to induce lipotoxicity (Listenberger et al. 2003). However, the contribution of lipid droplet formation to C18:1 induced C16:0 triglyceride formation is uncertain. Pancreatic β-cell exposure to C18:1, and C16:0 together with C18:1, increases expression of both the mRNA and protein of perilipin, a protein involved in lipid droplet formation (Plotz et al. 2016). Upon silencing of perilipin however, C18:1, or C18:1 combined with C16:0, is still not toxic to rodent β-cells, implying that perilipin synthesis is not essential for the protective effect of C18:1 (Plotz et al. 2016).

C18:1 has been shown to protect against C16:0-induced β-cell death at concentrations as low as 100μM, under conditions, when the concentration of C16:0 is five times higher than that of C18:1 (Plotz et al. 2016). In rodent β-cells, C16:1 attenuates C16:0-induced β-cell death even when C16:1 is introduced as late as 10h after the initial treatment with C16:0 (Dhayal et al. 2008). The potency and rapid action of C18:1 suggests that LC-MUFA may prevent C16:0-induced β-cell death through a receptor-mediated process. One potential candidate is the intracellular receptors, peroxisome proliferator-activated receptors (PPAR), a family of transcription factors whose ligands include FFA, and which act to regulate lipid homeostasis (Grygiel-Gorniak, 2014). In rodent β-cells, C18:1 but not C16:0, increase the activity of PPARδ, leading to the

induction of genes involved in fatty acid oxidation (Ravnskjaer et al. 2010). However, C18:1 has been shown to have no effect on the gene expression of other PPAR isoforms expressed in β-cells (Nolan & Larter, 2009). Consequently, there is insufficient evidence to conclusively show a role for PPAR activity in the protective effect of C18:1. A further receptor candidate for the protective mechanism of C18:1 against LC-SFA induced β-cell death, is the cell-surface G-protein coupled receptor, FFAR1 (free fatty acid receptor 1). The endogenous ligands for β-cell FFAR1 (previously known as GPR40) include unsaturated and saturated LC-FFA (Stoddart et al. 2008; Wang et al. 2018). Upon binding to FFAR1 on the β-cell plasma membrane, LC-FFA can act to stimulate insulin secretion, but with chronic exposure, it has been suggested that they may induce apoptosis. However, whether FFAR1 plays a pro- or anti-lipoapoptotic role remains a matter of debate. Certain studies have proposed that FFAR1 may contribute to C16:0 induced rodent β-cell death by contributing towards the phosphorylation of the apoptogenic kinases JNK and p38 mitogen-activated protein kinase (MAPK) (Natalicchio et al. 2013). Conversely, Zhang et al. (2007) reported that silencing of FFAR1 suppressed the anti-apoptotic activity of C18:1 in response to C16:0. Researchers identified that the activation of the extracellular signal-regulated kinase (ERK)/MAPK pathway was required for C18:1 to attenuate C16:0-induced murine β-cell apoptosis (Zhang et al. 2007). The differential effects of LC-FFA on FFAR1 and the fact that FFAR1 appears to bind LC-SFA and LC-MUFA with almost equal affinity indicates that FFAR1 is unlikely to be the receptor which mediates the cytoprotective properties of C18:1 in β-cells (Newsholme et al. 2007). The role of other FFAR subtypes (such as GPR119 and GPR120) in β-cells are yet to be characterised fully, but potentially other FFARs may play a role in the protective effect of C18:1 against C16:0-induced β-cell lipotoxicity.

In summary, there is a large body of literature which supports a role for C18:1 in preventing C16:0-induced apoptosis of pancreatic β-cells. Mechanisms by which C18:1 may protect the β-cell from lipoapoptosis include attenuating ER stress, cardiolipin, increasing the expression of those proteins with anti-oxidant activity, rerouting C16:0 into triglyceride pools, and through an unknown receptor-mediated process.

1.9 Gaps in research

The cause of LC-SFA induced β-cell death remains unclear, as do the mechanisms by which C18:1 acts to attenuate LC-SFA induced β-cell apoptosis. Literature supports the role of ER stress, autophagy, ceramide metabolism, mitochondrial dysfunction and intracellular fatty acid storage, in the cytotoxic and cytoprotective mechanisms of LC-FFA. It is likely that the mechanism of LC-SFA induced β-cell death and the cytoprotective mechanism of C18:1 is multifaceted, although the interplay of these processes is yet to be determined.

There are numerous discrepancies in the literature which can, in part, be attributed to the model being used. The majority of research investigating the mechanism of lipotoxicity has been conducted in rodent β-cells or human islets. Rodent β-cells have been shown to differ in: their expression of genes for insulin as rodent β-cells have two genes and humans have one (Shiao et al. 2008), glucose transporters (De Vos et al. 1995) and islet structure (Brissova et al. 2005); which raises questions as to whether rodent β-cells are a suitable model to study T2D. Moreover, human islets contain β-cells as well as α-cells, δ-cells, pancreatic polypeptide (PP) cells and Ɛ-cells (figure 1.4) (Elayat et al. 1995; Wierup et al. 2002); which makes them an unsuitable model for specifically studying β-cells. Further, post-mortem pancreatic tissue has

been used to study lipotoxicity although post-mortem tissue can only offer insight into the end point of T2D and not the progression of β-cell dysfunction and death. Although these models have played a critical role in the exploration and characterisation of β-cell LC-FFA lipotoxicity, it is imperative that the mechanisms of lipotoxicity be investigated in a cell and species-specific model, namely live human pancreatic β-cells. By gaining insight into the mechanisms of lipotoxicity in a live human β-cell, only then can strategies be devised which reduce the toxicity of LC-SFA in β-cells by therapeutic intervention. Researchers have long attempted to generate a human-derived pancreatic β-cell for use in the field of diabetes research. Ravassard et al. have finally achieved this, developing the EndoC-βH1 cells, a stable insulin-secreting human-derived β-cell line which was made available to study in 2011 (Ravassard et al. 2011). Studies which have characterised the functionality of EndoC-βH1 cells have identified that they function in a manner similar to human islets. However, EndoC-βH1 cells consist only of β-cells, unlike human islets which comprise of a number of different cell types (Andersson et al. 2015; Gurgul-Convey et al. 2015). There are a limited number of studies which have investigated the effect of C16:0 and C18:1 on EndoC-βH1 cell viability (Tsonkova et al. 2018; Krizhanovskii et al. 2017; Plotz et al. 2017). To the best of our knowledge, however, we are the first to study lipotoxicity in a human-derived β-cell line using a range of LC-FFA.

The LC-SFA C16:0 and C18:0 are the most abundant circulating fatty acids and as such C18:0, and particularly C16:0, are most often employed when investigating β-cell lipotoxicity (Abdullah et al. 2015). However, C16:0 and C18:0 are not the only LC-SFA in circulation, pentadecanoic acid (C15:0), heptadecanoic acid (C17:0) and nonadecanoic acid (C19:0) are also present in blood plasma and as such merit further investigation into their toxicity profile in β-cells (Abdelmagid et al. 2015; Forouhi et al.

2014). A recent epidemiological study shows that higher circulating concentrations of C15:0 and C17:0 are associated with a lower the risk of developing T2D. This implies that C15:0 and C17:0 may exert a positive effect on β-cell survival, although this is yet to be tested directly (Forouhi et al. 2014).

Extensive work has been conducted into the mechanisms underlying LC-SFA-induced β-cell death and the cytoprotective properties of LC-MUFA. Insight into these mechanisms have been gained predominantly using molecular biology and multi-omics techniques (including lipidomics, proteomics and transcriptomics); identifying many of the intracellular signalling pathways which contribute towards β-cell lipotoxicity, more often than not with conflicting results. A feature of many of these mechanisms is that they are compartmentalised, occurring at subcellular organelles such as the ER, mitochondria, lipid droplets, cell membrane etc. Subsequently, the work of this thesis proposes to investigate lipotoxicity by 'zooming out' of the molecular mechanisms, in favour of studying the subcellular organelle distribution of LC-FFA. We predict that by studying lipotoxicity in this manner will provide new insight on how lipotoxicity occurs. Investigating the disposition of LC-FFA in β-cells may also serve to elucidate the extent to which each subcellular organelle contributes towards lipotoxicity. For example, if LC-FFA accumulates in the ER and alters ER morphology, it can be assumed that the ER may play a greater role in β-cell lipotoxicity compared to fully functioning mitochondria with no alterations in morphology and no accumulation of LC-FFA. Further, by studying the distribution of LC-FFA, it can be determined how β-cells handle LC-FFA, if this differs with fatty acid chain length and degrees of saturation, and if there are interspecies differences in the handling of LC-FFA. Ultimately, these investigations will serve as a means to devise a strategy to reduce the toxicity of LC-SFA in β-cells by therapeutic intervention.

1.10 Thesis aims and objectives

The overall aim of this thesis is to elucidate the mechanisms of lipotoxicity in human pancreatic β-cells. The objectives of this study are, therefore:

1. To characterise the toxicity profile of LC-FFA (odd and even LC-SFA, and LC-MUFA) in the human-derived EndoC-βH1 cell line
2. Compare the effects of LC-FFA on the viability of EndoC-βH1 cells with those in the rat-derived INS-1E β-cell line.
3. To elucidate the mechanisms of lipotoxicity by studying the subcellular distribution of LC-FFA in both human-derived EndoC-βH1 and rodent-derived INS-1 β-cell lines.

In order to meet these objectives, pancreatic β-cell viability will be assessed using a vital dye stain and flow cytometry. The distribution of LC-FFA will be studied with the aid with fluorescent dyes and confocal and electron microscopy. Further, the Seahorse extracellular flux analyser will be employed to measure the oxidation of unlabelled LC-FFA in real time. In this way, the mechanisms underlying β-cell lipotoxicity can be elucidated.

Chapter 2.

Materials and Methods

2.1 Source of reagents

The sources of all reagents are stated in table 2.1.

The contents of all buffers are stated in table 2.2.

Table 2.1 Sources of reagents

Processes	Reagent with manufacturer
Cell culture	Bovine fraction V (fatty acid free) (Roche Diagnostics); β-mercaptoethanol (Fisher); Extracellular Matrix (ECM) (Sigma); Fetal bovine serum (FBS) (Gibco); Fibronectin from bovine plasma (Sigma); High glucose DMEM (Gibco); L-glutamine (Gibco). Low glucose Dulbecco's Modified Eagles Medium (DMEM) (Gibco); Nicotinamide (VWR); Penicillin-streptomycin (Life Technology); Phosphate buffered saline (PBS) (Lonza); RPMI-1640 (Lonza); Sodium selenite (Sigma); Transferrin (Sigma); 0.05% Trypsin (v/v) 0.53mM EDTA (Life Technologies);
Fatty acids	All fatty acids were purchased from Sigma, except heptadecanoic acid, 9,11-CLA and 10,12-CLA which

	were purchased from Cayman Chemicals. Bovine fraction V (fatty acid-free) (Roche Diagnostics).
Viability assays	Glucose, propidium iodide and trypan blue were purchased from Sigma. All other flow cytometer reagents were purchased from BD Biosciences.
Microscopy	BODIPY FL C_{16} (ThermoFisher Scientific), CellLight Golgi-RFP, BacMam 2.0 (ThermoFisher Scientific).
Radioimmunoassay	All reagents purchased from Sigma
Seahorse XF96[e]	All reagents purchased from Agilent.

Table 2.2 Buffers	
Krebs Ringer bicarbonate buffer (McClenaghan, 1996)	115mM NaCl, 4.7mM KCl, 1.2mM $MgSO_4$, 10mM $NaHCO_3$, 20mM HEPES, and 1.28mM $CaCl_2$.
Insulin assay buffer	40mM Na_2HPO_4, 10mM KH_2PO_4, 150mM NaCl, 10mM EDTA and 5% (w/v) BSA.
FACS buffer	PBS with 2% (w/v) BSA
Antibody diluting solution (ADS)	0.1M lysine, 10% (v/v) donor calf serum 0.02% (w/v) sodium azide, made up in PBS

2.2 Cell lines

Immortalised clonal β-cell lines, the rodent-derived INS-1 (INS-1E and INS-1 823/13) and human-derived EndoC-βH1 cells, were used in this study. The INS-1 rodent beta cell line originated from cells that had been isolated from an x-ray induced rat insulinoma, with continuous growth requiring thiol β-mercaptoethanol (Asfari *et al.* 1992). Hohmeirer *et al*. (2000) stably transfected the INS-1 cell line with a human proinsulin gene to enhance their response to glucose, thereby generating INS-1 823/13 cells. Merglen *et al.* (2004) isolated INS-1E cells from parental INS-1 cells, based on their responsiveness to glucose and insulin content. The EndoC-βH1 human-derived beta cell line was established using targeted oncogenesis of human foetal tissue. Briefly, this consisted of transducing human foetal pancreatic buds with a lentiviral vector encoding the oncoprotein, SV40LT. The oncoprotein SV40LT was under the control of the insulin promoter, thereby facilitating proliferation. The transduced buds were then grafted into mice to facilitate their development and differentiation into mature β-cells. The β-cells proliferated and formed insulinomas, which were subsequently transfected with human telomerase reverse transcriptase (hTERT) (to immortalise the cell line) and expanded in vitro (Ravassard, 2011).

INS-1 and EndoC-βH1 cells were both found to secrete insulin and express β-cell markers, such as the transcription factor PDX1 (Wang, 2001; Ravassard, 2011).

2.2.1 Cell culture conditions

Clonal INS-1E cells were cultured in RPMI-1640 medium containing 11mM glucose, supplemented with 10% (v/v) foetal bovine serum, 100U/ml penicillin and 100µg/ml streptomycin, 2mM L-glutamine and 50mM/L β-mercaptoethanol. INS-1 823/13 cells were cultured in the same media as INS-1E cells but with a further supplement of

10mM HEPES and 1mM sodium pyruvate. Cells were cultured in complete medium (containing supplemental reagents to facilitate growth) which had been pre-warmed to 37ºC. Cells were maintained in 75cm^2 flasks at 37°C in a 5% CO_2 humidified atmosphere. Culture medium was changed twice weekly.

EndoC-βH1 were seeded into flasks that were coated 1h prior to seeding in DMEM (25mM glucose) supplemented with 1% (v/v) penicillin/streptomycin (P/S), 2µg/ml fibronectin, 1% (v/v) extracellular matrix (ECM). Coating medium was kept at 4ºC while coating the flasks, and at 37°C for the 1h incubation period before cell seeding. EndoC-βH1 were cultured in DMEM medium containing 5.6mM glucose, supplemented with 2% (w/v) bovine serum fraction V (BSA), 100U/ml penicillin and 100µg/ml streptomycin, 10mM Nicotinamide, 5.5µg/ml transferrin, 50mM/L β-mercaptoethanol, and 2.7nM sodium selenite. Cells were maintained in 25cm^2 flasks at 37°C in a 5% CO_2 humidified atmosphere. Culture medium was changed twice weekly.

2.2.2 Cell passage

Both cell lines were subcultured when they reached a confluency of approximately 80%.

INS-1 cells were detached from the culture vessel with the aid of 0.05% trypsin-0.53mM EDTA for 5min at 37°C. Trypsin was neutralised with culture medium containing 10% (v/v) FBS and centrifuged at 200g for 5min. INS-1 cells were seeded into a fresh flask at one-tenth of the original growing population.

To aid the detachment of EndoC-βH1 cells from the culture vessel, cells were washed twice in PBS and then incubated in 0.05% (v/v) trypsin-0.53mM EDTA for 5min at 37°C. The trypsin was then neutralised in 20% FBS/ 80% (v/v) PBS and centrifuged

at 700g for 4min. To maintain the cell line, EndoC-βH1 cells were seeded into a fresh flask at $2.5x10^6$ cells per flask.

2.2.3 Cell Seeding

In this study, cells were seeded in a monolayer at the densities stated in Table 2.3.

Table 2.3 Cell seeding densities

Cell line	Plate size	Seeding density (per well)
EndoC-βH1	6-well plates	$1x10^6$
EndoC-βH1	12-well plate	$0.5x10^6$
EndoC-βH1	24-well plates	$0.25x10^6$
EndoC-βH1	FluoroDish sterile microscopy culture dishes	$0.5x10^6$
EndoC-βH1	Seahorse XF96^e 96-well cell culture plates	$0.06x10^6$
INS-1 cell lines	FluoroDish sterile microscopy culture dishes	$0.5x10^6$
INS-1 cell lines	6-well plate	$1x10^6$
INS-1 cell lines	12-well plate	$0.5x10^6$
INS-1 cell lines	24-well plates	$0.25x10^6$
INS-1 cell lines	Seahorse XF96^e 96-well cell culture plates	$0.02x10^6$

In those experiments which used fixed cells for microscopy, cells were seeded onto glass coverslips that had been sterilised in 95% (v/v) ethanol (EtOH) for 30min, repeated three times.

2.3 Preparation of fatty acids and treatment of cells

All fatty acids were dissolved in 90% (v/v) EtOH, except oleic (C18:1) and palmitoleic (C16:1) acids which were dissolved in 50% (v/v) EtOH. Fatty acids were dissolved in EtOH by heating at 70ºC for 10min. The dissolved fatty acids were then conjugated to albumin by combining the fatty acids with a 10% (w/v) bovine fatty acid-free albumin solution for 1h at 37ºC, at a 1:10 dilution. The fatty acids conjugated to BSA were then added to BSA free media at a 1:10 dilution. This gave a final concentration of either 0.9% (v/v) or 0.5% (v/v) EtOH and 1% (w/v) BSA. Cells were seeded (Table 2.3) 24h before being treated with the fatty acid-BSA complexes. EndoC-βH1 cells were exposed to fatty acid-BSA complexes for 72h, whereas INS-1 cells were treated for only 24h (shown to be a sufficient time for lipotoxicity to occur in INS-1 cells by Kwak et al. (2017)). Controls received vehicle alone which consisted of a final concentration of 0.9% (v/v) or 0.5% (v/v) EtOH, 1% (w/v) BSA, and no fatty acids.

2.4 Bafilomycin

Bafilomycin A1 is an inhibitor of vacuolar (H^+)-ATPase (V-ATPases), which play a role in receptor-mediated endocytosis, intracellular membrane trafficking and protein degradation (Toei, 2011; Xu, 2003). In this study, bafilomycin A1 was used to investigate the role of specific fatty acid trafficking pathways (such as lipophagy) inside the cell. Bafilomycin A1 (Sigma) was prepared in 100% EtOH and applied to the culture medium at a concentration of 100nM, 1h before being treated with fatty acid-BSA

complexes (see section 2.3). A concentration of 100nM bafilomycin was used as recommended in the literature (Yamamoto et al. 1998).

2.5 Cell viability assays

2.5.1 Vital dye staining

Trypan blue is a dye commonly used to assess cell viability. In living cells, where the membrane is intact, trypan blue is excluded causing the cell to have a clear cytoplasm. In dead cells, where the membrane has been damaged, the dye is retained causing the cell to have a blue cytoplasm (Strober, 1997). In this study, cells were treated with fatty acid-BSA complexes (see section 2.3) and subsequently harvested by collecting adhered and floating cells from each well. Cells were then centrifuged (INS-1 were centrifuged at 200g for 5min, EndoC-βH1 at 700g for 4min), the supernatant removed and the cell pellet resuspended in 500µl culture medium and 500µl trypan blue (0.4% (w/v) in PBS) and incubated at room temperature for 5min. The total number of dead (blue) and live (yellow) cells were then counted on a haemocytometer (figure 2.1) under a light microscope, enabling the percentage of dead cells in each well to be determined.

2.5.2 Propidium iodide staining

Propidium iodide (PI) is a red-fluorescent stain which, when the plasma membrane integrity is lost in cell death, intercalates with DNA. Adhered and floating cells were harvested as described for vital dye staining (see section 2.4.1). The pellet was resuspended in 200µl medium. The PI staining solution was prepared by combining 20µg/ml propidium iodide (PI) suspended in FACS buffer (PBS and 2% (v/v) FBS). 200µl of PI solution was then added to each sample, and the samples incubated at 4ºC for 15min. Following this, the PI-stained cells were assessed using a BD Accuri™

C6 Plus flow cytometer. PI stain was excited at 535nm, with a gate created to aid in the identification of dead cell populations. The gate was defined to differentiate cells with high PI fluorescence intensity, increased granulation and small size, which are indicative of reduced viability (figure 2.2) (Cummings et al. 2013).

All viability experiments were performed a minimum of three occasions with either duplicate or triplicate wells for each experimental condition.

2.6 Determining the action of fatty acid uptake and distribution

2.6.1 Imaging with BODIPY-labelled palmitic acid

BODIPY FL C_{16} (4,4-difluoro-5,7-dimethyl-4-bora-3a,4a-diaza-s-indacene-3-hexadecanoic acid) is a fluorescent C16:0 analogue, employed to study the subcellular disposition of fatty acids (Ziessel et al. 2007). BODIPY FL C_{16} (Life Technologies, USA) was prepared in 100% EtOH. When preparing the fatty acid-BSA complexes (see section 2.3) BODIPY FL C_{16} was also added and the fatty acid-BSA-BODIPY FL C_{16} complex incubated for 1h at 37ºC. The bound fatty acid-BSA-BODIPY FL C_{16} complexes were then applied to cells at a final exposure concentration of 250µM FFA, 1% (w/v) BSA and 400nM BODIPY FL $C_{16.}$ Cells were seeded on coverslips in a 24 well plate (section 2.2.3) 24h before fatty acid-BSA-BODIPY FL C_{16} treatment.

The subcellular disposition of the fatty acids was discovered by exposing cells to 500µM C16:0 containing 400nM BODIPY FL C_{16}, or 250µM C16:0 plus 400nM BODIPY FL C_{16} plus either 250 µM C17:0, 250 µM C19:0, 250 µM C18:1 or 250 µM methyl C18:1; for 2, 6 and 24hrs. Control cells received 400nM BODIPY FL C_{16} bound to BSA only. Cells were maintained at 37°C in a 5% CO_2 humidified atmosphere.

To image the BODIPY FL C_{16}, cells were fixed in 250µl 4% (w/v) paraformaldehyde (at 4ºC) and incubated at room temperature for 15min. Fixed cells were then washed

three times in PBS, and mounted on coverslips with the aid of a fluorescent mounting medium (Dako, Denmark). Images were captured with a Leica DMI8 confocal microscope (63x/1.40 oil immersion objective) with excitation at 488-552nm, using Leica Application Suite X software. Intracellular BODIPY FL C_{16} accumulation (identified in the study as cytosolic puncta) was quantified using FIJI software (Schindelin, 2012). Using FIJI software, a region of interest (ROI) was drawn around the plasma membrane to identify the total cell area (figure 2.3a). ROI were drawn around the cytosolic puncta to identify the total area occupied by the puncta in the cell (figure 2.3b). The area of the cell covered by cytosolic puncta was then divided by the total cell area, and the results expressed as a percentage of the total. This was repeated for each individual cell and a minimum of 5 cells per condition. All experiments were performed on either two or three separate occasions using either two or three replicate wells for each experimental condition. Statistical analysis was carried out as described in section 2.10.

The results from each experimental condition in each cell line are expressed as mean ± SEM, with each data point representing an individual well containing a monolayer of cells at the seeding densities specified in Table 2.3.

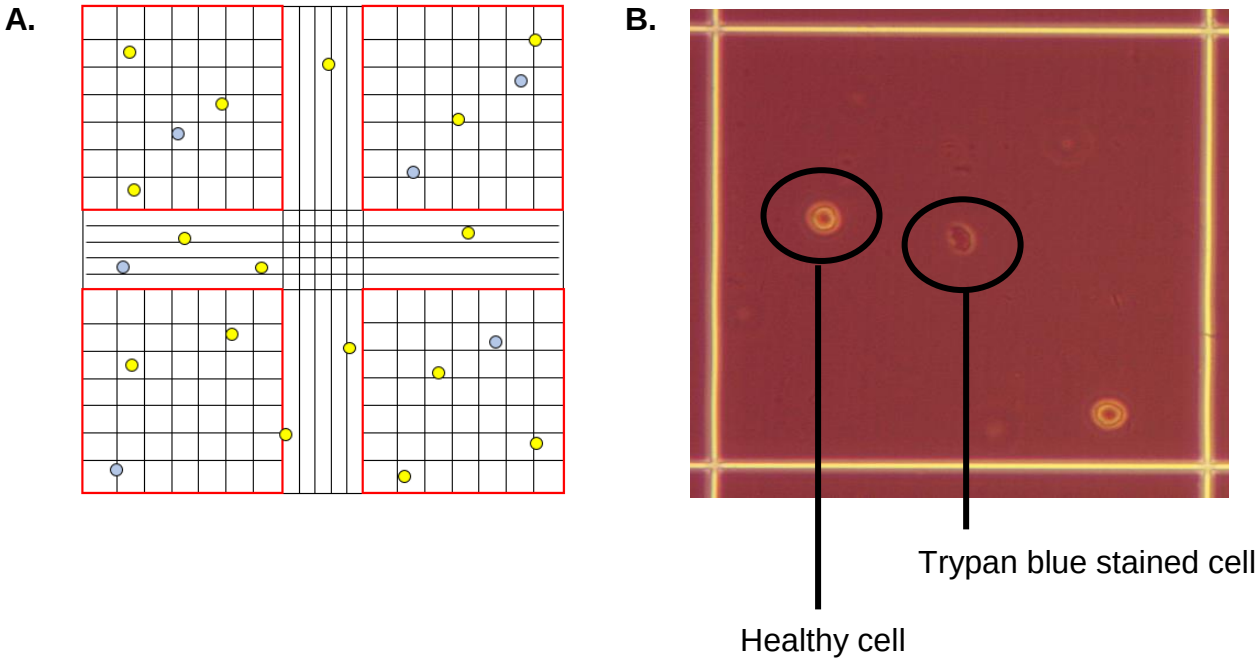

Figure 2.1 Counting dead and live cells on a haemocytometer. (A) Dead (blue) and live (yellow) cells were counted by eye in all four large squares (red) of a haemocytometer. The number of dead cells was expressed as a percentage of total cells counted in all four squares. **(B)** Trypan blue stained and healthy cells, imaged and recorded with the x4 objective on a Zeiss Primovert inverted microscope with an Axiocam camera.

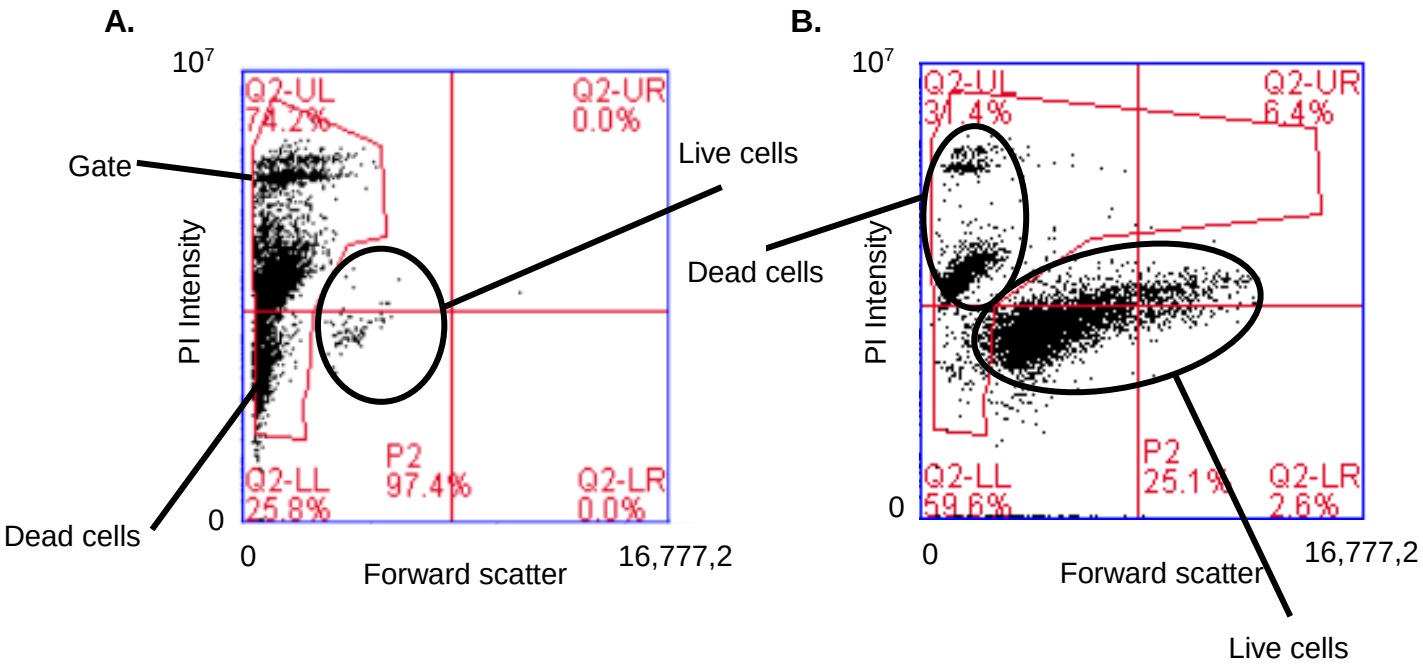

Figure 2.2 Detection of cell death using flow cytometry. (A) Cell death was induced in β-cell lines using fatty acid-BSA complexes. **(B)** Cells treated with vehicle control did not undergo cell death. Cells were stained with PI. The gate was established to differentiate dead (and dying) from live cells as shown.

A. **B.**

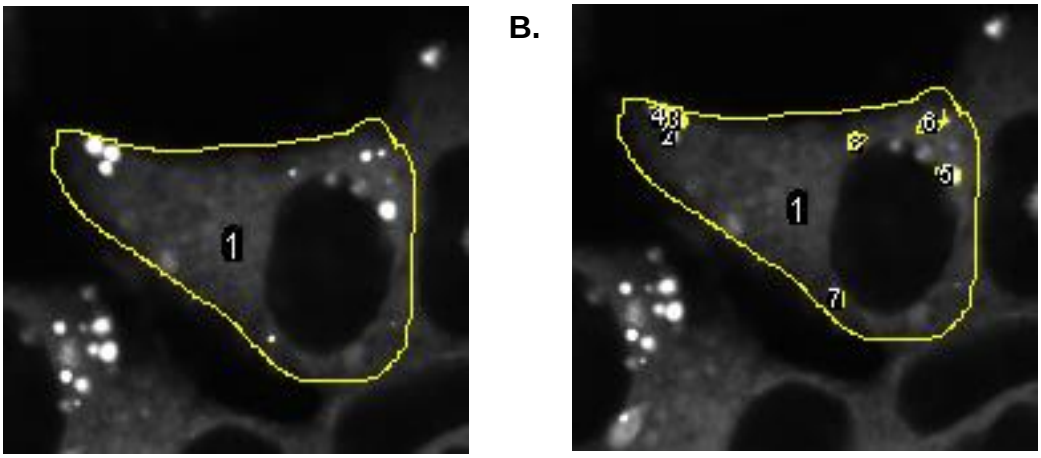

Figure 2.3 Determining the total area of the cell covered by cytosolic puncta (BODIPY FL C_{16} accumulation) in ImageJ/FIJI software. (A) A region of interest was drawn around the plasma membrane and **(B)** cytosolic puncta. The area of the cell covered by cytosolic puncta was then divided by the total cell area to determine the total area (%) of the cell occupied by the puncta.

2.6.2 Golgi-BODIPY FL C_{16} co-localisation

Cells were transfected with CellLight Golgi-RFP, BacMam 2.0 (Life Technologies), a fusion construct of a red fluorescent protein and human Golgi resident enzyme (N-acetylgalactosaminyltransferase) to identify co-localisation. Golgi-RFP was prepared according to the manufacturer's instructions and added to cells at 50 viral particles per cell (100µl reagent in 1.5ml culture medium) directly in culture medium 24hrs after seeding. Fatty acid-BSA complexes containing BODIPY FL C_{16} (see section 2.6.1), were added after 24hr and fixed in 4% (v/v) PFA (as described in section 2.6.1) for 1 hr. To image the Golgi-RFP and BODIPY FL C_{16} treated cells, images were taken using confocal microscopy as described in section 2.6.1 above. Golgi-RFP was excited at 555-584nm. Cells were maintained at 37°C during imaging and imaged directly in culture medium or Live Cell Imaging Solution (Life Technologies). These experiments were conducted in collaboration with and by Dr Jenna Corcoran, University of Exeter.

A quantitative colocalisation analysis was conducted using the fluorescent intensity analysis (FIA) plugin (as described in Dunn et al. 2011) in FIJI software (Schindelin et al. 2012). Briefly, the FIA plug-in converts the microscopy image into two RGB matrices: a pixel array of the Golgi-RFP red channel and a pixel array of the BODIPY FL C_{16} green channel. The fluorescent intensity analysis then overlaps the matrices to measure the degree of an overlay of the red and green pixels. The degree of colocalisation is then expressed as Pearson's correlation coefficient, where a value close to 1 is indicative of a high degree of co-localisation.

2.7 Transmission electron microscopy

INS-1 and EndoC-βH1 cells were seeded on coverslips in a 6 well plate (refer to Table 2.3 for seeding density) and exposed to 500µM C16:0, 500µM C18:1 or C16:0 co-incubated with C18:1 (final concentration of 500µM) (as fatty acid-BSA complexes described in section 2.3) for 6h. Control cells were treated with BSA vehicle only. INS-1 and EndoC-βH1 cells were then fixed in an osmium tetroxide fixative before being imaged with TEM. Fixing of the cells and TEM was undertaken within the Bioimaging Unit at the University of Exeter.

2.7.1 Immunogold labelling with transmission electron microscopy

Cryo-immunogold electron microscopy was used to determine the localisation of proinsulin and insulin in the EndoC-BH1 cell line. EndoC-βH1 cells were seeded in 10cm dishes at $5x10^6$ cells per dish. Cells were exposed to 500µM C16:0 or vehicle control (as fatty acid-BSA complexes described in section 2.3) for 6h. Cells were then treated as described in Slot *et al.* (2007). Briefly, this included fixing the cells in 4% (v/v) PFA supplemented with 0.1% (v/v) glutaraldehyde, scraping the cells in fixative, centrifuging at 800g for 30min to form a pellet, and embedding the pellet in 12% (w/v) gelatin. The gelatin embedded pellet was then immersed in 2.3M sucrose (made up in PBS at 4ºC) before being frozen in liquid nitrogen and cryo-sectioned. The sections were then incubated for 45min at room temperature in PBS containing 1% (w/v) BSA and the appropriate antibodies (insulin or proinsulin). The sections were then washed in PBS and incubated for 20 min in protein A-gold labelled antibodies (5nm or 20nm diameter gold spheres; G. Posthuman, Utrecht) diluted in 0.1% (w/v) BSA and PBS. The 5nm protein A-gold labelled antibody bound to the insulin antibody, and a bridging antibody was used to increase the stability of binding the 20nm protein A-gold label to

the proinsulin antibody. The sections were then incubated briefly in 1% (v/v) glutaraldehyde to stabilise the interactions and stained with 2% (w/v) neutral uranyl acetate (to stabilise the membrane lipids and enhance the final contrast) in water for 5 minutes. Sections were then embedded for 10 minutes on ice with 2% (w/v) methylcellulose supplemented with 0.4% uranyl acetate (w/v) and imaged with a Jeol 1400 microscope. Cryosectioning, immunolabelling and imaging were kindly conducted by Dr Varpu Marjomäki at the University of Jyväskyla, Finland.

2.8 Insulin secretion

2.8.1 Insulin secretion assay

INS-1 and EndoC-βH1 cells were seeded in a 24 well plate (table 2.3) 24h before the experiment. Cells were washed and pre-incubated for 1h in Krebs Ringer bicarbonate buffer (Krebs henceforth) (table 2.2) supplemented with 0.1% (w/v) BSA and 2mM D-glucose. The medium was then removed, and cells were treated for 1.5h (at 37ºC) with Krebs buffer supplemented with:

1. 0.1% (w/v) BSA and 2mM D-glucose
2. 0.1% (w/v) BSA and 20mM D-glucose
3. 0.1% (w/v) BSA and 25mM KCl (30mM final concentration as Krebs recipe contained 5mM KCl).
4. 20mM D-glucose and 500µM of either C16:0, C17:0, C18:0, C18:1 or vehicle only (as fatty acid-BSA (1% w/v) complexes described in section 2.3)

EndoC-βH1 cells did not secrete insulin in response to 20mM glucose. To amplify the release of insulin from the cells, test reagents were applied with and without 100µM IBMX (3-isobutyl-1-methylxanthine) in the incubation medium. IBMX was used to raise the level of cAMP, which amplifies the release of insulin (Siegal, 1980). After the 1.5h

treatment period, 500µl of the supernatant was removed from each well and insulin levels determined by radioimmunoassay.

2.8.2 Radioimmunoassay

Crystalline human insulin (8ng/ml) was serially diluted to create a standard curve. To each of the standards and samples, 50µl guinea pig anti-bovine insulin antibody (1:20,000 in insulin assay buffer) and 50µl of ^{125}I insulin (0.5µCi in 10ml insulin assay buffer) was added, and the tubes incubated overnight at 4°C. 1ml of precipitating reagent (PBS with 2mg/ml γ-globulins plus 30% PEG 6000 (w/v) (1:1) and 0.05% (v/v) Tween) was added to precipitate the insulin bound to the Ab. This was collected by centrifugation and the radioactivity of each pellet measured using a Perkin Elmer 2470 Automatic Gamma Counter with Wizard^2 software. A standard curve was constructed and used to calculate the insulin concentration of each experimental sample. Results were standardised by expressing insulin secretion as a fold change relative to those cells treated with either 2mM D-glucose alone (which acted as a control for 20mM glucose and 30mM KCl) or fatty acid vehicle control (see section 2.3).

All insulin secretion experiments were performed a minimum of three times with either duplicates or triplicates for each experimental condition.

2.8.3 EndoC-βH1 pseudoislet insulin secretion

To generate pseudoislets, EndoC-βH1 cells were grown as described in section 2.2, omitting the Matrigel-fibronectin from the culture flasks before seeding. The growing cells formed pseudoislets over a 72h period (figure 2.4).

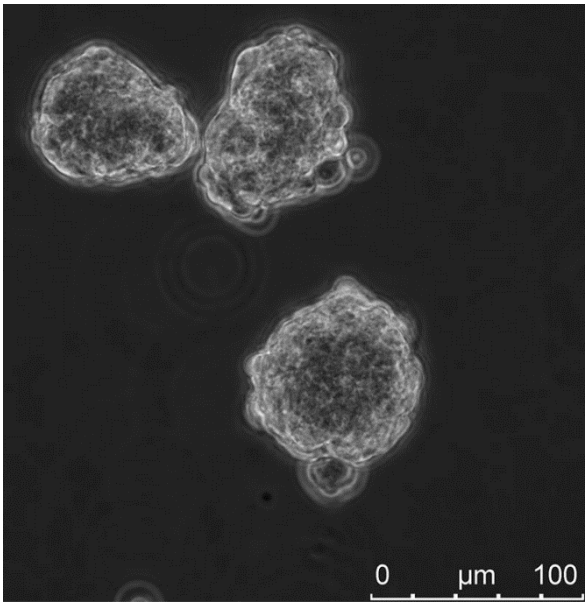

Figure 2.4 Pseudoislet formation after 72h. EndoC-βH1 were seeded in cell culture flasks that had not been coated with Matrigel-fibronectin before seeding. Cells were left to form pseudoislets over a 72h period. The formation of pseudoislets after this period was documented using a Leica DMi8 Widefield and Live Cell microscope (images courtesy of Dr Holly Hardy, University of Exeter).

EndoC-βH1 pseudoislet insulin secretion was determined by perfusion. Perfusion experiments were undertaken by Dr Mark Russell (University of Exeter) as described in Russell et al. (2011). Briefly, this consisted of suspending pseudoislets on a pre-wetted glass wool plug (in tubing) inside a Stuart bench incubator at 37ºC. Warm Krebs buffer (supplemented with 0.1% (w/v) BSA and 2mM D-glucose) was pumped over the pseudoislets at a rate of ~1ml/min for 1h before the start of the experiment. Insulin release was stimulated by adding 20mM glucose and ~20mins later, 30mM KCl. The supernatant was collected every minute for 50min. At the end of the assay, the glass wool was examined by eye under a Zeiss Primovert inverted microscope, to confirm that the islets were still present. The insulin content of the supernatant was determined by radioimmunoassay as described in section 2.2.

2.8.4 Immunocytochemistry

INS-1 and EndoC-βH1 cells were seeded on coverslips in a 24-well plate (Table 2.3) and left to adhere for 24hrs. Cells were exposed to the fatty acid-BSA complexes (section 2.3) for 4h before being fixed with 4% (v/v) PFA (as described in 2.6.1). Cells were then treated for 30min with antibody diluting solution (ADS) (table 2.2) supplemented with 0.2% (v/v) Triton X-100 (ADST) to permeabilise the cell membrane. The ADST was removed, and the cells probed with a primary insulin antibody (polyclonal guinea pig IgG anti-insulin [Dako, Agilent] at a 1:400 dilution in ADST) and incubated for 1h. The cells were washed five times in PBS and incubated for 1hr with the secondary antibody (anti-guinea pig 568nm (Thermo Fisher) at a 1:400 dilution in ADST) and DAPI (4',6-Diamidino-2-Phenylindole, Dihydrochloride) (Thermo Fischer) (at a 1:1000 dilution in ADST) to stain the nucleus. Cells were washed a further five times in PBS and mounted face down onto 3µl of fluorescent mounting medium (DAKO, Agilent). Samples were then viewed under a Leica DM4000 B LED

Fluorescent microscope, where DAPI was excited at 400nm and anti-guinea pig IgG at 568nm. Images were captured using Leica Application Suite X software.

2.9 Mitochondrial respiration

In this study, the Seahorse XF96^{e} flux analyser was used to measure the oxygen consumption rate (OCR) (pmol/minute) of live β-cells in response to an acute injection of glucose or fatty acid-BSA complexes (as described in section 2.3). INS-1 and EndoC-βH1 cells were seeded in a Seahorse XF96^{e} 96-well cell culture plate (table 2.3) 24h prior to running the assay. The 96-well culture microplate was coated in 100µg/ml poly-D-lysine (Sigma) 30 minutes prior to seeding cells to facilitate adhesion.

As per the manufacturer instructions, a Seahorse XF96^{e} sensor cartridge was hydrated (to hydrate the solid sensor probes which monitor changes in O_2) in Seahorse XF calibrant (200µl/well) and incubated overnight at 37°C with only atmospheric CO_2. Cell media were replaced 2h before running the assay with Krebs-Ringer buffer (table 2.2) supplemented with 1mM pyruvate, 2mM L-glutamine and either 0mM or 10mM glucose, and the pH adjusted to 7.4. Cells were further incubated at 37°C without CO_2 for 1h before the XF assay. Reagents to be injected were adjusted to a pH 7.4. Reagents were loaded into the injection ports of the sensor cartridge (25µl per port) ready for sequential injection during the assay. After injection, the machine mixed the well for 3 minutes, rested for 2 minutes, and took measurements for 3 minutes. The total assay time was between 60-90 minutes, including 20 minutes for reading basal respiration. The Seahorse instrument maintained the cells at a pH of 7.4 and at 37°C for the duration of the experiment. Each experiment was repeated a minimum of three times and eight replicates were included for each experimental condition.

2.9.1 Mito stress test

A Seahorse XF Cell Mito Stress Test kit was used to produce a mitochondrial bioenergetic profile of INS-1 and EndoC-βH1 cells, as an indicator of the metabolic function and bioenergetic health of the β-cell lines (figure 2.5). As per the manufacturer's instructions, oligomycin, FCCP (fluoro-carbonyl cyanide phenylhydrazone) and rotenone/antimycin A mix were reconstituted in supplemented Krebs buffer (Table 2.2). Compounds were loaded into the injection ports in the sensor cartridge (25µl per port) ready for sequential injection during the assay. Oligomycin was injected after 15 minutes (with the first 15mins measuring basal respiration), FCCP was injected after 35mins and the rotenone/antimycin mix after 61mins. Respiration was measured for approximately 20mins after each injection. The cells were exposed in the well to a final concentration of 1µM oligomycin, 1µM FCCP and 0.5µM rotenone/antimycin mix.

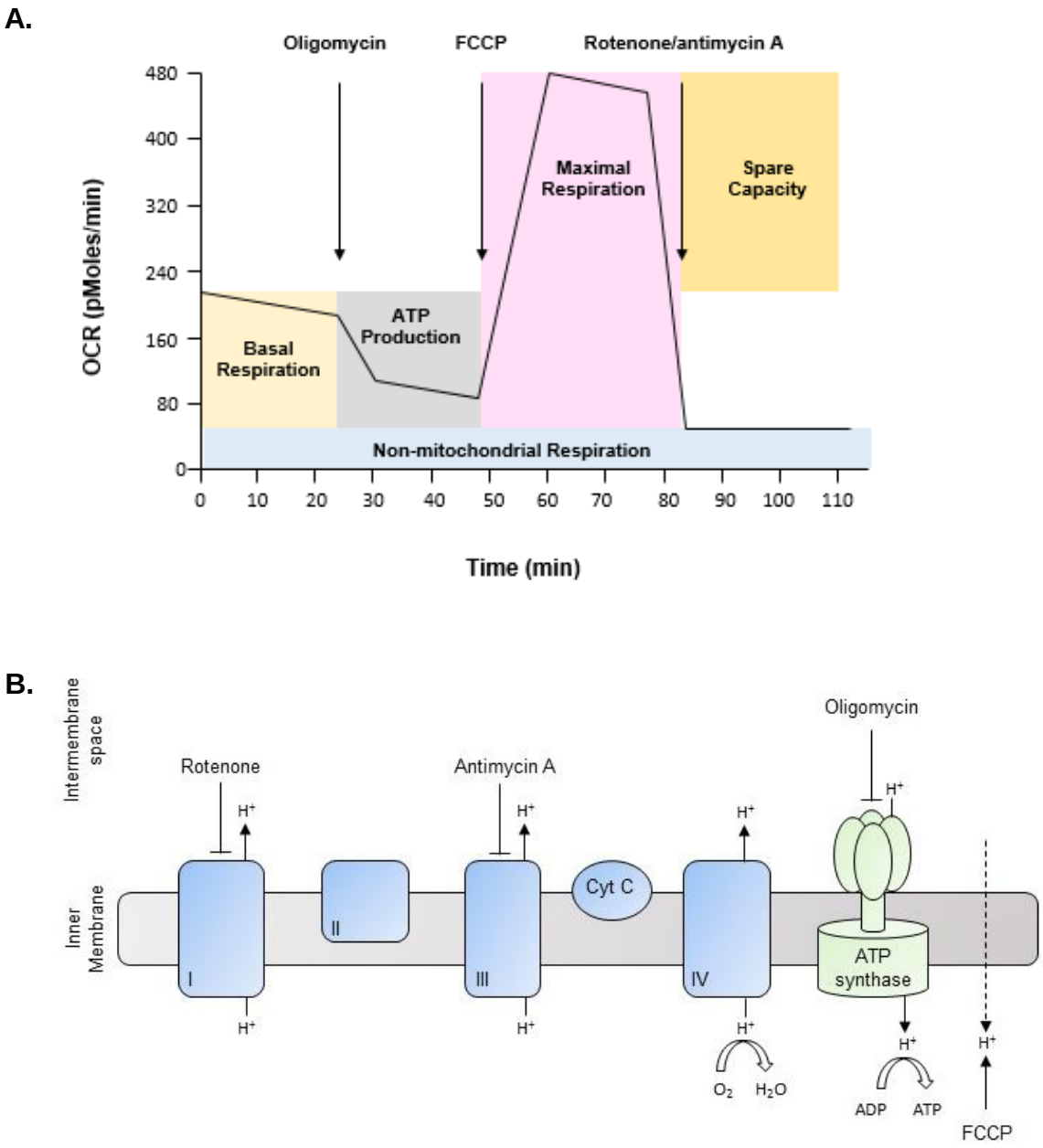

Figure 2.5 Agilent Seahorse XF Cell Mito Stress Test. The mitostress test produces a mitochondrial energetic profile of cells. **(A)** Oligomycin, FCCP and rotenone antimycin mix are sequentially injected during the assay which facilitates the measurement of ATP production, proton leak, maximal respiration and the spare metabolic capacity of cells. **(B)** Oligomycin inhibits ATP synthase, FCCP disrupts the proton gradient of the ETC, rotenone and antimycin A inhibit complex I (NADH Coenzyme Q oxidoreductase) and complex III (ubiquinol-cytochrome c oxidoreductase), respectively (adapted from Agilent, 2017).

2.9.2 Seahorse statistical analysis

All statistical analysis was conducted using the R statistical language, and GraphPad software. To standardise the data, all experimental values were normalised to baseline and $\log_e$ transformed. The area under the curve was calculated by taking the sum of all data points recorded after the substrate injection. The statistical differences between groups was conducted as described in section 2.10.

2.10 Statistical Analysis

Statistical significance was established using the R statistical language, and GraphPad software. Experimental replicates from each independent experiment were collated and the statistical difference between groups calculated using an analysis of variance (ANOVA) (Box, 1954). To compare differences between all treatment groups, a Tukey post-hoc (Tukey, 1949) test was used. The difference between groups or control was regarded as significant if $P < 0.05$.

Chapter 3.

Effects of long-chain fatty acids on human β-cell viability

3.1 Introduction

Fatty acids (FFA) are mainly bound to serum albumin in the blood and are present at total concentrations between 100µM-1mM (Ralston et al. 2013). The concentration of circulating FFA is tightly regulated, but with metabolic disturbances (such as insulin resistance) circulating FFA concentrations can become elevated and their circulating profile altered (Mika et al. 2016). When sustained, the dysregulation and elevation of circulating FFA are linked with an increase in an individual's risk of developing T2D (Mooradian, 2009; Fourouhi et al. 2014).

Lee et al. (1994) was one of the earliest studies to recognise that elevated FFA and triglyceride levels in the pancreas caused β-cell dysfunction and death. However, in subsequent years it has been realised that not all FFAs exert the same toxic effects on pancreatic β-cells. The LC-SFA C16:0 and C18:0 are the most abundant LC-SFAs in the human body (Mika et al. 2016), and it is widely understood that in excess they are extremely toxic to rodent β-cells and human islets at least, in vitro (Maedler et al. 2003; Welters et al. 2004). The short to medium chain SFAs (such as myristate; C14:0) however are much less toxic (Welters et al. 2004). Moreover, a recent epidemiological study revealed that higher levels of circulating C16:0 and C18:0 correlate with an increased risk of developing T2D, whereas an elevation in certain odd numbered LC-SFA (C15:0 and C17:0) is associated with a decreased risk (Fourouhi et al. 2014). This might suggest that C15:0 (pentadecanoic acid) and C17:0 (heptadecanoic acid) exert a positive effect on β-cell survival, although this has yet to be tested directly. Therefore, this evidence poses the following questions: 1) does LC-SFA toxicity correlate with carbon chain length in β-cells? 2) are the odd-chain FFA cytoprotective to β-cells?

Strikingly, the long-chain monounsaturated fatty acids (LC-MUFA) (such as oleic (C18:1) and palmitoleic acid (C16:1)) are well tolerated by β-cells, and even have the ability to attenuate C16:0 induced toxicity in rodent β-cells and human islets (Maedler et al. 2003; Maedler et al. 2001; Welters et al. 2004). It has been suggested that LC-MUFA may inhibit C16:0 induced cell death as a protective mechanism against lipotoxicity in tissues such as the liver (Silbernagel et al. 2012). In the liver and pancreas, C16:0 can be desaturated to yield C16:1 by SCD-1 (stearoyl-CoA desaturase) and this could be a mechanism to prevent C16:0 accumulation (Silbernagel et al. 2012; Hellemans et al. 2009). Interestingly, SCD1 has been shown to be upregulated in specific clones of rodent-derived β-cells which are resistant to C16:0-induced apoptosis (Busch, 2005). Further, inducing SCD1 expression protects against C16:0-induced cell death in rodent and human β-cells (Hellemans et al. 2009). Thus, the balance between the levels of various long-chain FFA (LC-FFA) species, particularly LC-SFA and LC-MUFA, is likely to be critical to the health of β-cells, as is the activity of desaturase enzymes such as SCD1.

Investigating the lipotoxic profile of individual FFAs in human β-cells has proved challenging. Isolating homogenous populations of β-cells is difficult due to the fact that β-cells comprise only 1-2% of the total pancreatic mass and they are located in islets of Langerhans, which also contain other cell types (Weir et al. 2011). With recent developments in florescence activated cell sorting (FACS) however, it is becoming increasingly feasible to purify β-cell populations (Basu et al. 2010), but accessing human islets remains a challenge in many countries as the majority of viable human islets are used in transplant programmes. Until recently, reliance has been placed on rodent models, post-mortem pancreatic sections and isolated human islets to study the pathophysiology of T2D. Although rodent models have historically played a critical

role in the exploration and characterisation of diabetes, there are marked interspecies differences between rodent and human β-cells. For example, the principal glucose transporter expressed in rodent β-cells is GLUT2 (glucose transporter 2), whereas in human β-cells GLUT1 and GLUT3 are the main glucose transporters (Chandrasekera et al. 2013). Interspecies differences call into question whether rodent cells are an appropriate model to study human β-cell lipotoxicity. However, investigating β-cell lipotoxicity in human islets also has limitations, as the islets consist of a number of cell types in addition to β-cells. In order to understand the impact of elevated FFAs on human pancreatic β-cells, it is essential to determine the mechanisms by which lipotoxicity occurs. For the first time, however, lipotoxicity in human β-cells can now be addressed as, in 2011, the stable insulin-secreting human-derived β-cell line, EndoC-βH1, was generated and has subsequently been made available for study (Ravassard et al. 2011).

With access to the EndoC-βH1 cell line, glucolipotoxicity can also be investigated. Human islets and rodent β-cells are well documented to undergo cell death when exposed to C16:0, although whether C16:0-induced β-cell death is affected by the presence of elevated glucose concentrations is species dependent. C16:0-induced cell death in isolated human islets does not increase when glucose concentrations are raised from 5.5mM to >20mM (Sargsyan et al. 2011; Poitout et al. 2010). Conversely, an increase in C16:0-induced cell death is observed when rodent β-cells are exposed to >11mM glucose (Sargsyan et al. 2011). Therefore, with the availability of EndoC-βH1 cells, it is now possible to establish whether human β-cells are sensitive to C16:0 and, if so whether cell viability is adversely affected by glucose concentrations.

The aim of the studies presented in this chapter is to characterise the toxicity profile of LC-FFA. Specifically, we wanted to determine which LC-FFA are toxic to human-

derived β-cells and over which concentration range. The studies further determined if toxicity correlates with FFA carbon chain length, if the odd-chain LC-SFA are cytoprotective to β-cells, and whether the presence of high glucose accentuates C16:0-induced cell death. Moreover, to assess whether lipotoxicity in rodent β-cells is reflective of the human situation, a comparison of the LC-FFA toxicity profile of the rodent-derived INS-1E β-cell line with that of the human-derived EndoC-βH1 cells were also made.

3.2 Methods

EndoC-βH1 and INS-1E cell lines were used in all experiments described in this chapter. The cells were cultured as described in section 2.2 and seeded into 6 or 12 well plates at a seeding density given in table 2.3. Cells were seeded 24h prior to treatment with fatty acid-BSA complexes (see section 2.3). Vital dye staining and propidium iodide were used to estimate cell death (see section 2.5).

Foetal bovine serum (FBS) is a necessary constitute of INS-1E culture medium, although it contains varying fatty acids (mainly polyunsaturated FFA) (Stoll, 1984). All experiments described in this chapter, therefore, were conducted in FBS FFA free media to ensure that FFA concentrations were not altered in an uncontrolled manner. Moreover, fatty acids were conjugated to fatty acid-free bovine serum albumin (BSA).

3.3 Results

3.3.1 Effects of the LC-SFA C16:0 on human β-cell viability

It is well understood that the LC-SFA C16:0 causes a loss of viability in rodent β-cells cultured for periods of 24-96h (Welters et al. 2004; Dhayal et al. 2011). Accordingly, in this study when INS-1E cells were exposed to increasing concentrations of C16:0 (0-500µM), there was a dose-dependent increase in cell death within 24h as judged

by vital dye staining. Cell death was significantly increased in INS-1E cells with concentrations of ≥250μM C16:0 after a 24h period of exposure (figure 3.1). To investigate the effects of C16:0 on the human-derived EndoC-βH1 cell line, EndoC-βH1 cells were also treated with increasing concentrations of C16:0 (0-500μM). Surprisingly, after 24, 48, and 72h there was no increase in cell death as assessed by flow cytometry (only 72h data shown) (figure 3.2). EndoC-βH1 cells exposed to 500μM C16:0 for 72h, also showed no significant increase in cell death when viability was estimated by vital dye staining (appendix 1). EndoC-βH1 cells, therefore, were more resistant to the toxic effects of C16:0 than rodent β-cells.

To investigate if the human-derived β-cell line, EndoC-βH1, undergoes cell death when exposed to C16:0 in the presence of glucose at high concentrations (glucolipotoxicity), EndoC-βH1 cells were treated with 500μM C16:0 in both low (5.5mM) and high (20mM) glucose for 72h. Compared to vehicle controls, there was no increase in cell death when EndoC-βH1 cells were exposed to 500μM C16:0 with low (5.5mM) or high (20mM) glucose in the extracellular medium (figure 3.3).

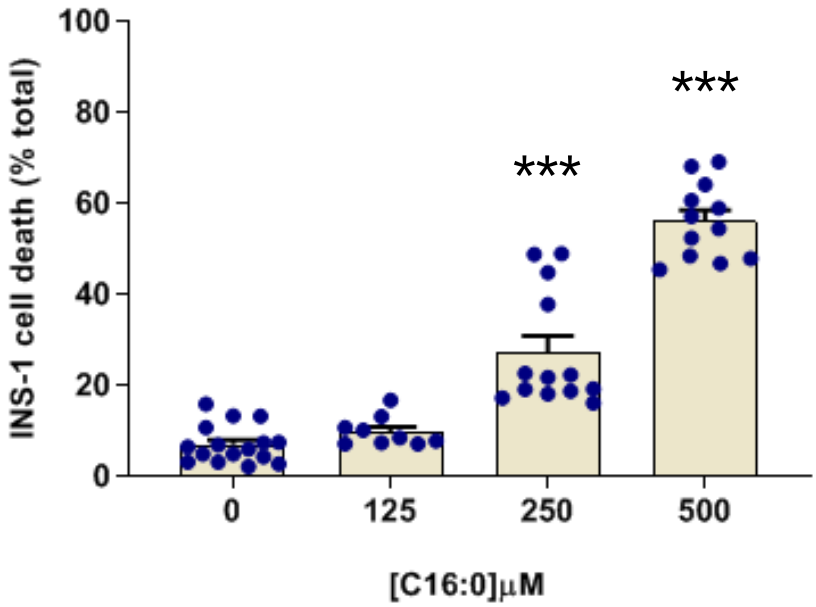

Figure 3.1 Effect of increasing concentrations of C16:0 on the viability of INS-1E cells. INS-1E cells were treated with 0μM, 125μM, 250μM and 500μM C16:0 for 24h. Cell death was estimated using vital dye staining. Dots represent data points from four independent experiments. Data are expressed as the mean values with error bars representing the SEM. *** $p<0.001$ relative to 0μM.

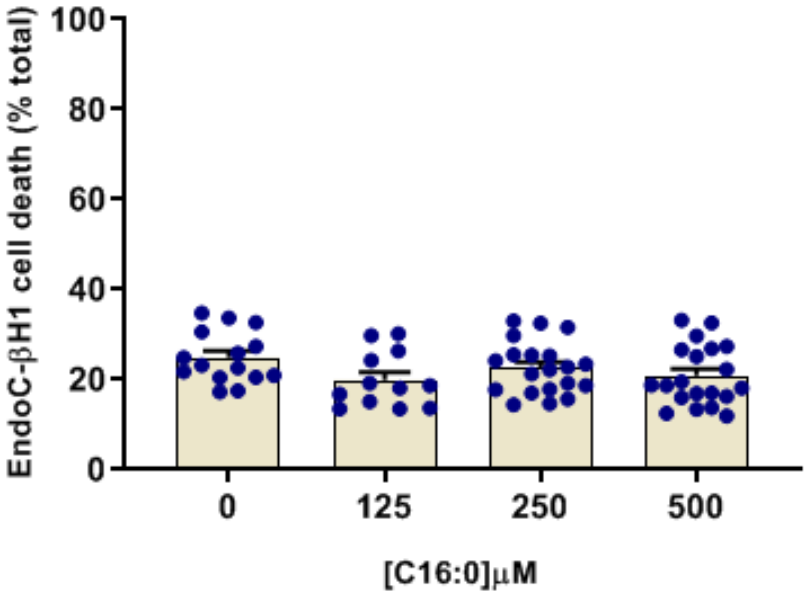

Figure 3.2 Effect of increasing concentrations of C16:0 on the viability of EndoC-βH1 cells. EndoC-βH1 cells were treated with 0μM, 125μM, 250μM and 500μM C16:0 for 72h. Dots represent data points from four independent experiments. Cell death was estimated using flow cytometry. Data are expressed as the mean values with error bars representing the SEM.

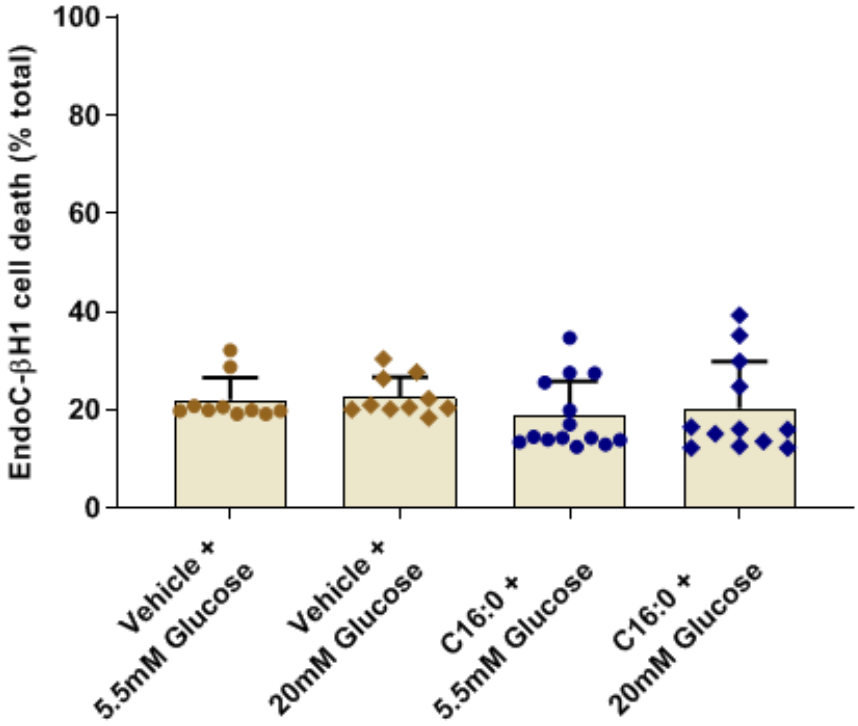

Figure 3.3 Effect of C16:0 on the viability of EndoC-βH1 cells in the presence of low and high glucose. EndoC-βH1 cells were treated with 0.5mM C16:0 in the presence of 5.5mM or 20mM glucose, for 72h. Control cells were treated with BSA vehicle only, with either 5.5mM or 20mM glucose in the extracellular medium. Cell death was estimated using flow cytometry. Dots represent data points from three independent experiments. Data are expressed as the mean values with error bars representing the SEM

3.3.2 Effects of fatty acid chain length on human β-cell viability

Welters et al. (2004) have previously shown that SFAs with a chain length greater than 14 carbon atoms are toxic to pancreatic β-cells, whereas SFAs with 14 carbon atoms or less are much less toxic to rodent β-cells. Moreover, it has been suggested that β-cell lipotoxicity is induced to a greater extent by C18:0 compared to C16:0 (Lu et al. 2016). Therefore, in this study, it was sought to explore if fatty acid chain length correlated with toxicity. The toxicity profile of C15:0, C16:0, C17:0, C18:0 and C19:0 were determined in both rodent-derived INS-1E and human-derived EndoC-βH1 cells. Seemingly, this is the first time that the toxicity profile of odd-chain LC-SFA has been determined directly in pancreatic β-cells.

In the rodent-derived INS-1E β-cell line, when used at 500μM and after an exposure time of 24h, C15:0, C16:0, C17:0, C18:0 and C19:0 all significantly increased β-cell death relative to control (figure 3.4). C19:0, however, was the most efficacious LC-SFA when used at 500μM, triggering cell death in almost 100% of cells. The odd-chain LC-SFA C15:0, C17:0 and C19:0 are therefore toxic to rodent INS-1E cells. LC-SFA toxicity, however, did not correlate directly with carbon chain length (i.e. there was no increase in cell death with increased chain length) since C15:0 caused a greater degree of INS-1E cell death compared to C17:0. Importantly, C17:0 and C19:0 were both found to cause cell death in a dose-dependent manner (figure 3.5 and 3.6). After 24h exposure, C17:0 induced INS-1E cell death at concentrations as low as 125μM (figure 3.5) with >50% of cells losing viability at concentrations ≥250μM. After 24h treatment, C19:0, however, caused >50% cell death at a concentration as low as 125μM (figure 3.6). In the INS-1E cell line, therefore, all LC-SFA are toxic, with C19:0 causing the greatest loss in viability even at lower concentrations. It must be noted that in figure 3.4, those cells treated with vehicle control had a higher amount of cell

death relative to those cells treated with vehicle control in figure 3.1. This was due to using a different method to estimate cell death, where flow cytometry gives a greater percentage cell death in the vehicle control-treated group compared to vital dye staining.

In the human-derived EndoC-βH1 cell line, C19:0 (500μM) was the only LC-SFA to significantly induce cell death over 72h, causing cell death in a dose-dependent manner (figure 3.7 and figure 3.8). Approximately 50% of total EndoC-βH1 cells underwent cell death after being treated with C19:0 for 72h at a concentration of 500μM, although there was no significant increase in cell death at concentrations <500μM. EndoC-βH1 cells are therefore resistant to the toxic effects of C15:0, C16:0, C17:0 and C18:0, but undergo cell death with exposure to high concentrations of C19:0.

C16:0 is present in the blood in combination with other FFA (Abdelmagid et al. 2015; Mika et al. 2016). To study the toxicity profile of LC-SFAs in combination, EndoC-βH1 cells were simultaneously treated for 72h with 250μM C16:0 and either 250μM C17:0 or 250μM C19:0 (total concentration of LC-SFA per well, 500μM) (figure 3.9). Individually and in combination, C16:0 and C17:0 did not increase EndoC-βH1 cell death relative to vehicle control. Conversely, C19:0 significantly increased β-cell death but surprisingly, when in combination with C16:0, C19:0-induced EndoC-βH1 cell death was significantly decreased. This may indicate that C16:0 exerts a protective effect against C19:0-induced EndoC-βH1 cell death. Alternatively, EndoC-βH1 cells may not have undergone C19:0-induced cell death as cells were treated with only 250μM C19:0 (and 250μM C16:0) which, as shown in figure 3.8, is not a sufficient concentration to induce cell death. In summary, human-derived EndoC-βH1 cells appear to respond differently to LC-SFA (C15:0-C18:0) compared to rodent-derived

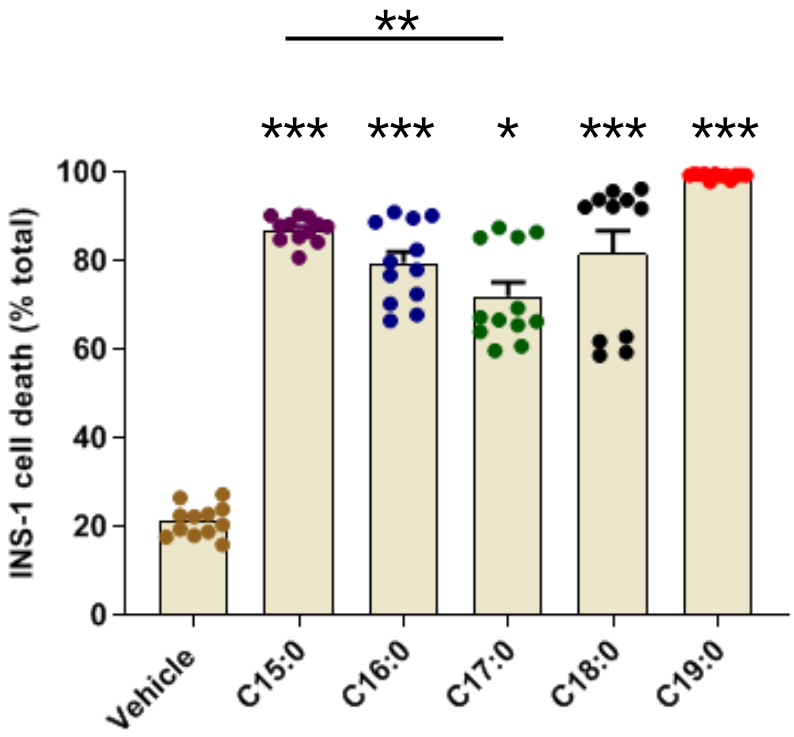

Figure 3.4 Effect of increasing chain length LC-SFA on the viability of INS-1E cells. INS-1E cells were treated with 500μM C15:0, C16:0, C17:0, C18:0 and C19:0 for 24h. Control cells were treated with BSA vehicle only. Cell death was estimated using flow cytometry. Dots represent data points from three independent experiments. Data are expressed as the mean values with error bars representing the SEM. *p<0.05, ***p<0.001 relative to vehicle.

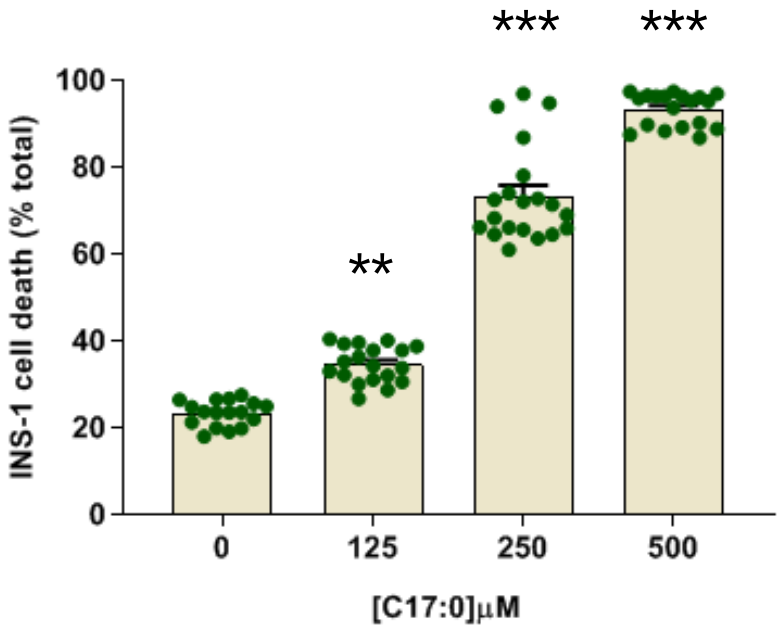

Figure 3.5 Effect of increasing concentrations of C17:0 on the viability of INS-1E cells. INS-1E cells were treated with 0μM, 125μM, 250μM and 500μM C17:0 for 24h. Cell death was estimated using flow cytometry. Dots represent data points from four independent experiments. Data are expressed as the mean values with error bars representing the SEM. **p<0.01,***p<0.001 relative to 0μM.

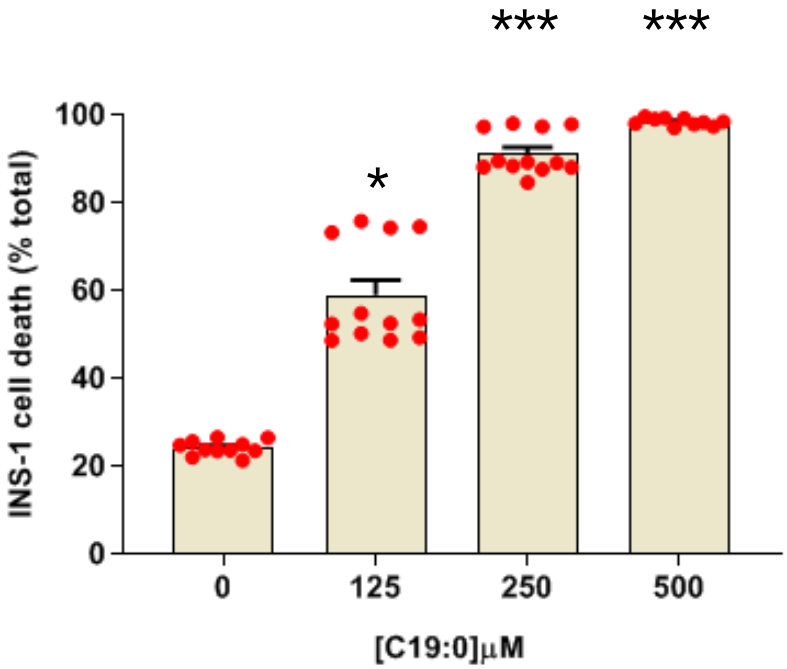

Figure 3.6 Effect of increasing concentrations of C19:0 on the viability of INS-1E cells. INS-1E cells were treated with 0µM, 125µM, 250µM and 500µM C19:0 for 24h. Cell death was estimated using flow cytometry. Dots represent data points from four independent experiments. Data are expressed as the mean values with error bars representing the SEM. *p<0.05, ***p<0.001 relative to 0µM.

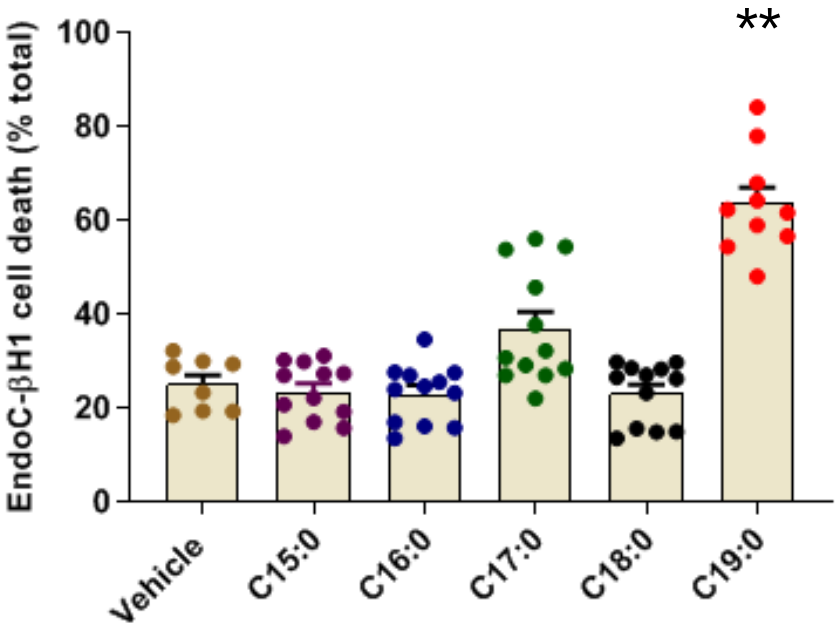

Figure 3.7 Effect of increasing chain length of LC-SFA on the viability of EndoC-βH1 cells. EndoC-βH1 cells were treated with 500μM C15:0, C16:0, C17:0, C18:0 and C19:0 for 72h. Control cells were treated with BSA vehicle only. Cell death was estimated using flow cytometry. Dots represent data points from three independent experiments. Data are expressed as the mean values with error bars representing the SEM. **p<0.01 relative to the vehicle.

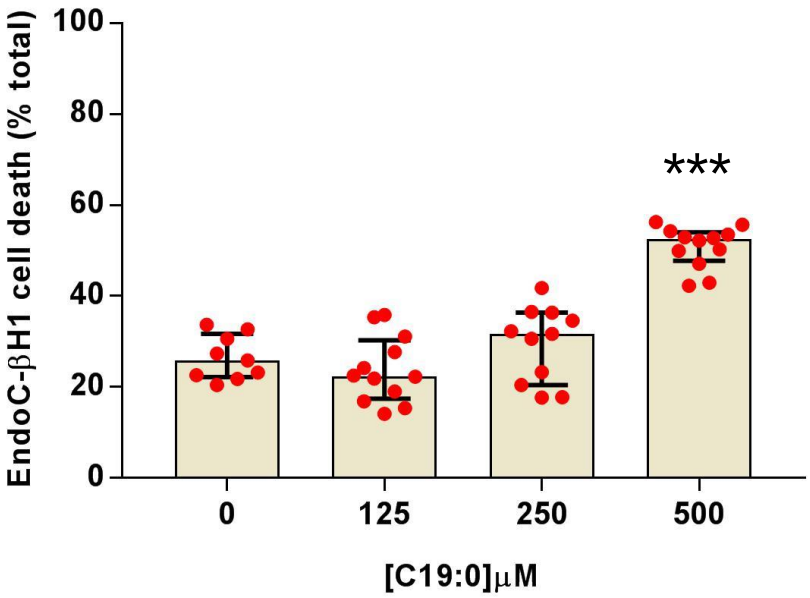

Figure 3.8 Effect of increasing concentrations of C19:0 on the viability of EndoC-βH1 cells. EndoC-βH1 cells were treated with 0μM, 125μM, 250μM and 500μM C19:0 for 72h. Cell death was estimated using flow cytometry. Dots represent data points from four independent experiments. Data are expressed as the mean values with error bars representing the SEM. ***p<0.001 relative to 0μM.

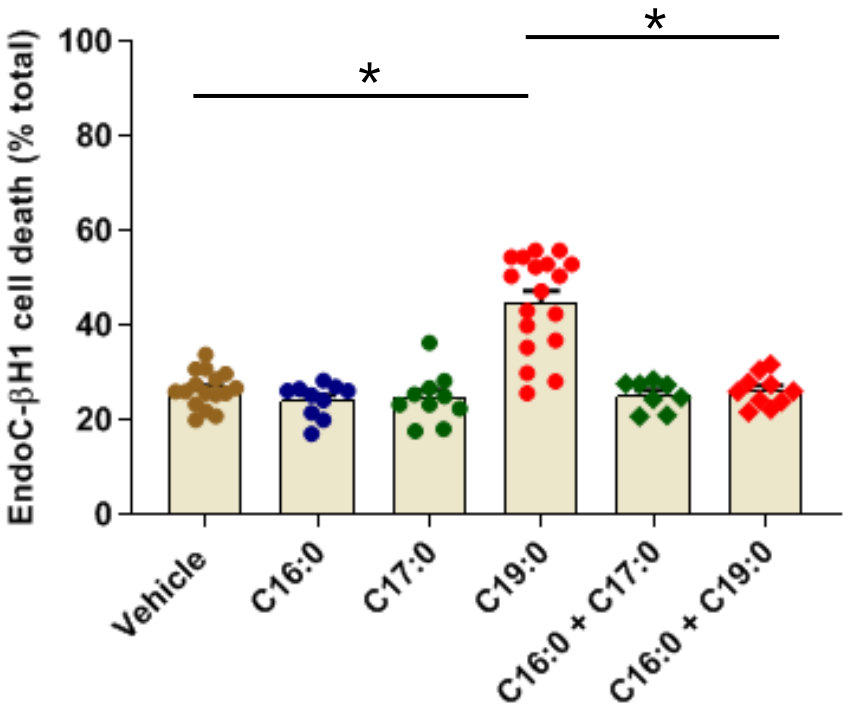

Figure 3.9 Effect of combined LC-SFA on the viability of EndoC-βH1 cells. EndoC-βH1 cells were treated with either 500μM C16:0, C17:0 and C19:0 (circles) for 72h, or 250μM C16:0 in combination with 250μM C17:0 or C19:0 (diamonds) (total concentration per well 500μM) for 72h. Control cells were treated with BSA vehicle only. Cell death was estimated using vital dye staining. Dots represent data points from three independent experiments. Data are expressed as the mean values with error bars representing the SEM. *p<0.05

INS-1E cells. C19:0, however, is the most efficacious LC-SFA causing the loss of viability in both EndoC-βH1 and INS-1E cells. EndoC-βH1 cells, however, appear more resistant to the toxic effects of C19:0 only losing viability with high concentrations (≥500μM) and with exposure periods extending up to 72h.

3.3.3 Effects of co-incubating LC-SFA with LC-MUFA on human β-cell viability

Contrary to LC-SFA, LC-MUFA have mostly proven to be benign in rodent β-cells and human islets. Strikingly, LC-MUFA have been shown to completely attenuate the cytotoxic effects of C16:0 in rodent β-cells and human islets (Maedler et al. 2003; Maedler et al. 2001). In confirmation of previous in vitro experiments (Welters et al. 2004), INS-1E cells were treated simultaneously with C16:0 and C18:1 and cell viability monitored. As previously observed in rodent β-cells, C18:1 was not toxic to INS-1E cells. Further, C18:1 completely attenuated C16:0 induced cell death, with the extent of cell death being even lower than in cells treated only with vehicle (figure 3.10). C16:0-induced INS-1E cell death was also attenuated by C18:1 methyl ester (figure 3.10). Due to the carboxyl group of the C18:1 being esterified to a methyl group, methyl-C18:1 cannot be further esterified to Co-enzyme A and is therefore metabolically inert. Thus, this result is indicative of C18:1 promoting β-cell viability by a mechanism that does not require its metabolism, as the non-metabolised methyl-C18:1 also mitigates C16:0-induced cell death in rodent-derived β-cells.

To determine if C18:1 blocks only C16:0-induced cell death in rodent-derived β-cells, INS-1E cells were treated simultaneously for 72h with C18:1 and either C15:0, C17:0 or C19:0. The LC-MUFA C18:1 completely attenuated cell death induced by each odd-chain LC-SFA in INS-1E cells (figure 3.11). In rodent-derived INS-1E cells, therefore,

LC-SFAs cause extensive cell death, except when simultaneously exposed to certain LC-MUFA.

To determine the effect of co-incubating C16:0 with LC-MUFA on the viability of EndoC-βH1 cells, these were simultaneously exposed to C16:0 and C18:1 (figure 3.12). Surprisingly, unlike in rodent β-cells, C18:1 modestly (18%) increased cell death relative to vehicle control, at a concentration of 500μM and an exposure time of 72h. Interestingly, methyl-C18:1 did not induce EndoC-βH1 cell death (figure 3.12), indicating that the toxic effects of C18:1 were due to a mechanism that requires its activation. To investigate if other LC-MUFA were also toxic to human-derived β-cells, EndoC-βH1 cells were treated for 72h with increasing concentrations of the LC-MUFA, palmitoleate (C16:1) (figure 3.13). No increase in cell death was observed in EndoC-βH1 cells treated with concentrations as high as 500μM C16:1 during an exposure period of 72h.

In summary, the LC-MUFA C18:1 can completely attenuate rodent β-cell death induced by the LC-SFA C15:0, C16:0, C17:0 and C19:0. Further, the cytoprotective effect of C18:1 in rodent-derived β-cells does not require its activation. Conversely, C18:1 causes a modest increase in human-derived β-cell death, but this is not reproduced by the methyl ester of C18:1. Unlike C18:1 however, the LC-MUFA C16:1 does not induce EndoC-βH1 cell death.

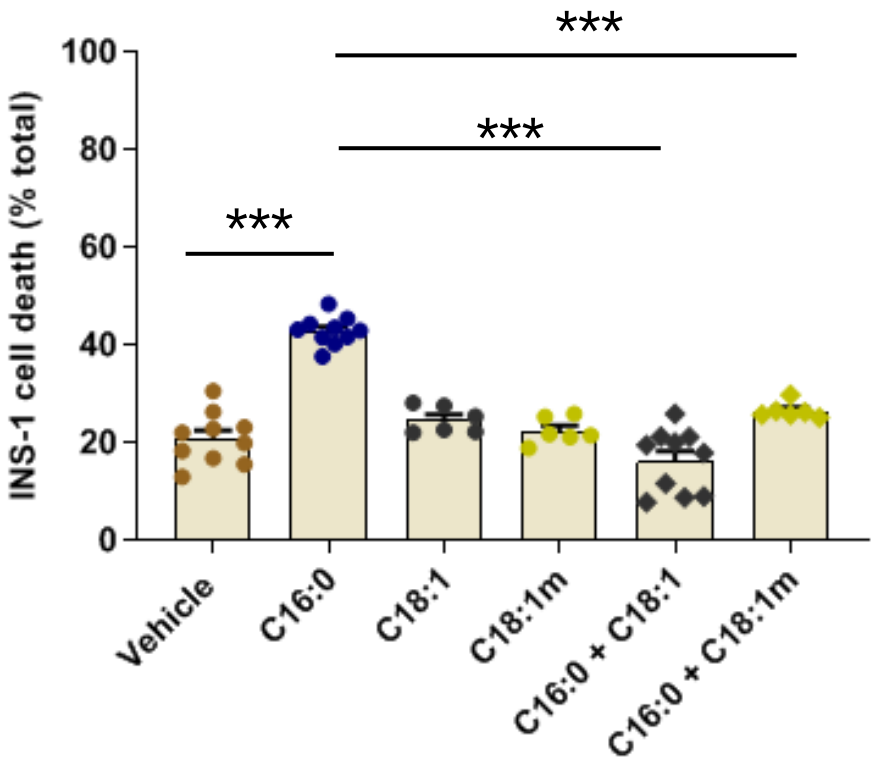

Figure 3.10 Effect of C16:0 in the presence or absence of C18:1 and C18:1 methyl on the viability of INS-1E cells. INS-1E cells were treated with either 500μM C16:0, 500μM C18:1, 500μM methyl C18:1 (C18:1m), or 250μM C16:0 combined with either 250μM C18:1 or 250μM methyl-C18:1 (final total concentration 500μM); for 24h. Control cells were treated with BSA vehicle only. Cell death was estimated using vital dye staining. Dots represent data points from four independent experiments. Data are expressed as the mean values with error bars representing the SEM. ***p<0.001.

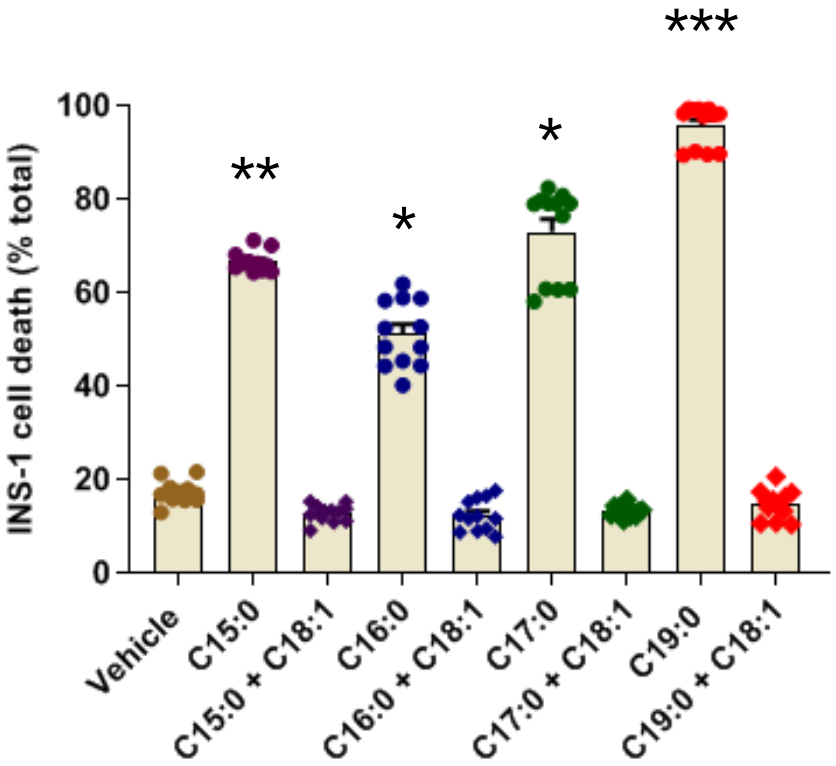

Figure 3.11 Effect of varying chain length LC-SFA in combination with C18:1 on the viability of INS-1E cells. INS-1E cells were treated for 24h with 500μM C15:0, C16:0, C17:0, C18:0 and C19:0, or 250μM C15:0, C16:0, C17:0, C18:0 and C19:0 in combination with 250μM C18:1., giving a final total concentration of 500μM fatty acids in each well. Control cells were treated with BSA vehicle only. Cell death was estimated using flow cytometry. Dots represent data points from three independent experiments. Data are expressed as the mean values with error bars representing the SEM. *p<0.05, **p<0.01, ***p<0.001 relative to vehicle.

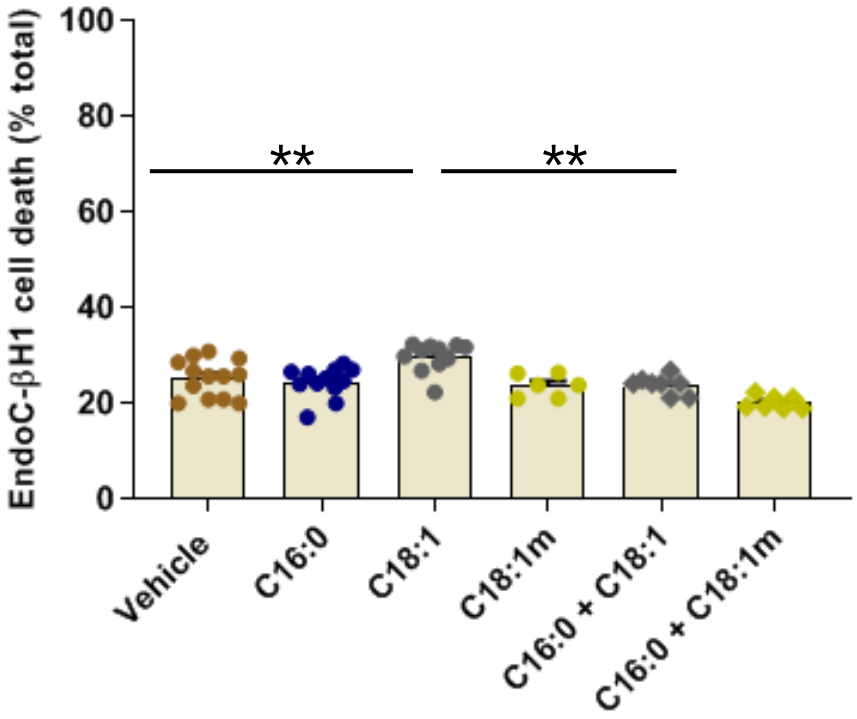

Figure 3.12 Effect of C16:0 in combination with C18:1 and methyl-C18:1 on the viability of EndoC-βH1 cells. EndoC-βH1 cells were treated for 72h with 500μM C16:0, 500μM C18:1, 500μM C18:1 methyl or 250μM C16:0 in combination with 250μM C18:1 (500μM total final concentration). Control cells were treated with BSA vehicle only. Cell death was estimated using flow cytometry. Dots represent data points from four independent experiments. Data are expressed as the mean values with error bars representing the SEM. **p<0.01.

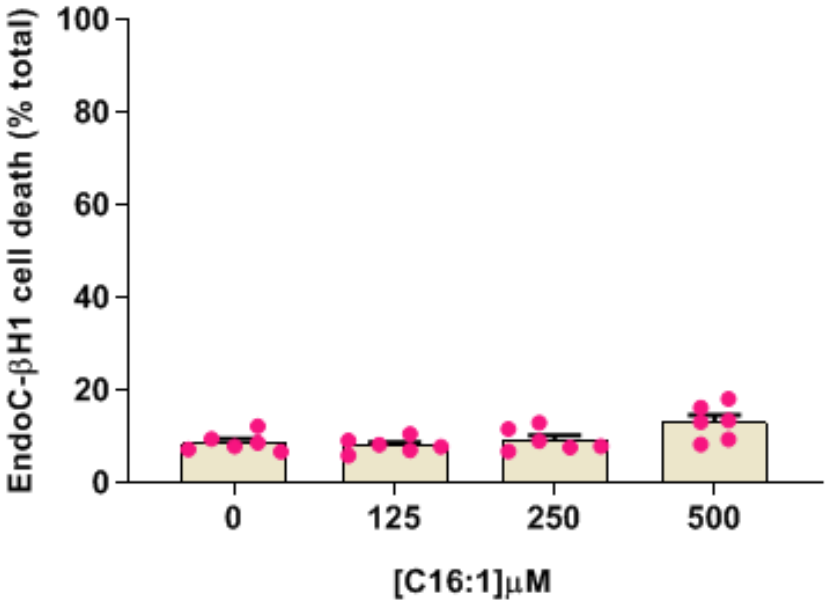

Figure 3.13 Effect of increasing concentrations of C16:1 on the viability of EndoC-βH1 cells. EndoC-βH1 cells were treated with 0μM, 125μM, 250μM and 500μM C16:1 for 72h. Cell death was estimated using flow cytometry. Dots represent data points from three independent experiments. Data are expressed as the mean values with error bars representing the SEM.

3.3.4 Effects of bafilomycin A1 on human β-cell viability in cells exposed to LC-SFA

Bafilomycin A1 is an inhibitor of vacuolar H^+-ATPase (V-ATPase), an electrogenic H^+ pump which regulates the pH of intracellular compartments including autophagosomes, endosomes and lysosomes (Maxson et al. 2014). V-ATPase, therefore, plays a regulatory role in intracellular processes including intracellular membrane trafficking, endocytosis and protein degradation (Jefferies et al. 2008). The effect of inhibiting these processes on EndoC-βH1 cell viability was investigated with the rationale that EndoC-βH1 cells may be resistant to the toxic effects of C16:0 through increased activity of V-ATPase dependent processes (e.g. autophagy). Inhibiting V-ATPase dependent mechanisms using 100nM bafilomycin alone significantly increased EndoC-βH1 cell death during an exposure time of 72h (figure 3.14). Moreover, bafilomycin-induced β-cell death was not altered in the presence of 500μM C16:0 or 500μM C18:1. Strikingly, treatment of EndoC-βH1 cells with both C16:0 and C18:1 for 72h (total concentration of LC-FFA per well, 500μM) caused a marked decrease in bafilomycin-induced β-cell death. This indicates that the combination of C16:0 and C18:1 is cytoprotective against bafilomycin-induced EndoC-βH1 cell death.

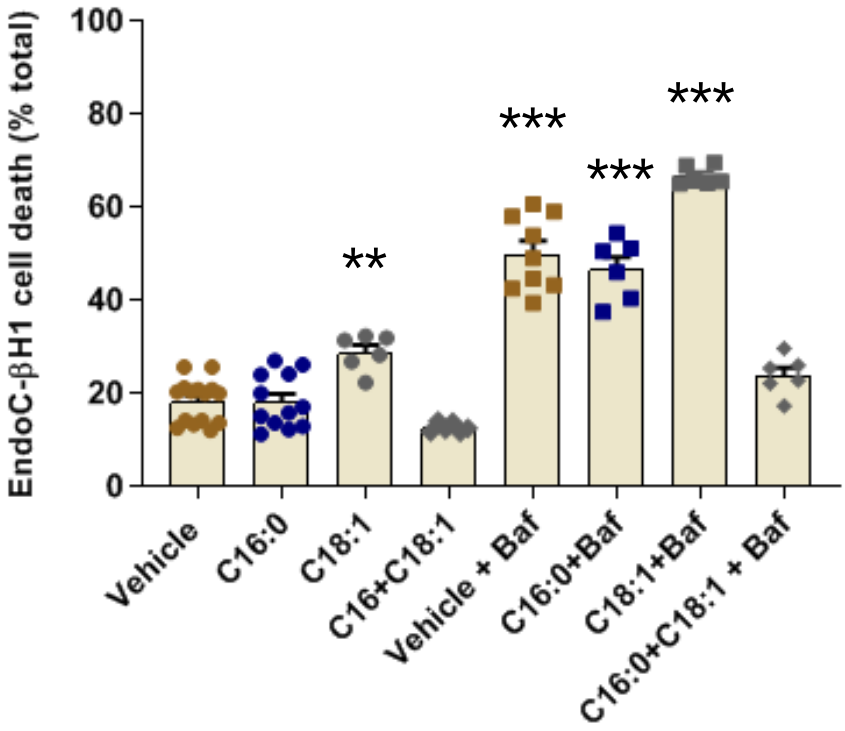

Figure 3.14 Effects of bafilomycin A1 on EndoC-βH1 cells exposed to LC-SFA. EndoC-βH1 cells were incubated for 1h with 100nM bafilomycin in the extracellular medium. 500µM C16:0, 500µM C18:1, or 250µM C16:0 combined with 250µM C18:1 was then added to cells which had previously been treated with and without bafilomycin. Control cells were treated with BSA vehicle only. EndoC-βH1 cells were treated with vehicle or LC-FFA for 72h, and cell death was estimated using flow cytometry. Dots represent data points from three independent experiments. Data are expressed as the mean values with error bars representing the SEM. **p<0.01, ***p<0.001 relative to vehicle (without bafilomycin).

3.3.5 The effect of conjugated linoleic acid (CLA) on human β-cell viability

The results obtained so far have shown that the human-derived EndoC-βH1 β-cell line is resistant to LC-SFA-induced β-cell death, whereas the rodent-derived INS-1E β-cell line is more susceptible. It was next investigated if EndoC-βH1 cells were resistant to the toxic effects of C16:0 through an increase in SCD1 activity; SCD1 being a desaturase enzyme which catalyses the biosynthesis of LC-MUFA from LC-SFA (as reviewed by Paton, 2009). Transcriptomic analyses of rodent β-cells rendered resistant to the toxic effects of C16:0 have shown an upregulation of SCD1 (Busch et al. 2005), and in rodent and human β-cells the overexpression of SCD1 protects against C16:0-induced apoptosis (Hellemans et al. 2009). Subsequently, cells were treated with the selective SCD1 inhibitor, cis-10,12-conjugated linoleic acid (10,12-CLA), to determine if EndoC-βH1 cells would undergo cell death when exposed to C16:0 in the presence of 10,12-CLA. The effects of SCD1 inhibition by 10,12-CLA were also compared with those of the structural analogue, cis-9, trans-11-conjugated linoleic acid (9,11-CLA), which does not inhibit SCD1 (Busch et al. 2005). Investigations using the SCD1 inhibitor were also undertaken in the rodent-derived INS-1E cell line. This was to compare the effects of SCD1 inhibition on cell viability in a cell line which is known to undergo C16:0-induced cell death (INS-1E) and one which is resistant to the toxic effects of C16:0 (EndoC-βH1 cells).

Initially, rodent-derived INS-1E cells were treated with increasing concentrations of either 9,11-CLA or 10,12-CLA for 24h. There was no significant increase in cell death in INS-1E cells treated with 0-80μM 10,12-CLA. Moreover, 10,12-CLA did not protect against C16:0-induced INS-1E cell death at 10,12-CLA concentrations ≤80μM (figure 3.15). The non-functional analogue, 9,11-CLA also did not increase INS-1E cell death with increasing concentrations (0-80μM). Surprisingly, however, 9,11-CLA significantly

decreased C16:0-induced cell death (compared to C16:0 alone) at concentrations ≥40μM. This unexpected result indicates that 9,11-CLA is cytoprotective against the toxic effects of C16:0 at concentrations ≥40μM (figure 3.16). Subsequently, 9,11-CLA and 10,12-CLA do not alter the viability of INS-1E cells, and 9,11-CLA is cytoprotective against C16:0-induced rodent-derived β-cell death at concentrations ≥40μM.

Human-derived EndoC-βH1 cells were also treated with increasing concentrations (0-80μM) of either 9,11-CLA or 10,12-CLA for 72h with and without 250μM C16:0. Strikingly EndoC-βH1 cells treated with ≥40μM 10,12-CLA had a significant increase in cell death relative to cells treated with 0μM 10,12-CLA. Moreover, EndoC-βH1 cells treated with ≥20μM 10,12-CLA in the presence of C16:0 also had significantly more cell death compared to cells treated with C16:0 only (figure 3.17). Thus, inhibiting SCD-1 with ≥40μM 10,12-CLA causes an increase in EndoC-βH1 cell death both in the presence and absence of C16:0. Conversely, the structural analogue, 9,11-CLA did not promote cell death in the absence or presence of C16:0 (figure 3.18) in EndoC-βH1 cells. This indicates that 9,11-CLA is not toxic to EndoC-βH1 cells. It can, therefore, be inferred that inhibiting SCD1 activity is detrimental to EndoC-βH1 cell viability.

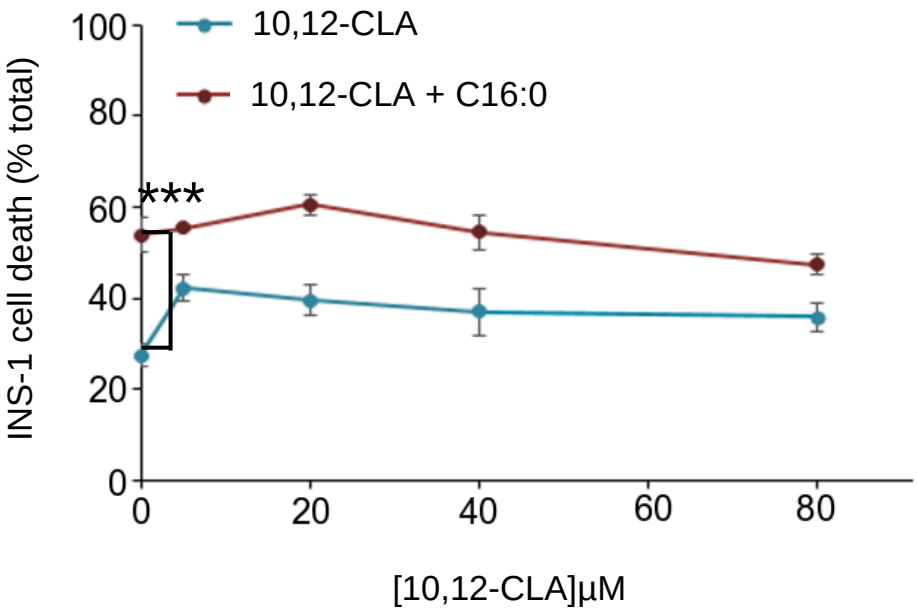

Figure 3.15 Effect of 10,12-conjugated linoleic acid (CLA) with and without C16:0 on the viability of INS-1E cells. INS-1E cells were treated with 0µM, 5µM, 20µM, 40µM or 80µM 10,12-CLA with (mauve) and without (turquoise) 250µM C16:0; for 24h. Cell death was estimated using flow cytometry. Data points are from five independent experiments. Data are expressed as the mean values with error bars representing the SEM. ***p<0.001

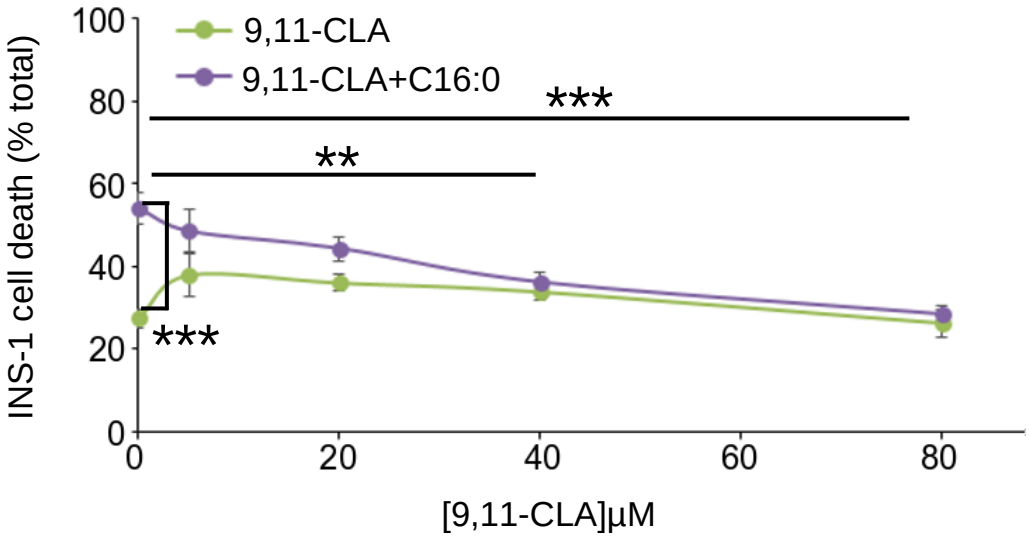

Figure 3.16 Effect of 9,11-conjugated linoleic acid (CLA) with and without C16:0 on the viability of INS-1E cells. INS-1E cells were treated with 0µM, 5µM, 20µM, 40µM or 80µM 9,11-CLA with (purple) and without (green) 250µM C16:0; for 24h. Cell death was estimated using flow cytometry. Data points are from three independent experiments. Data are expressed as the mean values with error bars representing the SEM. **p<0.01, ***p<0.001.

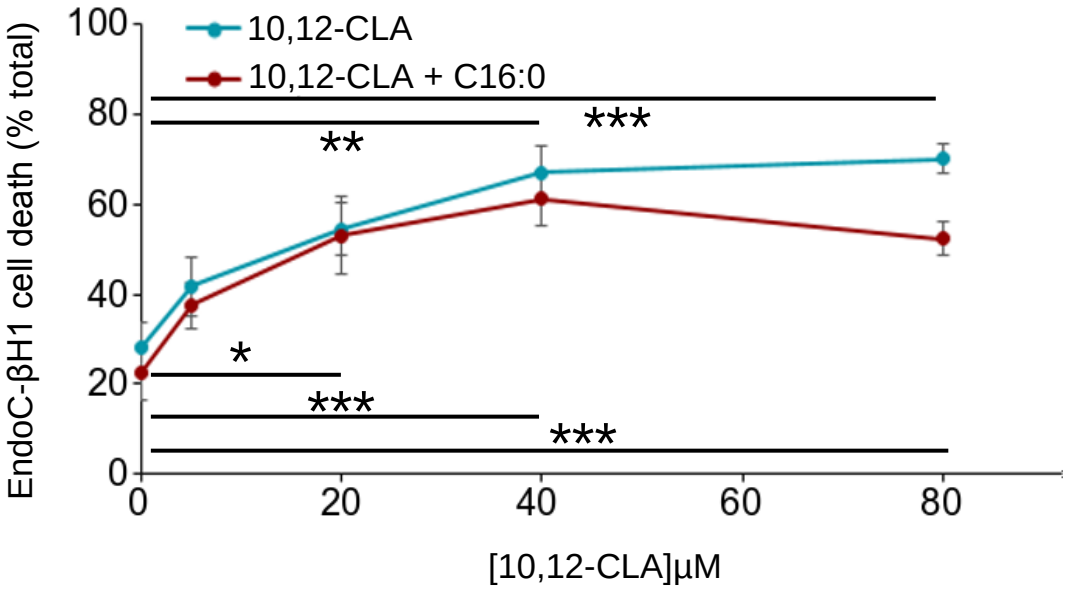

Figure 3.17 Effect of 10,12-conjugated linoleic acid (CLA) with and without C16:0 on the viability of EndoC-βH1 cells. EndoC-βH1 cells were treated with 0µM, 5µM, 20µM, 40µM or 80µM 10,12-CLA with (mauve) and without (turquoise) 250µM C16:0; for 72h. Cell death was estimated using flow cytometry. Data points are from four independent experiments. Data are expressed as the mean values with error bars representing the SEM. *p<0.05, **p<0.01, ***p<0.001.

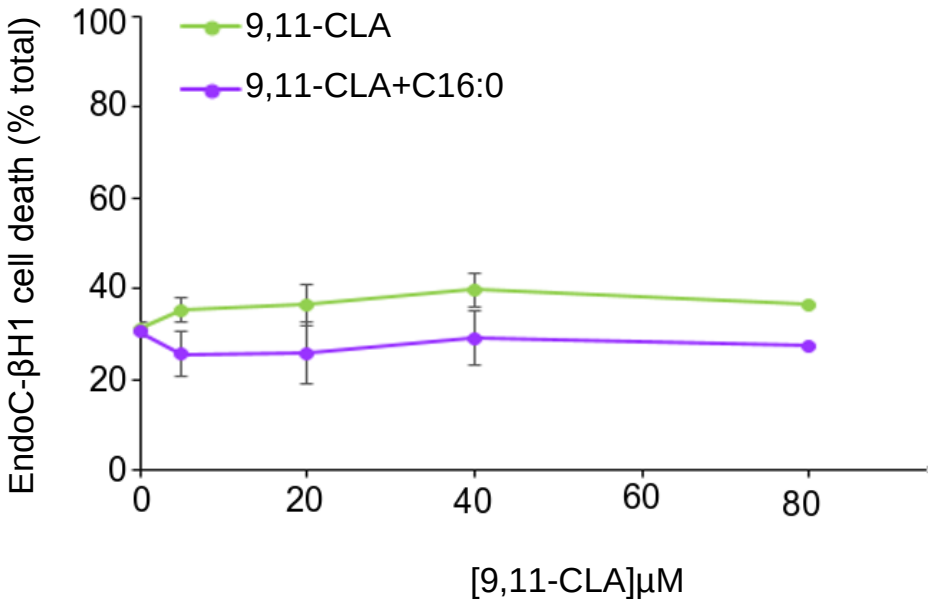

Figure 3.18 Effect of 9,11-conjugated linoleic acid (CLA) with and without C16:0 on the viability of EndoC-βH1 cells. EndoC-βH1 cells were treated with 0µM, 5µM, 20µM, 40µM or 80µM 9,11-CLA with (purple) and without (green) 250µM C16:0; for 72h. Cell death was estimated using flow cytometry. Data points are from three independent experiments. Data are expressed as the mean values with error bars representing the SEM.

3.4 Discussion

The aim of this study was to characterise the toxicity profile of LC-FFA in human-derived β-cells. The LC-FFA chosen for these investigations were C15:0, C16:0, C17:0, C18:0 and C19:0, in order to elucidate the role of chain length in toxicity and whether the odd-chain LC-FFA are cytoprotective to human-derived β-cells.

3.4.1 Effects of the LC-SFA C16:0 on human β-cell viability

It is well understood that the LC-SFA C16:0 induces cell death in both rodent-derived β-cells and human islets (Welters et al. 2004; Maedler et al. 2004). In this study, exposing rodent pancreatic β-cells to C16:0 caused a significant increase in cell death compared to vehicle, confirming previous observations (Dhayal et al. 2011; Welters et al. 2004). In contrast, EndoC-βH1 cells were found to be resistant to the toxic effects of C16:0. This finding is supported by the work of Tsonkova et al. (2018) and Krizhanovskii et al. (2017), who conducted their studies while the work of this study was taking place. Tsonkova et al. (2018) treated EndoC-βH1 cells with 100-700μM C16:0 for 72h and observed no increase in cell death relative to control. Krizhanovskii et al. (2017) treated EndoC-βH1 cells with 1mM C16:0 for 24h and failed to induce cell death. Conversely, however, another group treated EndoC-βH1 cells with 500μM C16:0 for 48h and reported a significant increase in cell death compared to cells treated with vehicle only (Plotz et al. 2017). Thus, three groups have found that EndoC-βH1 cells are resistant to the toxic effects of C16:0 even when treated at concentrations as high as 1mM and for an exposure period of 72h. This result, however, is not universally observed, and thus the ongoing ambiguity is yet to be resolved.

Next, we investigated whether EndoC-βH1 cells maintain viability when co-treated with C16:0 and high concentrations of glucose (glucolipotoxicity). Glucolipotoxicity is a phenomenon whereby the combination of C16:0 and high glucose synergistically cause β-cell death (Poitout et al. 2010). As described in the results of this study, EndoC-βH1 cells do not die when exposed to 20mM glucose either in the presence or absence of C16:0. These findings correlate with that of Tsonkova and colleagues (Tsonkova et al. 2018) who also observed no increased cell death in EndoC-βH1 cells treated with 100-700μM C16:0 for 72h in the presence of 20mM glucose (Tsonkova et al. 2018). Likewise, Krizhanovskii et al. (2017) found EndoC-βH1 viability to be maintained when co-exposed to 1mM C16:0 and 22mM glucose for 24h. Studies which have characterised the functionality of EndoC-βH1 cells have reported that these cells function in a manner similar to human islets, for example in terms of insulin secretion and respiratory response to glucose (Andersson et al. 2015; Gurgul-Convey et al. 2015). In human islets, Maedler et al. (2004) and Sargsyan et al. (2011) observed no further increase in cell death when human islets were treated with C16:0 in the presence of high glucose concentrations. Clearly, EndoC-βH1 cells do not respond to glucolipotoxic stress, and therefore, they appear to respond in a similar manner to human islets, whereby cell death is not exacerbated by co-treatment with high glucose and C16:0.

3.4.2 Carbon chain length does not correlate with toxicity in human-derived β-cells, and odd-chain LC-SFA are not cytoprotective in these cells

The results described in this chapter do not support the hypothesis that LC-SFA induced cell death correlates with chain length. Previous studies have found C18:0 to cause a greater amount of cell death compared to C16:0 in the rodent-derived β-cell lines (Lu et al. 2016; Nemcova-Furstova et al. 2011). However, In this study treating

rodent-derived β-cells with C15:0, C16:0, C17:0 and C18:0 all caused a similar increase in cell death compared to INS-1 cells treated with vehicle only, with C15:0 causing a greater degree of cell death compared to C17:0. In the rodent-derived INS-1E cells, there was no significant difference in cell death in those cells treated with C16:0 compared to C18:0. In rodent-derived β-cells, increasing chain-length (above C16:0) is not associated with an increase in cell death.

Similarly to C16:0, EndoC-βH1 cells did not die when exposed to C15:0, C17:0 or C18:0. Seemingly, this study is the first to identify that carbon chain length does not correlate with toxicity as LC-SFA molecules with 15-18 carbons had the same toxicity profile in rodent-derived (i.e. they all induced a comparable amount of cell death) and human-derived (i.e. viability was maintained) β-cells. This is important because epidemiological studies have identified a correlation between an increased concentration of odd-chained LC-SFA (C15:0 and C17:0) in the blood and a decreased risk of developing T2D (Forouhi et al. 2014; Santaren et al. 2014). From the results presented in this chapter, there was no difference in the toxicity profile of odd- and even-chained LC-SFA in rodent-derived or human-derived β-cells. This implies that if higher concentrations of circulating odd-chain LC-SFA do decrease the risk of developing T2D, it is unlikely to be through odd-chain LC-SFA exerting a protective effect on pancreatic β-cells.

3.4.3 Effects of the LC-SFA C19:0 on human β-cell viability

Strikingly, C19:0 was the most toxic LC-SFA in rodent β-cells. In addition, when used at a concentration of 500µM, C19:0 also caused EndoC-βH1 cell death. The effect on the viability of C19:0 has previously not been investigated in pancreatic β-cells. However, C19:0 was found to be toxic to the human macrophage cell line, THP-1, as

well as to a range of human cancer cell lines (Yoo et al. 2002). Collectively, this supports the view that C19:0 is toxic to a range of human-derived cell types including human-derived pancreatic β-cells, as shown in this study.

In this study, all LC-FFA, including C19:0, was conjugated to bovine serum albumin (BSA) prior to being applied to β-cells. This is because LC-FFA is transported to the β-cell bound to albumin in vivo prior to their release from the protein carrier for uptake into the cell (Thompson et al. 2010). However, this study found that C19:0 was prone to precipitate in the BSA solution (potentially due to its chain length) as this phenomenon was not observed with other LC-SFA. Hence, the true concentration of C19:0 to which the β-cells were exposed may have been less than that for other LC-SFA and cell death estimated less accurately.

3.4.4 Effects of co-incubating LC-SFA with LC-MUFA on human β-cell viability

Contrary to LC-SFA, LC-MUFA has mostly proven to be benign in rodent β-cells and human islets. A number of studies (Maedler et al. 2003; Maedler et al. 2001; Welters et al. 2004; Dhayal et al. 2008) have demonstrated that LC-MUFA can attenuate the cytotoxic effects of C16:0 in rodent β-cells and human islets. However, some studies have found LC-MUFA to promote β-cell death in immortal rodent-derived cell lines (Wrede et al. 2003; Martinez et al. 2008; Yuan et al. 2010). The results presented within this chapter verify previous observations (Dhayal et al. 2008). Namely, that C18:1 does not kill INS-1E cells and that it attenuates C16:0-induced cell death. Further, C18:1 also prevented cell death in INS-1E cells treated with either C15:0, C17:0, C18:0 or C19:0. This implies that in rodent-derived β-cells C18:1 can protect against the toxic effects of a range of LC-SFA, not just C16:0.

Surprisingly, in this study, when EndoC-βH1 cells were treated with 500μM C18:1 a modest but significant increase in cell death relative to control was seen. Another group have also noted that C18:1 can induce cell death in EndoC-βH1 cells (Plotz et al. 2017). Plotz and colleagues, however, also found EndoC-βH1 cells to undergo significant cell death when co-exposed to both C16:0 and C18:1 (Plotz et al. 2017), which differed from the observations detailed in the results section of this chapter. The difference observed between this study's results and those of Plotz and colleagues was that a higher total concentration of LC-FFA was applied by Plotz et al. when co-treating EndoC-βH1 cells with C16:0 and C18:1. In our investigations, we applied a combined concentration of C16:0 and C18:1 at 500μM, whereas Plotz et al. applied C16:0 combined with C18:1 at 1mM. It could be proposed, however, that these may be unphysiological concentrations which could account for the response.

In summary, the human-derived EndoC-βH1 cell line appears to respond differently to rodent cells when exposed to C18:1. The modest increase in EndoC-βH1 cell death induced by C18:1 is apparently mediated by a metabolic process as methyl-C18:1 did not induce cell death. C16:1 was not toxic to EndoC-βH1 cells, but further work is required to determine whether LC-MUFA toxicity correlates directly with carbon chain length in these cells.

3.4.5 The role of SCD1 in maintaining human-derived β-cell viability

An interesting conclusion is that the desaturase enzyme, SCD1, may be necessary for maintaining EndoC-βH1 cell viability. As presented in the results section of this chapter, the SCD1 inhibitor 10,12-CLA induced cell death in the EndoC-βH1 cells both in the absence and presence of C16:0.

Increased SCD1 expression has been identified in rodent-derived β-cells resistant to the toxic effects of C16:0 (Busch et al. 2005). Rodent cells can contain sub-populations which are resistant to the toxic effects of C16:0. Busch et al. (2005) isolated populations of MIN6 cells which did not undergo cell death when treated with C16:0. They then analysed the transcriptome of the C16:0-resistant MIN6 cells and identified that SCD1 expression was significantly upregulated compared to MIN6 cells which die when exposed to C16:0 (Busch et al. 2005). Busch and colleagues (2005) subsequently inhibited SCD1 using 10,12-CLA and, similar to the observations detailed in this chapter, EndoC-βH1 cell death occurrs both in the absence and presence of C16:0 (Busch et al. 2005). This implies that in those β-cells which are resistant to the toxic effects of C16:0, the capacity for β-cells to desaturate LC-FFA is critical for their survival. Busch et al. (2005) further suggested that the increased activity of SCD1 causes the resultant excess unsaturated fatty acids to accumulate in neutral lipids which are stored intracellularly as lipid bodies (Busch et al. 2005). Whether the C16:0-resistant EndoC-βH1 cells store a greater amount of intracellular lipids compared INS-1 cells, which undergo C16:0-induced cell death, merits further investigation. The expression of SCD1 in EndoC-βH1 cells also requires characterisation.

3.4.6 Effects of bafilomycin on human β-cell viability

Bafilomycin is known to inhibit V-ATPase dependent processes. However bafilomycin is most commonly used to block late-stage autophagy, inhibiting autophagosome to autolysosomal fusion (Yamamoto et al. 1998). In β-cells, autophagy has shown to be an essential process in maintaining cellular function and viability (Twig et al. 2008; Jung et al. 2008). This coincides with the observations of this study whereby EndoC-βH1 cell death was induced when the human-derived β-cells were exposed to

bafilomycin alone. This indicates that if bafilomycin does inhibit autophagy, then inhibiting autophagic flux is detrimental to EndoC-βH1 cell viability.

In rodent-derived β-cells, LC-FFA has been shown to alter autophagic turnover (Las et al. 2011; Choi et al. 2009; Chu et al. 2018). However, whether LC-FFA increases or block autophagic flux, and if LC-FFA with varying degrees of saturation act on autophagy, in the same manner, remains a matter of debate. For example, in rodent-derived β-cells, both C16:0 and C18:1 have both been shown to induce autophagy (Choi et al. 2009; Chu et al. 2018), with Choi et al. reporting that C16:0-induced β-cell death was augmented in the presence of bafilomycin A1. Conversely, our group have recently investigated the role of autophagy in rodent β-cell lipotoxicity and found that C16:0 actively increases autophagic flux while C16:1 decreases it (Dhayal S – personal communication). This observation is supported by the work of Wu et al. (2017) who found C16:0 to induce autophagy unlike C18:1 which inhibited autophagy in the human breast cancer cell line, MDA-MB-231. However, EndoC-βH1 cells had the same viability profile when treated with either C16:0 or C18:1 in the absence (viability was maintained) or presence (cell death was induced) of bafilomycin. This implies that C16:0 or C18:1 do not exert differential effects on autophagy in EndoC-βH1 cells.

Surprisingly, treating EndoC-βH1 cells with bafilomycin in combination with C16:0 and C18:1 led to a reduction in cell death compared to cells exposed to bafilomycin alone. This indicates that the inhibitory effects of bafilomycin on either autophagy or another V-ATPase dependent mechanism is overcome in EndoC-βH1 cells treated with both C16:0 and C18:1. Our investigations (Dhayal S – personal communication) show the co-incubation of C16:1 with C16:0 reduce autophagic flux in both rodent-derived β-cells and human islets (unpublished data). This indicates that the presence of one LC-

FFA can alter the activity of another LC-FFA in relation to autophagy. It is clear that the role of autophagy in EndoC-βH1 cell viability and β-cell lipotoxicity requires further investigation.

3.4.7 Summary

In summary, human-derived EndoC-βH1 cells appear to respond differently to C16:0 and C18:1 compared to rodent-derived INS-1E β-cells. Moreover, EndoC-βH1 cells also respond differently to C15:0, C17:0 and C18:0 compared to INS-1E cells. Nonadecyclic acid (C19:0) is the most efficacious LC-SFA and causes loss of viability in both human and rodent β-cells. Finally, human-derived β-cells undergo cell death when SCD1 is inhibited, suggesting that EndoC-βH1 cells may be resistant to LC-SFA induced cell death through an increase in fatty acid desaturase activity. However, the potential protective role of SCD1 in EndoC-βH1 cells requires further investigation.

Chapter 4.

The intracellular distribution of long-chain fatty acids in rodent and human β-cells

4.1 Introduction

Historically, lipotoxicity research has focused on characterising the molecular pathways which lead to FFA-induced β-cell apoptosis in T2D (as discussed in section 1.11). Mitochondrial dysfunction, ER stress, autophagy and the cytosolic accumulation of fatty acids have all been identified to play a role in the pathological process of β-cell lipotoxicity (reviewed in Sharma et al. 2014). A feature shared by these pathological processes is that they are often compartmentalised, occurring at organelles including the ER, mitochondria, lipid droplets and autophagosomes. Overloading of the β-cell with fatty acids is thought to disrupt the morphology, organisation and communication networks of these organelles. This leads to alterations in organelle biomechanics and in the activation of biochemical cascades (such as the unfolded protein response) which can ultimately lead to β-cell death (Chang et al. 2015).

The evidence is conflicting, however, as to which organelles LC-FFA predominantly act upon to cause β-cell death. For example, it has been suggested that excess LC-FFA metabolism in the mitochondria, leads to mitochondrial dysfunction and ultimately activation of the intrinsic arm of the apoptotic pathway, through the release of cytochrome c (Elsner et al. 2011; Maedler et al. 2003). However, an opposing argument is that high glucose concentrations, which are also present in the T2D milieu, increase the production of malonyl-CoA which inhibits CPT-1, thereby preventing the entry of LC-FFA into the mitochondria (McGarry et al. 1977). Rather, LC-FFA are rerouted into esterification pathways leading to the cytosolic accumulation of LC-FFA esters which eventually cause β-cell death (Kim et al. 2011; Cnop et al. 2001). There is, therefore, a need to characterise the intracellular distribution of exogenously applied LC-FFA, to determine which subcellular organelles are affected in β-cell lipotoxicity.

Past research has mostly studied the biochemical and biomechanical processes underlying LC-FFA induced β-cell death. Although this approach has played a critical role in the exploration and characterisation of β-cell LC-FFA lipotoxicity, new insight may also be gained from taking a more 'birds eye' view. To our knowledge, research is yet to simply apply LC-FFA to β-cells and monitor their distribution and the subsequent alterations in the morphology of organelles. This method, however, has only relatively recently become feasible with the development of lipid-bound probes (as reviewed in Daemen et al. 2016). BODIPY (boron-dipyrromethene) fluorophores are one such example; these dyes can be conjugated with certain FFA and are relatively insensitive to their environment (for example changes in pH), making them appropriate tools for studying the intracellular distribution of FFA in live and fixed cells (Loudet et al. 2007).

In this study, the fluorescent C16:0 analogue, BODIPY FL $C_{16,}$ was applied to clonal β-cells to investigate the distribution of the LC-FFA, C16:0. In parallel, electron microscopy was conducted to determine the changes occurring in the subcellular morphology of β-cells upon exposure to C16:0. By studying the distribution of BODIPY FL C_{16}, and changes to the morphology of β-cells after exposure to C16:0, we aimed to provide new insights into the mechanisms of lipotoxicity. A limitation of this study, however, is that BODIPY FL C_{16} is seemingly the longest LC-FFA BODIPY dye available and subsequently only the distribution of C16:0 could be analysed and not longer chain FFAs (for example C18:0). As shown in section 3.3.3, in combining C16:0 and C18:1, cell death is attenuated in both INS-1 823/13 and EndoC-βH1 cells. Moreover, C19:0-induced cell death is inhibited in the presence of C16:0 in EndoC-βH1 cells. Seemingly, there are currently no fluorescent derivatives routinely available for study of these other LC-FFA. Therefore, LC-FFA (C17:0, C19:0 and C18:1) were

applied in combination with BODIPY FL C_{16} to determine if their presence altered the intracellular distribution of BODIPY FL C_{16}. Subsequently, the changes in β-cell morphology were also examined using electron microscopy after exposure to C16:0 in the presence, or absence of C18:1.

Investigations in this study were conducted in both the rodent-derived INS-1 823/13 and the human-derived EndoC-βH1, clonal β-cell lines, to determine interspecies differences in the distribution and changes to β-cell morphology induced by C16:0.

4.2 Methods

EndoC-βH1 and INS-1 823/13 cell lines were used in all experiments described in this chapter. The cells were grown in culture and seeded onto 24 well plates for use in microscopy experiments as described in section 2.2. LC-FFA were dissolved in either 50% or 90% EtOH (final concentration 0.5% (v/v) or 0.9% (v/v) respectively) and then bound to 10% (w/v) BSA 1h before the addition to cells. In those experiments using tracer BODIPY FL C_{16} (400nM) was also added to the fatty acid-BSA complex 1h prior to treating cells (section 2.6.1).

The distribution of BODIPY FL C_{16} was measured in fixed cells (see section 2.6.1). Cells were imaged, and the total area covered by cytosolic puncta (BODIPY FL C_{16}) was calculated as described in section 2.6.1. Throughout this thesis the accumulation of C16:0 is referred to as ‘cytosolic puncta’, as the presence of the BODIPY FL C_{16} tracer within the C16:0 accumulated within the cytoplasm has a puncta-like appearance.

The distribution of BODIPY FL C_{16} and its co-localisation with organelles was studied with the aid of fluorescent dyes and confocal microscopy (see section 2.6.1). The impact of LC-FFA on β-cell organelle morphology was analysed by TEM, as detailed

in section 2.7. All electron microscopy images were assessed by an expert (Dr Christian Hacker, University of Exeter) to identify intracellular structures, including the Golgi apparatus and endoplasmic reticulum. The insulin localisation in β-cells was investigated using TEM after immunogold labelling and by immunocytochemistry (section 2.7.1 and 2.8.4).

4.3 Results

4.3.1 C16:0 cytosolic distribution in rodent- and human-derived β-cells

The following set of experiments were performed to determine the intracellular distribution of C16:0 with the tracer BODIPY FL C_{16} and whether C16:0 distribution was altered in the presence of other LC-SFA. INS-1 823/13 and EndoC-βH1 cells were treated with 500µM C16:0 plus 400nM BODIPY FL C_{16} for 2h, 6h and 24h. In INS-1 823/13 cells treated with both C16:0 and BODIPY FL C_{16} cytosolic puncta were not detected after 2h, 6h, or in those cells which had not undergone cell death at 24h (figure 4.1a). Conversely, in EndoC-βH1 cells, there was a significant time-dependent increase in the total area of the cell covered by cytosolic puncta when cells were exposed to both C16:0 and BODIPY FL C_{16} for 2-24h (figure 4.1a). When treated with tracer only (400nM BODIPY FL C_{16}), no cytosolic puncta were observed in either INS-1 823/13 or EndoC-βH1 cells (figure 4.1b+c). This indicates that the cytosolic distribution of BODIPY FL C_{16} is dictated by C16:0 and not by the fluorophore. In summary, C16:0 accumulates in the cytoplasm in human-derived, but not in rodent-derived, β-cells.

To study whether the cytosolic distribution of C16:0 is altered in the presence of other LC-FFAs, INS-1 823/13 and EndoC-βH1 cells were treated with C16:0 and BODIPY FL C_{16} in combination with either C17:0, C19:0, C18:1 or the methyl ester of C18:1; for

2h, 6h and 24h (figure 4.2+4.3). Cytosolic puncta were not observed in INS-1 823/13 cells treated with C16:0 and BODIPY FL C_{16} in the presence of C17:0 or C19:0 (figure 4.2). Surprisingly, however, a significant increase in cytosolic puncta was observed in INS-1 823/13 cells treated for 24h with C16:0 and BODIPY FL C_{16} in combination with C18:1 (figure 4.3). Interestingly, an increase in cytosolic puncta was not observed in INS-1 823/13 cells treated for 24h with BODIPY FL C_{16} and the metabolically inert, methyl ester of C18:1. Collectively, this indicates that C18:1 reroutes C16:0 in INS-1 823/13 cells, although, in order to do so it must be metabolised as this phenomenon does not occur with the metabolically inert, methyl ester of C18:1.

In EndoC-βH1 cells, there was no significant increase in cytosolic puncta in those cells treated with both C16:0 and BODIPY FL C_{16} compared to those treated with C16:0 and BODIPY FL C_{16} in the presence of C17:0, C19:0, C18:1 or the methyl ester of C18:1 (figure 4.4 and 4.5). Further, upon inspection, the distribution pattern of the cytosolic puncta in EndoC-βH1 cells is often polarised (for example in figure 4.4), accumulating in one region of the cell, and increased in size over time both with and without other LC-FFA being present. Collectively, this implies that C17:0, C19:0 and C18:1 do not alter the cytosolic distribution of C16:0 in EndoC-βH1 cells.

In summary, C16:0 accumulates in the cytoplasm of human-derived but not rodent-derived β-cells. C17:0 and C19:0 do not reroute C16:0 in either human-derived or rodent-derived β-cells. C18:1 does not alter the cytosolic distribution of C16:0 in human-derived β-cells. However, in rodent-derived β-cells the metabolism of C18:1 acts to reroute C16:0 causing it to accumulate in the cytoplasm. It could be speculated that the cytosolic puncta observed are in fact lipid droplets. However, this is yet to be tested directly.

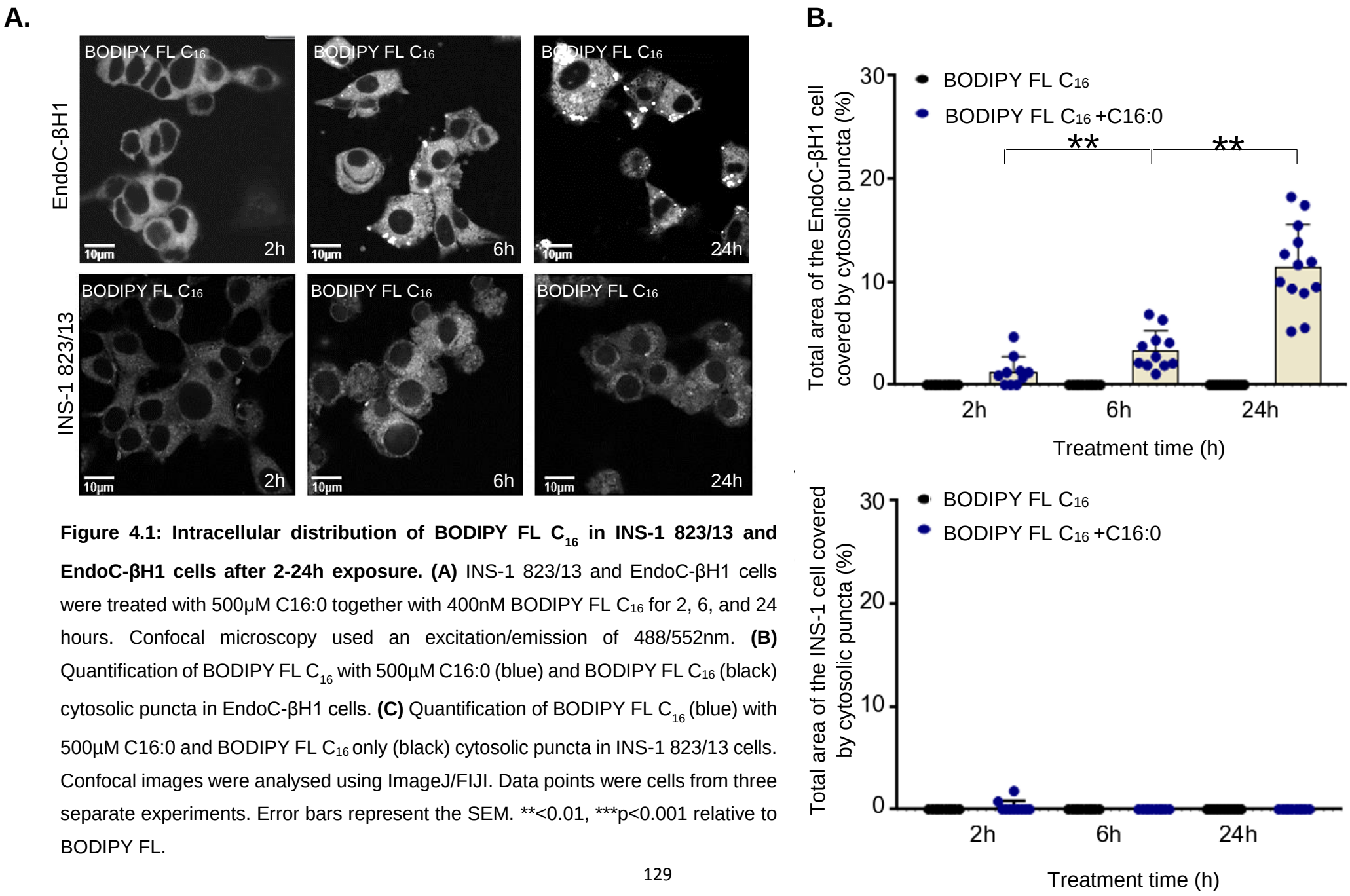

Figure 4.1: Intracellular distribution of BODIPY FL C_{16} in INS-1 823/13 and EndoC-βH1 cells after 2-24h exposure. (A) INS-1 823/13 and EndoC-βH1 cells were treated with 500µM C16:0 together with 400nM BODIPY FL C_{16} for 2, 6, and 24 hours. Confocal microscopy used an excitation/emission of 488/552nm. **(B)** Quantification of BODIPY FL C_{16} with 500µM C16:0 (blue) and BODIPY FL C_{16} (black) cytosolic puncta in EndoC-βH1 cells. **(C)** Quantification of BODIPY FL C_{16} (blue) with 500µM C16:0 and BODIPY FL C_{16} only (black) cytosolic puncta in INS-1 823/13 cells. Confocal images were analysed using ImageJ/FIJI. Data points were cells from three separate experiments. Error bars represent the SEM. **<0.01, ***p<0.001 relative to BODIPY FL.

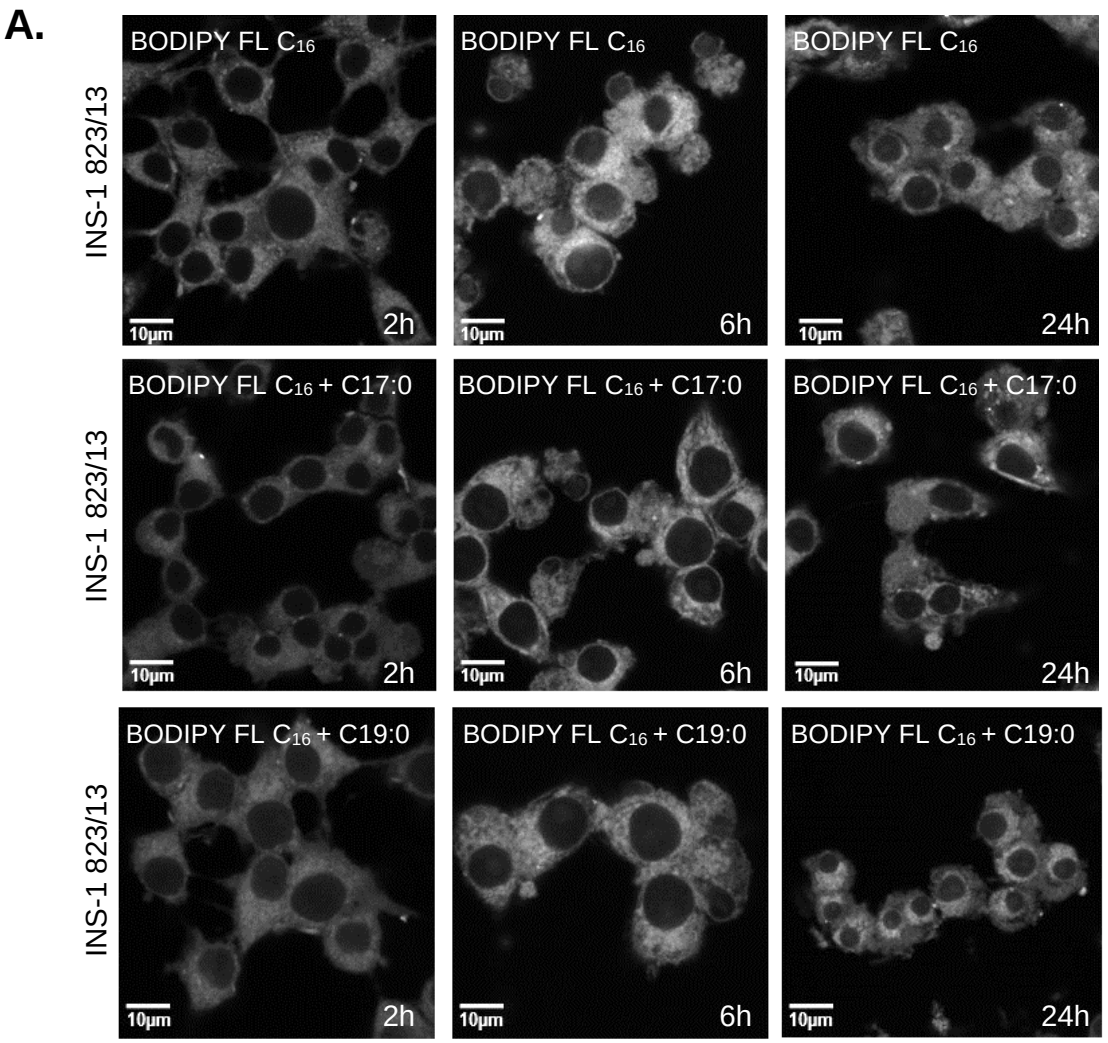

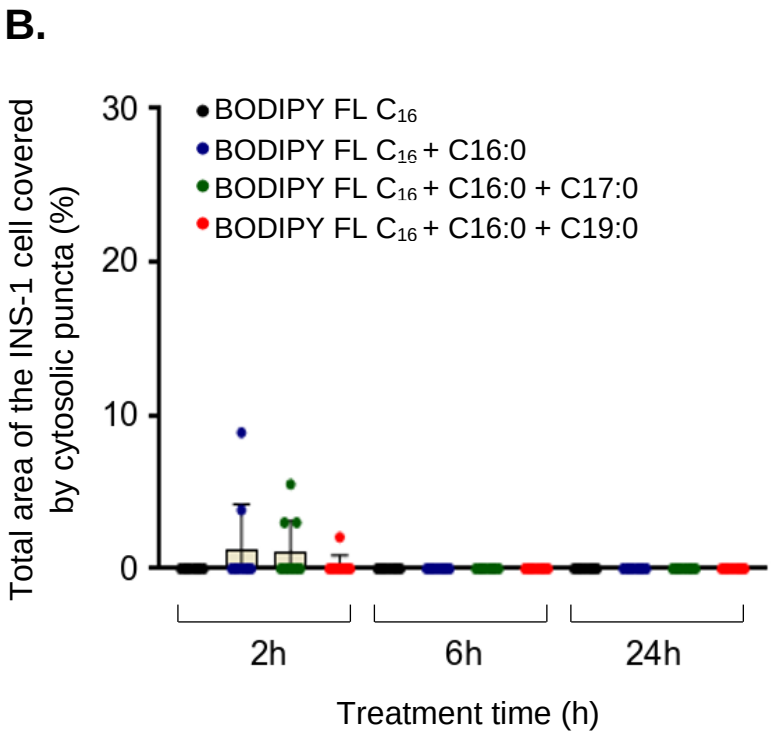

Figure 4.2: Intracellular distribution of BODIPY FL C_{16} in INS-1 cells after 2-24h exposure to BODIPY FL C_{16} in the presence of absence of C17:0 or C19:0. INS-1 cells were treated for 2, 6 and 24h with 400nM BODIPY FL C_{16} only, or 400nM BODIPY FL C_{16} and 500µM C16:0, or 400nM BODIPY FL C_{16} and 250µM C16:0 with either 250µM C17:0 or 250µM C19:0.

(A) INS-1 cells were treated for 2, 6 and 24h with BODIPY FL C_{16} in the presence or absence of C17:0 or C19:0. Images taken with a confocal microscope using an excitation/emission of 488/552nm. **(B)** Quantification of BODIPY FL C_{16}, cytosolic puncta in INS-1 cells. Confocal images were analysed using ImageJ/FIJI. Data points were cells from two separate experiments. Error bars represent the SEM.

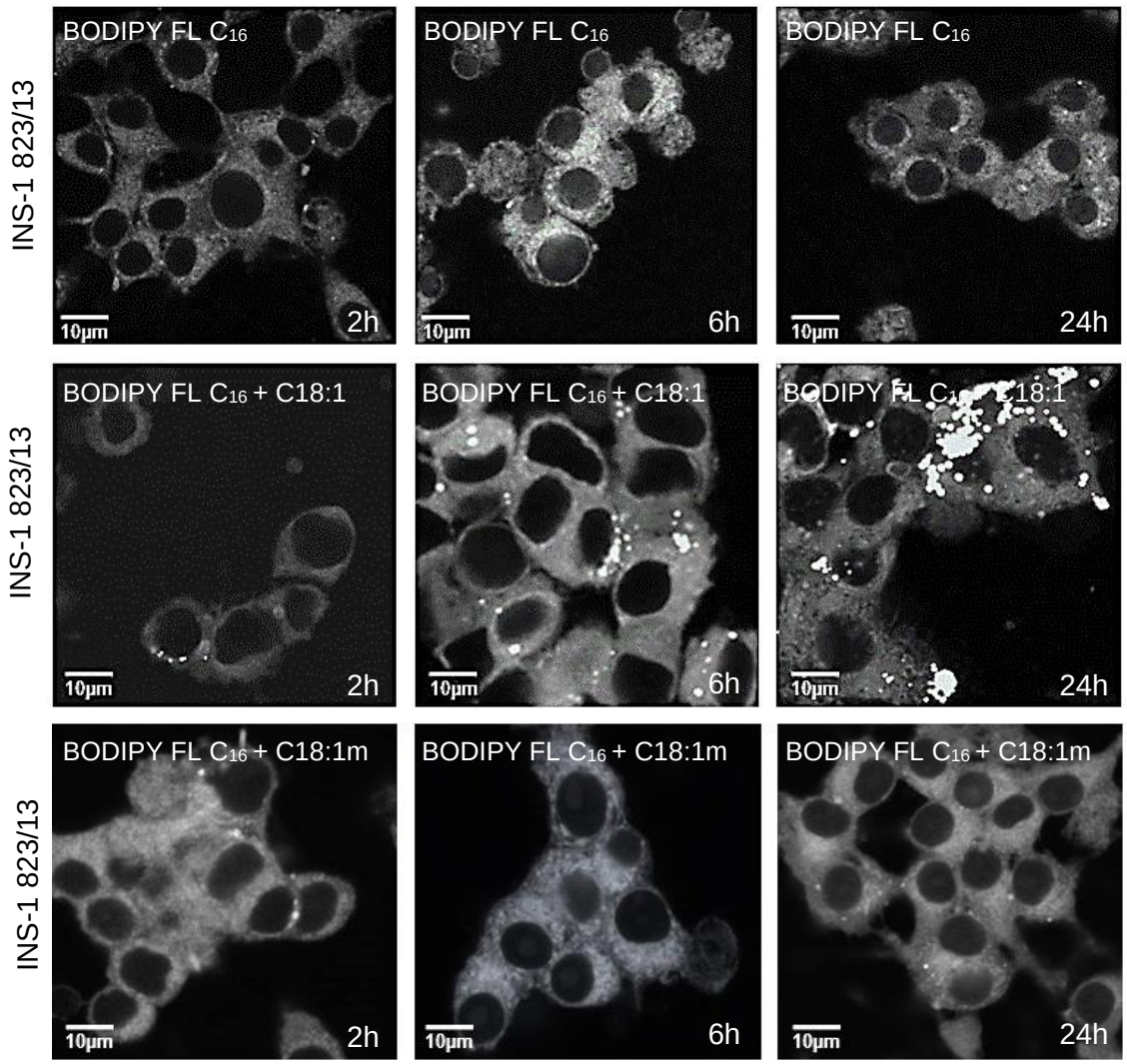

Figure 4.3: Intracellular distribution of BODIPY FL C_{16} in INS-1 823/13 cells after 2-24h exposure to BODIPY FL C_{16} in the presence or absence of C18:1 or the methyl ester of C18:1 (C18:1m). INS-1 823/13 cells were treated for 2, 6 and 24h with 400nM BODIPY FL C_{16} only, or 400nM BODIPY FL C_{16} with 500µM C16:0; or 400µM BODIPY FL C_{16} with 250µM C16:0 and either 250µM C18:1 or 250µM C18:1m.

(A) INS-1 823/13 cells treated for 2, 6 and 24h with BODIPY FL C_{16} in the presence or absence of C18:1 or C18:1m. Images taken with a confocal microscope using an excitation/emission of 488/552nm. INS-1 823/13 cells treated with C16:0+C18:1 for 2, 6 and 24h provided courtesy of Jenna Corcoran. **(B)** Quantification of BODIPY FL C_{16}, cytosolic puncta in INS-1 cells. Confocal images were analysed using ImageJ/FIJI. Data points were cells from three separate experiments. Error bars represent the SEM. ***p<0.001 relative to BODIPY FL C_{16}.

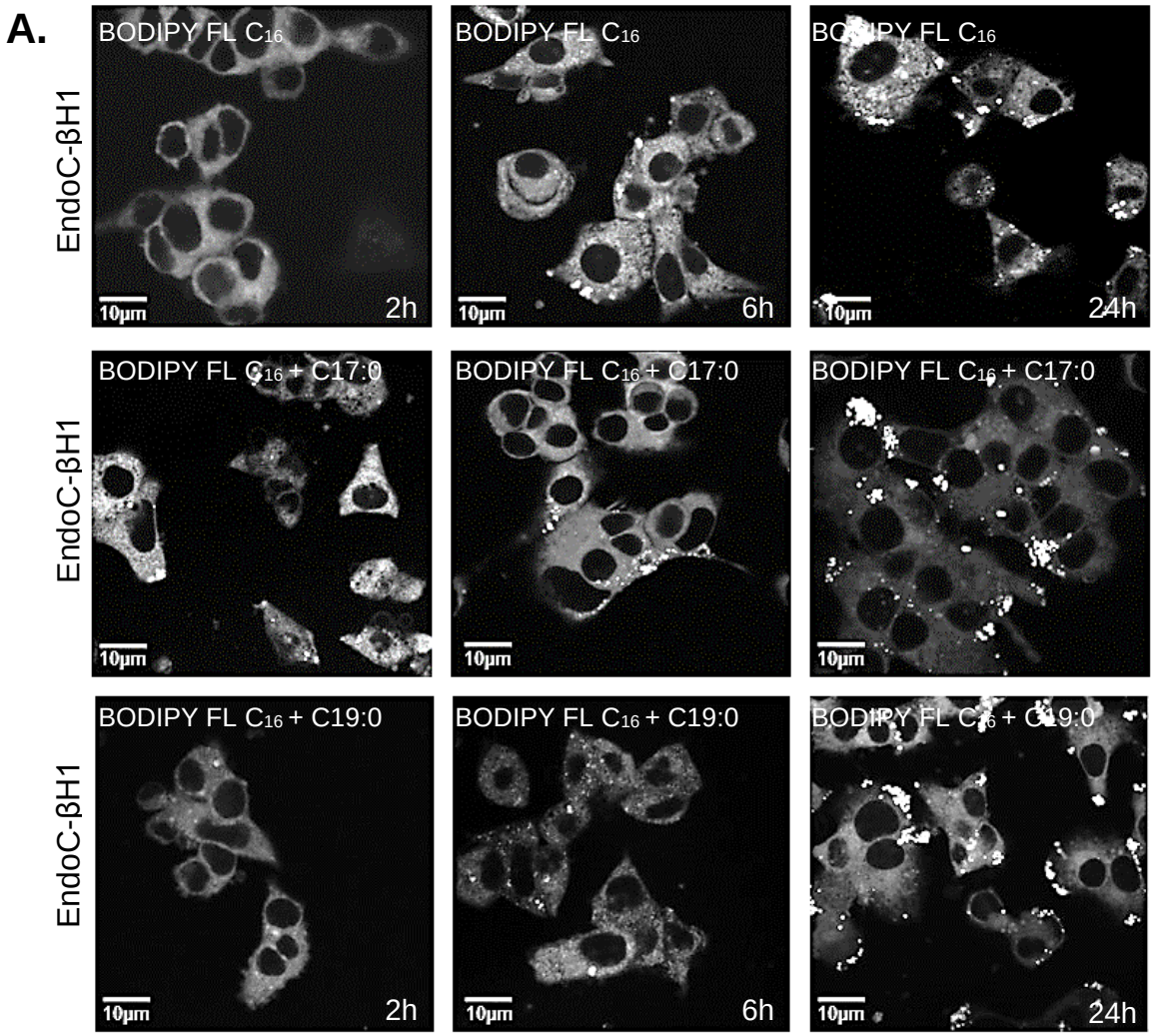

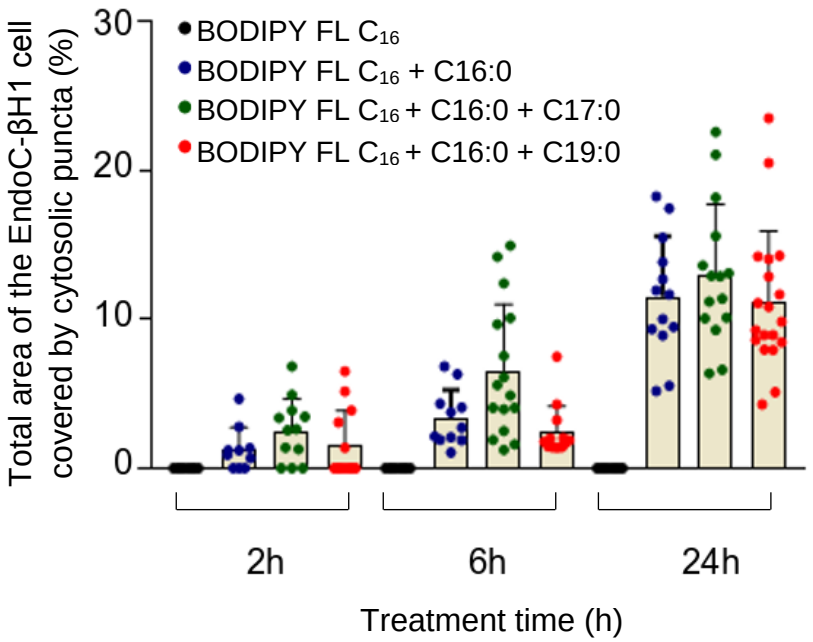

Figure 4.4: Intracellular distribution of BODIPY FL C_{16} in EndoC-βH1 cells after 2-24h exposure to BODIPY FL C_{16} in the presence of absence of C17:0 or C19:0. EndoC-βH1 cells were treated for 2, 6 and 24h with 400nM BODIPY FL C_{16} only, or 400nM BODIPY FL C_{16} with 500µM C16:0, or 400nM BODIPY FL C_{16} with 250µM C16:0 and either 250µM C17:0 or 250µM C19:0.

(A) EndoC-βH1 cells were treated for 2, 6 and 24h with BODIPY FL C_{16} in the presence or absence of C17:0 or C19:0. Images taken with a confocal microscope using an excitation/emission of 488/552nm. **(B)** Quantification of BODIPY FL C_{16}, cytosolic puncta in EndoC-βH1 cells. Confocal images were analysed using ImageJ/FIJI. Data points were cells from three separate experiments. Error bars represent the SEM.

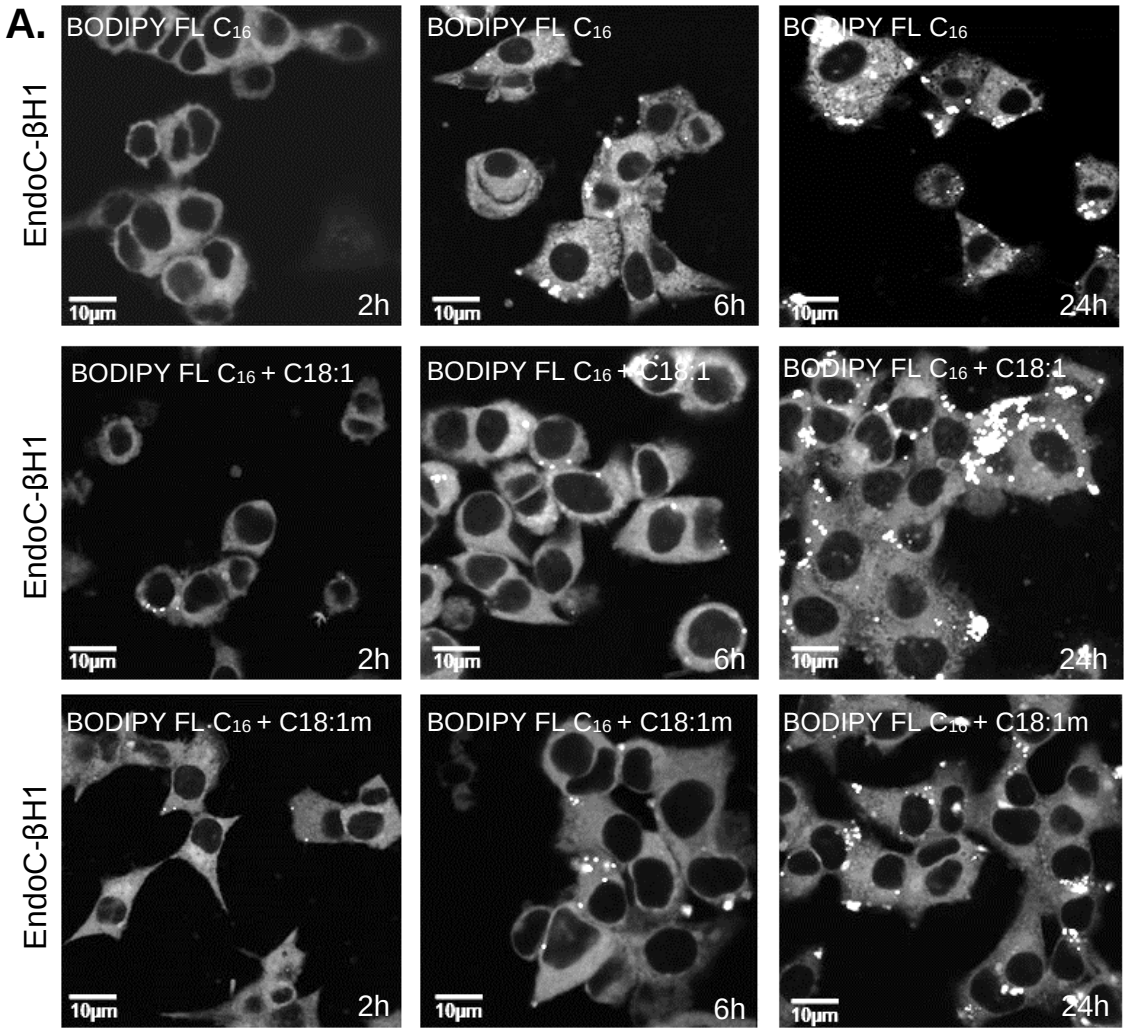

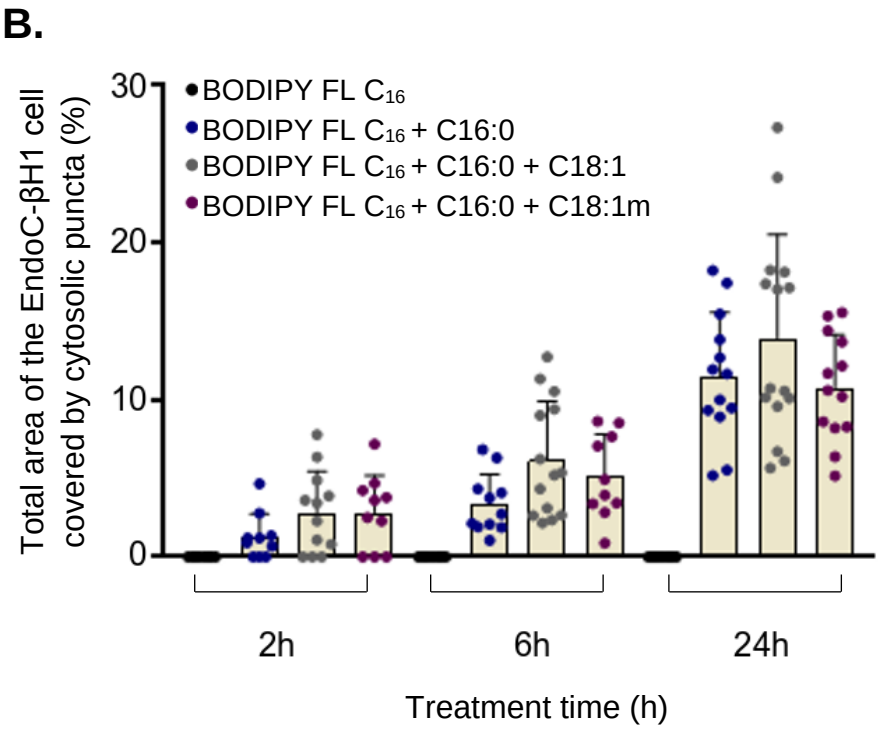

Figure 4.5: Intracellular distribution of BODIPY FL C_{16} in EndoC-βH1 cells after 2-24h exposure to BODIPY FL C_{16} in the presence of absence of C18:1 or the methyl ester of C18:1 (C18:1m). EndoC-βH1 cells were treated for 2, 6 and 24h with 400nM BODIPY FL C_{16} only, or 400nM BODIPY FL C_{16} with 500µM C16:0, or 400nM BODIPY FL C_{16} with 250µM C16:0 with either 250µM C18:1 or 250µM C18:1m.

(A) EndoC-βH1 cells were treated for 2, 6 and 24h with BODIPY FL C_{16} in the presence or absence of C18:1 or C18:1m. Images taken with a confocal microscope using an excitation/emission of 488/552nm. **(B)** Quantification of BODIPY FL C_{16}, cytosolic puncta in EndoC-βH1 cells. Confocal images were analysed using ImageJ/FIJI. Data points were cells from three separate experiments. Error bars represent the SEM. ***p<0.001 relative to BODIPY FL C_{16}.

4.3.2 Investigating LC-FFA distribution in human-derived β-cells using transmission electron microscopy (TEM)

Next, electron microscopy was employed to study the morphology of EndoC-βH1 cells and INS-1 823/13 cells after being exposed to LC-FFA (figure 4.6 and 4.7a). EndoC-βH1 and INS-1 823/13 cells were exposed for 6h to 250µM C16:0, 250µM C18:1, or 250µM C16:0 and 250µM C18:1 combined; and imaged using transmission electron microscopy (TEM).

Upon examination of the INS-1 823/13 cells, cellular organelles were visible in the cytoplasm whereas strikingly, in the cytoplasm of EndoC-βH1 cells, there were also numerous granular structures (figure 4.7b). Seemingly, the granular structures were present in the EndoC-βH1 cells to a greater extent compared to the INS-1 823/13 cells. The work of Anderson et al. (2015) has found that EndoC-βH1 cells contain 3-times more insulin granules than INS-1 823/13 cells. Considering the lack of cytosolic granules in INS-1 823/13 cells, and the presence of the granules in EndoC-βH1 cells treated with vehicle only, it was hypothesised that the cytosolic granules were, in fact, insulin secretory granules.

Electron microscopy-immunogold labelling for insulin and proinsulin was conducted in EndoC-βH1 cells for verification that the granules observed in the cytoplasm of EndoC-βH1 cells were indeed insulin secretory granules. EndoC-βH1 cells were treated for 6h with either 500µM C16:0 or vehicle only. Cells were then exposed to protein-A-gold labelled antibodies for either insulin or proinsulin and imaged with TEM (figure 4.8a). Proinsulin and insulin were shown to present in the cytosolic granules of EndoC-βH1 cells treated with both C16:0 and vehicle only. Isotype controls for proinsulin were also applied to EndoC-βH1 cells as a negative control to determine whether non-specific

binding had occurred. Electron-microscopy immunogold images of EndoC-βH1 cells treated with isotype controls showed that non-specific binding had not occurred in those cells probed with the isotype control antibody. To further verify the presence of insulin granule stores, and their distribution pattern within EndoC-βH1 after being treated with LC-FFA, cells were probed for insulin using immunocytochemistry. EndoC-βH1 cells were treated for 6h with either vehicle, 250µM C16:0, 250µM C18:1, or 250µM C16:0 and 250µM C18:1. Cells were then stained with an insulin antibody. Insulin was found to be distributed throughout the cytoplasm of EndoC-βH1 cells, and there was no observable difference in the presence or distribution patterns of insulin in EndoC-βH1 cells treated with either vehicle or LC-FFA (figure 4.8b). Collectively, this indicates that the granular structures observed in the cytoplasm of EndoC-βH1 cells after 6h treatment with vehicle or LC-FFA are insulin secretory granules.

Upon further examination of the morphology of INS-1 823/13 cells, it was observed that the Golgi apparatus appeared swollen after the rodent-derived β-cells had been treated for 6h with C16:0 (figure 4.9; appendix 2). Conversely, when INS-1 823/13 cells were treated with C16:0 in the presence of C18:1, the Golgi apparatus was not swollen (figure 4.9). Moreover, there was only a moderate swelling of the Golgi apparatus of EndoC-βH1 cells treated for 6h with C16:0 (figure 4.10). This implies that C16:0 is being trafficked to the Golgi apparatus in INS-1 823/13 cells to a greater extent relative to EndoC-βH1 cells. To verify these morphological observations, the Golgi apparatus of INS-1E and EndoC-βH1 cells were labelled with the red fluorescent marker, Golgi-RFP, to assess whether BODIPY FL C_{16} co-localised to the Golgi, BODIPY FL C_{16} co-localised with Golgi-RFP in INS-1E cells but not in EndoC-βH1 cells (figure 4.11 and figure 4.12). An intensity correlation analysis (Schindelin et al. 2012) was conducted to quantify the colocalisation of BODIPY FL C_{16} and Golgi-RFP

within these images (figure 4.11b and figure 4.12b). There was found to be a greater positive correlation for BODIPY FL C_{16} co-localising with Golgi-RFP in INS-1E (Pearson's correlation: 0.61) compared to EndoC-BH1 cells (Pearson's correlation: 0.25). Collectively, this implies that C16:0 becomes concentrated in the Golgi apparatus in rodent-derived, but not in human-derived β-cells.

A further observation in INS-1 823/13 cells treated with 250μM C16:0 for 6h and imaged with TEM was that the cells were torn in the region of the cell which corresponded with the endoplasmic reticulum (ER) (figure 4.13; appendix 3). This observation was interpreted as dilation of the ER as the same alterations in ER morphology have been observed previously by Diakogiannaki et al. 2008 who reported C16:0 to dilate the ER membrane and activate the ER stress response pathway of BRIN-BD11 cells treated with C16:0. Tears in the region of the ER in INS-1 823/13 cells treated with C16:0 were not observed when cells were treated with C16:0 in the presence of C18:1. Moreover, no observable changes in morphology were noted in the ER of EndoC-βH1 cells treated with 500μM C16:0 (figure 4.14). Further, using Western blotting with densitometry, C16:0 was shown to cause a 5-fold increase in the phosphorylation of the ER stress marker eIF2α in INS-1E cells (figure 4.14b). The increase in eIF2α stimulated by C16:0 was similar to that of tunicamycin, a known inducer of ER stress (Guha et al. 2017), which also caused a 6-fold increase in the phosphorylation of eIF2α (figure 4.14b). This indicates that in rodent-derived β-cells C16:0 causes ER stress to occur. As no changes to ER morphology were observed in EndoC-βH1 cells, it could be assumed that C16:0 does not have the same deleterious effects to the ER in the human-derived β-cell line.

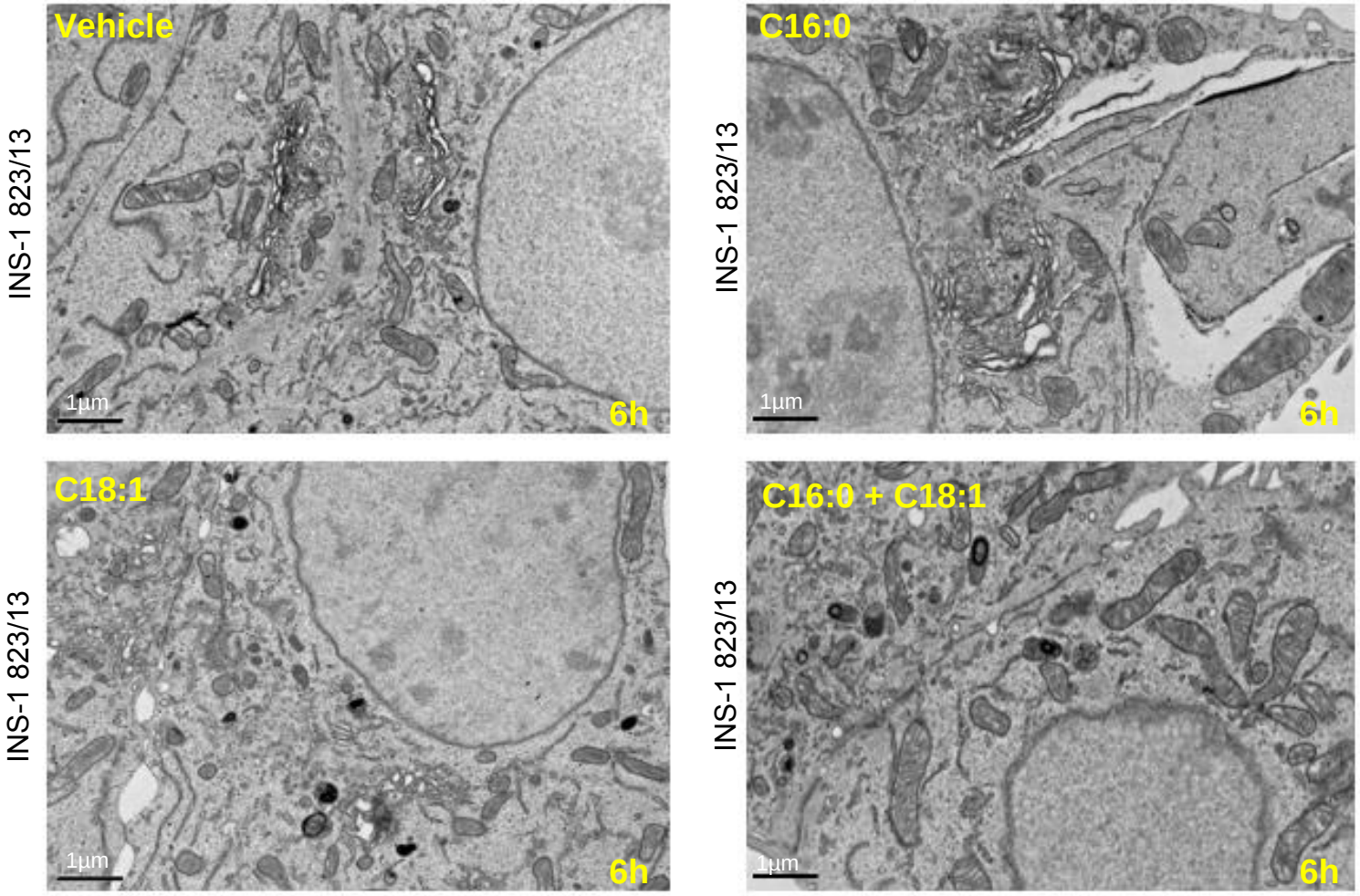

Figure 4.6 INS-1 cell structure as visualised by transmission electron microscopy (TEM). INS-1 cells were treated for 6hrs with 250µM C16:0 or 250µM C18:1 or 250µM C16:0 with 250µM C18:1. Control cells were treated with BSA vehicle only. INS-1 cells were then fixed in an osmium tetroxide fixative before being imaged with TEM. Scale bar represents 1µm.

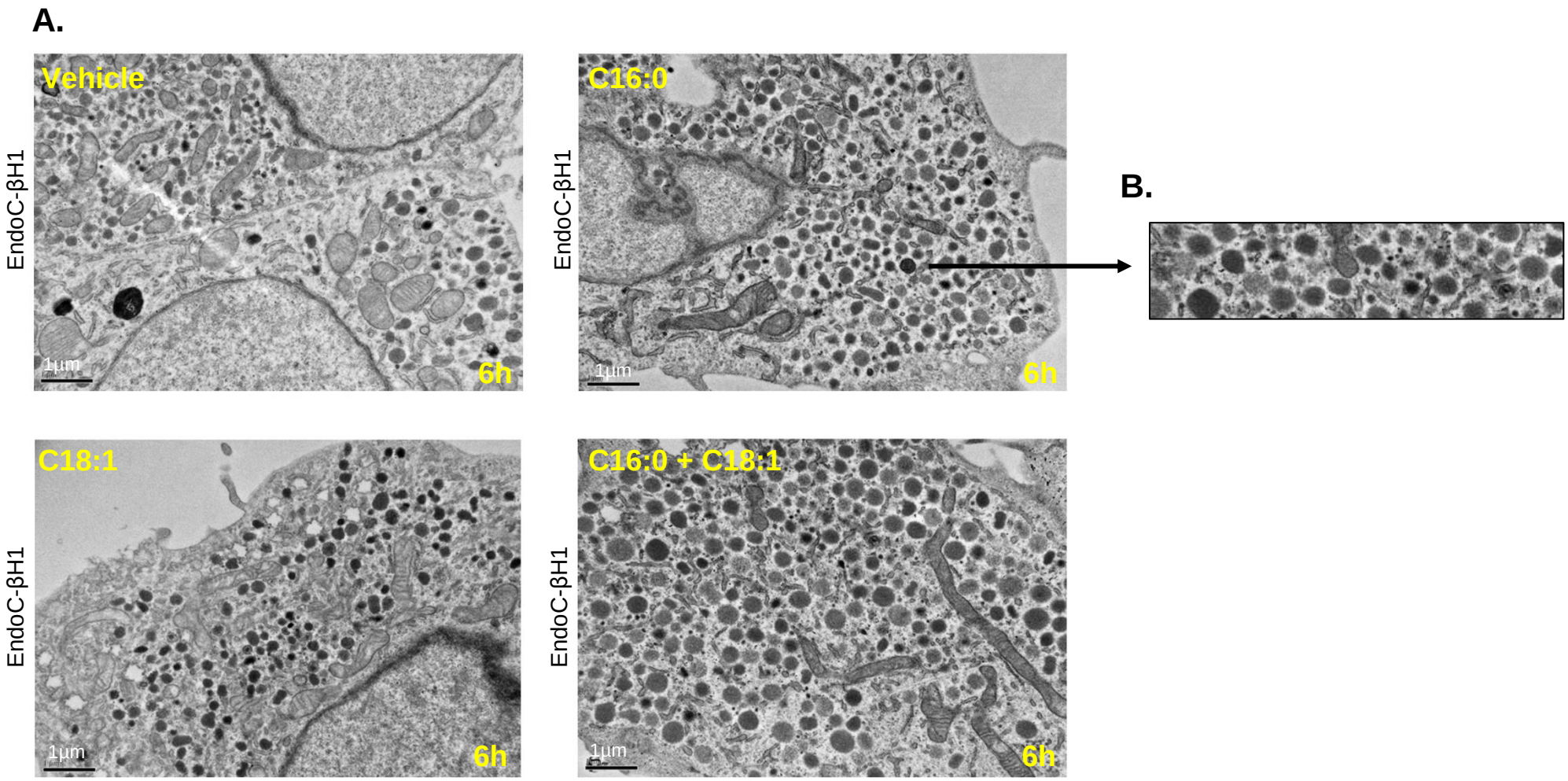

Figure 4.7 EndoC-βH1 cell structure as visualised by transmission electron microscopy (TEM). EndoC-βH1 cells were treated for 6hrs with 250µM C16:0, 250µM C18:1 or 250µM C16:0 with 250µM C18:1. Control cells were treated with BSA vehicle only. EndoC-βH1 cells were then fixed in an osmium tetroxide fixative before being imaged with TEM. Scale represents 1µm.

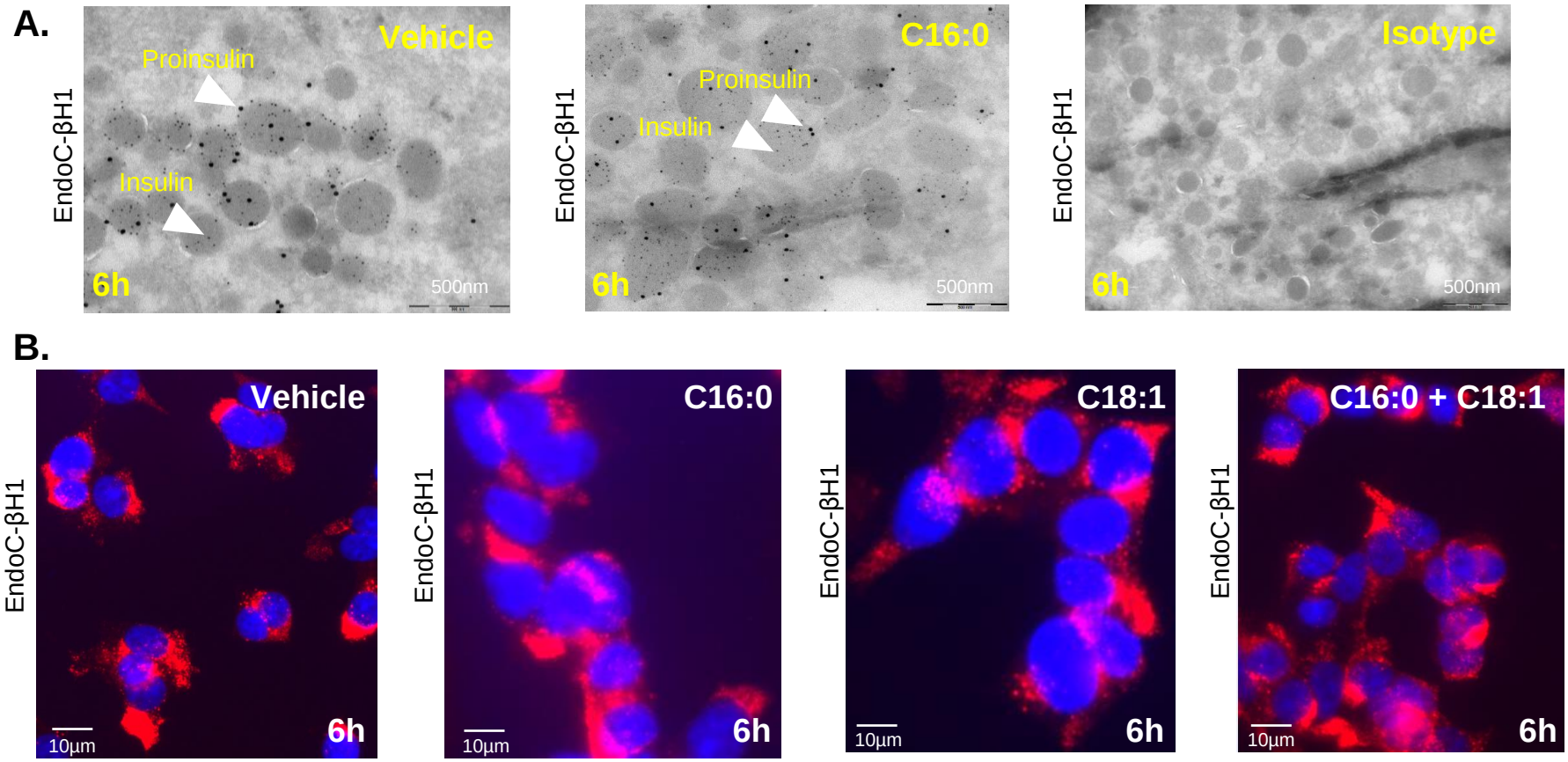

Figure 4.8 EndoC-βH1 cells are positive for insulin and proinsulin. (A) EndoC-βH1 cells were treated for 6hrs with vehicle only, 500µM C16:0 or isotype control. Insulin and proinsulin primary antibodies were then applied to cells. A 5nm protein A-gold labelled antibody was bound to the insulin antibody whereas a 20nm protein A-gold labelled antibody was bound the proinsulin antibody with the aid of a bridging antibody for stability. Cells were then imaged with electron microscopy to localise proinsulin and insulin. **(B)** EndoC-βH1 cells were treated for 6h with 500µM C16:0, 500µM C18:1 or 250µM C16:0 with 250µM C18:1 (final concentration 500µM). Control cells were treated with BSA vehicle only. Cells were then immunolabelled using an anti-insulin antibody (shown in red). The nuclei of EndoC-βH1 cells were counterstained with DAPI (shown in blue). Cells were then imaged using a fluorescent microscope.

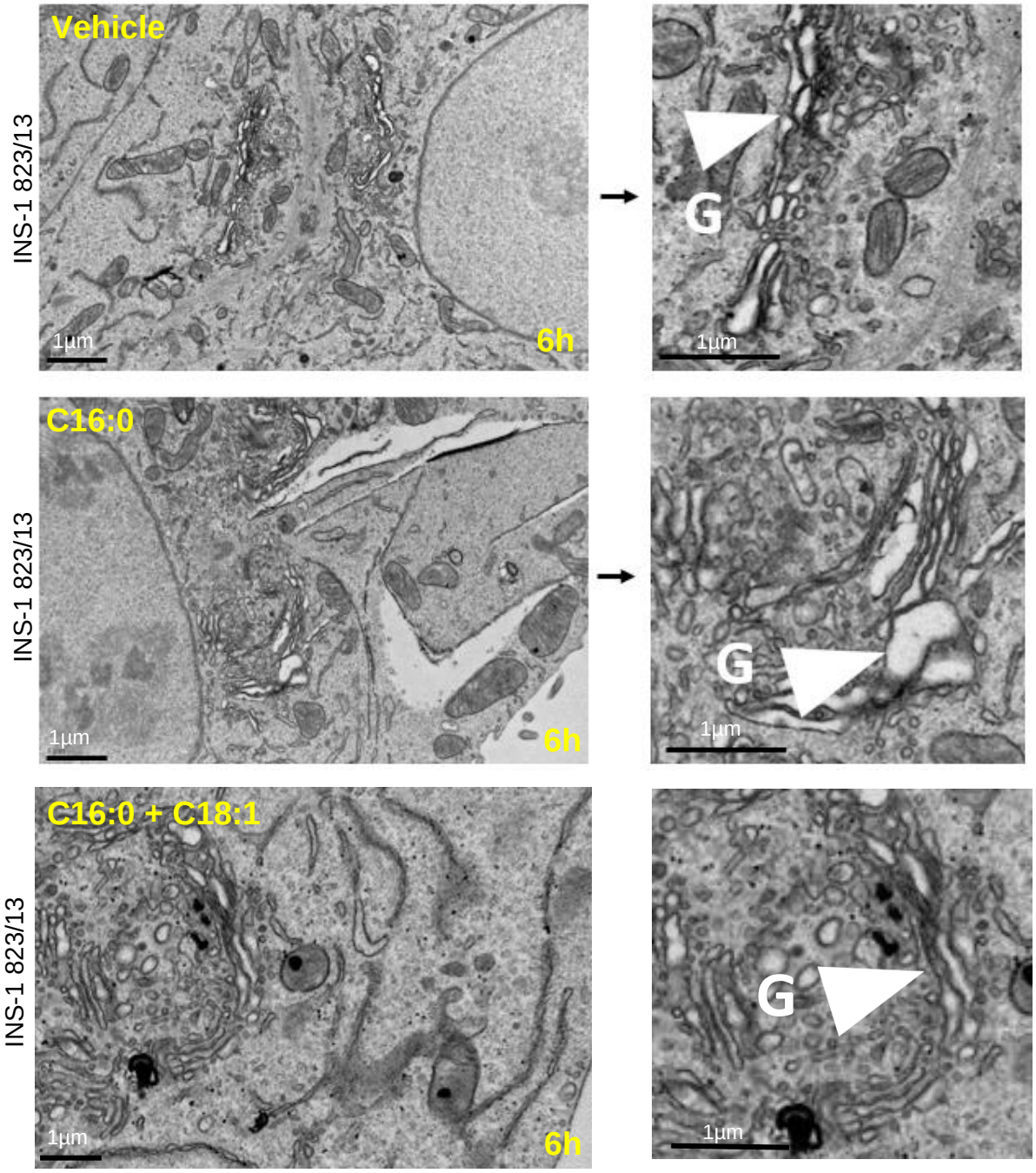

Figure 4.9 C16:0 causes the Golgi (G) apparatus to become swollen in INS-1 823/13 cells as visualised by TEM. INS-1 823/13 cells were treated for 6hrs with 250µM C16:0 or 250µM C16:0 combined with 250µM C18:1. Control cells were treated with BSA vehicle only. INS-1 823/13 cells were then fixed in an osmium tetroxide fixative before being imaged with TEM. Scale represents 1µm.

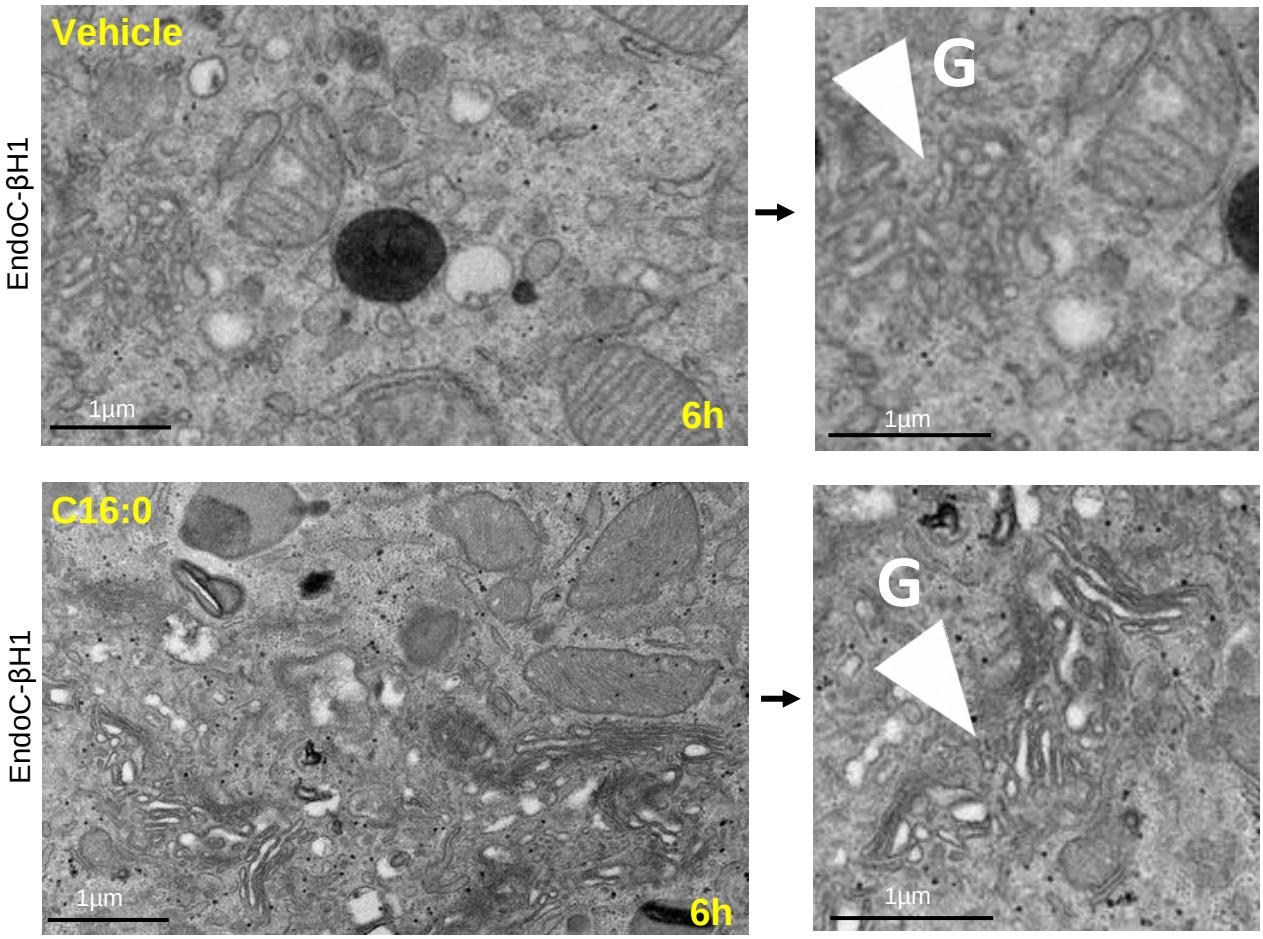

Figure 4.10 C16:0 does not cause the Golgi (G) apparatus to become swollen in EndoC-βH1 cells as visualised by TEM. EndoC-βH1 cells were treated for 6hrs with 250µM C16:0. Control cells were treated with BSA vehicle only. EndoC-βH1 cells were then fixed in an osmium tetroxide fixative before being imaged with TEM. Scale represents 1µm.

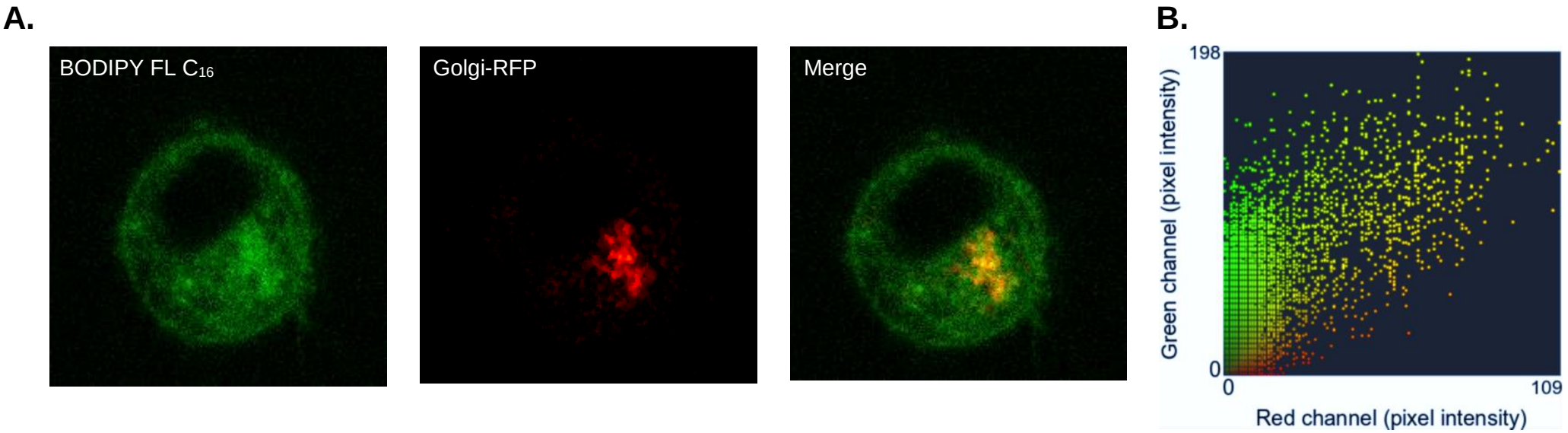

Figure 4.11 Colocalisation of BODIPY FL C_{16} with the Golgi apparatus in INS-1E cells. (A) INS-1E cells were incubated with 250μM C16:0 plus 400nM BODIPY FL and 50ppc (define ppc) Golgi-RFP for 24hr. Golgi-RFP was added 24 hours prior to BODIPY FL C_{16}. Confocal microscopy used an excitation/emission of 555/584nm for the red channel and of 488/552nm for the green. **(B)** ImageJ/FIJI intensity correlation analysis showed that when plotted against each other, the green and red pixels overlap in INS-1E cell images, with a Pearson correlation coefficient of 0.61 for C16:0: Golgi colocalisation.

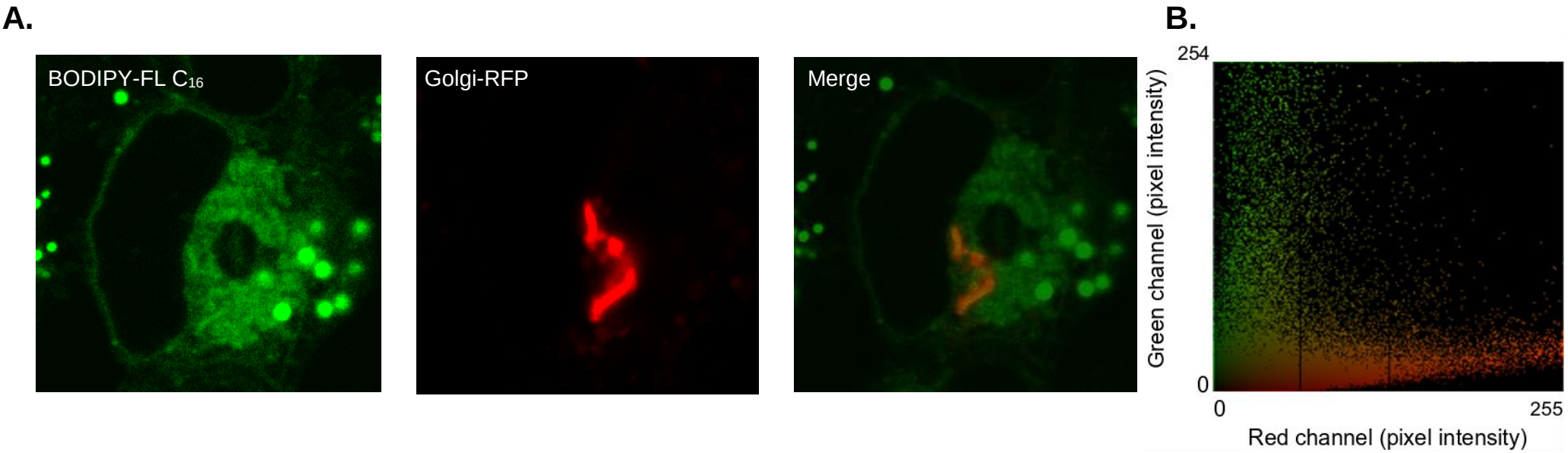

Figure 4.12 BODIPY FL C_{16} does not colocalise with the Golgi apparatus EndoC-βH1 cells. (A) EndoC-βH1 cells were incubated with 250μM C16:0 plus 400nM BODIPY FL C_{16} and 50ppc Golgi-RFP for 24hr. Golgi-RFP was added 24 hours prior to C16:0 and BODIPY FL C_{16}. Confocal microscopy used an excitation/emission of 555/584nm. **(B)** ImageJ/FIJI intensity correlation analysis showed that when plotted against each other, the green and red pixels overlap in EndoC-βH1 cell images, with a Pearson correlation coefficient of 0.25 for C16:0: Golgi colocalisation.

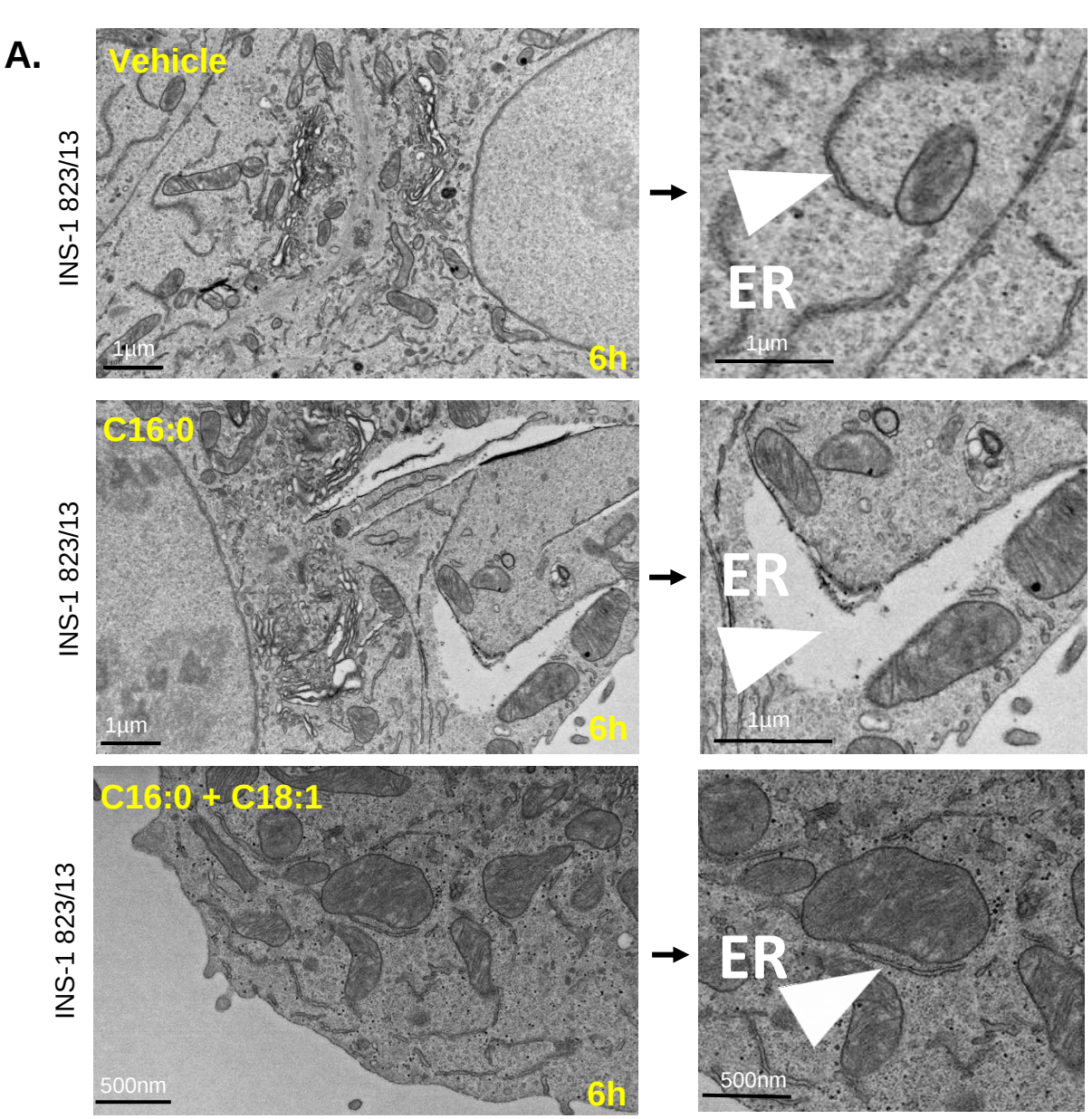

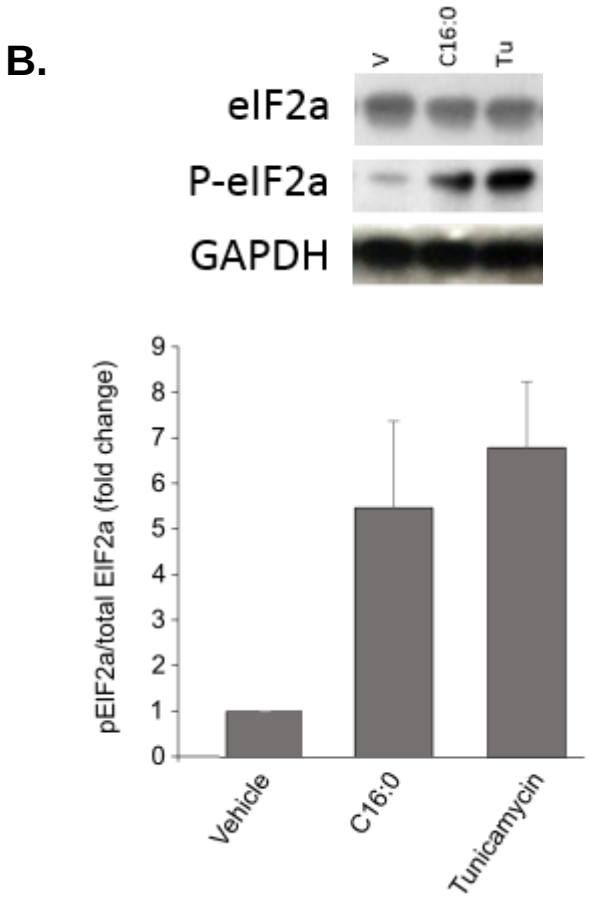

Figure 4.13 C16:0 dilates the ER membrane and EIF2α is phosphorylated in INS-1 823/13 cells. (A) INS-1 823/13 cells were treated for 6hrs with 250µM C16:0 or C16:0 with C18:1 (500µM total concentration). Control cells were treated with BSA vehicle only. INS-1 823/13 cells were then fixed in an osmium tetroxide fixative before being imaged with TEM. Scale represents 1µm.

(B) INS-1E cells were incubated with 250µM C16:0 for 16hr. Protein extracts were probed with an antiserum to phosphorylated EIF2α (pEIF2α) or total EIF2α. Glyceraldehyde 3-phosphate dehydrogenase (GAPDH) was used as a loading control and the bands were quantified by densitometry. Tunicamysin = 1µg/ml. Western blot courtesy of Catherine Arden, Newcastle University.

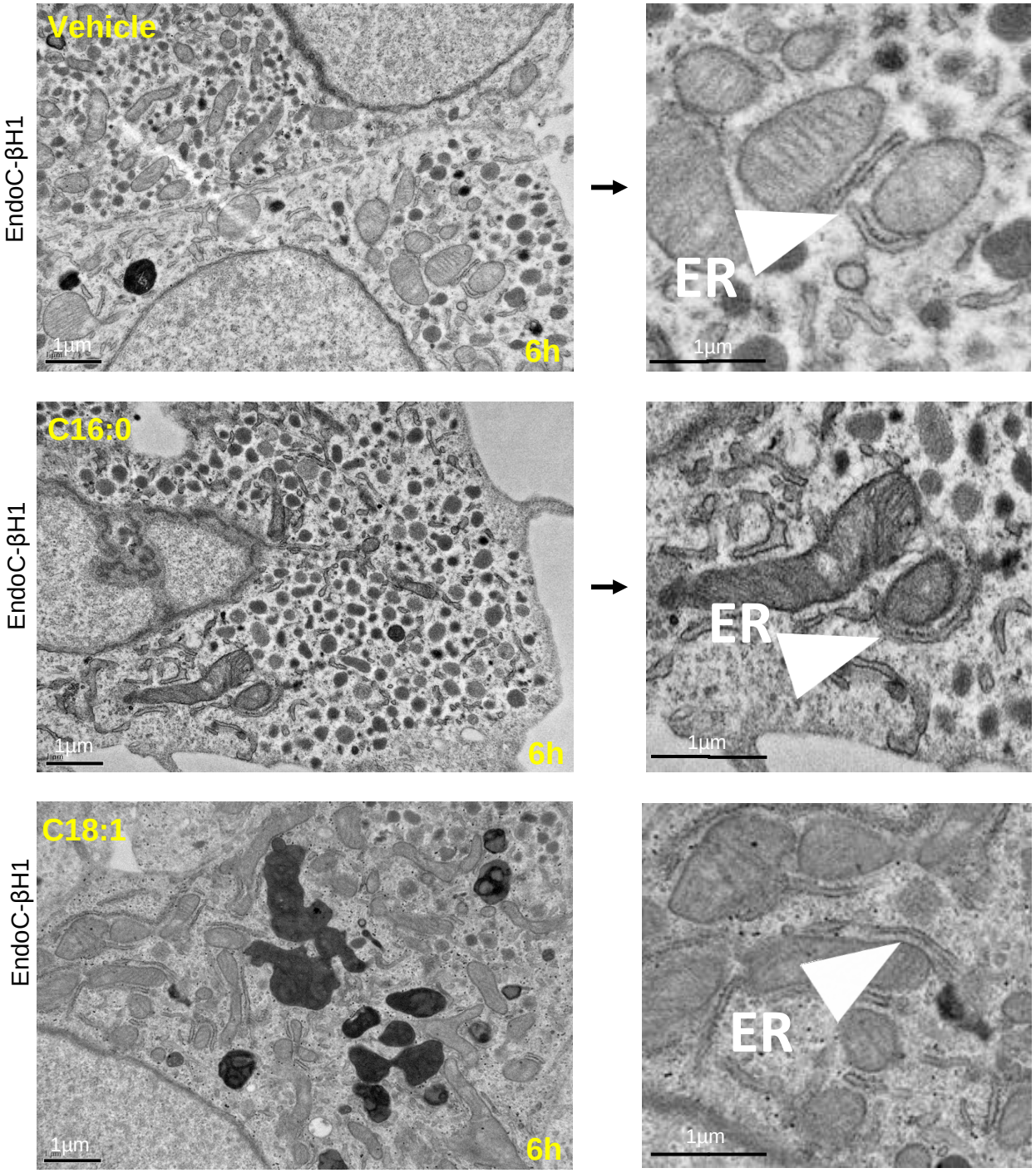

Figure 4.14 C16:0 does not dilate the ER membrane in EndoC-βH1 cells. EndoC-βH1 cells were treated for 6hrs with 250µM C16:0 or 250µM C18:1. Control cells were treated with BSA vehicle only. EndoC-βH1 cells were then fixed in an osmium tetroxide fixative before being imaged with TEM. Scale represents 1µm.

In summary, within rodent β-cells, C16:0 accumulates in the Golgi apparatus and seemingly causes dilation of the ER membrane. Conversely, in human β-cells, C16:0 does not become concentrated at the Golgi and does not cause alterations to ER morphology.

4.4 Discussion

In this chapter, the distribution and changes to β-cell morphology induced by C16:0 were investigated. It was also determined whether the distribution and changes in β-cell morphology induced by C16:0 were altered in the presence of other LC-FFA. Moreover, investigations were conducted in both rodent- and human-derived β-cells to determine if there were interspecies differences in the way β-cells distribute LC-FFA within the cell.

4.4.1 C16:0 cytosolic distribution in rodent- and human-derived β-cells

It was observed that C16:0 accumulates in the cytoplasm of human but not rodent-derived β-cells after 2-24h. Throughout this study, the accumulation of C16:0 is referred to as cytosolic puncta as the presence of the BODIPY FL C_{16} tracer within the C16:0 accumulated within the cytoplasm has a puncta-like appearance. In EndoC-βH1 cells, C17:0, C19:0, C18:1 and the methyl ester of C18:1 did not alter the cytosolic distribution of C16:0 or the total area of the cell covered by cytosolic puncta.

This is seemingly the first study to report the cytosolic distribution of C16:0 in EndoC-βH1 cells. This study is not, however, the first to show the cytosolic distribution of C16:0 in rodent-derived β-cells. Using the lipophilic stain, Nile Red, Vernier and colleagues (2012) reported lipid droplet formation in rat β-cells treated with C16:0 in combination with C18:1, and these steadily increased in number over 4 days. Further, Plotz et al. (2016) analysed lipid droplet formation in rodent-derived β-cells (RIN-m5F)

using the lipid stain Oil Red O coupled with Western blotting for the lipid droplet specific proteins, perilipin 1 and 2. Plotz et al. (2016) reported that lipid droplets form in RIN-m5F cells treated for <24h with C16:0 and C18:1, but not in those cells treated with C16:0 only. This correlates with our observations whereby cytosolic puncta formed in INS-1 823/13 cells when treated with both C16:0 and C18:1, but not when exposed to C16:0 only. However, contrary to Vernier et al. (2012) and Plotz et al. (2016) the work detailed in the results of this study is yet to verify whether the cytosolic puncta observed in either the INS-1 823/13 or EndoC-βH1 cells are lipid droplets.

Previously BODIPY dyes have been named in certain methodological reviews (Listenberger et al. 2016; Elle et al. 2010) as a valid method for the visualisation of lipid droplets. However, fatty acids may be present in the cytoplasm in more organelles than just lipid droplets. For example, lipid droplets can be sequestered by autophagosomes so that lipids can be degraded within lysosomes and the fatty acids recycled (Singh et al. 2009). Further, fatty acids can be transported in early endosomes as part of membrane trafficking pathways (Liu et al. 2007). Therefore, it is not clear whether BODIPY FL C_{16} in the cytoplasm of EndoC-βH1 cells (and INS-1 cells treated with both C16:0 and C18:1) is contained within lipid droplets or an alternative cytosolic vesicle. Further work is, therefore, necessary to characterise the mode of BODIPY FL C_{16} cytoplasmic accumulation in EndoC-βH1 cells.

4.4.2 Investigating LC-FFA distribution in rodent- and human-derived β-cells

The apparent dilation of the ER in INS-1 823/13 cells treated with C16:0 supports previous observations whereby BRIN-BD11 showed structural changes to the ER when exposed to C16:0 for 18h (Diakogiannaki et al. 2008). However, structural changes in the β-cells were examined when cells had been acutely exposed (6h) to

LC-FFA rather than after a prolonged exposure (>18h), indicating that the dilation of the ER occurs rapidly. Similar to our observation in INS-1 823/13 cells, Karaskov et al. (2006) found dilation of the ER in INS-1E cells exposed to 1mM C16:0 for as little as 30min. Laybutt et al. (2007), Kharroubi et al. (2004) and Baldwin et al. (2012) also report a significant upregulation in genes associated with ER-stress in rodent-derived β-cells treated with C16:0 for a time period of ≤6h. Collectively, this suggests that the structure and function of the ER are altered with both acute (<6h) and prolonged (≥18h) exposure to C16:0 in rodent-derived β-cells. This indicates that alterations to the ER may play a role in the induction of LC-SFA induced β-cell death in rodent models.

Interestingly, no alteration in ER morphology was observed when INS-1 823/13 cells were co-treated with C16:0 and C18:1 for 6h. This coincides with Diakogiannaki et al. (2008) whereby alterations to the ER morphology were also not observed in BRIN-BD11 cells exposed for 18h to both C16:0 and C16:1 combined (Diakogiannaki et al. 2008). This implies that the structure of the ER remains unaltered when rodent-derived β-cells are treated for ≤18h with C16:0 in combination with an LC-MUFA. Further, Sommerweiss et al. (2013) observed no increase in mRNA or protein expression of ER stress markers in INS-1E cells treated with C16:0 in combination with C18:1 at 1h, 6h or 24h; relative to control. Conversely, Cunha et al. (2008) reported a 2-2.5 fold increase in the expression of the chaperone protein, BiP, in INS-1E cells treated with C16:0 only or C16:0 combined with C18:1, indicating the activation of the ER stress response. However, Cunha et al. (2008) also reported no increase in the expression of those genes associated with PERK pathway, and only a moderate increase in genes associated with the IRE1 pathway, in INS-1E cells treated with both C16:0 and C18:1

for 6-24h. Collectively, this indicates that the ER stress response induced by C16:0 in rodent-derived β-cells is counteracted by C18:1.

This study is the first to report that LC-FFAs do not induce ER morphological changes in EndoC-βH1 cells. Similarly, in β-cell populations (MIN6 cells) resistant to the toxic effects of C16:0 it has been reported that genes associated with ER stress are not upregulated upon chronic exposure to C16:0 (Laybutt et al. 2007; Busch et al. 2005). Interestingly, Oleson et al. (2015) failed to activate ER stress in EndoC-βH1 cells using thapsigargin, a well-known activator of ER stress which acts to deplete ER Ca^{2+} stores. Oleson et al. (2015) reported EndoC-βH1 cells to have a dysfunctional ER stress response due to having high concentrations of basal Hsp70 (i.e. in the absence of cell stressors). In the same study, INS-1 823/13 cells were found not to have high concentrations of basal Hsp70, with thapsigargin inducing an ER stress response in as little as 6h (Oleson et al. 2015). Collectively, this indicates that, unlike rodent-derived β-cells, EndoC-βH1 cells may be resistant to the toxic effects of LC-SFA through a failure of LC-SFA to stimulate ER stress due to high levels of Hsp70. Future experiments could aim to knock out Hsp70 in EndoC-βH1 cells to determine if C16:0 is then toxic.

Along with dilation of the ER membrane, the Golgi apparatus was also found to be swollen in INS-1 823/13 cells treated with C16:0 for 6h. Moreover, C16:0 was found to localise to the Golgi in INS-1E cells after a 24h treatment period. These results correspond with Karaskov et al. (2006) who reported an alteration in Golgi morphology in INS-1 cells treated for 30min with 1mM C16:0. Seemingly, however, the results detailed in this chapter are the first to observe that C16:0 truly accumulates at the Golgi, ultimately altering the organelle's morphology.

Intracellular fatty acid trafficking is not well studied. However, it is thought that in fed states, intracellular fatty acids are stored in lipid droplets thus supporting the observations of this study. Conversely, in starvation, fatty acids are believed to be mobilised to the mitochondria for oxidation or alternatively, incorporated into the autophagy pathway to replenish lipid droplet stores (Rambold et al. 2015). Moreover, fatty acids and their derivatives (for example ceramide) are known to be trafficked from the ER to the Golgi for the synthesis of membrane phospholipids (as reviewed in Fagone et al. 2009). Subsequently, it was surprising to observe that C16:0 accumulates at the Golgi in rodent-derived β-cells as detailed in the results section of this study. It suggests that C16:0 is being routed via the Golgi in rodent-derived β-cells which is most likely a consequence of ER stress. This coincides with the work of Phelps et al. (2016) who reported C16:0 to accumulate at the Golgi in the form of palmitoylated glutamate decarboxylase 65 (GAD65). GAD65 is a peripheral membrane protein which undergoes a cycle of palmitoylation to control its endomembrane distribution. Upon inducing ER stress using thapsigargin or C16:0, the palmitoylation cycle of GAD65 is disrupted resulting in its Golgi accumulation (Phelps et al. 2016). Potentially, the observation that C16:0 localises to the Golgi (figure 4.9 and 4.11) may be palmitoylated GAD65 and thus requires further investigation. For example, using immunocytochemistry and confocal microscopy it could be determined if GAD65 localises to the Golgi apparatus.

4.4.4 Summary

In summary, C16:0 accumulates in the cytoplasm of human-derived β-cells and its cytosolic distribution is not altered by the presence of other LC-FFA. Conversely, C16:0 does not accumulate in the cytoplasm of rodent-derived β-cells unless C18:1 is present then, like human-derived β-cells, it accumulates within the cytoplasm.

Moreover, within rodent β-cells, C16:0 accumulates in the Golgi apparatus and seemingly causes dilation of the ER. Conversely, in human β-cells, C16:0 does not become concentrated at the Golgi and does not cause the ER to dilate.

Chapter 5.

Measuring the mitochondrial bioenergetics profile of β-cells using the Seahorse Extracellular Flux assay

5.1 Introduction

Since its introduction in 2006, the Seahorse Extracellular Flux Analyser (EFA) has been used in >2500 peer-reviewed publications. It is classed as the current gold standard for determining metabolic function in the fields of drug toxicology, biochemistry and genetics. The Seahorse EFA uses a respirometry assay and operates using a two sensor probe system, which simultaneously measures the extracellular acidification rate (ECAR) and oxygen consumption rate (OCR) of live cells. The OCR and ECAR of cells are measured; allowing the impact of nutrients and metabolic inhibitors on these parameters to be measured in real time. The output of the Seahorse EFA is a trace, giving a reading of OCR or ECAR every 3-7mins, to determine the bioenergetic profile of cells (van der Windt et al. 2016).

In the Seahorse EFA, the OCR is a measure of mitochondrial respiration; the amount of O_2 consumed by the cells is recorded and used as an indicator of oxidative phosphorylation, the primary use of O_2 in cells (figure 2.5) (Gerencser et al. 2009). The ECAR is determined by recording pH changes of the extracellular medium. ECAR can be used as a measure of anaerobic glycolysis as the extracellular medium is acidified predominantly from the release of lactic acid derived from the regeneration of NAD^+ in the glycolytic pathway (TeSlaa & Teitell, 2014). However, a limitation of using the Seahorse EFA for investigating the bioenergetics of β-cells is that any rise in ECAR is unlikely to be derived from glycolysis. Pancreatic β-cells express low levels of lactate dehydrogenase, the enzyme which catalyses the conversion of pyruvate (the end product of glycolysis) to lactate, and they lack monocarboxylate transporters which export lactate across the plasma membrane (Zhao et al. 2001). Subsequently, acidification of the extracellular medium is unlikely to be due to β-cells exporting

lactate. However, a rise in ECAR in β-cells is regularly observed when using the Seahorse EFA technology (figure 5.1). ECAR rises following the injection of glucose, decreases upon the injection of oligomycin, which inhibits ATP synthase, and decreases further with rotenone/antimycin mix, which inhibits complex I and complex III of the electron transport chain (van der Windt, 2016). In β-cells, it is likely that the rise in ECAR is a bi-product of mitochondrial respiration of glucose. To facilitate postprandial glucose-stimulated insulin secretion (GSIS), β-cells express low levels of lactate dehydrogenase *and* high levels of pyruvate carboxylase and pyruvate dehydrogenase, driving pyruvate into mitochondrial metabolic pathways (Khan, 1996; Schuit, 1997). Consequently, the TCA cycle generates large quantities of CO_2 as a byproduct of glucose (and FFA) oxidation which contributes towards a rise in ECAR by a reversible reaction, whereby CO_2 is hydrated to H_2CO_3, which then dissociates to $HCO_3^- + H^+$ (Mookerjee, 2015):

$$H_2O+CO_2 \leftrightarrow H_2CO_3 \leftrightarrow HCO_3^- + H^+$$

In the past, the contribution of mitochondrial CO_2 to extracellular acidification has been overlooked in the Seahorse EFA literature (e.g. Cen et al. 2016). It is now however becoming common practice to omit ECAR data in studies using the Seahorse EFA to investigate the bioenergetics of β-cells (Andersson et al. 2015; Barlow et al. 2016). For this reason, this study only reports and discusses the OCR of pancreatic β-cells.

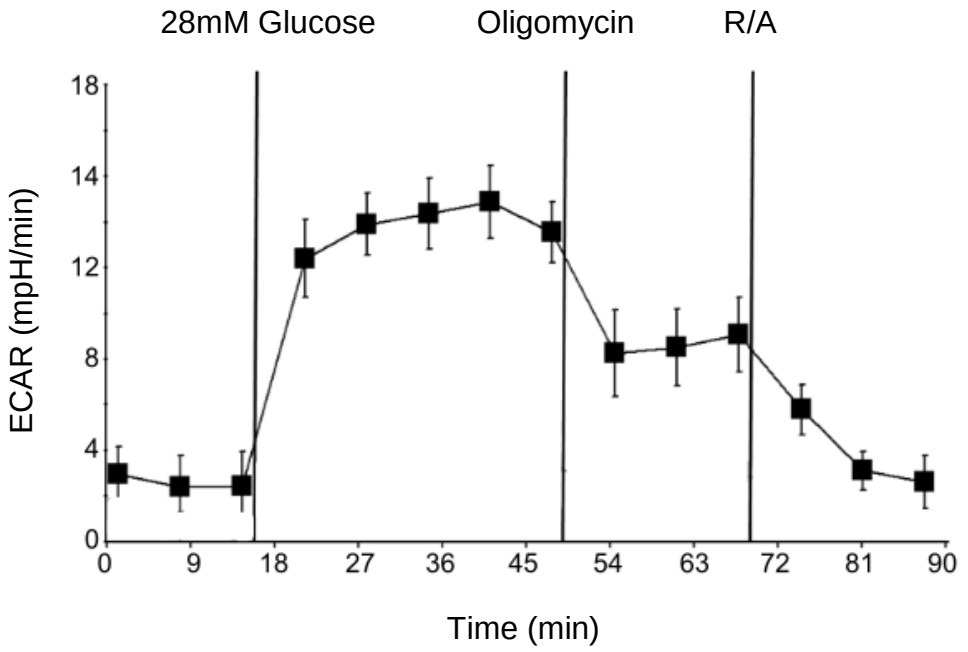

Figure 5.1 Typical extracellular acidification rate (ECAR) trace of INS-1E cells. Basal ECAR was recorded for 18mins, after which 28mM glucose was injected and respiration measured for approximately 31mins. At 49mins 2µg/mL oligomycin was introduced to inhibit ATP synthase, and respiration measured for approximately 20mins. At 69mins 2µM rotenone plus 2µM antimycin A (R/A) was added to inhibit mitochondrial respiration. Error bars represent SEM. Trace courtesy of Dr Charles Affourtit, University of Plymouth (Unpublished data).

In pancreatic β-cells, mitochondria oxidation of nutrients facilitates insulin secretion (Komatsu et al. 2013). Nutrient overloading of mitochondrial oxidative pathways, however, is well documented to contribute towards β-cell dysfunction and death in the pathophysiology of T2D (Stiles, 2012). Consequently, the Seahorse EFA is an ideal platform to study the mechanisms underlying nutrient-induced β-cell dysfunction and death in T2D, which currently remain unclear. This includes studying the effects of overloading the mitochondria with fatty acids, to investigate the effects of lipotoxicity on the mitochondria.

Mitochondrial dysfunction is thought to play a role in LC-FFA induced β-cell death (see section 1.7.4). However, literature is conflicting as to whether the mitochondrial oxidation of LC-FFA contributes towards β-cell death (see section 1.7.5). By employing the Seahorse EFA to monitor cellular bioenergetics in real time, the O_2 consumption of β-cells could be recorded, thereby providing a direct read-out of the oxidation rate of LC-FFA. By investigating the oxidation rate of LC-FFA species, it could be determined whether LC-FFA are indeed routed via the mitochondria in β-cells upon acute exposure. Moreover, by determining the OCR of both LC-SFA and LC-MUFA, it could be revealed whether a change in LC-FFA structure impacts on the efficiency of their oxidation in the mitochondria. By investigating these factors, it could be elucidated whether LC-FFA are routed to the mitochondria of β-cells upon acute exposure and if there was a link between LC-FFA mitochondrial oxidation and toxicity in pancreatic β-cells, which would merit further investigation. This work was conducted in the rodent-derived INS-1 and human-derived EndoC-βH1 cell lines, to determine if the two species respond similarly to LC-FFA mitochondrial oxidation.

Seemingly, this is the first study to use the Seahorse EFA technology to record the oxidation of LC-FFA in β-cells following an acute injection. Further, there is

only one study (Andersson et al. 2015) which has assessed the mitochondrial bioenergetics of EndoC-βH1 cells; other studies have used rodent β-cells (e.g. Barlow, 2015; Barlow; 2016). As glucose-stimulated insulin secretion (GSIS) is tightly controlled by β-cell mitochondrial respiration, an insulin secretion assay was used to verify that the mitochondria of EndoC-βH1 and INS-1E cells were not dysfunctional. Next using the Seahorse EFA, the bioenergetics of the cells was studied to verify that the metabolic machinery of the β-cells was functional. Finally, the response of INS-1 and EndoC-βH1 cells to an acute injection of LC-FFA species was conducted.

5.2 Methods

EndoC-βH1, INS-1E and INS-1 823/13 cell lines were cultured as described in section 2.2. The Seahorse EFA experiments were conducted as described in section 2.9. To ensure that the cells were metabolically responsive to glucose, insulin secretion assays were conducted as described in section 2.8.

The XF96^{e} 96-well cell culture plates were coated in 100µg/ml poly-D-lysine for 30min prior to seeding of cells to facilitate cellular adherence. The cells were then seeded at a constant number. To further facilitate cellular adhesion, when aspirating the supernatant from each well a 200µl tip was attached to the aspirator and the plate tilted forward to minimise the risk of the aspirator coming into contact with the cells. To ensure that cells were not lost during the Seahorse EFA assay, cells were examined by eye under a Zeiss Primovert inverted microscope before and after the assay.

Alterations in pH have the potential to alter cellular metabolic activity and thus OCR readings (Levin, 2013). Consequently, prior to running the Seahorse EFA, the media and compounds were all adjusted to a neutral pH of 7.4 at 37°C. The

temperature was maintained throughout the assay at 37°C by the Seahorse EFA machine.

Statistical analysis was conducted as described in section 2.9.2. Statistical significance was determined as described in section 2.10. The difference between groups or control was regarded as significant if $P<0.05$. The Mito Stress test report generator (Agilent, 2016) automatically calculated the mito stress test parameters from the Seahorse EFA technology report data. Each experiment was repeated a minimum of three times and ≥6 replicates were included for each experimental condition.

5.2.1 Optimising EndoC-βH1 cell seeding density

A cell titration assay was conducted to determine the optimum seeding density of EndoC-βH1 cells. The manufacturers recommend a cell seeding density of $5x10^3$-$40x10^3$ cells per well (Agilent, 2017) and basal OCR should be kept between 100-200pmol/min for the best signal-noise ratio and to be within the dynamic range of the Seahorse instrument (Rogers et al. 2011). INS-1E cells were seeded at $20x10^3$ cells per well to give a confluency of 70-80%, as recommended by Barlow et al. (2013), to give a basal respiration of approximately 100 pmol/min. EndoC-βH1 cells were seeded at higher densities than INS-1E cells as EndoC-βH1 are smaller. EndoC-βH1 cells were therefore seeded at $40x10^3$, $60x10^3$ and $80x10^3$ cells per well. Basal respiration was measured before the sequential injection of 20mM glucose and oligomycin (figure 5.2). Basal OCR was <100-200pmol/min when EndoC-βH1 cells were seeded at $40x10^3$ per well, and >100-200pmol/min at seeding densities of $60x10^3$ and $80x10^3$ cells per well. OCR did not increase in response to glucose but efficiently decreased when ATP synthase was inhibited by oligomycin, in EndoC-βH1 cells seeded at $40x10^3$,

$60x10^3$ and $80x10^3$ cells per well (figure 5.2). A seeding density of $60x10^3$ cells per well was chosen for the Seahorse EFA when using EndoC-βH1 cells, as OCR

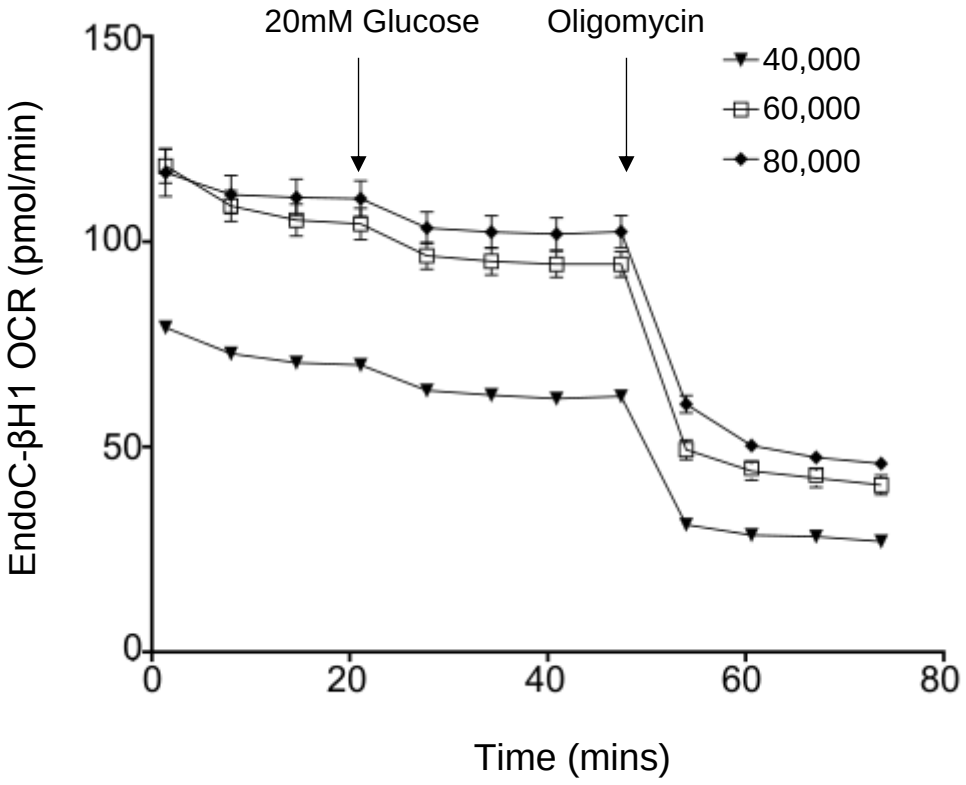

Figure 5.2 Raw OCR values for EndoC-βH1 cells to determine the optimum number of cells per well for the Seahorse EFA. EndoC-βH1 cells were seeded at either $40x10^3$, $60x10^3$ or $80x10^3$ cells per well. EndoC-βH1 cells were starved of glucose for 2h and incubated for 1h at 37°C under air prior to transferring to an XF96^e Seahorse analyser. Basal respiration (oxygen consumption rate (OCR)) was measured for 21mins. After 21mins, 20mM glucose was injected followed at 47mins by 1μM oligomycin (Oli) to inhibit ATP synthase; respiration was measured every 6-7mins. Experimental points were the mean of 7 replicates. Error bars represent SEM.

was >100-200pmol/min for the full duration of the assay, whereas OCR was <100-200pmol/min with a seeding density of $40x10^3$ cells per well.

5.3 Results

5.3.1 Glucose-induced insulin secretion of INS-1E and EndoC-βH1 cells

To test that the INS-1E and EndoC-βH1 cell lines were responsive to glucose, and thus had functional mitochondria, the insulin secretory response of both INS-1E and EndoC-βH1 was characterised. Insulin release was stimulated with either glucose (20mM) or KCl (30mM). Glucose-stimulated insulin secretion (GSIS) differed between the two cells lines. In the rodent-derived INS-1E cell line there was a 2-fold increase in insulin secretion at 20mM glucose compared to those cells treated with 2mM glucose ($p<0.001$). Moreover, depolarisation of the cells with 30mM KCl led to a 1.5-fold increase in basal insulin secretion (0mM glucose) in the INS-1E cell line ($p<0.05$) (figure 5.3).

Surprisingly, when configured in a monolayer, EndoC-βH1 cells were unresponsive to 20mM glucose even when glucose was combined with 3-isobutyl-1-methylxanthine (IBMX) which should amplify the release of insulin (figure 5.4). The EndoC-βH1 cell line was however responsive to KCl, exhibiting an 8-fold increase in insulin secretion. Further, when EndoC-βH1 cells in a monolayer were stimulated with 20mM glucose in the presence of 500µM C16:0 there was a 3.2-fold increase in insulin secretion in the presence of IBMX (figure 5.5a). A significant increase in insulin secretion was not observed however when EndoC-βH1 cells were stimulated with either 500µM C17:0, C18:0 or C18:1; in the presence of IBMX. Further, C16:0 did not amplify GSIS when IBMX was not present in the extracellular medium (figure 5.5b).

It is has been suggested that in vitro insulin secretory responses of cultured β-cells are greater when the cells are configured in a three-dimensional islet architecture (attributed to a greater degree of cell-cell communication) compared to when used as a monolayer (Green et al. 2015). To assess whether this was applicable to the EndoC-βH1 cell line, cells were configured as pseudoislets and insulin secretion quantified in response to 20mM glucose and 30mM KCl in a perifusion system. The insulin secretion trace (figure 5.6) revealed that neither 20mM glucose nor 30mM KCl elicited a significant increase in insulin secretion from EndoC-βH1 pseudoislets. The reason why EndoC-βH1 cells were responsive to 30mM KCl when in a monolayer but not in a pseudoislet configuration remains unclear.

In summary, the rodent-derived INS-1E cells have an intact GSIS response whereas the human-derived EndoC-βH1 cell line do not. Both cells lines were responsive to KCl indicating that both cell lines produce and secrete insulin, but EndoC-βH1 cells may be more reliant on canonical KATP-dependent pathways to secrete insulin. Moreover, secretion was increased by C16:0 in EndoC-βH1 cells, although this required the presence of IBMX.

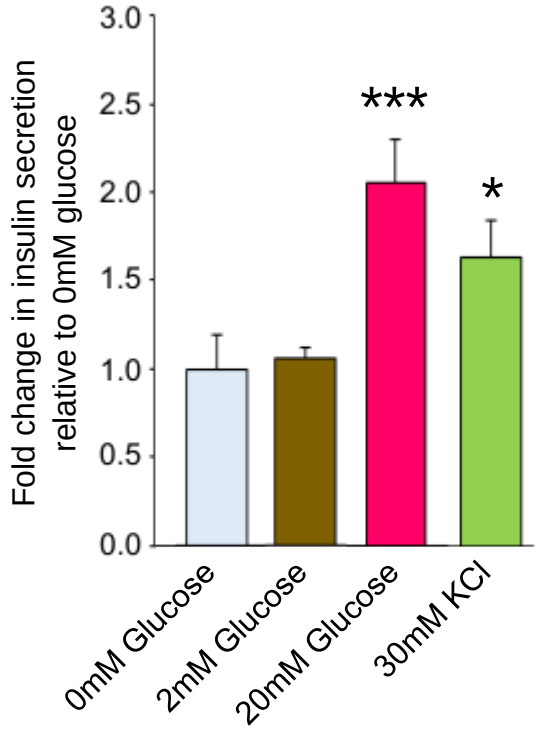

Figure 5.3 Glucose-induced insulin secretion of INS-1E cells. INS-1E cells were starved of glucose for 1.5h prior to being treated with 0mM glucose, 20mM glucose or 30mM KCl. Cells were treated for 1h and their insulin containing supernatant collected. A radioimmunoassay was then undertaken to measure the concentration of insulin in each sample. Data represent mean values from three independent experiments. Error bars represent SEM. *p<0.05, ***p<0.001 relative to 0mM glucose. Insulin secretion assay conducted by Mark Russell, University of Exeter.

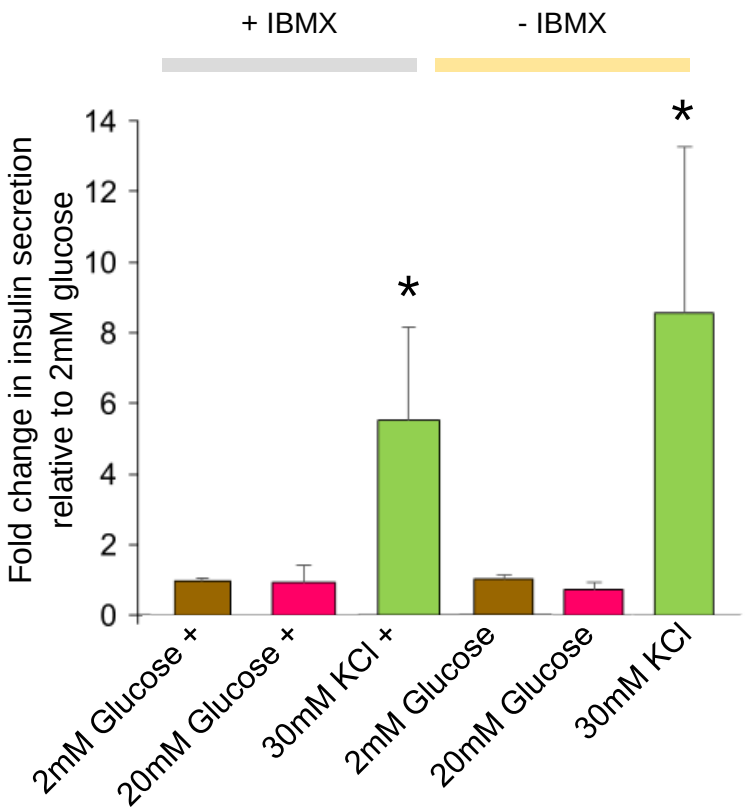

Figure 5.4 Glucose-induced insulin secretion in EndoC-βH1 cells. EndoC-βH1 cells were starved of glucose for 1.5h prior to being treated with 2mM glucose, 20mM glucose or 30mM KCl with (+) or without 100µM IBMX for 1h. The supernatant was then collected for use in a radioimmunoassay to measure the presence of insulin in each sample. Data represent mean values from three independent experiments. Error bars represent SEM. * $p<0.05$ relative to 2mM glucose with (+) and without IBMX.

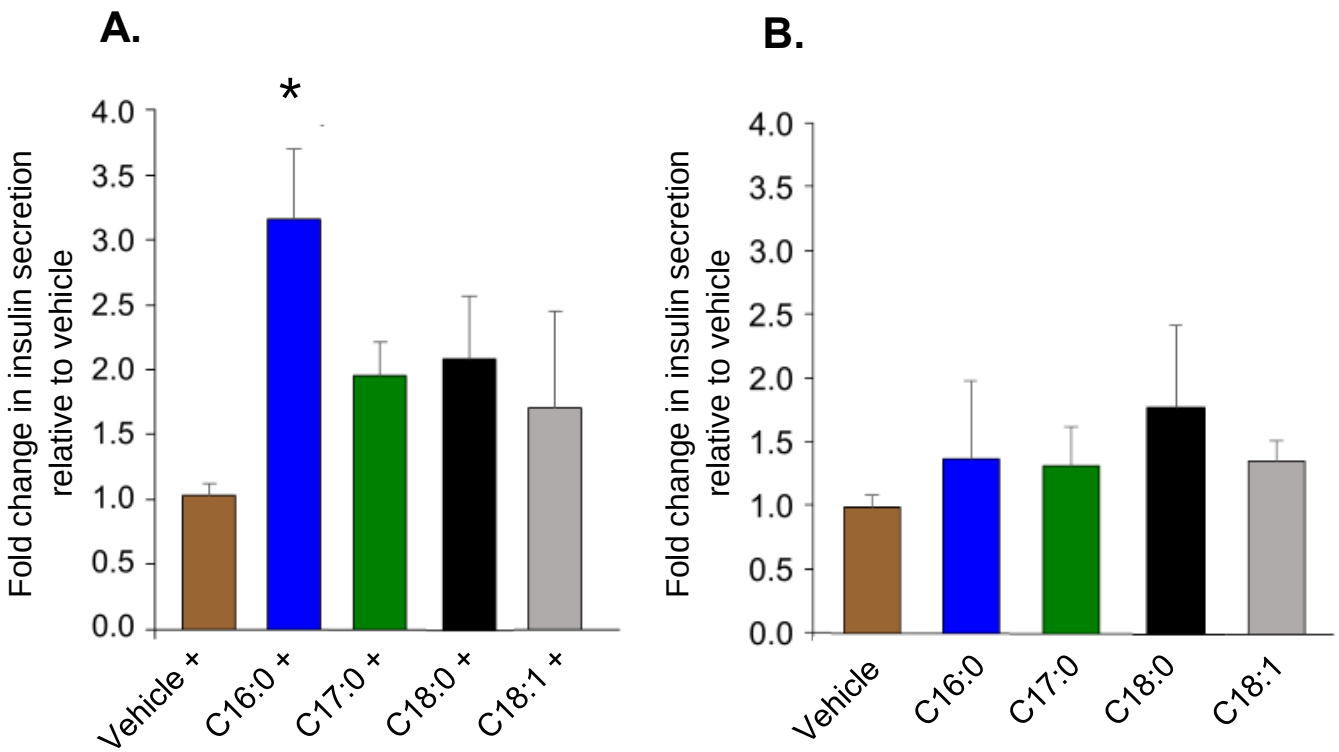

Figure 5.5 Fatty acid induced insulin secretion in EndoC-βH1 cells. EndoC-βH1 cells were starved of glucose for 1.5h prior to being treated with 20mM glucose and either 500μM C16:0, C17:0, C18:0 or C18:1 with (A) or without (B) 100μM IBMX. Control cells were treated with BSA vehicle only. Cells were treated for 1h and the supernatant collected. A radioimmunoassay was then undertaken to quantify the amount of insulin released. Data represent mean values from three independent experiments. Error bars represent SEM. * $p<0.05$ relative to vehicle.

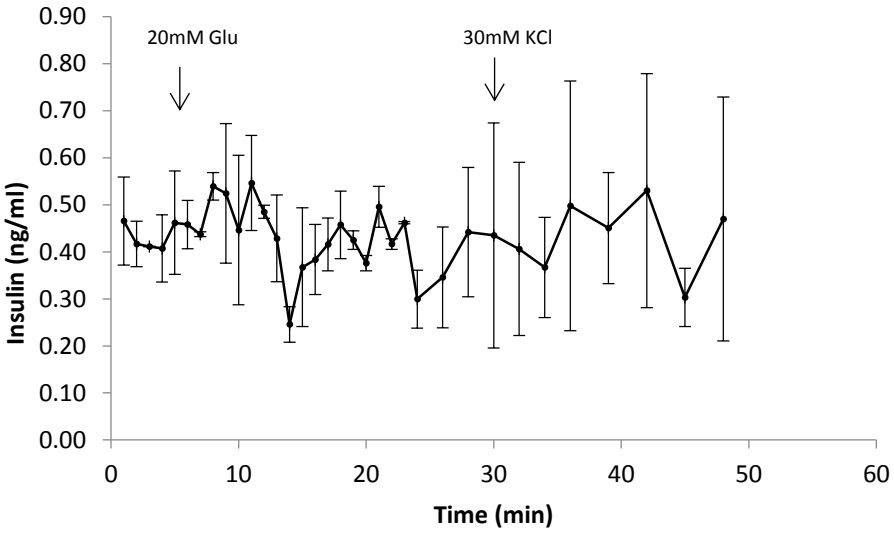

Figure 5.6 Insulin secretion profile of EndoC-βH1 pseudoislets during glucose and KCl perfusion. Pseudoislets were suspended inside a perifusion apparatus and warm Krebs buffer pumped over the pseudoislets at a rate of ~1ml/min for 1h prior to insulin release being stimulated with 20mM glucose (5-33mins) and 30mM KCl (33-50mins). Supernatant was collected every 1min for 50min and insulin content quantified using a radioimmunoassay. Data points represent the mean of two independent experiments. Error bars represent SEM.

5.3.2 The bioenergetics of clonal β-cells

A Mito Stress test (section 2.9.1) was conducted to verify that the mitochondrial machinery required for substrate oxidation in INS-1 and EndoC-βH1 cells were functional. The Seahorse EFA was used to record the OCR of cells after the sequential addition of mitochondrial inhibitors oligomycin, FCCP and a combination of rotenone and antimycin A. This enabled the mitochondrial respiration profile to be studied including ATP-linked respiration, respiration associated with the proton leak, and the maximal respiration rate (as reviewed by Brand, 2011). Healthy β-cell mitochondria will have a proton leak higher than other cell types as the proton leak is thought to be used by β-cells to regulate GSIS by decreasing ATP synthesis (Affourtit et al. 2011; Brand, 1993; Gohring, 2013). Moreover, healthy β-cell mitochondria have the ability to respond to increased energy demands by maximising cellular respiratory activity (reviewed in Brand & Nicholls, 2011).

INS-1 823/13 cells showed a decline in OCR upon inhibiting ATP synthase with oligomycin (figure 5.7a). From the trace, it could be determined that 55% of oxygen consumption is used by INS-1 823/13 cells to generate ATP, and the remaining 45% is associated with the proton leak (figure 5.7b). As shown in figure 5.7b, uncoupling the inner mitochondrial membrane proton gradient with carbonyl cyanide-4-(trifluoromethoxy) phenylhydrazone (FCCP) caused INS-1 823/13 cells to have an almost two-fold rise in OCR relative to basal respiration, demonstrating that INS-1 823/13 cells have the ability to respond to an increase in energy demand. Collectively, this indicates that the mitochondria of INS-1 823/13 cells are functional and have the capacity to metabolise high concentrations of substrates.

Similarly to INS-1 823/13 cells, INS-1E cells had a decline in OCR upon inhibiting ATP synthase with oligomycin (figure 5.8). From the trace, it could be determined that 56% of oxygen consumption is used to generate ATP with the remaining 44% being associated with the proton leak. Unlike INS-1 823/13 cells, however, INS-1E cells had a modest rise in OCR (one-fold increase relative to basal) upon uncoupling the inner mitochondrial membrane proton gradient with FCCP. Further, the spare capacity of INS-1E cells (5pmol/min) was substantially lower than INS-1 823/13 cells (95pmol/min). This indicates that INS-1E cells have a limited ability to respond to an increase in energy demand compared to INS-1 823/13 cells.

EndoC-βH1 cells had a marked decline in respiration upon the addition of oligomycin (figure 5.9), more so than INS-1 cells. Respiration associated with ATP generation accounted for 83% of basal respiration, whereas the proton leak only accounted for 17%. Respiration associated with ATP generation was much higher in the EndoC-βH1 cell line compared to INS-1 cells, and respiration associated with the proton leak was far less in EndoC-βH1 cells. Further, EndoC-βH1 cells had a 2.2-fold increase in OCR with the addition of FCCP indicating that human-derived β-cells can also increase respiration to meet increased cellular energy requirements. The increase in OCR in response to FCCP was similar to the increase in OCR observed in INS-1 823/13 cells upon the uncoupling of their inner mitochondrial membrane proton gradient.

In summary, the mitochondrial metabolic machinery of INS-1 823/13 and EndoC-βH1 cells are fully functional, although rodent-derived β-cells seemingly have a greater proton leak relative to human-derived β-cells. Moreover, INS-1E cells have the capacity to produce ATP, but they are not able to meet an increase in energy demands due to having a modest spare respiratory capacity.

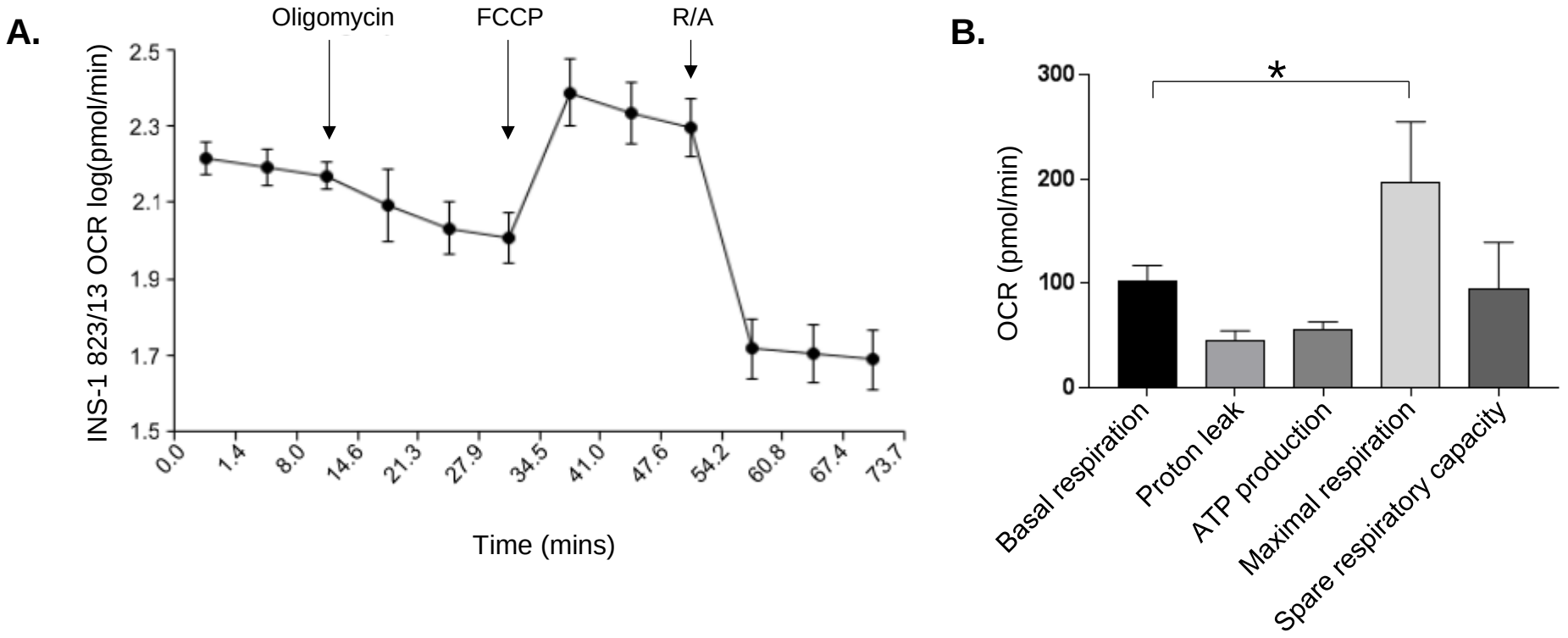

Figure 5.7 Bioenergetic profile of INS-1 823/13 cells. Cells were incubated in 10mM glucose for 2h and incubated for 1hr at 37°C under air prior to transferring to an XF96^{e} Seahorse EFA analyser. During the assay, glucose was maintained at 10mM for the full duration. Basal respiration (oxygen consumption rate (OCR)) was measured for 21.3mins. At 21.3mins 1μM oligomycin was injected, at 34.5mins 1.0μM FCCP was injected and at 54.2mins 0.5 μM rotenone/antimycin (R/A) was injected; respiration was measured every 6-7mins. **(A)** Bioenergetics trace of INS-1 823/13 cells. Data was normalized to baseline and log-transformed. **(B)** Parameters of mitochondrial functioning as determined by the Mito Stress test report generator (Agilent, USA). Data was the mean from 3 independent experiments. Error bars represent SEM. *p<0.05.

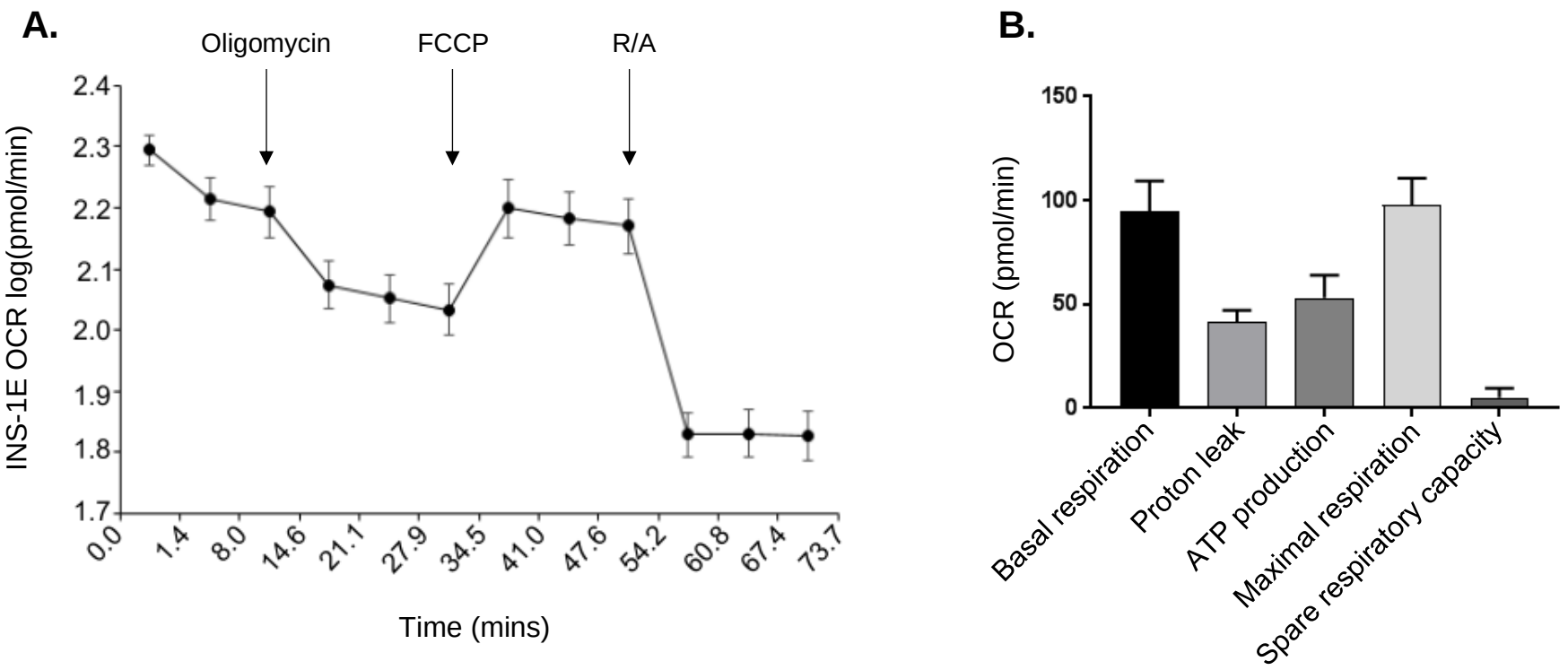

Figure 5.8 Bioenergetic profile of INS-1E cells. Cells were incubated in 10mM glucose for 2h and incubated for 1h at 37°C under air prior to transferring to an XF96^{e} Seahorse EFA analyser. During the assay, glucose was maintained at 10mM for the full duration. Basal respiration (oxygen consumption rate (OCR)) was measured for 21.3mins. At 21.3mins 1μM oligomycin was injected, at 34.5mins 1.0μM FCCP was injected and at 54.2mins 0.5 μM rotenone/antimycin (R/A) was injected; respiration was measured every 6-7mins. **(A)** Bioenergetics trace of INS-1E cells. Data was normalized to baseline and log-transformed. **(B)** Parameters of mitochondrial functioning as determined by the Mito Stress test report generator (Agilent, USA). Data was the mean from 3 independent experiments. Error bars represent SEM.

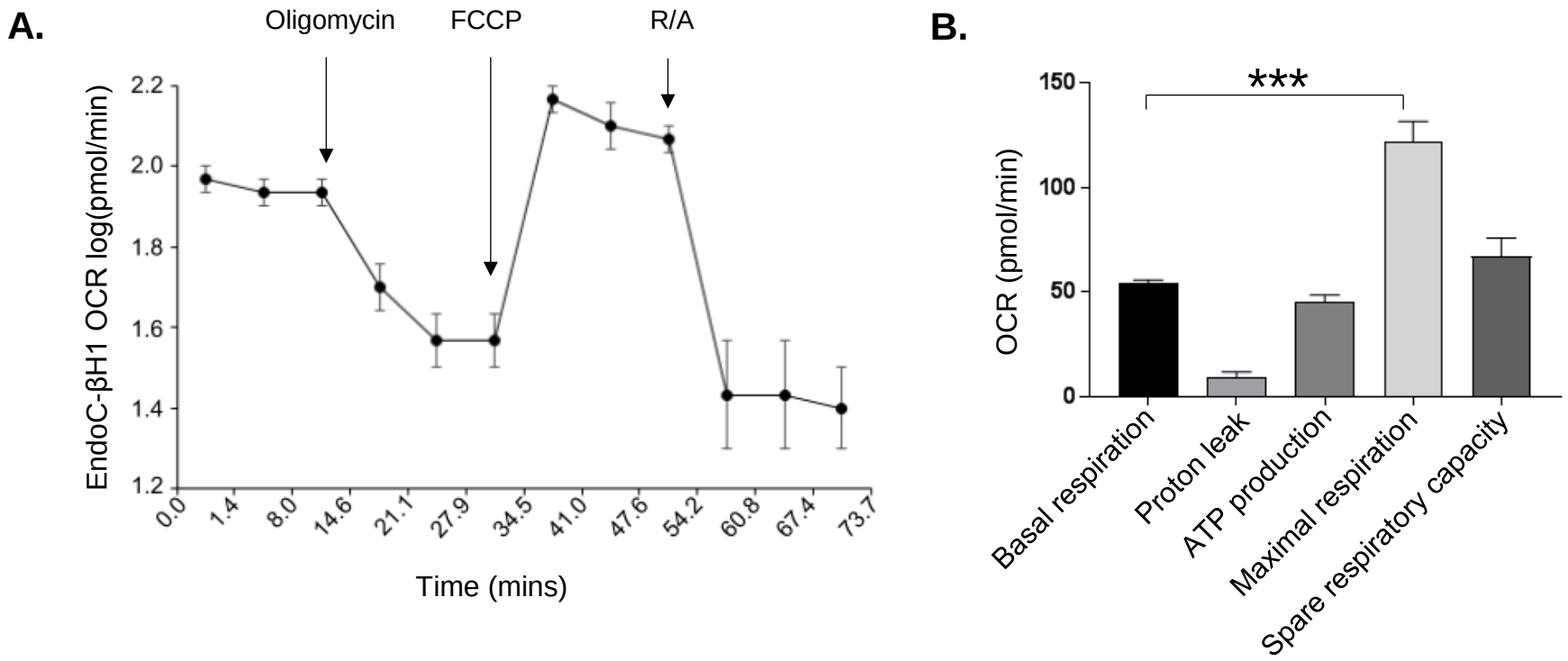

Figure 5.9 Bioenergetic profile of EndoC-βH1 cells. Cells were incubated in 10mM glucose for 2h and incubated for 1h at 37°C under air prior to transferring to an XF96^{e} Seahorse EFA analyser. During the assay, glucose was maintained at 10mM for the full duration. Basal respiration (oxygen consumption rate (OCR)) was measured for 21.3mins. At 21.3mins 1μM oligomycin was injected, at 34.5mins 1.0μM FCCP was injected and at 54.2mins 0.5 μM rotenone/antimycin (R/A) was injected; respiration was measured every 6-7mins. **(A)** Bioenergetics trace of EndoC-βH1 cells. Data was normalized to baseline and log-transformed. **(B)** Parameters of mitochondrial functioning as determined by the Mito Stress test report generator (Agilent, USA). Data was the mean from 3 independent experiments. Error bars represent SEM. ***p<0.001.

5.3.3 Changes in β-cell respiration in response to glucose

To verify that the INS-1E cell line had an increase in mitochondrial respiration in response to increasing glucose, OCR was measured in cells after an acute injection of 0mM, 16mM and 30mM glucose (figure 5.10). INS-1E cells oxidised glucose in a dose-responsive manner. With the injection of 0mM glucose, there was no rise in OCR. With the injection of 16mM glucose, there was a significant increase in OCR (18pmol/min) relative to 0mM. With the addition of 30mM glucose, there was also a significant elevation of OCR (41pmol/min) relative to 0mM. Moreover, 30mM glucose elicited a significant increase in OCR (23pmol/min) relative to 16mM glucose.

Contrary to INS-1E cells, however, an acute injection of 10mM, 16mM, 20mM or 30mM glucose failed to stimulate an increase in OCR (compared to 0mM glucose) in EndoC-βH1 cells (figure 5.11). This implies that glucose is not being oxidised by the mitochondria of EndoC-βH1 cells.

In summary, using the Seahorse EFA technology to record OCR, INS-1E cells were found to oxidise glucose in a dose-responsive manner whereas EndoC-βH1 cells seemingly do not oxidise glucose through mitochondrial respiration pathways.

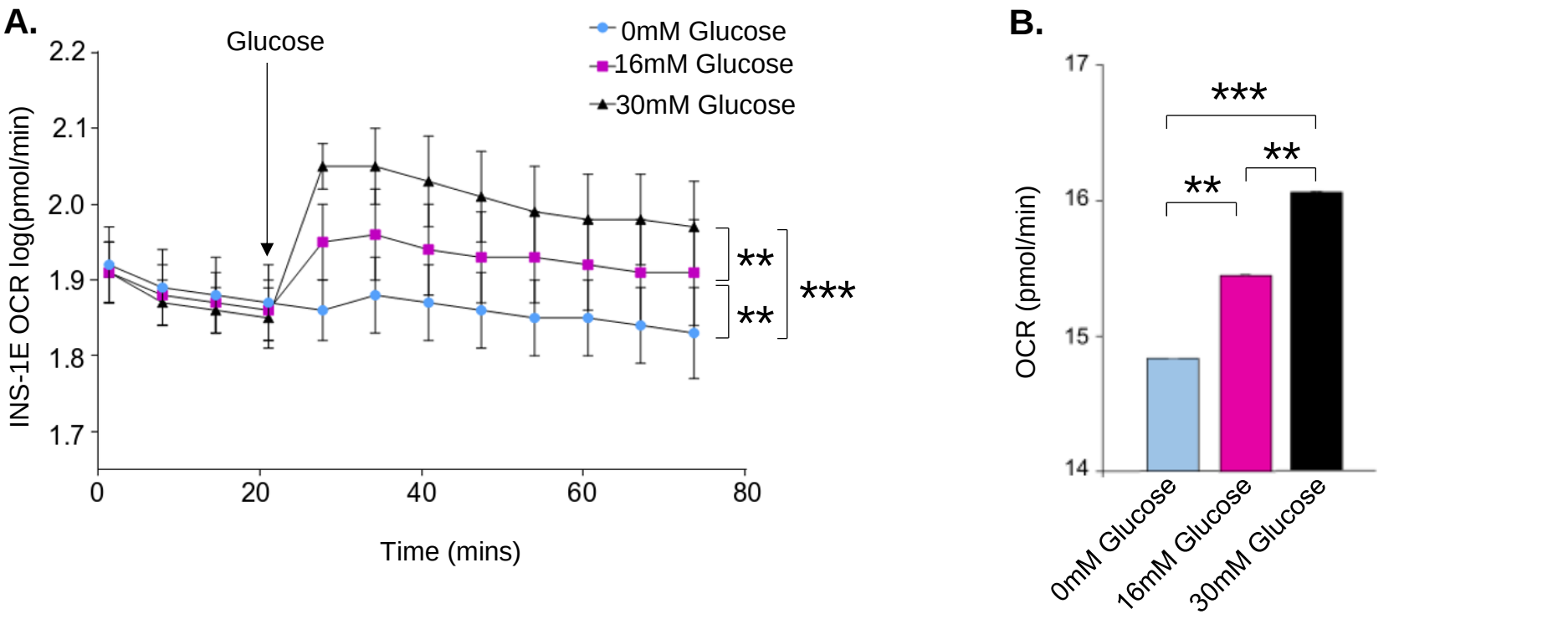

Figure 5.10 Cellular respiration upon acute injection of glucose in INS-1E cells. INS-1E cells were starved of glucose for 2h and incubated for 1h at 37°C under air prior to transferring to an XF96^{e} Seahorse analyser. **(A)** Basal respiration (oxygen consumption rate (OCR)) was measured for 21.1mins. 16mM and 30mM glucose was injected at 21.1mins and respiration recorded every 6-7mins thereafter. Data was normalized to baseline and log-transformed. Experimental points were the mean of 7 replicates from 3 independent experiments. **(B)** Area under the curve calculated by totaling the sum of data points post injection of glucose (i.e. those data points recorded after 21.1mins). Error bars represent SEM. **p<0.01, ***p<0.001.

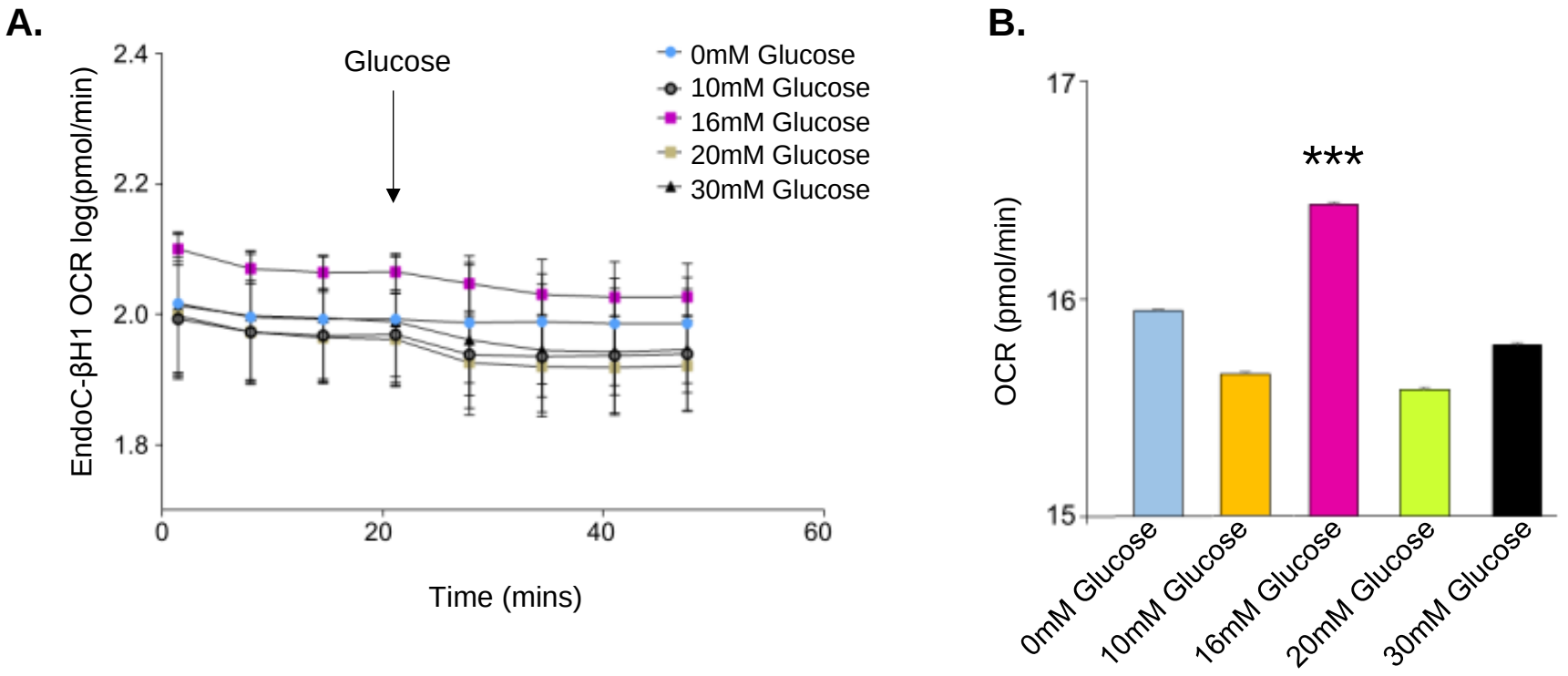

Figure 5.11 Cellular respiration upon acute injection of glucose in EndoC-βH1 cells. EndoC-βH1 cells were starved of glucose for 2h and incubated for 1h at 37°C under air prior to transferring to an XF96^{e} Seahorse analyser. **(A)** Basal respiration (oxygen consumption rate (OCR)) was measured for 20mins. At 20mins 0mM, 10mM, 16mM, 20mM or 30mM glucose was injected and respiration recorded every 6-7mins thereafter. Data was normalized to baseline and log-transformed. Experimental points were the mean of 7-11 replicates from 3 independent experiments. **(B)** Area under the curve calculated by totaling the sum of data points post injection of glucose (i.e. those data points recorded after 21.1mins). Error bars represent SEM. ***p<0.001 relative to 0mM glucose.

5.3.4 Changes in β-cell respiration in response to fatty acids

The oxidation rate of LC-FFA species routed via the mitochondria was next assessed in INS-1E cells using the Seahorse EFA. In INS-1E cells, an acute injection of 125µM, 250µM or 500µM C16:0 did not elicit a significant rise in OCR relative to control (figure 5.12). Further, 125µM, 250µM or 500µM C17:0 also did not stimulate a significant rise in OCR relative to vehicle in INS-1E cells (figure 5.13). To assess whether it was only LC-SFA which were not oxidised by the mitochondria, the OCR of INS-1E cells after an acute injection of the LC-MUFA was also recorded. 125µM, 250µM or 500µM of the LC-MUFA, C16:1, did not cause a significant increase in OCR relative to control in INS-1E cells (figure 5.14). Therefore, LC-FFA did not cause a significant increase in mitochondrial oxidation in INS-1E cells even at concentrations as high as 500µM.

It was observed in figure 5.8 that INS-1E cells have a modest mitochondrial spare capacity. Therefore, it could be inferred that INS-1E cells may not be able to increase their bioenergetic activity to oxidise the endogenous LC-FFA being acutely injected. Consequently, as an alternative to INS-1E cells the oxidation rate of LC-FFA was measured in INS-1 823/13 cells which are derived from the same parent cell line as INS-1E cells (Hohmeirer et al. 2000) but as shown in figure 5.7, have a greater spare respiratory capacity. Unlike INS-1E cells, INS-1 823/13 cells were responsive to an acute injection of LC-FFA (figure 5.15). After an acute injection of 500µM C16:0 there was no significant increase in OCR relative to vehicle control. However, with the injection of 500µM C18:1, there was a significant rise in OCR (19pmol/min) compared to vehicle and C16:0. Collectively, this shows that in INS-1 8233/13 cells C18:1 is routed to the mitochondria where it is oxidised. Conversely, C16:0 is not oxidised by the mitochondria of INS-1 823/13 cells.

Next, the oxidation rate of LC-FFA species routed via the mitochondria was assessed in EndoC-βH1 cells using the Seahorse EFA (figure 5.16). In my hands, no increase in OCR relative to control was observed after an acute injection of 500µM C16:0 or 500µM C18:1. In summary, LC-FFA are not routed via the mitochondria for oxidation in EndoC-βH1 cells.

In summary, no significant rise in OCR was observed in INS-1E or EndoC-βH1 cells in response to an acute injection of LC-FFA. Conversely, in INS-1 823/13 cells C18:1 but not C16:0 was routed to the mitochondria for oxidation.

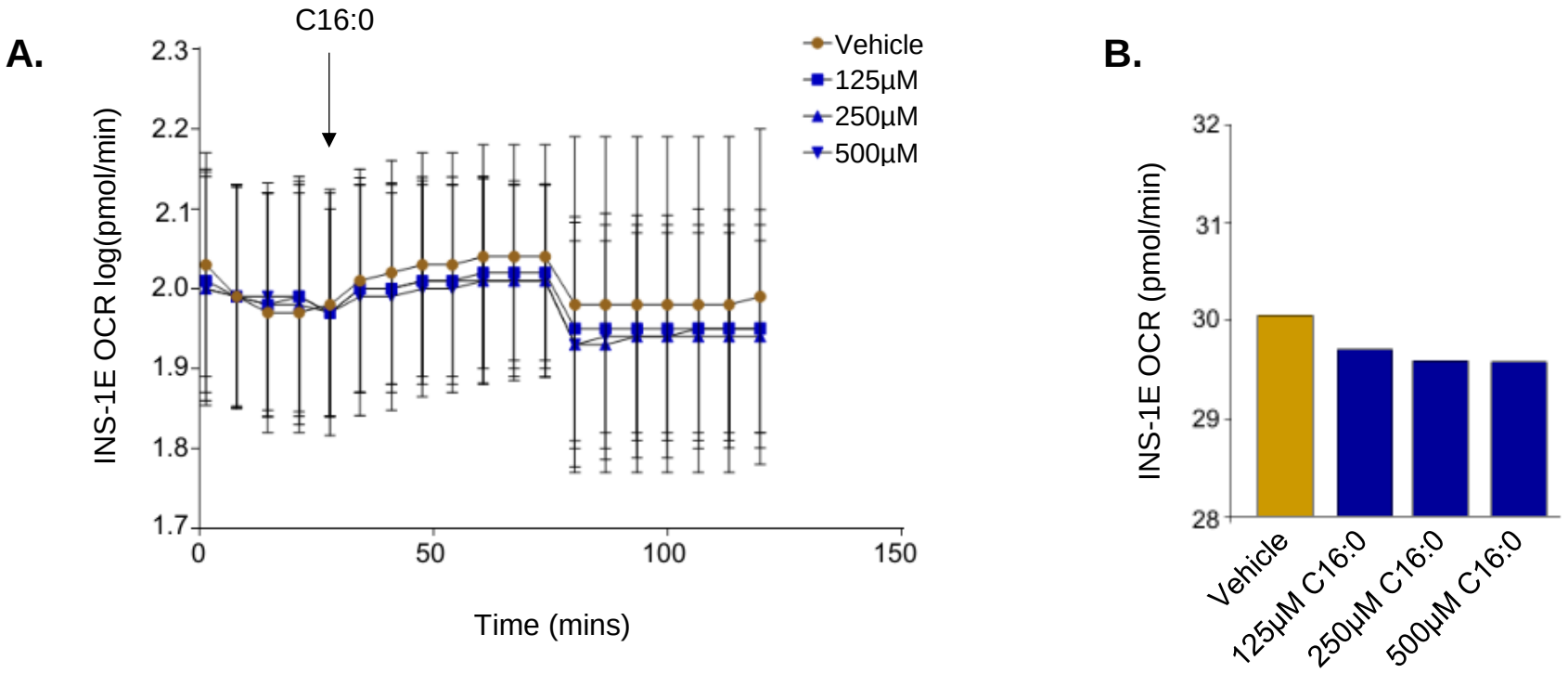

Figure 5.12 Cellular respiration upon acute injection of C16:0 in INS-1E cells. INS-1E cells were starved of glucose for 2h and incubated for 1h at 37°C under air prior to transferring to an XF96^{e} Seahorse analyser. **(A)** Basal respiration (oxygen consumption rate (OCR)) was measured for 21.3mins. LC-FFA conjugated to BSA was injected at 21.3mins and respiration recorded every ~6/7mins thereafter. Control cells received an injection of BSA vehicle only. **(B)** Area under the curve calculated by totaling the sum of data points post injection of C16:0 (i.e. those data points recorded after 21.1mins). Experimental points were the mean of 7 replicates from 3 independent experiments. Data was normalized to baseline and log-transformed. Error bars represent SEM.

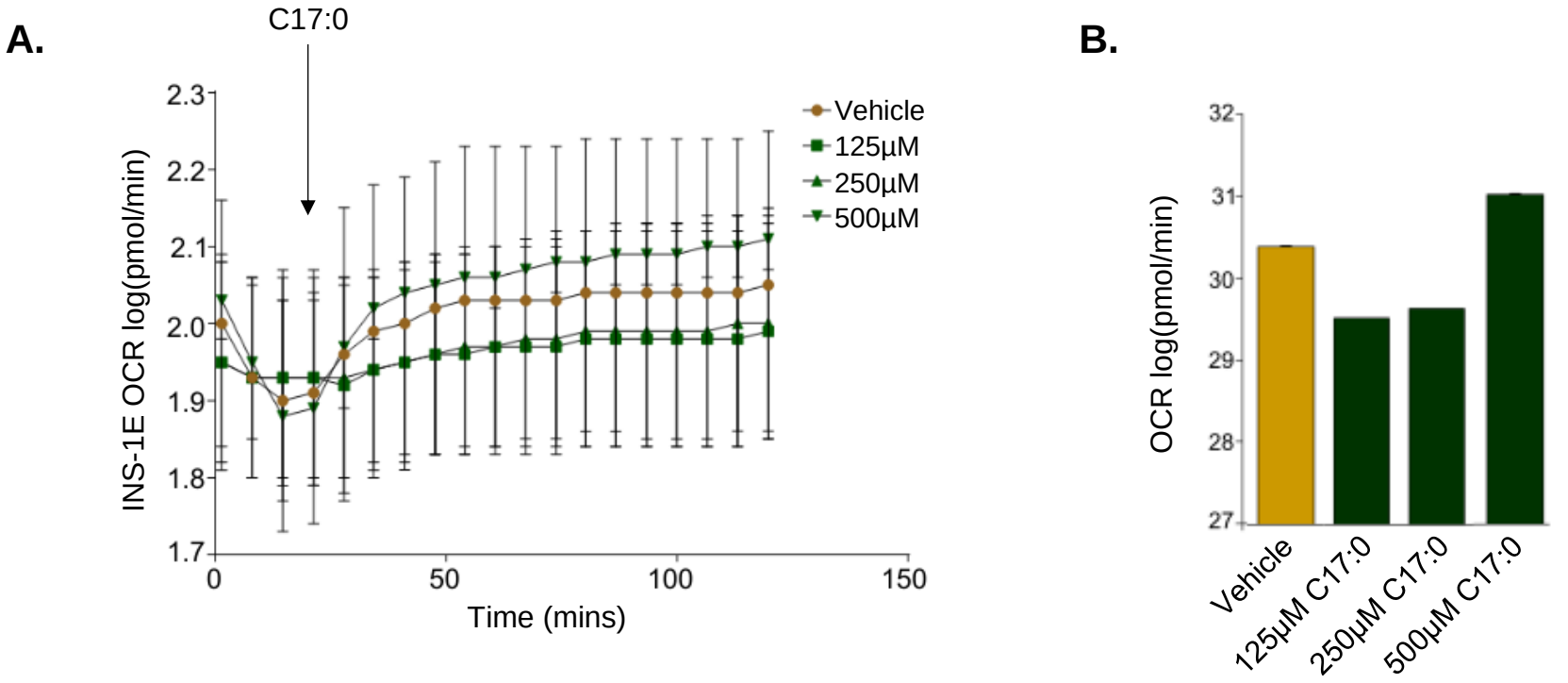

Figure 5.13 Cellular respiration upon acute injection of C17:0 in INS-1E cells. INS-1E cells were starved of glucose for 2h and incubated for 1h at 37°C under air prior to transferring to an XF96^{e} Seahorse analyser. **(A)** Basal respiration (oxygen consumption rate (OCR)) was measured for 21.3mins. LC-FFA conjugated to BSA was injected at 21.3mins and respiration recorded every ~6/7mins thereafter. Control cells received an injection of BSA vehicle only. **(B)** Area under the curve calculated by totaling the sum of data points post injection of C17:0 (i.e. those data points recorded after 21.1mins). Experimental points were the mean of 7 replicates from 3 independent experiments. Data was normalized to baseline and log-transformed. Error bars represent SEM.

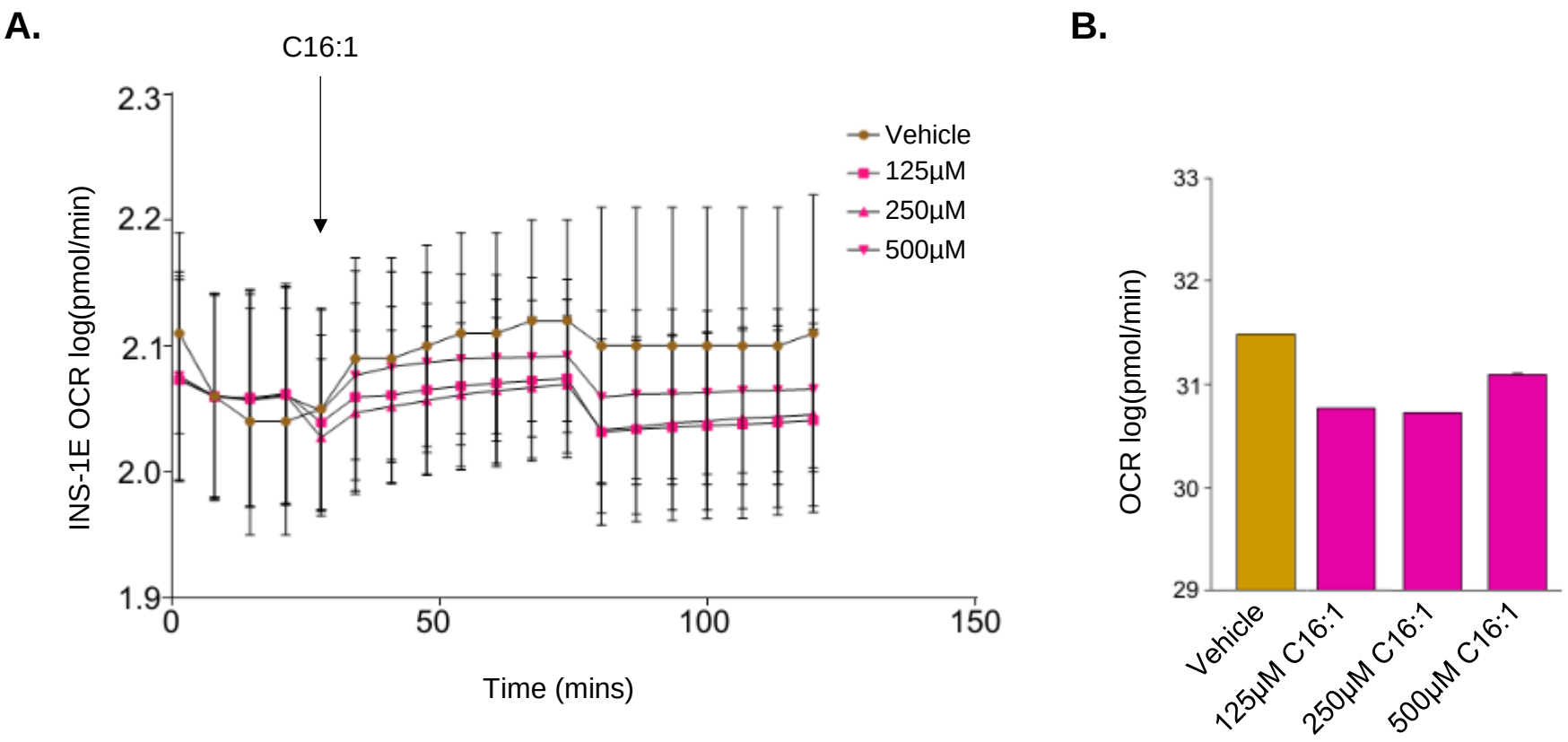

Figure 5.14 Cellular respiration upon acute injection of C16:1 in INS-1E cells. INS-1E cells were starved of glucose for 2h and incubated for 1h at 37°C under air prior to transferring to an XF96^{e} Seahorse analyser. **(A)** Basal respiration (oxygen consumption rate (OCR)) was measured for 21.3mins. LC-FFA conjugated to BSA was injected at 21.3mins and respiration recorded every ~6/7mins thereafter. Control cells received an injection of BSA vehicle only. **(B)** Area under the curve calculated by totaling the sum of data points post injection of C16:1 (i.e. those data points recorded after 21.1mins). Experimental points were the mean of 7 replicates from 3 independent experiments. Data was normalized to baseline and log-transformed. Error bars represent SEM.

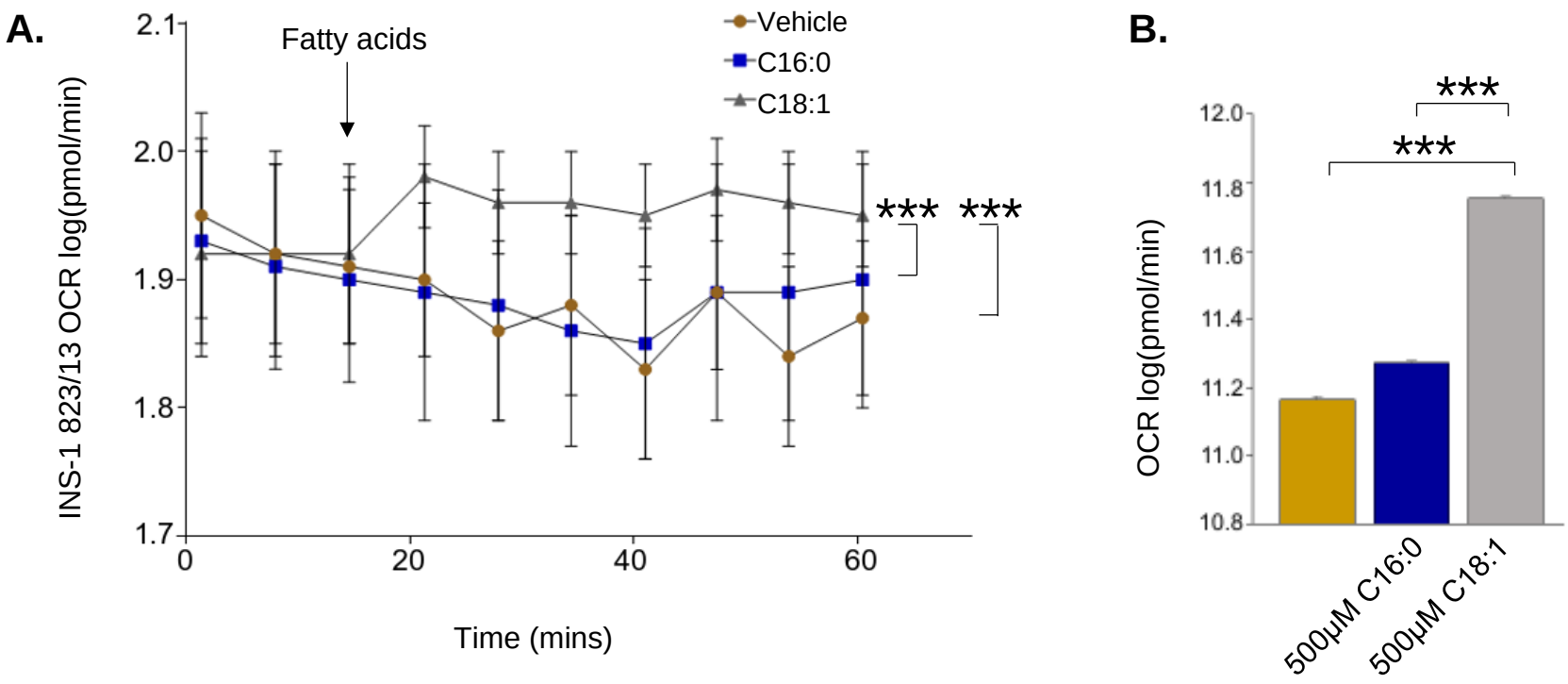

Figure 5.15 Cellular respiration upon acute injection of LC-FFA in INS-1 823/13 cells. INS-1 823/13 cells were starved of glucose for 2h and incubated for 1h at 37°C under air prior to transferring to an XF96^{e} Seahorse analyser. **(A)** Basal respiration (oxygen consumption rate (OCR)) was measured for 14.6mins. LC-FFA (500μM) conjugated to BSA was injected at 14.6mins and respiration recorded every ~6/7mins thereafter. Control cells received an injection of BSA vehicle only. **(B)** Area under the curve calculated by totaling the sum of data points post injection of LC-FFA (i.e. those data points recorded after 15mins). Experimental points were the mean of 7 replicates from 4 independent experiments. Data was normalized to baseline and log-transformed. Error bars represent SEM. ***p<0.001.

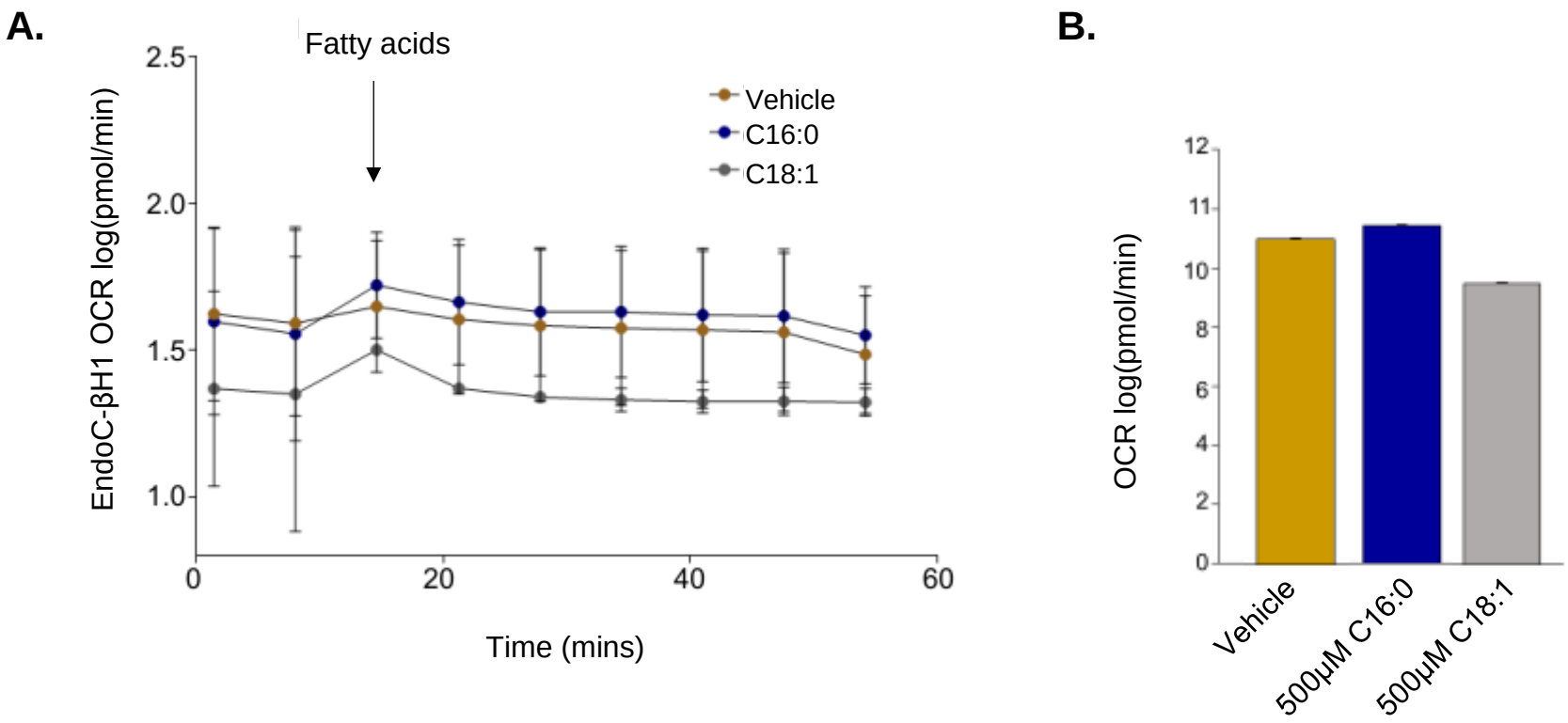

Figure 5.16 Cellular respiration upon acute injection of LC-FFA in EndoC-βH1 cells. EndoC-βH1 cells were starved of glucose for 2h and incubated for 1h at 37°C under air prior to transferring to an XF96^{e} Seahorse analyser. **(A)** Basal respiration (oxygen consumption rate (OCR)) was measured for 15mins. LC-FFA (500μM) conjugated to BSA was injected at 15mins and respiration recorded every ~6/7mins thereafter. Control cells received an injection of BSA vehicle only. **(B)** Area under the curve calculated by totaling the sum of data points post injection of LC-FFA (i.e. those data points recorded after 15mins). Experimental points were the mean of 7 replicates from 3 independent experiments. Data was normalized to baseline and log-transformed. Error bars represent SEM.

5.4 Discussion

The metabolic activity of INS-1 and EndoC-βH1 cells was studied by examining their insulin secretory responses, their bioenergetics profiles, and their respiratory responses to an acute injection of LC-FFA.

5.4.1 Insulin secretion

In this study, INS-1E cells were found to have a 2-fold increase in insulin secretion in response to 20mM glucose and a 1.5-fold increase in response to 30mM KCl. Insulin secretion by INS-1E cells in response to glucose and KCl was found to be less in this study compared to those reported by Merglen et al. (2004) who generated the INS-1E cell line. Merglen et al. (2004) provoked a 6.2-fold increase in insulin secretion in response to 15mM glucose and a 4.7-fold increase in response to 30mM KCl. Collectively, however, this supports the view that INS-1E cells secrete insulin in response to both glucose and KCl.

However, as detailed in the results section of this chapter, EndoC-βH1 cells did not secrete insulin in response to 20mM glucose. This contradicts the work of Andersson et al. (2015) who found EndoC-βH1 cells to have a 2.4-fold increase in insulin secretion after treatment with 20mM glucose. The results detailed in this chapter also differ to the observations of Ravassard et al. (2011) and Gurgul-Convey et al. (2015) who reported EndoC-βH1 cells to secrete insulin in response to ≥11mM glucose. Gurgul-Convey et al. (2015) also found the insulin secretory response of EndoC-βH1 cells to be amplified when cells were exposed to both 10mM glucose in combination with 100µM IBMX. In this study, EndoC-βH1 cells failed to secrete insulin in response to 20mM glucose in the presence of 100µM IBMX. However, 30mM KCl stimulated an 8-fold increase in insulin secretion relative to control in EndoC-βH1 cells. This was

much higher than reported by Andersson et al. (2015) who found 35mM KCl to stimulate only a 2.8-fold increase in insulin secretion relative control. Both in this study and in the work of Andersson et al. (2015), EndoC-βH1 cells were found to secrete more insulin in response to KCl compared to glucose, whereas Gurgul-Convey et al. (2015) reported EndoC-βH1 cells to secrete a comparable concentration of insulin in response to glucose and KCl.

Interestingly, a 3.2-fold rise in insulin secretion (relative to control) was observed after exposing EndoC-βH1 cells to 19mM glucose in combination with 500μM C16:0 and 100μM IBMX for 1h. This finding supports those studies which have shown LC-FFA to augment GSIS (Prentki at al. 1992; Vara et al. 1986; Yaney et al. 2000). Gravena et al. (2002) also found human islets to have a marked increase in insulin secretion when treated with both 16.7mM glucose and 500μM C16:0, relative to control. Cen et al. (2016) also induced a 1.5-fold increase in insulin secretion after exposing human islets to both 5.5mM glucose and 500μM C16:0. This agrees with the observations detailed in the results section of this study, although EndoC-βH1 cells only secreted insulin in response to 20mM glucose and C16:0 in the presence of IBMX. Conversely, EndoC-βH1 cells treated with 20mM glucose in combination with either C17:0, C18:0 or C18:1; did not have a significant increase in insulin secretion (relative to control) either in the presence or absence of IBMX. This result does not accord with Gravena et al. (2002) who stimulated insulin secretion from human islets after exposing islets to 16.7mM glucose in combination with either C18:0 or C16:1. Further, Cen et al. (2016) also found human islets to secrete insulin in response to C18:0 and C18:1 in the presence of 5.5mM glucose. The difference in insulin secretory response to C18:0 and C18:1 between human islets and EndoC-βH1 cells may be due to EndoC-βH1 cells containing only β-cells whereas human islets also contain other cells types which may

release messengers in response to LC-FFA to amplify insulin secretion. Collectively, this implies that in my hands, EndoC-βH1 cells can secrete insulin via membrane depolarisation as evidenced by the 8-fold increase in insulin secretion relative to control induced by KCl. Moreover, insulin secretion can also be stimulated in EndoC-βH1 cells when co-treated with C16:0, glucose and IBMX. The lack of insulin secretion in response to glucose may also imply that EndoC-βH1 cells have dysfunctional mitochondria.

5.4.2 The mitochondrial bioenergetics of clonal β-cells

The bioenergetic profile of INS-1E, INS-1 823/13 and EndoC-βH1 cells was studied to verify that the mitochondrial machinery required for oxidation in INS-1 and EndoC-βH1 cells was functional. The most striking difference between the INS-1 and EndoC-βH1 cell lines was that 44-45% of oxygen consumption in INS-1 cells was associated with the mitochondrial proton leak, whereas only 17% of oxygen consumption was associated with this proton leak in EndoC-βH1 cells. The mitochondrial proton leak acts to uncouple oxidative phosphorylation from ATP synthesis (Affourtit et al. 2011). Similar to what we observed, Andersson et al. (2015) also reported the relative proton leak of INS-1 823/13 cells to be greater than that of EndoC-βH1 cells.

Affourtit et al. (2008) have shown INS-1E cells to have a proton leak four times higher than that of myoblasts, and Brand et al. (1993) have shown that only 30% of oxygen consumption is associated with the proton leak in hepatocytes. It has been proposed that pancreatic β-cells have a higher proton leak compared to other cell types (Affourtit et al. 2008) as the proton leak is thought to be used by β-cells to regulate GSIS by decreasing ATP synthesis (Affourtit et al. 2011). However, if a small proton leak increases GSIS, then it can be inferred that EndoC-βH1 cells should have secreted

more insulin in response to glucose relative to INS-1E cells as EndoC-βH1 cells had considerably less O_2 consumption associated with the proton leak. As shown in section 5.3.1, EndoC-βH1 cells did not secrete insulin in response to glucose, unlike INS-1E cells. This indicates that the small proton leak in EndoC-βH1 cells is not the cause of the different insulin secretory responses to glucose by INS-1E and EndoC-βH1 cells. The cause of impaired GSIS by EndoC-βH1 cells requires further investigation.

The mechanism by which the proton leak regulates GSIS is currently the subject of ongoing investigation. Uncoupling protein-2 (UCP2) is thought to be a key regulator of the proton leak and its knock-down in INS-1E cells has been shown to enhance GSIS (Affourtit & Brand, 2008). Moreover, it has been proposed that UCP2 acts to attenuate GSIS by decreasing ROS production (Affourtit et al. 2011). The UCP2 associated decrease in ROS production would interfere with ROS metabolic signalling thereby attenuating insulin secretion (Pi et al. 2007) and would protect the β-cell from oxidative stress (Affourtit et al. 2011). The expression of UCP2 in response to LC-FFA therefore requires further investigation as if UCP2 is upregulated in INS-1 cells (which have an increased proton leak activity) then it could be inferred that an elevation in mitochondrial-derived ROS, produced by the increased oxidation of excess LC-FFA, is not the cause of LC-FFA induced β-cell death (as proposed by Graciano et al. (2011)). However, according to Barlow et al. (2015), the expression of UCP2 is challenging to quantify as commercially available UCP2 antibodies non-specifically bind to other proteins. However, Barlow et al. (2015) reported INS-1E cells exposed to C16:0 for 24h have an elevated concentration of mitochondrial-derived ROS (determined using MitoSOX oxidation) and a loss in viability. In their study knock down of UCP2 accentuated the protective effects of C18:1 against C16:0-induced β-cell

death (Barlow et al. 2015), implying that UCP2 was not protective against C16:0-induced β-cell death. The high proton leak of INS-1 cells and, as detailed in chapter 3 of this thesis, the fact that INS-1E cells undergo LC-SFA induced β-cell death support the work of Barlow et al. (2015) that the proton leak does not act to protect INS-1E cells from lipotoxicity.

In summary, a higher degree of O_2 is consumed by the proton leak in rodent-derived β-cells relative to human-derived β-cells. An increase in proton leak activity of INS-1 cells relative to EndoC-βH1 cells does not offer an explanation however as to why INS-1E cells, but not EndoC-βH1 cells, secrete insulin in response to glucose. Further, the role of UCP2 in LC-FFA induced β-cell death requires further investigation.

5.4.3 Glucose and fatty acid oxidation in rodent-derived β-cells

The results detailed in this chapter have shown the metabolic machinery of INS-1E cells to be functional (albeit with a modest spare respiratory capacity). Consequently, INS-1E cells oxidise glucose in a dose-responsive manner, and in response to an acute exposure (1h) of glucose they secrete insulin. However, INS-1E cells were found not to route LC-SFA nor LC-MUFA to the mitochondria for oxidation. Conversely, INS-1 823/13 cells, which are derived from the same parent cell line INS-1E cells but contain a human proinsulin gene (Hohmeirer, 2000); were found to oxidise C18:1 but not C16:0 upon acute exposure. The difference in the respiratory response to LC-FFA between INS-1E cells and INS-1 823/13 cells may be due to the difference in spare respiratory capacity between the cell types (figure 5.7 and 5.8). INS-1 823/13 cells have a much greater spare respiratory capacity (95.3pmol/min) compared to INS-1E cells (5.03pmol/min). Consequently, INS-1E cells may not be able to meet the increased energy demands imposed on the cell by the acute exposure of LC-FFA.

Seemingly, this study is the first to show that during acute exposure, C16:0 is not routed to the mitochondria in rodent-derived β-cells, whereas C18:1 is. Those studies which have previously investigated the effect of LC-FFA on mitochondrial bioenergetics of β-cells using the Seahorse EFA have pre-incubated β-cells in LC-FFA prior to running the Seahorse EFA (Barlow & Affourtit, 2013; Barlow et al. 2016; Cen et al. 2016). The observation that C18:1 but not C16:0 is routed to the mitochondria and oxidised in INS-1 823/13 cells agrees with the work of Cen et al. (2016). These authors preincubated human islets in 500μM LC-FFA for 1h before measuring OCR with the Seahorse EFA (Cen et al. 2016). Cen and colleagues (2016) reported OCR to be elevated by 50% in those islets treated with the LC-MUFA C16:1 and C18:1 relative to control. In human islets pre-incubated with the LC-SFA C16:0 and C18:0, OCR was elevated 20% relative to control (Cen et al. 2016). The fact that human islets had an increase in OCR in response to C16:0 may be due to cells other than β-cells oxidising C16:0.

In the work of Barlow et al. (2013) using Seahorse EFA technology, INS-1E cells were found to have defective mitochondria after they had been exposed to C16:0 for 24h. Mitochondrial defects included a dampening of the mitochondrial respiratory response to 28mM glucose (a 25% decrease) and a lower coupling efficiency compared to INS-1E cells treated with vehicle only (Barlow et al. 2013). Barlow et al. (2016) also found the mitochondrial respiratory response to glucose to be impaired in mouse islets exposed to C16:0 for 48h, although the respiratory response to glucose was not impaired when mouse islets were exposed to C16:0 for 24h. Collectively, these results imply that C16:0 is not oxidised by the mitochondria in rodent-derived β-cells and that any mitochondrial defects generated by exposing β-cells to LC-SFA are not due to their oxidation but by an alternative mechanism. The ability of rodent-derived β-cells

to oxidise C18:1 may be a potential mechanism as to why C16:0 has been shown to kill rodent-derived β-cells whereas C18:1 is mostly benign.

5.4.4 Glucose and fatty acids in human-derived β-cells

EndoC-βH1 cells were found not to oxidise glucose or LC-FFA via mitochondrial oxidation pathways. Although, the metabolic machinery of EndoC-βH1 cells was functional and consequently EndoC-βH1 cells do have the capacity to oxidise glucose and LC-FFA. The observation that EndoC-βH1 cells do not oxidise glucose is supported by their not secreting insulin in response to an acute exposure to glucose. Conversely, Andersson et al. (2015) reported a modest but significant rise in OCR relative to control when measuring the respiration of 20mM glucose in EndoC-βH1 cells.

This study is the first to investigate the OCR of EndoC-βH1 cells after an acute injection of LC-FFA using the Seahorse EFA. According to the results in this study, EndoC-βH1 cells do not route LC-FFA to the mitochondria. These results do not accord with the work of Cen et al. (2016) who observed an increase in OCR of human islets following a 1h incubation in either LC-MUFA or LC-SFA.

In summary, EndoC-βH1 cells appear not to oxidise glucose or LC-FFA via mitochondrial pathways. However, it can be questioned whether this is a true reflection of the oxidative capacity of EndoC-βH1 cells or whether it is due to the limitations of the Seahorse EFA.

5.4.5 Limitations of the Seahorse EFA

Initially, the Seahorse EFA was to be used within the work of this PhD as a tool for investigating the role of LC-FFA metabolism in β-cell death. The initial aim was to use the Seahorse EFA to investigate whether the structure or length of the LC-FFA

impacted on its ability to be metabolised by the mitochondria. Moreover, the Seahorse EFA was to be used to determine whether the presence of one LC-FFA altered the metabolic fate of another. However, the Seahorse EFA technology proved to be challenging.

The Seahorse EFA technology has an accessible graphical user interface, and the machine itself is simple to operate. However, the preparatory steps of the Seahorse EFA increase the likelihood for error and the data output from the machine is timely to process (this was overcome by writing a Seahorse EFA script in the R statistical programming language). To obtain the results of section 5.3.3 and 5.3.4, it took a total of three years of intermittent work. In this time the advice of the Seahorse manufacturer and experts within the field was sought. In an attempt to record the oxidation rate of β-cells in response to an acute injection of glucose and LC-FFA the following steps were taken:

- Optimised the time (1-24h) required to starve the cells of serum and glucose prior to running the Seahorse EFA
- Devised a method to ensure the cells remained adhered to the Seahorse XF Cell Culture Microplate
- Devised a method to deliver the fatty acids in a way which did not induce BSA bubble formation. This included: altering the BSA: fatty acid conjugation ratios, using the Seahorse XF Palmitate-BSA FAO substrate kit, varying the BSA solvent, and trialling pre-incubating the fatty acids instead of an acute injection.
- Varying the usage of pipettes (i.e. manual, multi-dispenser and electronic) for each stage of the Seahorse EFA
- Trialing a range of cell types including INS-1E, INS-1 823/13, EndoC-βH1, BRIN-BD11 and HEK cells

- Trialing compounds which alter glucose and LC-FFA metabolism including etomoxir, methyl succinate and 2-Deoxy-D-glucose (2DG)

Consequently, due to the extensive optimisation steps required to obtain results from the Seahorse EFA, the number of repeats required in one experiment to obtain data, and the high degree of inter-experimental variability between wells; any results obtained from the Seahorse EFA technology require verification.

As literature has shown (Barlow & Affourtit, 2013; Barlow et al. 2016; Cen et al. 2016), the Seahorse EFA technology is seemingly an ideal tool for measuring the extent of fatty acid-induced mitochondrial dysfunction in β-cells after they have been pre-incubated in fatty acids. However, as a tool to measure changes in OCR of β-cells after an acute injection of fatty acids, the Seahorse EFA technology does not fit this purpose.

Measuring changes in OCR of β-cells after an acute injection of glucose or fatty acids is also confounded by the design of the Seahorse EFA technology. The Seahorse EFA is a “semiclosed” design where the cells and the probes are exposed to leakage of atmospheric O_2 (Gerencser et al. 2009). Moreover, the XF96^e 96-well cell culture plates are also made of a polystyrene material which is permeable to, and stores substantial amounts of O_2 further distorting OCR readings (Gerencser et al. 2009).

A further limitation of the Seahorse EFA is that the assay medium requires supplementation with 1mM pyruvate (as sodium pyruvate) and 2mM L-glutamine. The Seahorse EFA manufacturer training manual recommends inclusion of pyruvate and L-glutamine in the assay medium as 'their consumption is necessary for mitochondrial respiration’ (Agilent, 2018). Furthermore, upon contacting the manufacturer helpline (personal communication, 2017) for further clarification, Agilent explained that they

had identified certain cell types (such as neurons) which fail to elicit respiration without pyruvate supplementation (data not provided by the manufacturer). Subsequently, in this study, an assay was undertaken to determine whether pyruvate and L-glutamine supplementation were necessary for the EFA medium when using the Seahorse technology for β-cell lines (figure 5.17).

In INS-1E cells whose assay medium had not been supplemented with pyruvate and L-glutamine, basal respiration was significantly lower than those cells who had received pyruvate/L-glutamine. Moreover, with the addition of oligomycin, cells not treated with pyruvate/L-glutamine had only a slight decline in OCR. Conversely, INS-1E cells treated with pyruvate/L-glutamine had a greater decline in OCR with the addition of oligomycin. Consequently, it is questionable whether changes in OCR in response to glucose and LC-FFA are actual responses to these compounds or an artefact of L-glutamine and sodium pyruvate metabolism.

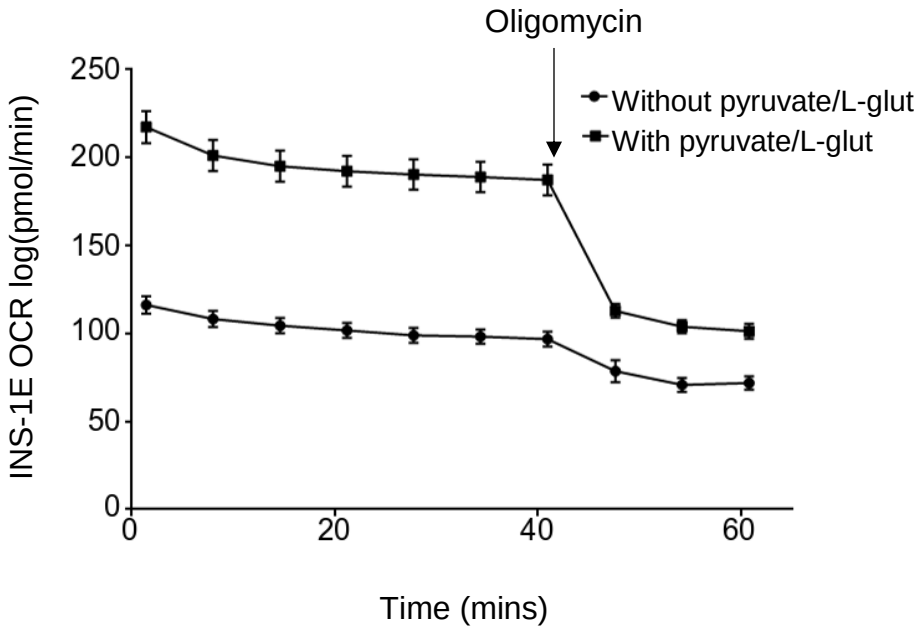

Figure 5.17 The effect of pyruvate on INS-1E cellular respiration. INS-1E cells were seeded at $20x10^3$ cells per well. INS-1E cells were starved of glucose for 2hrs and incubated for 1hr at 37°C under air prior to transferring to an XF96^e Seahorse analyser. The extracellular medium of each well-contained media either not supplemented (without pyruvate) or supplemented with 1mM sodium pyruvate (with pyruvate). Basal respiration (oxygen consumption rate (OCR)) was measured for approximately 42mins. At 42mins 1µM oligomycin was introduced to inhibit ATP synthase. Respiration was measured very 6-7mins. Experimental points were the mean of 7 replicates. Error bars represent SEM.

Future work to record the OCR of β-cells after an acute exposure to glucose or fatty acids should subsequently be verified using techniques such as oxygen microsensors which record the OCR of individual cells (Jung et al. 1999). Using tools such as microsensors to measure the OCR of individual cells would overcome many of the limitations of this technology as discussed above.

5.4.6 Summary

This study aimed to investigate the mitochondrial bioenergetics of clonal β-cells including their insulin secretory and respiratory response after an acute injection of glucose and LC-FFA. INS-1E cells secrete insulin in response to both glucose and KCl. EndoC-βH1 cells secrete insulin in response to KCl or glucose in combination with C16:0 and IBMX. EndoC-βH1 cell insulin secretory response to insulin was not enhanced by the cells being in a pseudo islet configuration. INS-1E cells oxidise glucose in a dose-responsive manner although they do not oxidise LC-FFA via mitochondrial oxidative pathways. INS-1 823/13 cells, however, oxidise C18:1 but not C16:0. The ability of INS-1 823/13 cells to oxidise C18:1 but not C16:0 may offer a potential explanation as to why INS-1 823/13 cells do not die when exposed to C18:1 but do die when treated with C16:0 (Kawai et al. 2001; Tuo et al. 2012). This is indicative that C16:0-induced cell death is not due to mitochondrial oxidation. EndoC-βH1 cells probably do not oxidise either glucose or LC-FFA. However, due to the limitations of the Seahorse EFA technology these results require verification using an alternate low-throughput method.

Chapter 6.

Discussion

The overall aim of this thesis was to elucidate the mechanisms of lipotoxicity in human-derived pancreatic β-cells. Upon beginning the study, the toxicity profile of LC-FFA was yet to be determined in the human-derived EndoC-βH1 cell line. In the period in which this PhD was being conducted, Tsonkova et al. (2018), Krizhanovskii et al. (2017) and Plotz et al. (2017) also studied the effect of LC-FFA on EndoC-βH1 cell viability, although these studies did not investigate the toxicity profile of the odd and even-chained LC-FFA. Moreover, unlike the investigations detailed in this thesis, those studies (Tsonkova et al. 2018; Krizhanovskii, 2017; Plotz et al. 2017) which have investigated lipotoxicity in EndoC-βH1 cells have not studied the subcellular distribution of LC-FFA.

Surprisingly, the EndoC-βH1 cell line proved to be the ideal model for studying β-cell lipotoxicity, as EndoC-βH1 cells are seemingly resistant to the toxic effects of LC-SFA. As rodent-derived INS-1 β-cells undergo LC-SFA induced cell death, the difference in the way human and rodent-derived β-cell lines handle LC-FFA could be compared, thereby furthering our understanding of lipotoxic mechanisms. However, as EndoC-βH1 cells are a human-derived β-cell, it poses the question: is β-cell lipotoxicity a rodent phenomenon?

Studies which have characterised the functionality of EndoC-βH1 cells have identified that they function in a manner similar to human islets (Andersson, 2015; Gurgul-Convey, 2015). Like EndoC-βH1 cells, Hall (2014) and Staff (2016) both found human islets to be resistant to the toxic effects of C16:0. Hall et al. (2014) found that treating human islets for 48h with 1mM C16:0 did not induce cell death. Moreover, Staff et al. (2016) found no increase in apoptotic markers in human islets treated with 500μM C16:0 for 2-4d. Conversely, however, Sargsyan and colleagues (2011) observed a significant increase in cell death in human islets treated for 24h with 500μM C16:0. Moreover, Maedler (2004) reported a ≥2.1 fold

increase in cell death relative to control in human islets exposed to C16:0 for 96h, at concentrations as low as 100µM. Subsequently, as EndoC-βH1 cells were found to be resistant to the toxic effects of LC-SFA, the results detailed in this study seemingly support those studies which report C16:0 not to be toxic to human islets (Hall et al. 2014; Staff et al. 2016).

In my hands, however, EndoC-βH1 cells did not secrete insulin in response to glucose and neither did they oxidise glucose via mitochondrial pathways, even at a concentration as high as 30mM (section 5.4.1). This implies that EndoC-βH1 cells do not act in a β-cell like manner as the key feature of a β-cell is its ability to secrete insulin in response to glucose. Further, Hastoy et al. (2018) found EndoC-βH1 cells to be polyhormonal, expressing somatostatin as well as insulin, which is normally secreted by islet delta cells. This may be due to EndoC-βH1 cells being foetal in origin (Ravassard et al. 2011) and subsequently they may function differently to adult β-cells for example, by being polyhormonal and not secreting insulin (Riedel et al. 2011). Although, Hastoy et al. (2018) found the transcriptomic profile of EndoC-βH1 cells to be more similar to that of adult β-cells compared to foetal. Consequently, the transcriptomic profile of EndoC-βH1 cells is likely to be different from that of human β-cells in vitro. It cannot, therefore, be reported that LC-SFA induced β-cell death is a rodent phenomenon and does not occur in human β-cells, as the genes which regulate fatty acid metabolism may also be differentially expressed in EndoC-βH1 cells. The likelihood that resistance to LC-SFA induced cell death is a feature of the EndoC-βH1 cell line cannot be discounted. Differences in the transcriptomic profile of fatty acid associated genes in EndoC-βH1 cells compared to human β-cells can now, however, be verified. Using multi-omic maps of EndoC-βH1 cells and human-derived β-cells generated by Lawlor et al. (2019) a bioinformatic investigation can

be conducted to assess differences and similarities in the transcriptomic profile of those genes associated with fatty acid metabolism in EndoC-βH1 cells relative to human β-cells.

In summary, the resistance to the toxic effects of LC-SFA by EndoC-βH1 cells supports those studies which have reported human islets also to be resistant to the toxic effects of LC-SFA. However, human islets contain more cell types than just β-cells and their resistance to LC-SFA is not universally observed. Further, EndoC-βH1 cells have features which do not coincide with β-cells such as having a modest response to, or failing to, secrete insulin in response to glucose and being polyhormonal. It can therefore not be stated with certainty that lipotoxicity is a phenomenon only seen in rodent-derived β-cells.

6.1.1 LC-FFA trafficking

In rodent derived β-cells, C16:0 became concentrated in the Golgi apparatus and activated the ER stress response. Moreover, C16:0 failed to elicit changes in mitochondrial respiration upon acute injection. With the metabolism of C18:1 however, C16:0 was found to accumulate in the cytoplasm, although, cytoplasmic accumulation of C16:0 in rodent-derived β-cells did not occur in the presence of other LC-SFA. When rodent-derived β-cells were treated with C16:0 in the presence of C18:1, the Golgi apparatus did not swell, and the ER stress response was seemingly not activated as the morphology of the ER remained unaltered. Moreover, unlike C16:0, C18:1 is oxidised by the mitochondria of rodent-derived β-cells, although to what extent remains unclear. As reported previously (Welters et al. 2004; Dhayal et al. 2008), C16:0-induced cell death was attenuated in the presence of C18:1 in rodent-derived β-cells. Strikingly, human-derived β-cells were found not to die when exposed to C16:0. Interestingly, human-derived β-cells displayed a similar C16:0 distribution to rodent-derived β-cells when they

are co-treated with both C16:0 and C18:1. In human-derived β-cells, C16:0 did not accumulate at the Golgi and neither did it cause alterations to the morphology of the ER but instead distributed in a punctate manner throughout the cytosol. The accumulation of C16:0 in the cytoplasm may be a potential mechanism for the differential toxicity profiles of C16:0 and C18:1 in rodent and human β-cells. The accumulation of C16:0 in the cytoplasm is a potential mechanism whereby C16:0 does not accumulate at organelles such as the Golgi and ER which may trigger cell death.

In Chapter 1 of this study, it was observed that inhibiting SCD1 activity was detrimental to human-derived β-cell viability. A study in murine renal proximal tubular epithelial cells (PTEC) found SCD-1 overexpression to prevent C16:0-induced cell death (Iwai et al. 2016). Moreover, C16:0-induced ER stress was attenuated upon overexpression of SCD1, and there was a reported increase in lipid droplet formation. Interestingly, treating PTEC on its own with C16:0 did not stimulate lipid droplet formation (Iwai et al. 2016). Similarly, in the murine PTEC, the LC-MUFA, C18:1 also prevented C16:0-induced cell death, inhibited C16:0-induced ER stress and increased lipid droplet formation when cells were treated with both C16:0 and C18:1 (Iwai et al. 2016). Consequently, the role of SCD1 in the resistance to LC-SFA induced cell death in human-derived β-cells requires further investigation.

In summary, the routing of C16:0 is similar in human-derived β-cells relative to rodent-derived β-cells when C18:1 is also present (and metabolised). When treated with C16:0, EndoC-βH1 cells do not die and C16:0 accumulates in the cytoplasm. Similarly, when rodent-derived β-cells are treated with both C16:0 and C18:1, cells do not die and C16:0 accumulated in the cytoplasm. The cytoplasmic accumulation of C16:0 in both human and rodent-derived β-cells requires further

investigation as does the role of SCD1 in this process. Moreover, the results detailed within this study support a role for ER stress and the accumulation of C16:0 at the Golgi apparatus in the underlying mechanism of LC-SFA induced β-cell death.

6.1.2 Limitations of this study

The main limitation of this study was the rate at which EndoC-βH1 cells proliferate. Andersson et al. (2015) reported a doubling rate of approximately 174h, which is much slower than that of INS-1 823/13 cells which replicated at a rate of approximately 44h. This made it challenging to obtain results as it often took a number of weeks to grow up enough cells to undertake three repeats of an experiment. Moreover, in the early stages of this PhD study, a working protocol to facilitate EndoC-βH1 proliferation was developed. The main points observed whilst developing this protocol included:

1. Maintaining cells in a 25cm^2 culturing vessel at a confluency of 60-70%, EndoC-βH1 cells seemingly grew best when in close proximity to one another.
2. Using sterile BSA which has been opened and stored at 4°C for more than 2 months seemingly kills EndoC-βH1 cells although the reason for this remains unclear.
3. EndoC-βH1 cells do not proliferate when CO_2 levels fluctuate at regular intervals: the cells must, therefore, reside at the back of a CO_2 incubator.

However, despite these challenges, the results recorded using EndoC-βH1 cells were consistent, and upon developing a culturing protocol which facilitated proliferation, the cells were relatively easy to handle, albeit slow in growth.

6.1.3 Overall summary

The work of this thesis aimed to elucidate the mechanisms of lipotoxicity in pancreatic β-cells. The first objective of this study was to characterise the toxicity profile of LC-FFA (odd and even LC-SFA, and LC-MUFA) in the EndoC-βH1 cell line. The LC-SFA C15:0, C16:0, C17:0 and C18:0 were not toxic to EndoC-βH1 cells, and neither was the LC-MUFA C16:1. Conversely, C19:0 caused EndoC-βH1 cell death, as did the LC-MUFA, C18:1, bafilomycin and the SCD-1 inhibitor 10,12-CLA.

The second objective of this study was to compare the effects on the viability of LC-FFA in EndoC-βH1 cells with those in the rat-derived INS-1E β-cell line. Unlike EndoC-βH1 cells, C15:0, C16:0, C17:0, C18:0 and similarly, C19:0, were all highly toxic to INS-1E cells. The LC-MUFA, C18:1 was, however, not toxic to INS-1E cells and attenuated the toxic effects of C16:0.

The final objective of this thesis was to study the subcellular distribution of LC-FFA in both human-derived EndoC-βH1 and rodent-derived INS-1 β-cell lines. In INS-1 cells C16:0 stimulated ER stress, caused apparent alterations to the ER morphology, and accumulated at the Golgi apparatus. C17:0 and C19:0 did not cause C16:0 to be routed to the cytoplasm in INS-1 cells. However, the metabolism of LC-MUFA, C18:1 caused C16:0 to accumulate in the cytoplasm in rodent-derived β-cells. Further, C16:0 was found not to be routed to the mitochondria for oxidation whereas C18:1 was. Moreover, in rodent-derived β-cells treated with both C16:0 and C18:1, the ER morphology was maintained, and the Golgi apparatus did not become swollen.

In EndoC-βH1 cells, C16:0 accumulated in the cytoplasm, with cytoplasmic distribution being unaltered in the presence of C17:0, C19:1 and C18:1. Moreover, C16:0 did not alter the morphology of the ER or Golgi apparatus of

EndoC-βH1 cells. Treatment with LC-FFA also did not alter the insulin content of EndoC-βH1 cells, although C16:0 was found to amplify GSIS in the presence of IBMX.

In summary, differences observed in the viability profile of LC-FFA in human compared to rodent β-cells may be due to differential routing of lipids.

6.1.4 Future work

Key future work should focus on determining whether lipotoxicity occurs in the pathophysiology of T2D in humans, or whether β-cell lipotoxicity is a phenomenon specific to rodent-derived β-cells. As discussed in section 1.7 of this thesis, the majority of studies which have investigated the mechanisms underlying β-cell lipotoxicity are conducted in rodent-derived β-cells. It is possible therefore that LC-SFA may not be overtly toxic to human β-cells but cause them to dedifferentiate, losing insulin production. Jeffery et al. (2019) reported an increase in somatostatin expression in EndoC-βH1 cells exposed to 500μM C16:0 for 24h. Consequently, key future experiments should aim to characterise the expression of β-cell specific markers and markers of dedifferentiation in EndoC-βH1 cells exposed to LC-FFA.

References

Aas V, Kase ET, Solberg R, Jensen J, Ruiabetstan. (2004). Chronic hyperglycaemia promotes lipogenesis and triacylglycerol accumulation in human skeletal muscle cells. *Diabetologia* 47(8): 1452-1461.

Abaraviciene SM, Lundquist I, Salehi A. (2008). Rosiglitazone counteracts palmitate-induced β-cell dysfunction by suppression of MAP kinase, inducible nitric oxide synthase and caspase 3 activities. *Cell Mol Life Sci.* 65: 2256-2265.

Abdelmagid SA, Clarke SE, Nielsen DE, Badawi A, El-Sohemy A, Mutch DM. (2015). Comprehensive profiling of plasma fatty acid concentrations in young healthy Canadian adults. *PLoS One* 10 (2): e0116195.

Abdullah A, Peeters A, de Courten M, Stoelwinder J. (2010). The magnitude of association between overweight and obesity and the risk of diabetes: a meta-analysis of prospective cohort studies. *Diabetes Res Clin Pract* 89 (3): 309-19.

Accili D, Talchai SC, Kim-Muller JY, Cinti F, Ishida E, Ordelheide AM, et al. (2016). When β-cells fail: lessons from dedifferentiation. *Diabetes Obes and Metab.* 18(1): 117-122.

Acosta-Montano P, Garcia-Gonzalez V. (2018). Effects of dietary fatty acids in pancreatic beta cell metabolism, implications in homeostasis. *Nutrients* 10(4): 393.

Affourtit C, Brand MD. (2008). Uncoupling protein-2 contributes significantly to high mitochondrial proton leak in INS-1E insulinoma cells and attenuates glucose-stimulated insulin secretion. *Biochem J* 409(1): 199-204.

Affourtit C, Jastroch M, Brand MD. (2011). Uncoupling protein-2 attenuates glucose-stimulated insulin secretion in INS-1E insulinoma cells by lowering mitochondrial reactive oxygen species. *Free Radic Biol Med* 50(5): 609-616.

Agilent technologies. (2016). Report generator user guide: Agilent Seahorse XF Cell Mito Stress Test. Retrieved 19.3.2019 from: https://www.agilent.com/cs/library/usermanuals/public/Report_Generator_User_Guide_Seahorse_XF_Cell_Mito_Stress_Test_Single_File.pdf

Agilent Technologies. (2018). XFp Intro training manual cell characterisation and stress tests. Retrieved 5.12.2018 from:

https://www.anatomy.uzh.ch/dam/jcr:0ff137db-a76b-44d9-aabd-94c3849eb86b/XFp%20Basic%20Procedures%20plus.pdf

Agilent. (2017). Agilent Mito stress user guide. Accessed 4.11.2018 from: https://www.agilent.com/cs/library/usermanuals/public/XF_Cell_Mito_Stress_Test_Kit_User_Guide.pdf.

Ahowesso C, Black PN, Saini N, Montefusco D, et al. (2015). Chemical inhibition of fatty acid absorption and cellular uptake limits lipotoxic cell death. *Biochem Pharmacol* 98(1): 167-181.

Aikin R, Maysinger D, Rosenberg L. (2004). Cross-talk between phosphatidylinositol 3-kinase/AKT and c-jun NH2-terminal kinase mediates survival of isolated human islets. *Endocrinology* 145 (10): 4522-4531.

Ainscow EK, Zhao C, Rutter GA. (2000). Acute overexpression of lactate dehydrogenase-A perturbs beta-cell mitochondrial metabolism and insulin secretion. *Diabetes* 49 (7):1140-1155.

Ali, O. (2013). Genetics of type 2 diabetes. *World J Diabetes* 4 (4): 114-123

Amisten S, Salehi A, Rorsman P, Jones PM, Persaud SJ. (2013). An atlas and functional analysis of G-protein coupled receptors in human islets of Langerhans. *Pharmacol Ther* 139 (3): 359-391.

Andersson LE, Valtat B, Bagge A, Sharoyko VV, et al. (2015). Characterisation of stimulus-secretion coupling in the human pancreatic EndoC-BH1 beta cell line. *PLoS One* 10 (3): e0120879.

Anello M, Lupi R, Spampinato D, Piro S, Masini M, Boggi U, et al. (2005). Functional and morphological alterations of mitochondria in pancreatic beta cells from type 2 diabetic patients. *Diabetologia* 48 (2): 282-289.

Arner P, Kulyte A, Batchelor K, Larenchikiene J, Livingston J, Ryden M. (2018). Mapping of biguanide transporters in human fat cells and their impact on lipolysis. *Diabetes Obes Metab* 20 (10): 2416-2425

Asfari M, Janjic D, Meda P, Halban PA, Wollheim CB. (1992). Establishment of 2-mercaptoethanol-dependent differentiated insulin-secreting cell lines. *Endocrinology* 130 (1): 167-178.

Ashcroft FM, Rorsman P. (2018). Diabetes mellitus and the β-cell: the last ten years. *Cell* 148 (6): 1160-1171.

Bachar E, Ariav Y, Ketzinel-Gilad M, Cerasi E, Kaiser N, Leibowitz G. (2009). Glucose amplifies fatty acid-induced endoplasmic reticulum stress in pancreatic β-cells via activation of mTORC1. *PLoS One* 4 (3): e4954.

Bailey CJ, Tahrani AA, Barnett AH. (2016). Future glucose-lowering drugs for type 2 diabetes. *Lancet Diabetes Endocrinol* 4 (4): 350-359.

Baldwin AC, Green CD, Olson LK, Moxlet MA, Corbett JA. (2012). A role for aberrant protein palmitoylation in FFA-induced ER stress and β-cell death. *Am J Physiol Endocrinol Metab* 302 (11): E1390-E1398.

Bankaitis A, Garcia-Mata R, Mousley CJ. (2012). Review: Golgi Membrane Dynamics and lipid metabolism. *Curr Biol* 22 (10): 414-424.

Barlow J, Affourtit C. (2013). Novel insights into pancreatic β-cell glucolipotoxicity from real-time functional analysis of mitochondrial energy analysis of mitochondrial energy metabolism in INS-1E insulinoma cells. *Biochem J* 456 (3): 417-426.

Barlow J, Jensen VH, Affourtit C. (2015a). Uncoupling protein-2 attenuates palmitoleate protection against the cytotoxic production of mitochondrial reactive oxygen species in INS-1E insulinoma cells. *Redox Biol* 4: 14-22.

Barlow J, Jensen VH, Jastroch M, Affourtit C. (2016). Palmitate-induced impairment of glucose-stimulated insulin secretion preceded mitochondrial dysfunction in mouse pancreatic islets. *Biochem J* 473(4): 487-496.

Barlow J, Solomon TPJ, Affourtit C. (2018). Pro-inflammatory cytokines attenuate glucose-stimulated insulin secretion from INS-1E insulinoma cells by restricting mitochondrial pyruvate oxidation capacity. *PLoS One* 13(6): e0199505.

Barzilai N, Ferucci L. (2012). Insulin resistance and aging: a cause or a protective response? *J Gerontol A Biol Sci Med Sci*. 67(12): 1329-1331.

Bassi, M. Carmo JM, Silva AA. (2013). Chronic effects of centrally administered adiponectin on appetite, metabolism and blood pressure regulation in normotensive and hypertensive rats. *Peptides* 37 (1): 1-5.

Bastaki, S. (2005). Diabetes mellitus and its treatment. *Int J Diabetes & Metabolism* 13: 111-134.

Basu S, Campbell HM, Dittel BN, Ray A. (2010). Purification of specific cell population by fluorescence activated cell sorting (FACS). *J Vis Exp* 41: 1546.

Becam J, Walter T, Burgert A, Schlegel J, Sauer M, Seibel, Schubert-Unkmeir A. (2017). Antibacterial activity of ceramide and ceramide analogs against pathogenic Neisseria. *Sci Rep* 7: 17627.

Best CH, Scott DA. (1923). The preparation of insulin. *J Biol Chem* 57: 709-723.

Bikman BT, Summers SA. (2011). Ceramides as modulators of cellular and whole-body metabolism. *J Clin Invest* 121(11): 4222-4230.

Blair M. (2016). Diabetes Mellitus Review. *Urol Nurs* 36 (1): 27-36.

Boden G, Chen X, Ruiz J, White JV, Rossetti L. (1994). Mechanisms of fatty-acid inhibition of glucose uptake. *J Clin Invest* 93 (6): 2438-2446.

Boden G. (2008). Obesity and free fatty acids. *Endocrinol Metab Clin North Am.* 37 (3): 635-646.

Bonner-Weir S, Veld PAI, Weir GC. (2014). Reanalysis of study of pancreatic effects of incretin therapy: methodological deficiencies. *Diabetes Obese Metab*. 16 (7): 661-666.

Borg J, Klint C, Wierup N, Strom K, Larsson S, Sundler F, Lupi R, et al. (2009). Perilipin is present in islets of Langerhans and protects against lipotoxicity when overexpressed in the β-cell line INS-1. *Endocrinology* 150(7): 3049-3057.

Borradaile NM, Han X, Harp JD, Gale SE, Ory DS, Schafffer JE. (2006). Disruption of endoplasmic reticulum structure and integrity in lipotoxic cell death. *J Lipid Res* 47(12): 2726-37.

Boslem E, Weir JM, MacIntosh G, Sue N, Cantley J, Meikle PJ, Biden TJ. (2013). Alteration of endoplasmic reticulum lipid rafts contributes to lipotoxicity in pancreatic β-cells. *J Biol Chem* 288(37): 26569-26582.

Box GEP. (1954). Some theorems on quadratic forms applied in the study of analysis of variance problems, I. Effect of inequality of variance in the one-way classification. *Ann Math Statist.* 25(2): 290.

Brand MD, Harper ME, Taylor HC. (1993). Control of the effective P/O ratio of oxidative phosphorylation in liver mitochondria and hepatocytes. *Biochem J.* 291 (3): 739-48.

Brand MD, Nicholls DG. (2011). Assessing mitochondrial dysfunction in cells. *Biochem J* 435 (2): 297-312.

Breslow DK. (2013). Sphingolipid homeostasis in the endoplasmic reticulum and beyond. *Cold Spring Harb Perspect Biol.* 5(4); a013326.

Briscoe CP, Tadayyon M, Andrews JL, Benson WG, Chambers JK, Eilert MM, et al. (2002). The orphan G protein-coupled receptor GPR40 is activated by medium and long chain fatty acids. *J Biol Chem* 278: 11303-11311.

Brissova M, Fowler MJ, Nicholson WE, Chu A, Hirshberg B, Harlan DM, Powers AC. (2005). Assessment of human pancreatic islet architecture and composition by laser scanning confocal microscopy. *J Histochem Cytochem.* 53(9): 1087-97.

Brock B, Hermansen K. (2004). Long-term exposure to INS-1 cells to cis and trans fatty acids influences insulin release and fatty acid oxidation differentially. *Metabolism* 53 (9): 1158-1165.

Burdge GC. (2006). Metabolism of α-linoleic acid in humans. *Prostaglandins Leukot and Essent Fatty Acids*. 75 (3): 161-168.

Busch AK, Cordery D, Denyer GS, Biden TJ. (2002). Expression profiling of palmitate- and oleate- regulated genes provides novel insights into the effects of chronic lipid exposure on pancreatic β-cell function. *Diabetes* 51(4):977-987.

Busch AK, Gurisik E, Cordery DV, Sudlow M, Denyer GS, et al. (2005). Increased fatty acid desaturation and enhanced expression of Stearoyl Coenzyme A Desaturase protects pancreatic β-cells from lipoapoptosis. *Diabetes* 54(10): 2917-2924.

Butler AE, Janson J, Bonner-Weir S, Ritzel R, Rizza RA, Butler PC. (2003). Beta-cell deficit and increased beta-cell apoptosis in humans with type 2 diabetes. *Diabetes* 52 (1): 102-110.

Caicedo, A. (2013). Paracrine and autocrine interactions in the human islet: more than meets the eye. *Semin Cell Dev Biol.* 24 (1): 11-21.

Carta G, Murru E, Banni S, Manca C. (2017). Palmitic acid: physiological role, metabolism and nutritional implications. *Front Physiol* 8:902.

Carta G, Murru E, Lisai S, Sirigu A, Piras A, Collu M, et al. (2015). Dietary triacylglycerols with palmitic acid in the sn-2 position modulate levels of N-acylethanolmides in rat tissues. *PLoS ONE* 10(3): e0120424.

Cen J, Sargsyan E, Bergsten P. (2016). Fatty acids stimulate insulin secretion from human pancreatic islets at fasting glucose concentrations via mitochondria-dependent and –independent mechanisms. *Nutr Metab (Lond).* 13(1):59

Cerf ME. (2013). Beta cell dysfunction and insulin resistance. *Front Endocrinol* 4:37.

Chandra R, Liddle RA. (2009). Neural and hormonal regulation of pancreatic secretion. *Curr Opin Gastroenterol* 25 (5): 441-446.

Chandrasekera C, Pippin JJ. (2013). Of rodents and men: species-specific glucose regulation and type 2 diabetes research. *ALTEX* 31(2): 157-176.

Chang YC, Hee SW, Hseih ML, Jeng YM and Chuang LM. (2015). The role of organelle stresses in diabetes mellitus and obesity: implication for treatment. *Anal Cell Pathol (Amst)*: 972891.

Chang-Chen KJ, Mullue R, Bernal-Mizrachi E. (2008). β-cell failure as a complication of diabetes. *Rev Endocr Metab Disord* 9: 329-343.

Chen YY, Sun LQ, Wang BA, Zou XM, Mu YM, Lu JM. (2013). Palmitate induces autophagy in pancreatic β-cells via endoplasmic reticulum stress and its downstream JNK pathway. *Int J Mol Med* 32 (6): 1401-1406.

Choi SE, Lee SM, Lee YJ, Li LJ, Lee SJ et al. (2009). Protective role of autophagy in palmitate-induced INS-1 beta cell death. *Endocrinology* 150 (1): 126-34.

Choi SH, Ginsber HN. (2011). Increased very low density lipoprotein secretion, hepatic steatosis, and insulin resistance. *Trends Endocrinol Metab* 22(9): 353-363.

Choudhary A, Hu He K, Mertins P, Udeshi N. (2014). Quantitative-proteomic comparison of alpha and beta cells to uncover novel targets for lineage reprogramming. *PLoS ONE* 9(4): e95194.

Chu KY, O'Reilly L, Mellet N, Meikle PJ, Bartley C, Biden TJ. (2018). Oleate disrupts cAMP signalling, contributing to potent stimulation of pancreatic β-cell autophagy. *J Biol Chem* 294 (4): 1218-1229.

Cistola DP, Hamilton JA, Jackson D, Small DM. (1988). Ionisation and phase behaviour of fatty acids in water: application of the Gibbs phase rule. *Biochemistry* 27: 1881-1888.

Cnop M, Hannaert JC, Hoorens A, Eizirik DL, Pipeleers DG. (2001). Inverse relationship between cytotoxicity of free fatty acids in pancreatic islet cells and cellular triglyceride accumulation. *Diabetes* 50 (8): 1771-1777.

Crespin SR, Greenough WB, Steinberg D. (1973). Stimulation of insulin secretion by long-chain free fatty acids. A direct pancreatic effect. *J Clin Invest* 52 (8): 1979-1984.

Cummings BS, Wills LP, Schnellmann RG. (2013). Measurement of cell death in mammalian cells. *Curr Protoc Pharmacol* 1:1-12.

Cunha DJ, Hekerman P, Ladriere L, Bazarra-Castro et al. (2008). Initiation and execution of lipotoxic ER stress in pancreatic β-cells. *J Cell Sci* 121(014): 2308-2318.

Dabelea D, Mayer-Davis EJ, Saydah S, et al. (2014). Prevalence of type 1 and type 2 diabetes among children and adolescents from 2001 to 2009. *JAMA* 311(17): 1778-1786.

Daemen S, van Zandvoort MAMJ, Parekh SH, Hesselink KC. (2016). Microscopy tools for the investigation of intracellular lipid storage and dynamics. *Mol Metab* 5 (3): 153-163.

Davis, RJ. (2000). Signal transduction by the JNK group of MAP kinases. *Cell* 103(2): 239-252.

De Vos A, Heimberg H, Quartier E, Huypens P, Bouwens L, Pipeleers D, Schuit F. (1995). Human and rat beta cells differ in glucose transporter but not in glucokinase gene expression. *J Clin Invest* 96(5): 2489-2495.

Del Guerra S, Bugliania M, D'Aleo V. et al. (2010). G-protein coupled receptor 40 (GPR40) expression and its regulation in human pancreatic islets: the role of type 2 diabetes and fatty acids. *Nutr Metab Cardiovasc Dis* 20 (1): 22-25.

Dhayal S, Morgan NG. (2011). Pharamacological characterisation of the cytoprotective effects of polyunsaturated fatty acids in insulin-secreting BRIN-BD11 cells. *Br J Pharmacol* 162 (6): 1340-1350.

Dhayal S, Morgan NG. (2011). Structure-activity relationships influencing lipid-induced changes in elf2α phosphorylation and cell viability in BRIN-BD11 cells. *FEBS Lett* 585 (14): 2243-2248.

Dhayal S, Welters HJ, Morgan NG. (2008). Structural requirements for the cytoprotective actions of monounsaturated fatty acids in the pancreatic β-cell line, BRIN-BD11. *Br J Pharmacol* 153(8): 1718-1727.

DiabetesUK. (2017). Diabetes Prevalence 2017 (November 2017). Retrieved 25.10.2018 from: https://www.diabetes.org.uk/professionals/position-statements-reports/statistics/diabetes-prevalence-2017

Diakogiannaki E, Dhayal S, Childs CE, Calder PC, Welters HJ, Morgan NG. (2007). Mechanisms involved in the cytotoxic and cytoprotective actions of saturated versus monounsaturated long-chain fatty acids in pancreatic β-cells. *J Endocrinol* 194 (2): 283-291.

Diakogiannaki E, Welter HJ, Morgan NG. (2008). Differential regulation of the endoplasmic reticulum stress response in pancreatic beta-cells exposed to long-chain saturated and monounsaturated fatty acids. *J Endocrinol* 197 (3): 553-63.

Diedisheim M, Oshima M, Albagli O, Huldt CW, Ahlstedt I, et al. (2018). Modelling human pancreatic beta cell dedifferentiation. *Mol Metab* (10): 74-86.

Donath MY, Ehses JA, Maedler K, Schumann DM, Ellingsgaard H. et al. (2005). Mechanisms of β-cell death in type 2 diabetes. *Diabetes* 54(2): S108-S113.

Donath MY, Storing J, Maedler K, Mandrup-Poulsen T. (2003). Inflammatory mediators and islet β-cell failure: a link between type 1 and type 2 diabetes. *J Mol Med (Berl)* 81 (8): 455-470.

Dong H, Czaja M. (2011). Regulation of lipid droplets by autophagy. *Trends Endocrinol Metab* 22 (6): 234-240.

Donnelly KL, Smith CI, Schwarzenberg SJ, Jessurun J, Boldt MD, Parks EJ. (2005). Sources of fatty acids stored in liver and secreted via lipoproteins in patients with non-alcoholic fatty liver disease. *J Clin Invest* 115 (5): 1343-1351.

Duncan BB, Schmidt MI, Pankow JS, Bang H, Couper D, Ballantyne CM, Hoogeveen RC, Heiss G. (2004). The atherosclerosis risk in communities study. *Diabetes* 53(9): 2473-2478.

Dunn KW, Kamocka MM, McDonald JH. (2011). A practical guide to evaluating colocalisation in biological microscopy. *Am J Physiol Cell Physiol* 300(4): 723-742.

Dunnett CW. (1964). New tables for multiple comparisons with a control. *Biometrics* 20: 482-491.

Boslem E, MacIntosh G, Preston AM, Bartlyey C, Busch AK, Fuller M, et al. (2011). A lipidomic screen of palmitate-treated MIN6 β-cells links sphingolipid metabolites with endoplasmic reticulum (ER) stress and impaired protein trafficking. *Biochem J* 435: 267-76.

Ebato C, Uchida T, Arakawa M, Kawamori R, Fujitani Y. (2008). Autophagy is important in islet homeostasis and compensatory increase of beta cell mass in response to high-fat diet. *Cell Metab* 8(4): 325-332

Eckel, R., H. Kahn, S., E. Ferrannini, E., Goldfine, A., B. Nathan, D., M. Schwartz, M., W. Smith, R., J. and Smith, S., R. (2011). Obesity and type 2 diabetes: what can be unified and what needs to be individualised? *J Clin Endocrinol Metab.* 96 (6): 1654-1663.

Eitel K, Staiger H, Rieger J, Mischak H, Brandhorst H, Brendel MD et al. (2003). Protein kinase C delta activation and translocation to the nucleus are required for fatty acid-induced apoptosis of insulin-secreting cells. *Diabetes* 52 (4): 991-997.

El-Assaad W, Buteau J, Peyot ML, Nolan C, Roduit R, Hardy S, Joly E, Dbaibo G, Rosenberg L, Prentki M. (2003). Saturated fatty acids synergise with elevated glucose to cause pancreatic beta-cell death. *Endocrinology* 144 (9): 4154-4163.

El-Assaad W, Joly E, Barbeau A, Sladek R, Buteau J, Maestre I, Pepin E, Zhao S, Iglesias J, Roche E, Prentki M. (2010). Glucolipotoxicity alters lipid partitioning and causes mitochondrial dysfunction, cholesterol, and ceramide deposition and

reactive oxygen species production in INS832/13 ss-cells. *Endocrinology* 151(7): 3061-3073.

Elayat AA, el-Naggar MM, Tahir M. (1995). An immunocytochemical and morphometric study of the rat pancreatic islets. *J Anat* 186 (3): 629-637.

Elle IC, Olsen LCB, Pultz D, Rodkaer SV, Faergeman J. (2010). Something worth dyeing for: molecular tools for the dissection of lipid metabolism in Caenorhabditis elegans. *FEBS Letts* 584 (11): 2183-2193.

Elsner M, Gehrmann W, Lenzen S. (2011). Peroxisome-generated hydrogen peroxide as important mediator of lipotoxicity in insulin-producing cells. *Diabetes* 60(1): 200-208.

Fagone P, Jackowski S. (2009). Membrane phospholipid synthesis and endoplasmic reticulum function. *J Lipid Res.* 50: S311-S316.

Farfari S, Schulz V, Corkey B, Prentki M. (2000). Glucose-regulated anaplerosis and cataplerosis in pancreatic β-cells. *Diabetes* 49 (5): 718-726.

Fariss MW, Chan CB, Patel M, van Houten B, Orrenius S. (2005). Role of mitochondria in toxic oxidative stress. *Mol Interv.* 5 (2): 94-111.

Ferdaoussi M, Bergeron V, Zarrouki B, Kolic J, Cantley J, Fielitz J, Olson EN, et al. (2012). G protein-coupled receptor (GPR) 40-dependent potentiation of insulin secretion in mouse islets is mediated by protein kinase D1. *Diabetologia* 55(10): 2682-2692.

Fernandez-Real JM, Vendrell J, Ricart W. (2005). Circulating adiponectin and plasma fatty acid profile. *Clin Chem.* 51(3): 603-609.

Festa A, Williams K, D'Agostino R, Wagenknecht LE, Haffner SM. (2006). The natural course of β-cell function in nondiabetic and diabetic individuals: The insulin resistance atherosclerosis study. *Diabetes* 55 (4): 1114-1120.

Fex M, Nitert MD, Wierup N, Sundler F, Ling C, Mulder H. (2007). Enhanced mitochondrial metabolism may account for the adaptation to insulin resistance in islets from C57BL/6J mice fed a high-fat diet. *Diabetologia* 50 (1): 74-83.

Flowers JB, Rabaglia ME, Schueler KL, Flowers MT, Lan H, Keller MP et al. (2007). Loss of stearoyl-CoA desaturase-1 improves insulin sensitivity in lean

mice but worsens diabetes in leptin-deficient obese mice. *Diabetes* 56(5): 1228-1239.

Fonseca SG, Gromada J, Urano F. (2011). Endoplasmic reticulum stress and pancreatic beta cell death. *Trends Endocrinol Metab.* 22(7): 266-274.

Forouhi NG, Koulman A, Sharp SJ, Imamura F, Kroger J, et al. (2014). Differences in the prospective association between individual plasma phospholipid saturated fatty acids and incident type 2 diabetes: the EPIC-InterAct case-cohort study. *Lancet Diabetes Endocrinol* 10 (2): 810-818.

Fox CS, Massaro JM, Hoffmann U, Pou KM, Maurovich-Horvat P, Liu CY, Vasan RS, et al. (2007). Abdominal visceral and subcutaneous adipose tissue compartments: association with metabolic risk factors in the Framingham Heart Study. *Circulation* 116 (1): 39-48.

Frayling TM, Timpson NJ, Weedon MN, Zeggini E, et al. (2007). A common variant in the *FTO* gene is associated with body mass index and predisposes to childhood and adult obesity. *Science* 316 (5826): 889-894.

Fu Z, Gilbert ER, Liu D. (2013). Regulation of insulin synthesis and secretion and pancreatic beta cell dysfunction in diabetes. *Curr Diabetes Rev.* 9 (1): 25-53.

Fuchsberger C, Flannick J, McCarthy MI. (2016). The genetic architecture of type 2 diabetes. *Nature* 536 (7614):41-47.

Furstova V, Kopska T, James RFL, Kovar J. (2008). Comparison of the effect of individual saturated and unsaturated fatty acids on cell growth and death induction in the human pancreatic β-cell line NES2Y. *Life Sci* 82 (13-14): 684-691.

Gehrmann W, Elsner M, Lenzen S. (2010). Role of metabolically generated reactive oxygen species for lipotoxicity in pancreatic β-cells. *Diabetes Obes Metab.* 12(2): 149-158.

Gehrmann W, Wurdemann W, Plotz T, Jorns A, Lenzen S, Elsner M. (2015). Antagonism between saturated and unsaturated fatty acids in ROS mediated lipotoxicity in rat insulin-producing cells. *Cell Physiol Biochem* 36(3): 852-865.

Gerencser AA, Neilson A, Choi SW, Edman U, Yadava N, Oh RJ, et al. (2009). Quantitative microplate-based respirometry with correction for oxygen diffusion. *Anal Chem* 81(61): 6868-6878.

Gidalevitz T, Stevens F, Argon Y. (2013). Orchestration of secretory protein folding by ER chaperones. *Biochim Biophys Acta* 1833(11): 2410-2424.

Giussani P, Maceyka M, Le Stunff H, Mikami A, Lepine S, Wang E, Kelly S, Merrill AH, Milstein S, Spiegel S. (2006). Sphingosine-1-phosphate phosphohydrolase regulates endoplasmic reticulum-to-golgi trafficking of ceramide. *Mol Cell Biol.* 26 (13): 5055-69.

Glatz JF, Luiken JJ, Bonen A. (2010). Membrane fatty acid transporters as regulators of lipid metabolism: implications for metabolic disease. *Physiol Rev* 90(1): 367-417.

Gohring I, Sharoyko VV, Malmgren S, Andersson LE, Spegal P, Nicholls DG, Mulder H. (2013). Chronic high glucose and pyruvate levels differentially affect mitochondrial bioenergetics and fuel-stimulated insulin secretion from clonal INS-1 823/13 cells. *J Biol Chem* 289 (6): 3786-3798.

Graciano MF, Valle MM, Kowluru A, Curi R, Carpinelli AR. (2011). Regulation of insulin secretion and reactive oxygen species production by free fatty acids in pancreatic islets. *Islets* 3(5): 213-23.

Grapov D, Adams SH, Pedersen TL, Garvey WT, Newman JW. (2012). Type 2 diabetes associated changes in the plasma non-esterified fatty acids, oxylipins and endocannabinoids. *PLoS One* 7(11): e48852.

Gravena C, Mathias PC, Ashcroft SJH. (2002). Acute effects of fatty acids on insulin secretion from rat and human islets of Langerhans. *J Endocrinol* 173 (1): 73-80.

Green AD, Vasu S, McClenaghan NH, Flatt PR. (2015). Pseudoislet formation enhances gene expression, insulin secretion and cytoprotective mechanisms of clonal human insulin-secreting 1.1B4 cells. *Pflugers Arch* 467(10): 2219-2228.

Grygiel-Gorniak B. (2014). Peroxisome proliferator-activated receptors and their ligands: nutritional and clinical implications. *Nutr J* 13:17.

Guha P, Kaptan E, Gade P. Kalvakolanu DV, Ahmed H. (2017). Tunicamycin induced endoplasmic reticulum stress promotes apoptosis of prostate cancer cells by activating mTORC1. *Oncotarget* 8(40): 68191-68207.

Gurgul-Convey E, Kaminski MT, Lenzen S. (2015). Physiological characterisation of the human EndoC-βH1 β-cell line. *Biochem Biophys Res Commun* 464(1): 13-9.

Hagman DK, Hays LB, Parazzoli SD, Poitout V. (2005). Palmitate inhibits insulin gene expression by altering PDX-1 nuclear localisation and reducing MAFA expression in isolated rat islets of Langerhans. *J Biol Chem.* 280(37): 32413-32418.

Halban PA, Polonsky KS, Bowden DW, Hawkins MA, Ling C, Mather KJ, Powers AC, Rhodes CJ, Sussel L, Weir GC. (2014). B-cell failure in type 2 diabetes: postulated mechanisms and prospects for prevention and treatment. *J Clin Endocrinol Metab* 37(6): 1751-1758.

Hall E, Volkov P. Dayeh T, Bacos K, Ronn T, Nitert MD, Ling C. (2014). Effects of palmitate on genome-wide mRNA expression and DNA methylation patterns in human pancreatic islets. *BMC Med* 12:103.

Hamid YH, Vissing H, Holst B et al. (2005). Studies of relationships between variation of the human G protein-coupled receptor 40 gene and type 2 diabetes and insulin resistance. *Diabet Med* 22 (1): 74-80.

Hamilton JA. (2003). Fast flip-flop of cholesterol and fatty acids in membranes: implications for membrane transport proteins. *Curr Opin in Lipidol* 14(3): 263-271.

Han J, Kaufman RJ. (2016). The role of ER stress in lipid metabolism and lipotoxicity. *J Lipid Res* 57(8): 1329-1338.

Hannigan AM, Gorski SM. (2009). Macroautophagy: the key ingredient to a healthy diet. *Autophagy* 5(2): 140-151.

Hannun YA, Obeid LM. (2008). Principles of bioactive lipid signalling: lessons from sphingolipids. *Nat Rev Mol Cell Biol* 9 (2): 139-150.

Hannun YA, Obeid LM. (2018). Sphingolipids and their metabolism in physiology and disease. *Nat Rev Mol Cell Biol* 19 (3): 175-191.

Hardy OT, Czech MP, Corvera S. (2012). What causes the insulin resistance underlying obesity. *Curr Opin Endocrinol Diabetes Obes* 19(2): 81-97.

Haus JM, Kashyap SR, Kasumov T, Zhang R, Kelly KR, Defronzo RA, Kirwan JP. (2009). Plasma ceramides are elevated in obese subjects with type 2 diabetes and correlate with the severity of insulin resistance. *Diabetes* 58 (2): 337-343.

Health Survey for England. (2013). The Health and Social Care Information Centre. Health Survey for England – 2012 trend tables. Retrieved 11.5.2019 from: https://digital.nhs.uk/data-and-information/publications/statistical/health-survey-for-england/health-survey-for-england-2012-trend-tables.

Hegarty BD, Furler SM, Ye J, Cooney GJ, Kraegen EW. (2003). The role of intramuscular lipid in insulin resistance. *Acta Physiol Scand* 178(4): 373-83.

Hellemans KH, Hannaert JC, Denys B, Steffensen KR, Raemdonck C, Martens GA, Van Veldhoven PP, Gustafsson JA, Pipeleers D. (2009). Susceptibility of pancreatic beta cells to fatty acids is regulated be LXR/PPARα-dependent stearoyl-coenzyme A desaturase. *PLoS One* 4(9): e7266.

Heredia FP, Sanchez J, Priego T, Laque E, Portillo MP, Palou A, Zamora S. (2009). Adiponectin is associated with serum and adipose tissue fatty acid composition in rats. *J Endocrinol Invest* 32(8): 659-665.

Hex N, Bartlett C, Wright D, Taylor M, Varley D. (2012). Estimating the current and future costs of type 1 and type 2 diabetes in the UK, including direct health costs and indirect societal and productivity costs. *Diabet. Med* 29 (7): 855-862.

Higa M, Shimabukuro M, Shimajiri Y, Takasu N, Shinjyo T, Inaba T. (2006). Protein kinase B /Akt signalling is required for palmitate-induced β-cell lipotoxicity. *Diabetes Obes Metab* 8 (2): 228-233.

Hohmeier HE, Mulder H, Chen G, Henkel-Rieger R, Prentki M, Newgard CB. (2000). Isolation of INS-1 derived cell lines with robust ATP-sensitive K^+ channel-dependent and independent glucose-stimulated insulin secretion. *Diabetes* 49(3): 424-430.

Holman N, Forouhi NG, Goyder E, et al. (2010). The Association of Public Health Observatories (APHO) Diabetes Prevalence Model: estimates of total diabetes prevalence for England. *Diabet Med* 28(5): 575-582.

Holness MJ, Smith ND, Greenwood GK, Sugden MC. (2007). PPAR alpha activation reverses adverse effects induced by high-saturated fat feeding on pancreatic beta-cell function in late pregnancy. *Am J Physiol Endocrinol Metab* 292 (4): E1087-E1094.

Hoppa MB, Collins S, Ramracheya R, Hodson L, Amisten S, Zhang Q, Johnson P, Ashcroft FM, Rorsman P. (2013). Chronic palmitate exposure inhibits insulin secretion by dissociation of Ca^{2+} channels from secretory granules. *Cell Metab* 10 (6): 455-465.

Huang-Doran I, Sleigh A, Rochford JJ, Rahilly S, Savage DB. (2010). Lipodystrophy: metabolic insights from a rare disorder. *J Endocrinol* 207 (3): 245-255.

Huber AH, Kleinfeld AM. (2017). Unbound free fatty acid profiles in human plasma and the unexpected absence of unbound palmitoleate. *J Lipid Res* 58(3): 578-585.

Hue L, Taegtmeyer H. (2009). The Randle cycle revisited: a new head for an old hat. *Am J Physiol Endocrinol Metab* 297(3): E578-E591.

Iglesias J, Barg S, Vallois D, Lahiri S, Roger C, et al. (2012). PPARβ/δ affects pancreatic β cell mass and insulin secretion in mice. *J Clin Invest* 122(11): 4105-4117.

Igoillo-Esteve M, Marselli L, Cunha DA, Ladriere L, Ortis F, et al. (2010). Palmitate induces a pro-inflamatory response in human pancreatic islets that mimics CCL2 expression by beta cells in type 2 diabetes. *Diabetologia* 53(7): 1395-1405.

Indulekha K, Anjana RM, Surendar J, Mohan V. (2011). Association of visceral and subcutaneous fat with glucose intolerance, insulin resistance, adipocytokines and inflammatory markers in Asian Indians. *Clin Biochem* 44(4): 281-287.

Ionescu-Tirgoviste, C., Gagniuc, P., A., Gubceac, E., Mardare, L., Popescu, I., Dima, S., Militaru, M. (2015). A 3D map of the islet routes throughout the healthy human pancreas. *Sci Rep* 5: 14634.

Ishii M, Maeda A, Tani S, Akagawa M. (2015). Palmitate induces insulin resistance in human HepG2 hepatocytes by enhancing ubiquitination and proteasomal degradation of key insulin signalling molecules. *Arch Biochem Biophys* 566: 26-35.

Itoh Y, Kawamata Y, Harada M, Kobayashi M, Fujii R, et al. (2003). Free fatty acids regulate insulin secretion from pancreatic β cells through GPR40. *Nature* 422 (6928): 173-176.

Iverson SL, Orrenius S. (2004). The cardiolipin-cytochrome c interaction and the mitochondrial regulation of apoptosis. *Arch Biochem Biophys* 423(1): 37-46.

Jang IS, Hwang DY, Lee JE, Kim YK, Kang TS, et al. (2003). Effects of conjugated linoleic acid and stearic acid on apoptosis of the INS-1 β-cells and pancreatic islets isolated from Zucker Obese (fa/fa) rats. *Asian-Australas J Anim Sci* 16(7): 1060-1065.

Jefferies KC, Cipriano DJ, Forgac M. (2008). Function, structure and regulation of the vacuolar (H^+)-ATPases. *Arch Biochem Biophys* 476(1):33-42.

Jeffery N, Richardson S, Chambers D, Morgan NG, Harries LW. (2019). Cellular stressors may alter islet hormone cell proportions by moderation of alternative splicing patters. *Hum Mol Genet*. Doi: 10.1093/hmg/ddz094.

Jensen MV, Joseph JW, Ronnebaum SM, Burgess SC, Sherry D, Newgard CB. (2008). Metabolic cycling in control of glucose-stimulated insulin secretion. *Am J Physiol Endocrinol Metab* 295(6): E1287-E1297.

Jezek P, Jaburek M, Holendova B and Plecita-Hlavata. (2018). Fatty acid-stimulated insulin secretion vs. lipotoxicity. *Molecules* 23:1483

Jung HS, Chung KW, Kim JW, Kim KW, Shin J. (2008). Loss of autophagy diminishes pancreatic β-cell mass and function with resultant hyperglycaemia. *Cell Metab* 8(4): 318-324.

Jurgens CA, Toukatly MN, Fligner CL, Udayasankar J, et al. (2011). β-cell loss and β-cell apoptosis in human type 2 diabetes are related to islet amyloid deposition. The *Am J Pathol* 178(6): 2632-2640

Karaskov E, Scott C, Zhang L, Teodoro T, Ravazzola M, Volchuk A. (2006). Chronic palmitate but not oleate exposure induced endoplasmic reticulum stress, which may contribute to INS-1 pancreatic β-cell apoptosis. *Endocrinology* 147 (7): 3398-3407.

Kawai T, Hirose H, Seto Y, Fujita H, Saruta T. (2001). Chronic effects of different fatty acids and leptin in INS-1 cells. *Diabetes Res Clin Pract* 51 (1): 1-8.

Khan A, Ling ZC, Landau BR. (1996). Quantifying the carboxylation of pyruvate in pancreatic islets. *J Biol Chem* 271 (5): 2539-2542.

Kharroubi I, Ladriere L, Cardozo AK, Dogusan Z, Cnop M, Eizirik DL. (2004). Free fatty acids and cytokines induce pancreatic β-cell apoptosis by different mechanisms: role of nuclear factor-KB and endoplasmic reticulum stress. *Endocrinology* 145(11): 5087-5096.

Kikukawa H, Sakuradani E, Nishibaba Y, Okuda T, Ando A, Shima J, Shimizu S, Ogawa J. (2014). Production of *cis*-11-eicosenoic acid by Mortierella fungi. *J Appl Microbiol* 118(3): 641-647.

Kim JW, Yoon KH. (2011). Glucolipotoxicity in pancreatic β-cells. *Diabetes Metab J.* 35(5): 444-450.

Knowler WC, Barrett-Connor E, Fowler SE, Hamman RF, Lachin JM, Walker EA, Nathan DM. (2002). Reduction in the incidence of type 2 diabetes with lifestyle intervention or metformin. *N Engl J Med* 346: 393-403.

Koh XH, Liu X, Teo YY. (2014). Can evidence from genome-wide association studies and positive natural selection surveys be used to evaluate the thrifty gene hypothesis in east Asians? *PLoS One* 9(10): e110974.

Komatsu M, Takei M, Ishii H, Sato Y. (2013). Glucose-stimulated insulin secretion: a newer perspective. *J Diabetes Investig* 4(6): 511-516.

Koshkin V, Dai FF, Robson-Doucette CA, Chan CB, Wheeler MB. (2008). Limited mitochondrial permeabilisation is an early manifestation of palmitate-induced lipotoxicity in pancreatic beta-cells. *J Biol Chem* 283 (12): 7936-7948.

Koshkin V, Wang X, Scherer PE, Chan CB, Wheeler MB. (2003). Mitochondrial functional state in clonal pancreatic β-cells exposed to free fatty acids. *J Biol Chem* 278 (22): 19709-19715.

Krizhanovskii C, Kristinsson H, Elksnis A, Wang X, Gavali H, Bergsten P. (2017). EndoC-βH1 cells display increased sensitivity to sodium palmitate when cultured in DMEM/F12 medium. *Islets* 9(3): e1296995.

Krssak M, Peersen K, Dresner A, DiPietro L, Vogel SM, Rothman DL, Roden M, Shulman GI. (1999). Intramyocellular lipid concentrations are correlated with insulin sensitivity in humans: a 1H NMR spectroscopy study. *Diabetologia* 42(1): 113-116.

Kruskal WH, Wallis WA. (1952). Use of ranks in one-criterion variance analysis. *J Am Stat Assoc.* 47(26): 583-621.

Kulkarni, R., N. (2004). The islet β-cell. *Int J of Biochem Cell Biol* 36 (3): 365-371.

Kumar PR, Bhansali A, Ravikiran M, Bhansali S, Dutta P, et al. (2010). Utility of glycated haemoglobin in diagnosing type 2 diabetes mellitus: a community-based study. *J Clin Endocrinol Metab* 95(6): 2832-2835.

Kurokawa M, Kornbluth S. (2012). Caspases and kinases in a death grip. *Cell* 138(5): 838-854.

Kwak HJ, Yang D, Hwang Y, Jun HS, Cheon HG. (2017). Baicalein protects rat insulinoma INS-1 cells from palmitate-induced lipotoxicity by inducing HO-1. *PLoS One* 12(4): e0176432.

Laatsch A, Merkel M, Talmud PJ, Grewal T, Beisiegel U, Heeren J. (2009). Insulin stimulates hepatic low density lipoprotein receptor-related protein 1 (LRP1) to increase postprandial lipoprotein clearance. *Atherosclerosis* 204: 105-111.

Lalloyer F, Vandewalle B, Percevault F, Torpier G, Kerr-Conte J, Oosterveer M. (2006). Peroxisome proliferator-activated receptor α improves pancreatic adaptation to insulin resistance in obese mice and reduces lipotoxicity in human islets. *Diabetes* 55(6): 1605-1613.

Lameloise N, Muzzin P, Prentki M, Assimacopoulos-Jeannet F. (2001). Uncoupling protein 2: a possible link between fatty acid excess and impaired glucose-induced insulin secretion. *Diabetes* 50(4): 803-809.

Las G, Serada SB, Wikstrom JD, Twig G, Shirihai OS. (2011). Fatty acids suppress autophagic turnover in β-cells. *J Biol Chem* 286(49): 42534-42544.

Las G, Shirihai OS. (2010). The role of autophagy in β-cell lipotoxicity and type 2 diabetes. *Diabetes Obes Metab* 12(02): 15-19.

Laukkanen O, Pihlajamaki J, Lindstrom J, Eriksson J, Valle TT, et al. (2004). Polymorphisms of the SUR1 (ABCC8) and Kir6.2 (KCNJ11) genes predict the conversion from impaired glucose tolerance to type 2 diabetes. The Finnish Diabetes Prevention Study. *J Clin Endocrinol Metab* 89(12): 6286-90.

Laybutt DR, Preston AM, Akerfeldt MC, Kench JG, Busch AK, Biankin AV. (2007). Endoplasmic reticulum stress contributes to beta cell apoptosis in type 2 diabetes. *Diabetologia* 50(4): 752-763.

Lee JH, Jung IR, Choi SE, Lee SM, Lee SJ, et al. (2014). Toxicity generated through inhibition of pyruvate carboxylase and carnitine palmitoyl transferase-1 is similar to high glucose/palmitate-induced glucolipotoxicity in INS-1 β-cells. *Mol Cell Endocrinol* 383 (1-2): 48-59.

Lee Y, Hirose H, Ohneda M, Johnson JH, McGarry JD, Unger RH. (1994). Beta-cell lipotoxicity in the pathogenesis of non-insulin-dependent diabetes mellitus of obese rate: impairment in adipocyte-beta-cell relationships. *Proc Natl Acad Sci USA* 91 (23): 10878-10882.

Lee Y, Lingvay I, Ravazzola M, Orci L, Unger RH. (2010). Pancreatic steatosis: harbinger of type 2 diabetes in obese rodents. *Int J Obes (Lond)* 34 (2): 396-400.

Lee Y, Wang MY, Kakuma T, Wang ZW, Babcock E, et al. (2001). Liporegulation in diet-induced obesity. The antisteatotic role of hyperleptinemia. *J Biol Chem.* 276(8): 5629-35.

Lenzen S, Drinkgern J, Tiedge M. (1996). Low antioxidant enzyme gene expression in pancreatic islets compared with various other mouse tissues. *Free Radic Biol Med* 20(3); 463-466.

Lenzen S. (2008). Oxidative stress: the vulnerable β-cell. *Biochem Soc Trans* 36(3): 343-347.

Lettner A, Roden M. (2008). Ectopic fat and insulin resistance. *Curr Diab Rep* 8(3): 185-91.

Levin LR, Buck J. (2015). Physiological roles of acid-base sensors. *Annu Rev Physiol* 77: 347-362.

Lewis GF, Carpentier A, Adeli K, Giacca A. (2002). Disordered fat storage and mobilisation in the pathogenesis of insulin resistance and type 2 diabetes. *Endocr Rev* 23(2): 201-229.

Li LX, Skorpen F, Egeberg K, Jorgensen IH, Grill V. (2001). Uncoupling protein-2 participates in cellular defense against oxidative stress in clonal β-cells. *Biochem Biophys Res Commun* 282 (1): 273-277.

Li Z, Zhou Z, Huang G, Hu F, Xiang Y, He L. (2013). Extendin-4 protects mitochondria from reactive oxygen species induced apoptosis in pancreatic beta cells. *PLoS One* 8(10): e76172.

Linder ME, Deschenes RJ. (2007). Palmitoylation: policing protein stability and traffic. *Nat Rev Mol Cell Biol* 8: 74-84.

Listenberger LL, Han X, Lewis SE, Cases S, Farese RV, Ory DS, Schaffer JE. (2003). Triglyceride accumulation protects against fatty acid-induced lipotoxicity. *Proc Natl Acad Sci USA* 100(6): 3077-3082.

Listenberger LL, Studer AM, Brown DA, Wolins NE. (2016). Fluorescent detection of lipid droplets and associated proteins. *Curr Protoc Cell Biol* 71(1): 4.31.1-4.31.14.

Liu E, Kitajima S, Higaki Y, Morimoto M, Sun H, Watanabe T, Yamada N, Fan J. (2005). High lipoprotein lipase activity increases insulin sensitivity in transgenic rabbits. *Metabolism* 54(1): 132-138.

Liu P, Bartz R, Zehmer JK, Ying YS, Zhu M, Serrero G, Anderson RGW. (2009). Rab-regulated interactions of early endosomes with lipid droplets. *Biochim Biophys Acta 1773*(6): 784-793.

Liu YQ, Jetton TL, Leahy JL. (2002). Beta-cell adaptation to insulin resistance. Increased pyruvate carboxylase and malate-pyruvate shuttle activity in islets of nondiabetic Zucker fatty rats. *J Biol Chem* 277(42): 39163-8.

Lizcano, J., M., Alessi, D., R. (2002). The insulin signalling pathway. *Curr Biol* 12 (7): R236-R238.

Loudet, A., Burgess, K. (2007). BODIPY dyes and their derivatives: syntheses and spectroscopic properties. *Chem Rev.* 107(11): 4891-4932.

Lovis P, Roggli E, Laybutt DR, Gattesco S, Yang JY, Widmann C, Abderrahmani A, Regazzi R. (2008). Alterations in microRNA expression contribute to fatty acid-induced pancreatic β-cell dysfunction. *Diabetes* 57(10): 2728-2736.

Lu H, Hao L, Li S, Lin L, Chen Y, Cui H et al. (2016). Elevated circulating stearic acid leads to a major lipotoxic effect on mouse pancreatice beta cells in hyperlipidaemia via a miR-34a-5p-mediated PERK/p53-dependent pathway. *Diabetologia* 59(6): 1247-1257.

Luca C, Olefsky JM. (2008). Inflammation and insulin resistance. *FEBS Lett* 582(1):97-105.

Lucas R, Parikh SJ, Sridhar S, Guo DH, Bhagatwala J, Dong Y, et al. (2013). Cytokine profiling of young overweight and obese female African American adults with prediabetes. *Cytokine* 64: 310-315.

Lupi RR, Dotta F, Marselli L, Del Guerra S, et al. (2002). Prolonged exposure to free fatty acids has cytostatic and pro-apoptotic effects on human pancreatic islets: evidence that cell death is caspase mediated, partially dependent on ceramide pathway, and Bcl-2 regulated. *Diabetes* 51 (5): 1437-1442.

Lv W, Yang T. (2012). Identification of possible biomarkers for breast cancer from free fatty acid profiles determined by GC-MS and multivariate statistical analysis. *Clin Biochem* 45 (1-2): 127-133.

Lyssenko V, Lupi R, Marchetti P, Del Guerra S, et al. (2007). Mechanisms by which common variants in the TCF7L2 gene increase risk of type 2 diabetes. *J Clin Invest* 117(8): 2155-2163.

Ma H, Fukiage, C., Kin, Y., H., Duncan, M., K., Reed, N., A., Shih, M., Azuma, M., Shearer, T., R. (2001). Characterisation and expression of Calpain 10: A novel ubiquitous calpain with nuclear localisation. *J Biol Chem* 276 (30): 28525-28531.

MacDonald MJ, Fahien LA, Mertz RJ, Rana RS. (1989). Effect of esters of succinic acid and other citric acid cycle intermediates on insulin release and inositol phosphate formation by pancreatic islets. *Arch Biochem Biophys* 269(2): 400-6.

Maedler K, Oberholzer J, Bucher P, Spinas GA, Donath MY. (2003). Monounsaturated fatty acids prevent the deleterious effects of palmitate and high glucose on human pancreatic β-cell turnover and function. *Diabetes* 52(3): 726-733.

Maedler K, Spinas GA, Dyntar D, moritz W, Kaiser N, Donath MY. (2001). Distinct effects of saturated and monounsaturated fatty acids on beta-cell turnover and function. *Diabetes* 50(1): 69-76.

Maestre I, Jordan J, Calvo S, Reig JA, Cena V, et al. (2003). Mitochondrial dysfunction is involved in apoptosis induced by serum withdrawal and fatty acids in the β-ccell line INS-1. *Endocrinology* 144(1): 335-345.

Mahajan A, Taliun D, McCarthy MI. (2018). Fine-mapping type 2 diabetes loci to single-variant resolution using high-density imputation and islet-specific epigenome maps. *Nat Genet* 50 (11): 1505-1513.

Malaisse WJ, Malaisse-Lagae F, Wright PH. (1967). Effect of fasting upon insulin secretion in rat. *Am J Physiol* 213 (4):843-848.

Malmgren S, Nicholls DG, Taneera J, Bacos K, Koeck T, Tamaddon A, et al. (2009). Tight coupling between glucose and mitochondrial metabolism in clonal β-cells is required for robust insulin secretion. *J Biol Chem* 284 (47): 32395-32404.

Malmgren S, Spegal P, Anders PH, Nagorny CL, Andersson LE, Nitert MD, et al. (2012). Coordinate changes in histone modifications, mRNA levels, and metabolite profiles in clonal INS-1 823/13 β-cells accompany functional adaptations to lipotoxicity. *J Biol Chem* 288(17): 11973-11987.

Manigrasso MR, Ferroni P, Santilli F, Taraborelli T, Guagnano MT, Michetti N, et al. (2005). Association between circulating adiponectin and interleukin-10 levels in android obesity: effects of weight loss. *J Clin Endocrinol Metab* 90: 5876-5879.

Martens, GA. (2015). Species-related differences in the proteome of rat and human pancreatic beta cells. *J Diabetes Res* 2015: 549818.

Martinez SC, Tanabe K, Cras-Meneur C, Abumrad NA, Bernal-Mizrachi E, Permutt MA. (2008). Inhibition of Foxo1 protects pancreatic islet β-cells against fatty acid and endoplasmic reticulum stress-induced apoptosis. *Diabetes* 57(4): 846-859.

Masini M, Bugliani M, Lupi R, del Guerra S, Boggi U, Filipponi F, Marselli L, et al. (2009). Autophagy in human type 2 diabetes pancreatic beta cells. *Diabetologia* 52(6): 1083-1086.

Mathers CD, Loncar D. (2006). Projections of global mortality and burden of disease from 2002 to 2030. *PLoS Med* 3(11): e442.

Maxson ME, Grinstein S. (2014). The vacuolar-type H^+-ATPase at a glance – more than a proton pump. *J Cell Sci* 127 (23): 4987-4993.

McClenaghan NH, Barnett CR, Ah-Sing E, Yasser H, Abdel-Wahab A, Finbarr P, O'Harte M, Tai-Wook Y, Swanston-Flatt SK, Flatt PR. (1996). Characterisation of a novel glucose-responsive insulin-secreting cell line, BRIN-BD11, produced by electrofusion. *Diabetes* 45(8):1132-1140.

McGarry JD, Mannaerts GP, Foster DW. (1977). A possible role for malonyl-CoA in the regulation of hepatic fatty acid oxidation and ketogenesis. *J Clin Invest* 60(1): 265-270.

Medina-Gomez G, Gray SL, Yetukuri L, Shimomura K, Virtue S, Campbell M, et al. (2007). PPAR gamma 2 prevents lipotoxicity by controlling adipose tissue expandability and peripheral lipid metabolism. *PLoS Genet* 3 (4): e64.

Medina-Gomez G, Yetukuri L, Velagapudi V, Campbell M, Blount M, Jimenez-Linan M. et al. (2009). Adaption and failure of pancreatic β cells in murine models with different degrees of metabolic syndrome. *Dis Model Mech* 2 (11-12): 582-92.

Meigs JB, Cupples LA, Wilson PW. (2000). Parental transmission of type 2 diabetes: the Framingham Offspring Study. *Diabetes* 49 (12): 2201-2207.

Meijssen S, Cabezas MC, Ballieux CGM, Derksen RJ, Erkelens DW. (2001). Insulin medicated inhibition of hormone sensitive lipase activity in vivo in relation to endogenous catecholamines in heathy subjects. *J Clin Endocrinol Metab* 86(9): 4193-4197.

Merglen A, Theander S, Rubi B, Chaffard G, Wollheim CB, Maechler P. (2004). Glucose sensitivity and metabolism-secretion coupling studied during two-year continuous culture in INS-1E insulinoma cells. *Endocrinology* 145(2): 667-678.

Mika A, Stepnowski P, Kaska L, Proczko M, Wisniewski P, Sledzinski M et al. (2016). A comprehensive study of serum odd- and branched-chain fatty acids in patients with excess weight. *Obesity* 24 (8): 1669-1676.

Mir SU, George NM, Zahoor L, Harms R, Guinn Z and Sarvetnick NE. (2015). Inhibition of autophagic turnover in beta-cells by fatty acids and glucose leads to apoptotic cell death. *J Biol Chem*. 290: 6071-6085.

Moffitt JH, Fielding BA, Evershed R, Berstan R, Currie JM, Clark A. (2005). Adverse physicochemical properties of tripalmitin in beta cells lead to morphological changes and lipotoxicity in vitro. *Diabetologia* 48(9): 1819-29.

Molina AJ, Wikstrom JD, Stiles L. et al. (2009). Mitochondrial networking protects beta cells from nutrient-induced apoptosis. *Diabetes* 58 (10): 2303-2315.

Mookerjee SA, Brand MD. (2015). Measurement and analysis of extracellular acid production to determine glycolytic rate. *J Vis Exp* 106: e53464.

Mookerjee SA, Goncalves RLS, Gerencser AA, Nicholls DG, Brand MD. (2015). The contributions of respiration and glycolysis to extracellular acid production. *Biochim Biophys Acta* 1847 (2): 171-181.

Mooradian AD. (2009). Dyslipidemia in type 2 diabetes. *Nat Clin Pract Endocrinol Metab* 5 (3): 150-159.

Moore PC, Ugas MA, Hagman DK, Parazzoli SD, Poitout V. (2004). Evidence-against the involvement of oxidative stress in fatty acid inhibition of insulin secretion. *Diabetes* 53(10): 2610-2616.

Mulder H, Ling C. (2009). Mitochondrial dysfunction in pancreatic beta-cells in Type 2 diabetes. *Mol Cell Endocrinol* 297: 34-40.

Muraro MJ, Dharmadhikari G, Grun D, Dielen T, Jansen E, et al. (2016). A single-cell transcriptome atlas of the human pancreas. *Cell Syst* 3 (4): 385-394.

Murea, M, Lijun M, Freedman BI. (2012). Genetic and environmental factors associated with type 2 diabetes and diabetic vascular complications. *Rev Diabet Stud* 9(1): 6-22.

Nagasumi K, Esako R, Iwachidow K, Yasuhara Y, Ogi K, Tanaka H, Nakata M, et al. (2009). Overexpression of GPR40 in pancreatic β-cells augments glucose-stimulated insulin secretion and improves glucose tolerance in normal and diabetic mice. *Diabetes* 58(5): 1067-1076.

Natalicchio A, Labarbuta R, Tortosa F, Biondi G, Marrano N, Peschechera A, Carchia E, et al. (2013). Extendin-4 protects pancreatic β-cells from palmitate-induced apoptosis by interfering with GPR40 and the MKK4/7 stress kinase signalling pathway. *Diabetologia* 56 (11): 2456-2466.

National Institute for Health and Care Excellence. (2014). Obesity: Identification, assessment and management of overweight and obesity in children, young people and adults. Accessed 28.10.2018 from: https://www.nice.org.uk/guidance/cg189/evidence/obesity-update-full-guideline-pdf-193342429

National Institute for Health and Care Excellence. (2015). Type 2 diabetes in adults: management. Accessed 2.11.2018 from: https://www.nice.org.uk/guidance/ng28.

Nemcova-Furstova V, James RFL. Kovar J. (2011). Inhibitory effect of unsaturated fatty acids on saturated fatty acid-induced apoptosis in human pancreatic cells: activation of caspases and ER stress induction. *Cell Physiol Biochem* 27 (5): 525-538.

Nestel P, Clifton P, Noakes M. (1994). Effects of increasing dietary palmitoleic acid comparing with palmitic and oleic acids on plasma lipids of hypercholesterolemic men. *J Lipid Res* 35: 656-662.

Newsholme P, Keane D, Welters HJ, Morgan NG. (2007) Life and death decisions of the pancreatic beta-cell: the role of fatty acids. *Clin Sci (Lond)* 112(1):27-42.

NHS England. (2018). Type 2 diabetes and the importance of prevention. Accessed 9.4.2018 from: https://www.england.nhs.uk/blog/type-2-diabetes-and-the-importance-of-prevention/

Nickens KP, Wikstrom JD, Shirihai OS, Patierno SR, Ceryak S. (2014). A bioenergetic profile of non-transformed fibroblasts uncovers a link between death-resistance and enhanced spare respiratory capacity. *Mitochondrion* 13(6): 662-667.

Nolan CJ, Larter, CZ. (2009). Lipotoxicity: Why do saturated fatty acids cause and monounsaturates protect against is? *J Gastroenterol Hepatol* 24(5): 703-706.

Nolan CJ, Leahy JL, Delghingaro-Augusto V, Moibi J, et al. (2006). Beta cell compensation for insulin resistance in Zucker fatty rats: increased lipolysis and fatty acid signalling. *Diabetologia* 49 (9): 2120-2130.

Nolan CJ, Madiraju MSR, Delghingaro-Augusto V, Peyot ML, Prentki M. (2006). Fatty acid signalling in the β-cell and insulin secretion. *Diabetes* 55(2): S16-S23.

Oh YS, Bae GD, Baek DJ, Park EY, Jun HS. (2018). Fatty acid-induced lipotoxicity in pancreatic beta-cells during development of type 2 diabetes. *Front Endocrinol (Lausanne)* 9: 384.

Oh YS. (2015). Mechanistic insights into pancreatic beta-cell mass regulation by glucose and free fatty acids. *Anat Cell Biol* 48(1): 16-24.

Oleson BJ, McGraw JA, Broniowska KA, Annamalai M, Chen J, Buschkofsky JR, Davis DB, Corbett JA, Mathews CE. (2015). Distinct differences in the responses of the human pancreatic β-cell line EndoC-βH1 and human islets to proinflammatory cytokines. *Am J Physiol Regul Integr Comp Physiol* 309(5): R525-R534.

Ouchi N, Kihara S, Funahashi T, Nakamura T, Nishida M, Kumada M, et al. (2003). Reciprocal association of C-reactive protein with adiponectin in blood stream and adipose tissue. *Circulation* 107 (5): 671-674.

Park KS, Wiederkehr A, Kirkpatrick C, Mattenberger Y, et al. (2008). Selective actions of mitochondrial fission/fusion genes on metabolism-secretion coupling in insulin-releasing cells. *J Biol Chem*. 283(48): 33347-33356.

Paton CM, Ntambi JM. (2009). Biochemical and physiological function of stearoyl-CoA desaturase. *Am J Physiol Endocrinol Metab* 297(1): E28-E37.

Pederson TM, Kramer DL, Rondinone CM, (2001). Serine/threonine phosphorylation of IRS-1 triggers its degradation. *Diabetes* 50(1): 24-31.

Petersen M, Shulman GI. (2018). Mechanisms of insulin action and insulin resistance. *Physiol Rev* 98 (4): 2133-2223.

Phelps EA, Cianciaruso C, Michael IP, Pasquier M, Kanaani J, Nano R, Lavallard V, Billestrup N, Hubbell JA, Baekkeskov S. (2016). Aberrant accumulation of the diabetes autoantigen GAD65 in Golgi membranes in conditions of ER stress and autoimmunity. *Diabetes* 65 (9): 2686-2699.

Pi J, Bai Y, Zhang Q, Wong V, Floering LM et al. (2007). Reactive oxygen species as a signal in glucose-stimulated insulin secretion. *Diabetes* 56(7): 1783-1791.

Pi J, Zhang Q, Fu J, Woods CG, Hou Y, et al. (2010). ROS signalling, oxidative stress and Nrf2 in pancreatic beta-cell function. *Toxicol Appl Pharmacol* 244(1): 77-83.

Pickersgill L, Litherland GJ, Greenberg AS, Walker M, Yeaman SJ. (2007). Key role for ceramides in mediating insulin resistance in human muscle cells. *J Biol Chem*. 282 (17): 12583-12589.

Plaisance V, Perret V, Favrea D, Abderrahmania A, Yanga JY, Widmanna C, Regazzi R. (2009). Role of the transcription factor C/EBP in fatty acid-elicited β-cell failure. *Mol Cell Endocrinol* 305 (1-2): 47-55.

Plotz T, Hartmann M, Lenzen S, Elsner M. (2016). The role of lipid droplet formation in the protection of unsaturated fatty acids against palmitic acid induced lipotoxicity to rat insulin-producing cells. *Nutr Metab (Lond)* 13: 16.

Pohl J, Ring A, Korkmaz U, Ehehalt R, Stremmel W. (2005). FAT/CD36 Medicated long-chain fatty acid uptake in adipocytes requires plasma membrane rafts. *Mol Biol Cell* 16 (1): 24-31.

Poitout V, Amyot J, Semache M, Zarrouki B, Hagman D, Fontes G. (2010). Glucolipotoxicity of the pancreatic beta cell. *Biochim Biophys Acta* 1801(3): 289-298.

Poitout V, Hagman D, Stein R, Artner I, Robertson RP, Harmon JS. (2006). Regulation of the insulin gene by glucose and fatty acids. *J Nutr* 136 (4): 873-876.

Prause M, Christensen DP, Billestrip N, Mandrup-Poulsen T. (2014). JNK1 protects against glucolipotoxicity-mediated beta-cell apoptosis. *PLoS One* 9(1): e87067.

Prentki M, Joly E, El-Assaad W, Roduit R. (2002). Malonyl-CoA Signaling, lipid partitioning and glucolipotoxicity. *Diabetes* 51(3): S405-S413.

Prentki M, Matschinsky FM, Madiraju SRM. (2013). Metabolic signalling in fuel-induced insulin secretion. *Cell Metab* 18(2): 162-185.

Prentki M, Nolan CJ. (2006). Islet β-cell failure in type 2 diabetes. *J Clin Invest* 116(7): 1802-1812.

Prentki M, Vischer S, Glennon MC, Regazzi R, Deeney JT, Corkey BE. (1992). Malonyl-CoA and long chain acyl-CoA esters as metabolic coupling factors in nutrient-induced insulin secretion. *J Biol Chem* 267 (9): 5802-5810.

Preston AM, Gurisik E, Bartley C, Laybutt DR, Biden TJ. (2009). Reduced endoplasmic reticulum (ER)-to-Golgi protein trafficking contributes to ER stress in lipotoxic mouse beta cells by promoting protein overload. *Diabetologia* 52(11): 2369-2373.

Public Health England. (2014). Adult obesity and Type 2 diabetes. Accessed 31.10.2018:https://assets.publishing.service.gov.uk/government/uploads/system/uploads/attachment_data/file/338934/Adult_obesity_and_type_2_diabetes_.pdf

Qin J, Fang N, Lou L, Zhang W, Xu S, et al. (2014). TRB3 is involved in free fatty acid-induced INS-1 derived cell apoptosis via the protein kinase C δ pathway. *PLoS One* 9 (5): e96089.

Quan X, Zhang L, Li Y, Liang C. (2014). TCF2 attenuated FFA-induced damage in islet β-cells by regulating production of insulin and ROS. *Int J Mol Sci* 15 (8): 13317-13332.

Quehenberger O, Armando AM, Brown AH, Milne SB, Myers DS, Merril AH, et al. (2010). Lipodomics reveals a remarkable diversity of lipids in human plasma. *J Lipid Res*. 51 (11): 3299-3305.

Rachek LI, Thornley NP, Grishko VI, LeDoux SP, Wilson GL. (2006). Protection of INS-1 cells from free fatty-acid induced apoptosis by targeting hOGG1 to mitochondria. *Diabetes* 55(4): 1022-1028.

Rakatzi I, Mueller H, Ritzeler O, Tennagels N, Eckel J. (2004). Adiponectin counteracts cytokine- and fatty acid-induced apoptosis in the pancreatic beta-cell line INS-1. *Diabetologia* 47(2): 249-58.

Ralston JC, Zulyniak MA, Nielsen DE, Clarke S, Badawi A, El-Sohemy A, Ma DWL, Mutch DA. (2013). Ethnic- and sex-specific associations between plasma fatty acids and markers of insulin resistance in healthy young adults. *Nutr Metab (Lond)* 10 (1): 42.

Rambold AS, Cohen S, Lippincott-Schwarz J. (2015). Fatty acid trafficking in starved cells: regulation by lipid droplet lipolysis, autophagy, and mitochondrial fusion dynamics. *Dev Cell* 32(6): 678-692.

Randle PJ, Garland PB, Hales CN, Newsholme EA. (1963). The glucose fatty-acid cycle. Its role in insulin sensitivity and the metabolic disturbances of diabetes mellitus. *Lancet* 1: 785-789.

Rask-Madsen C, King GL. (2013). Vascular complications of diabetes: mechanisms of injury and protective factors. *Cell Metab* 17(1): 20-33.

Ravassard P, Hazhouz Y, Pechberty S, Bricout-Neveu E, Armanet M, Czernichow P, Scharfmann R. (2011). A genetically engineered human pancreatic β cell line exhibiting glucose-inducible insulin secretion. *J Clin Invest* 121(9): 3589-3597.

Ravnskjaer K, Frigerio F, Boergesen M, Nielsen T, Maechler P, Mandrup S. (2010). PPARδ is a fatty acid sensor that enhances mitochondrial oxidation in insulin-secreting cells and protects against fatty acid-induced dysfunction. *J Lipid Res* 51(6): 1370-1379.

Ray PD, Huang BW, Tsuji Y. (2013). Reactive oxygen species (ROS) homeostasis and redox regulation in cellular signalling. *Cell Signal* 24(5): 981-990.

Riedel MJ, Asadi A, Wang R, Ao Z, Warnock GL, Kieffer TJ. (2012). Immunohistochemical characterisation of cells co-producing insulin and glucagon in the developing human pancreas. *Diabetologia* 55 (2): 372-381.

Robertson RP, Harmon J, Tran POT, Poitout V. (2004). B-cell glucose toxicity, lipotoxicity, and chronic oxidative stress in type 2 diabetes. *Diabetes* 53(1): S119-S124.

Roden M, Stingl H, Chandramouli V, Schumann WC, Landau BR, Nowotny P, Waldhausl W, Shulman GI. (2000). Effects of free fatty acid elevation on postabsorptive endogenous glucose production and gluconeogenesis in humans. *Diabetes* 49(5): 701-707.

Roduit R, Morin J, Masse F, Segall L, Roche E, Newgard CB, et al. (2000). Glucose down-regulated the expression of peroxisome proliferator-activated receptor-α gene in the pancreatic β-cell. *J Biol Chem* 275: 35799-35806.

Rogers GW, Brand MD, Petrosyan S, Ashok D, Elorza AA, Ferrick DA, Murphy AN. (2011). High throughput microplate respiratory measurements using minimal quantities of isolated mitochondria. *PLoS One* 6(7): e21746.

Rogowski MP, Flowers MT, Stamatikos AD, Ntambi JM, Paton CM. (2013). SCD1 activity in muscle increases triglyceride PUFA content, exercise capacity, and PPARδ expression in mice. *J Lipid Res* 54(1 0): 2636-2646.

Rorsman P, Renstrom E. (2003). Insulin granule dynamics in pancreatic β-cells. *Diabetologia* 46 (8): 1029-1045.

Ruan H, Lodish HF. (2003). Insulin resistance in adipose tissue: direct and indirect effects of tumor necrosis factor alpha. *Cytokine Growth Factor Rev* 14 (5): 447-455.

Russell MA, Morgan NG. (2011). Conditional expression of the FTO gene product in rat INS-1 cells reveals a rapid turnover and a role in the profile of glucose-induced insulin secretion. *Clin Sci (Lond)* 120(9): 403-413.

Saisho Y, Butler AE, Butler PC. (2008). Pancreatic fat content and beta-cell function in men with and without type 2 diabetes: response to Tushuizen et al. *Diabetes Care* 31 (5):e38, author reply e39.

Sakuaba H, Mizukami H, Yagihashi N, Wada R, Hanyu C, Yagihashi S. (2002). Reduced β-cell mass and expression of oxidative stress related DNA damage in the islet of Japanese type II diabetic patients. *Diabetologia* 45 (1): 85-96.

Salaun C, Greaves J, Chamberlain LH. (2010). The intracellular dynamic of protein palmitoylation. *J Cell Biol* 191(7): 1229-1238.

Saltiel AR, Olefsky AM. (1996). Thiazolidinediones in the treatment of insulin resistance and type II diabetes. *Diabetes* 45(12): 1661-1669.

Sansone A, Tolika E, Louka M, Sunda V, Deplano S, Melchiorre M, Anagnostopoulos D, et al. (2016). Hexadecenoic fatty acid isomers in human blood lipids and their relevance for the interpretation of lipodomic profiles. *PLoS ONE* 11(4): e0152378.

Santaren ID, Watkins SM, Liese AD, Wagenknecht LE, Rewers MJ, Haffner SM, Lorenzo C, Hanley AJ. (2014). Serum pentadecanoic acid (15:0), a short-term marker of dairy food intake, is inversely associated with incident type 2 diabetes and its underlying disorders. *Am J Clin Nutr* 100(6): 1532-1540.

Sargsyan E, Artemenko K, Manukyan L, Bergquist J, Bersten P. (2016). Oleate protects beta-cells from the toxic effect of palmitate by activating pro-survival pathways of the ER stress response. *Biochim Biophys Acta* 1861(9): 1151-1160.

Sargsyan E, Bergsten P. (2011). Lipotoxicity is glucose-dependent in INS-1E cells but not in human islets and MIN6 cells. *Lipids Health Dis* 10: 115.

Sattar N, Gill JMR. (2014). Type 2 diabetes as a disease of ectopic fat. *BMC Medicine* 12: 123.

Schindelin J, Arganda-Carreras I, Frise E, et al. (2012). Fiji is an open source platform for biological-image analysis. *Nat Methods* 9(7): 676-682.

Schmidt FM, Weschenfelder J, Sander C, Minkwitz J, Thormann J, et al. (2015). Inflammatory cytokines in general and central obesity and modulating effects of physical activity. *PLoS One* 10(3): e0121971.

Schonfeld P, Wojtczak L. (2008). Fatty acids as modulators of the cellular production of reactive oxygen species. *Free Radic Biol Med* 45 (3): 231-241.

Schuit F, De Vos A, Farfari S, Moens K, Pipeleers D, Brun T, Prentki M. (1997). Metabolic fats of glucose in purified islet cells. *J Biol Chem* 272 (30): 18572-18579.

Scott RA, Scott LJ, Magi R, Marullo L, et al. (2017). An expanded genome-wide association study of type 2 diabetes in Europeans. *Diabetes* 66(11): 2888-2902.

Sears B, Perry M. (2015). The role of fatty acids in insulin resistance. *Lipids Health Dis* 14:121.

Shapiro SS, Wilk MB. (1965). An analysis of variance test for normality (complete samples). *Biometrika* 52 (3-4): 591-611.

Sharma RB, Alonso LC. (2014). Lipotoxicity in the pancreatic beta cell: not just survival and function, but proliferation as well. *Curr Diab Rep* 14(6): 492.

Shetty GK, Economides PA, Horton ES, Mantzoros CS, Veves A. (2004). Circulating adiponectin and resistin levels in relation to metabolic factors, inflammatory markers, and vascular reactivity in diabetic patients and subjects at risk for diabetes. *Diabetes Care* 27(10): 2450-2457.

Shiao MS, Liao BY, Long M, Yu HT. (2008). Adaptive evolution of the insulin two-gene system in mouse. *Genetics* 178(3): 1683-1691.

Shimabukuro M, Zhou YT, Levi M, Unger RH. (1998). Fatty acid-induced β-cell apoptosis: A link between obesity and diabetes. *Proc Natl Acad Sci USA* 95(5): 2498-2502.

Shojaee-Moradie F, Ma Y, Lou S, Hovorka R, Umpleby AM. (2013). Prandial hyperglyceridemia in metabolic syndrome is due to an overproduction of both chylomicron and VLDL triacylglycerol. *Diabetes* 62(12): 4063-4069.

Siegal EG. Wollheim CB, Kikuchi M, Renold AE, Sharp GW. (1980). Dependency of cyclic AMP-induced insulin release on intra- and extracellular calcium in rat islets of Langerhans. *J Clin Invest* 65(2): 233-241.

Silbernagel G. Kovarova M, Cegan A, Machann J, Schick F, Lehmann R. et al. (2012). High hepatic SCD1 activity is associated with low liver fat content in

healthy subjects under a lipogenic diet. *J Clin Endocrinol Metab* 97(12): E2288-E2292.

Simon MN, Azevedo-Martins AK, Amanso AM, Carvalho CRO, Curi R. (2008). Persistent activation of Akt or ERK prevents the toxicity induced by saturated and polyunsaturated fatty acids in RINm5F β-cells. *Toxicol. In Vitro* 22 (4): 1018-1024.

Singh R, Cuervo AM. (2012). Lipophagy: Connecting autophagy and lipid metabolism. *Int J Cell Biol* 2012: 282041.

Singh R, Kaushik S, Wang Y, Xiang Y, Novak I, Komatsu M, Tanaka K, Cuervo AM, Czaja MJ. (2009). Autophagy regulates lipid metabolism. *Nature* 458 (7242): 1131-1135.

Slot JW, Geuze HJ. (2007). Cryosectioning and immunolabeling. *Nat Protoc* 2(10): 2480-2491.

Smith J, Su X, El-Maghrabi R, Stahl PD, Abumrad NA. (2008). Opposite regulation of CD36 Ubiquitination by fatty acids and insulin: effects on fatty acid uptake. *J Biol Chem* 283 (20): 13578-13585.

Smith SR, De Jonge L, Volaufoya J, Xie H, Bray GA. (2005). Effect of pioglitazone on body composition and energy expenditure: a randomised controlled trial. *Metabolism* 54 (1): 24-32.

Sol EM, Sargsyan E, Akusjarvi G, Bergsten P. (2008). Glucolipotoxicity in INS-1E cells is counteracted by carnitine palmitoyltransferase 1 over-expression. *Biochem Biophys Res Commun* 375(4): 517-521.

Sommerweiss D, Gorski T, Richter S, Garten A, Kiess W. (2013). Oleate rescues INS-1E β-cells from palmitate-induced apoptosis by preventing activation of the unfolded protein response. *Biochem Biophys Res Commun* 441(4): 770-776.

Song X, Huang Y, Neuhouser ML, Tinker LF, Vitolins MZ, Prentice RL, Lampe JW. (2017). Dietary long-chain fatty acids and carbohydrate biomarker evaluation in a controlled feeding study in participants from the Women's Health Initiative cohort. *Am J Clin Nutr* 105(6): 1272-1282.

Southam L, Soranzo N, Montgomery SB, Frayling TM, McCarthy MI, Barroso I, Zeggini E. (2009). Is the thrifty genotype hypothesis supported by evidence based

on confirmed type 2 diabetes- and obesity-susceptibility variants? *Diabetologia* 52(9): 1846-1851.

Sowers JR. (2008). Endocrine functions of adipose tissue: focus on adiponectin. *Clin Cornerstone* 9(1): 32-40.

Sramek J, Furstova VN, Kovar J. (2016). Kinase signalling in apoptosis induced by saturated fatty acids in pancreatic β-cells. *Int J Mol Sci* 17(9): E1400.

Staaf J, Ubhayasekera SJKA, Sargsyan E, Chowdhury A, Kristinsson H, et al. (2016). Initial hyperinsulinemia and subsequent β-cell dysfunction is associated with elevated palmitate levels. *Pediatr Res* 80 (2): 267-274.

Steil GM, Trivedi N, Jonas JC, Hasenkamp WM, Sharma A, Bonner-Weir. (2001). Adaptation of beta-cell mass to substrate oversupply: enhanced function with normal gene expression. *Am J Physiol Endocrinol Metab* 280(5): E788-E796.

Stein DT, Esser V, Stevenson BE, Lane KE, Whiteside JH, Daniels MB, Chen S, McGarry JD. (1996). Essentially of circulating fatty acids for glucose-stimulated insulin secretion in the fasted rat. *J Clin Invest* 97 (12): 2728-2735.

Steneberg P, Rubins N, Bartoov-Shifman R, Walker MD, Edlund H. (2005). The FFA receptor GPR40 links hyperinsulinemia, hepatic steatosis, and impaired glucose homeostasis in mouse. *Cell Metab* 1 (4): 245-258.

Stern JH, Rutkowski JM, Scherer PR. (2016). Adiponectin, leptin, and fatty acids in the maintenance of metabolic homeostasis through adipose tissue crosstalk. *Cell Metab* 23 (5): 770-784.

Stevens S, Hollingsworth G, Small PK, Woodcock SA, Pucci A, Aribisala B, Al-Mrabeh A, Daly AK, Batterham RL, Taylor R. (2015). Weight loss decreases excess pancreatic triacylglycerol specifically in type 2 diabetes. *Diabetes Care* 39(1): 158-165.

Stiban J, Tidhar R, Futerman AH. (2010). Ceramide synthases: roles in cell physiology and signalling. *Adv Exp Med Biol* 688: 60-71.

Stiles L, Shirihai OS. (2012). Mitochondrial dynamics and morphology in beta-cells. *Best Pract Res Clin Endocrinol Metab* 26(6): 725-738.

Stoddart LA, Smith NJ, Milligan G. (2008). International union of pharmacology. LXXI. Free fatty acid receptors FFA1, -2 and -3: pharmacology and pathophysiological functions. *Pharmacol Rev* 60(4): 405-417.

Stoll LL, Spector AA. (1984). Changes in serum influence the fatty acid composition of established cell lines. *In Vitro* 20(9): 732-8.

Strable MS, Ntambi JM. (2010). Genetic control of de novo lipogenesis: role in diet-induced obesity. *Crit Rev Biochem Mol Biol* 45(3): 199-214.

Strober W. (1997). Trypan blue exclusion test of cell viability. *Curr Protoc Immunol* 21(1): A.3B.1-A.3B.2

Stuhlsatz-Krouper SM, Bennett NE, Schaffer JE. (1998). Substitution of alanine for serine 250 in the murine fatty acid transport protein inhibits long chain fatty acid transport. *J Biol Chem* 273 (44): 28642-28650.

Suen DF, Norris KL, Youle RJ. (2007). Mitochondrial dynamics and apoptosis. *Genes Dev* 22 (12): 1577-1590.

Summers SA, Garza LA, Zhou H, Birnbaum MJ. (1998). Regulation of insulin-stimulated glucose transporter GLUT4 translocation and Akt kinase activity by ceramide. *Mol Cell Biol* 18(9): 5457-5464.

Talchai C, Xuan S, Lin HV, Sussel L. Accili D. (2012). Pancreatic β-cell dedifferentiation as mechanism of diabetic β-cell failure. *Cell* 150(6): 1223-1234.

Tallima H, El Ridi R. (2018). Arachidonic acid: physiological roles and potential health benefits – a review. *J Adv Res* 11: 33-41.

Taskinen MR, Nikkila EA, Kuusi T, Harmo K. (1982). Lipoprotein lipase activity and serum lipoproteins in untreated type 2 (insulin-independent) diabetes associated with obesity. *Diabetologia* 22(1): 46-50.

TeSlaa T, Teitell MA. (2014). Techniques to monitor glycolysis. *Methods Enzymol* 542: 91-114.

Thiam AR, Beller M. (2017). The why, when and how of lipid droplet diversity. *J Cell Sci* 130 (2): 315-324.

Thomas NJ, Jones SE, Weedon MN, Shields BM, Oram RA, Hattersley AT. (2018). Frequency and phenotype of type 1 diabetes in the first six decades of

life: a cross-sectional, genetically stratified survival analysis from UK Biobank. *Lancet Diabetes Endocrinol* 6(2): 122-129.

Thompson BR, Lobo S, Bernlohr DA. (2010). Fatty acid flux in adipocytes; the in's and out's of fat cell lipid trafficking. *Mol Cell Endocrinol* 318(1-2): 24-33.

Thompson GR. (2004). Management of dyslipidaemia. *Heart* 90(8):949-955.

Thumm M, Egner R, Koch B, Schlumpberger M, Straub M, Veenhuis M, Wolf DH. (1994). Isolation of autophagocytosis mutants of Saccharomyces cerevisiae. *FEBS Lett* 349(2): 275-280.

Toei M, Saum R, Forgac M. (2011). Regulation and isoform function of the V-ATPases. *Biochemistry* 49(23): 4715-4723.

Tran K, Li Y, Duan H, Arora D, Lim HY, Wang W. (2014). Identification of small molecules that protect pancreatic beta cells against endoplasmic reticulum stress-induced cell death. *ACS Chem Biol* 9 (12): 2796-2806.

Trayhurn P, Wood IS. (2004). Adipokines: inflammation and the pleiotropic role of white adipose tissue. *Br J Nutr* 92 (3): 347-355.

Tsang KY, Chan D, Bateman JF, Cheah KS. (2010). In vivo cellular adaptation to ER stress: survival strategies with double-edged consequences. *J Cell Sci.* 123 (13): 2145-2154.

Tse G, Yan BP, Chan YWF, Tian XY, Huang Y. (2016). Reactive oxygen species, endoplasmic reticulum stress and mitochondrial dysfunction: the link with cardiac arrhythmogenesis. *Front Physiol* 7: 313.

Tsonkova VG, Sand FW, Wolf XA, Grunnet LG, et al. (2018). The EndoC-βH1 cell line is a valid model of human beta cells and applicable for screenings to identify novel drug target candidates. *Mol Metab* 8: 144-157.

Tsukada M, Ohsumi Y. (1993). Isolation and characterisation of autophagy-defective mutants of Saccharomyces cerevisiae. *FEBS Lett* 333(1-2): 169-174.

Tukey J. (1949). Comparing individual means in the analysis of variance. *Biometrics* 5(2): 99-114.

Tuo Y, Feng DD, Wang DF, Sun J, Li SB, Chen C. (2012). Long-term in vitro treatment of INS-1 rat pancreatic β-cells by unsaturated free fatty acids protects

cells against gluco- and lipotoxicity via activation of GPR40 receptors. *Clin Exp Pharmacol Physiol* 39 (5): 423-428.

Tushuizen ME, Bunck MC, Pouwels PJ, Bontemps S, van Waesberghe JH, et al. (2007). Pancreatic fat content and beta-cell function in men with and without type 2 diabetes. *Diabetes Care* 30(11): 2916-2921.

Twig G, Elorza A, Molina AJA, Mohamed H, Wikstrom JD, Walzer G, Stiles L, Haigh SE, Katz S, Las G, Alroy J, Wu M, Py BF, Yuan J, Deeney JT, Corkey BE, Shirihai OS. (2008). Fission and selective fusion govern mitochondrial segregation and elimination by autophagy. *EMBO J* 27(2): 433-446.

Tyagi S, Gupta P, Saini AS, Kaushal C, Sharma S. (2011). The peroxisome proliferator activated receptor: a family of nuclear receptors role in various diseases. *J Adv Pharm Technol Res.* 2(4): 236-240.

Upadhyay J, Polyzos SA, Perakakis N, Thakkar B, Paschou SA, Katsiki N, Underwood P, Park KH, Seufert J, Kang ES, Sternthal E, Karagiannis A, Mantzoros CS. (2018). Pharmacotherapy of type 2 diabetes: an update. *Metabolism* 78: 13-42.

Van Citters GW, Kabur M, Kim SP, Mittelman SD, Dea MK, Brubaker PL, Bergman RN. (2002). Elevated glucagon-like peptide-1-(7-36)-amide, but not glucose associated with hyperinsulinemic compensation for fat feeding. *J Clin Endocrinol Metab* 87(11): 5191-5198.

Van der Windt GJW, Chang CH, Pearce EL. (2016). Measuring bioenergetics in T cells using a Seahorse Extracellular Flux Analyser. *Curr Protoc Immunol* 113: 3.16B. 1-3. 16B.14

Van Raalte DH, van der Zijl NJ, Diamant M. (2010). Pancreatic steatosis in humans: cause or marker of liptoxicity. *Curr Opin Clin Nutr Metab Care* 13 (4): 478-485.

Vandewalle B, Moerman E, Lefebvre B, Defrance F, et al. (2008). PPARγ-dependent and –independent effects of Rosiglitazone on lipotoxic human pancreatic islets. *Biochem Biophys Res Commun* 366(4): 1096-1101.

Vara E, Tamarit-Rodriguez J. (1986). Glucose stimulation of insulin secretion in islets of fed and starved rats and its dependence on lipid metabolism. *Metabolism* 35 (3): 266-271.

Veret J, Belline L, Giussani P, Carl NG, Magnuan C, Stunff HL. (2014). Roles of sphingolipid metabolism in pancreatic β cell dysfunction induced by lipotoxicity. *J Clin Med* 3 (2): 646-662.

Verges B. (2015). Pathophysiology of diabetic dyslipidaemia: where are we? *Diabetologia* 58(5): 886-899.

Vernier S, Chiu A, Schober J, Weber T, Nguyen P, Luer M, et al. (2012). β-cell metabolic alterations under chronic nutrient overload in rat and human islets. *Islets* 4(6): 379-392.

Voight BF, Kudaravalli S, Wen X, Pritchard JK. (2006). A map of recent positive selection in the human genome. *PLoS Biol* 4 (3): e72.

Wahjudi PN, Yee JK, Martinez SR, Zhang J, Teitell M, et al. (2011). Turnover of nonessential fatty acid in cardiolipin from the rat heart. *J Lipid Res* 52(12): 2226-2233.

Wanders RJ, Ferdinandusse S, Brites P, Kemp S. (2010). Peroxisomes, lipid metabolism and lipotoxicity. *Biochim Biophys Acta* 1801 (3): 272-280.

Wang H, Maechler P, Ritz-Laser B, Hagenfeldt KA, Ishihara H, Philippe J, Wollheim CB. (2001). Pdx1 level defines pancreatic gene expression pattern and cell lineage differentiation. *J Biol Chem* 276(27): 25279-25286.

Wang Y, Xie T, Zhang D, Leung PS. (2018). GPR120 protects lipotoxicity-induced pancreatic beta-cell dysfunction through regulation of PDX1 expression and inhibition of islet inflammation. *Clin Sci (Lond)* 133 (1): 101-116.

Wang Z, York NW, Nichols CG, Remedi MS. (2014). Pancreatic β-cell dedifferentiation in diabetes and re-differentiation following insulin therapy. *Cell Metab* 19(5): 872-882.

Watt MJ, Barnett AC, Bruce CR, Schenk S, Horowitz JF, Hoy AJ. (2012). Regulation of plasma ceramide levels with fatty acid oversupply: evidence that the liver detects and secretes de novo synthesised ceramide. *Diabetologia* 55(10): 2741-2746.

Weir GC, Bonner-Weir S. (2004). Five stages of evolving beta-cell dysfunction during progression to diabetes. *Diabetes* 53(3): S16-S21.

Welters HJ, El Ouaamari A, Kawamori D, Meyer J, Hu J, Smith DM, Kulkarni RN. (2012). Rosiglitazone promoted PPARγ-dependent and –independent alterations in gene expression in mouse islets. *Endocrinology* 153(10): 4593-4599.

Welters HJ, McBain SC, Tadayyon M, Scarpello JHB, Smith SA, Morgan NG. (2004). Expression and functional activity of PPARγ in pancreatic β-cells. *Br J Pharmacol* 142(7): 1162-1170.

Welters HJ, Smith SA, Tadayyon M, Scarpello JH, Morgan NG. (2004b). Evidence that protein kinase Cdelta is not required for palmitate-induced cytotoxicity in BRIN-BD11 beta-cells. *J Mol Endocrinol* 32(1): 227-35.

Welters HJ, Tadayyon M, Scarpello JH, Smith SA, Morgan NG. (2004). Mono-unsaturated fatty acids protect against beta-cell apoptosis induced by saturated fatty acids, serum withdrawal or cytokine exposure. *FEBS Lett* 560 (1-3): 103-108.

Weyer C, Bogardus C, Mott DM, Pratley RE. (1999). The natural history of insulin secretory dysfunction and insulin resistance in the pathogenesis of type 2 diabetes mellitus. *J Clin Invest* 104(6): 787-794.

Weyer C, Funahashi T, Tanaka S, Hotta K, Matsuzawa, Pratley RE, Tataranni A. (2001). Hypoadiponectinemia in obesity and type 2 diabetes: close association with insulin resistance and hyperinsulinemia. *J Clin Endocrinol Metab.* 86 (5): 1930-1935.

WHO. (2006). Definition and diagnosis of diabetes mellitus and intermediate hyperglycaemia. Report of a WHO/IDF consultation. Accessed 10.11.2018 from http://www.who.int/diabetes/publications/diagnosis_diabetes2006/en/

WHO. (2018). Global Health Estimates 2016: Deaths by Cause, Age, Sex, by Country and by Region, 2000-2016. Geneva, World Health Organisation; 2018.

Wiederkehr A, Wollheim CB. (2009). Linking fatty acid stress to β-cell mitochondrial dynamics. *Diabetes* 58 (10): 2185-6.

Wierup N, Svensson H, Mulder H, Sundler F. (2002). The ghrelin cell: a novel developmentally regulated islet cell in the human pancreas. *Regul Pept* 107 (1-3): 63-69.

World Health Organisation. (2015). World report on ageing and health. Accessed 2.11.2018 from http://www.who.int/ageing/publications/world-report-2015/en/.

World Health Organisation. (2016). Global report on diabetes. Accessed 10.11.2018 from http://www.who.int/diabetes/global-report/en/

Wrede CE, Dickson LM, Lingohr MK, Briaud I, Rhodes CJ. (2003). Fatty acid and phorbol ester-mediated interference of mitogenic signalling via novel protein kinase C isoforms in pancreatic β-cells (INS-1). *J Mol Endocrinol* 30 (3): 271-286.

Wu J, Wu Q, Li JJ, Chen C, Sun S, Wang CH, Sun SR. (2017). Autophagy mediates free fatty acid effects on MDA-MB-231 cell proliferation, migration and invasion. *Oncol Lett* 14(4): 4715-4721.

Xiao C, Lewis GF. (2012). Regulation of chylomicron production in humans. *Biochim. Biophys Acta* 1821 (5): 736-746.

Xu J, Feng HT, Wang C, Yip KHM, Pavlos N, Papadimitriou JM, Wood D, Zheng MH. (2003). Effects of bafilomycin A1: an inhibitor of vacuolar H (+)-ATPases on endocytosis and apoptosis in RAW cells and RAW cell-derived osteoclasts. *J Cell Biochem* 88 (6):1256-1264.

Xue A, Wu Y, Zhu Z, Zhang F, Kemper KE, et al. (2018). Genome-wide association analyses identify 143 risk variants for putative regulatory mechanisms for type 2 diabetes. *Nat Commun* 9 (1): 2941.

Yamamoto A, Tagawa Y, Yoshimori T, Moriyama Y, Masaki R, Tashiro Y. (1998). Bafilomycin A1 prevents maturation of autophagic vacuoles by inhibiting fusion between autophagosomes and lysosomes in rat hepatoma cell line, H-4-II-E cells. *Cell Struct Funct* 23 (1): 33-42.

Yamauchi T, Kamon J, Minokoshi Y, Ito Y, Waki H, et al. (2002). Adiponectin stimulatesgluocse utilisation and fatty-acid oxidation by activating AMP-activated protein kinase. *Nat Med* 8 (11): 1288-1295.

Yaney GC, Korchak HM, Corkey BE. (2000). Long-chain acyl CoA regulation of protein kinase C and fatty acid potentiation of glucose-stimulated insulin secretion in clonal β-cells. *Endocrinology* 141 (6): 1989-1998.

Yano M, Watanabe K, Yamamoto T, Ikeda K, Senokuchi T, et al. (2011). Mitochondrial dysfunction and increased reactive oxygen species impair insulin secretion in sphingomyelin synthase 1-null mice. *J Biol Chem* 286 (5): 3992-4002.

Yli-Jama P, Meyer HE, Ringstad J, Pederson JI. (2002). Serum free fatty acid pattern and risk of myocardial infarction: a case-control study. *J Intern Med* 251(1): 19-28.

Yoo JC, Han JM, Nam SK, Ko OH. (2002). Characterisation and cytotoxic activities of nonadecanoic acid produced by Streptomyces scabiei subsp. Chosunensis M0137 (KCTC 9927). *J Microbiol* 40: 331-334.

Yoon KH, Ko SH, Cho JH, Lee JM, Ahn YB, Song KH, Yoo SJ, Kang MI, Cha BY et al. (2003). Selective beta-cell loss and alpha-cell expansion in patients with type 2 diabetes mellitus in Korea. *J Clin Endocrinol Metab* 88 (5): 2300-2308.

Yuan H, Zhang X, Huang X, Lu Y, Tang W, Man Y, Wang S, Xi J, Li J. (2010). NADPH oxidase 2-derived reactive oxygen species media FFAs-induced dysfunction and apoptosis of β-cells via JNK, p38 MAPK and p53 pathways. *PLoS One* 5(12): e15726.

Zhang Y, Ranta F, Tang C, Shumilina E, Mahmud H, Foller M, Ullrich S, Haring HU, Lang F. (2009). Sphingomyelinase dependent apoptosis following treatment of pancreatic beta-cells with amyloid peptides A beta(1-42) or IAPP. *Apoptosis* 14(7): 878-889.

Zhang Y, Xu M, Zhang S, Yan L, Yang C, Lu W, Li Y, Cheng H. (2007). The role of G protein-coupled receptor 40 in lipoapoptosis in mouse beta-cell line NIT-1. *J Mol Endocrinol* 38(6): 651-661.

Zhao C, Wilson MC, Schuit F, Halestrap AP, Rutter GA. (2001). Expression and distribution of lactate/monocarboxylate transporter isoforms in pancreatic islets and the exocrine pancrease. *Diabetes* 50 (2): 361-366.

Zhao M, Xia L, Chen GQ. (2012). Protein kinase Cδ in apoptosis: a brief overview. *Arch Immunol Ther Exp (Warsz)* 60(5): 361-372.

Ziessel R, Ulrich G, Harriman A. New J. (2007). The chemistry of Bodipy: A new El Dorado for fluorescence tools. *New J Chem* 31 (4): 496.

Appendix 1

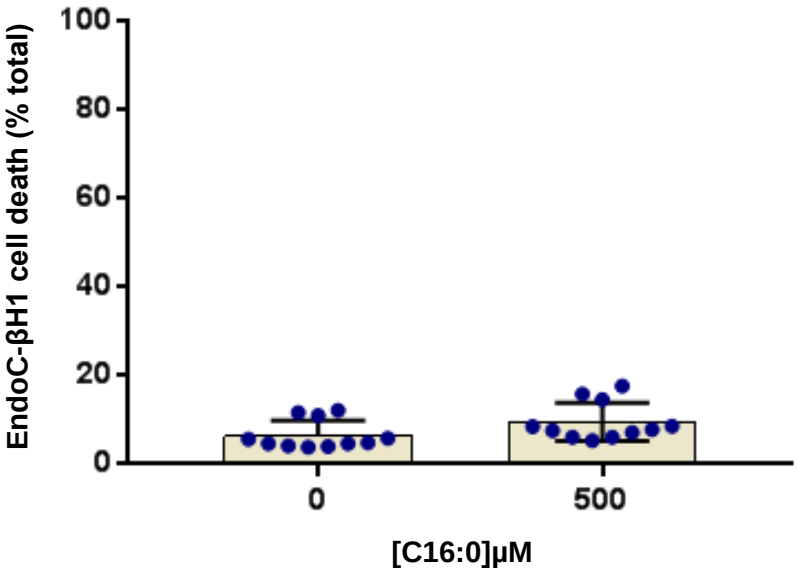

Effect of C16:0 on the viability of EndoC-βH1 cells. EndoC-βH1 cells were treated with 0μM and 500μM C16:0 for 24h. Cell death was estimated using vital dye staining. Dots represent data points from four independent experiments. Data are expressed as the mean +/- SEM.

Appendix 2

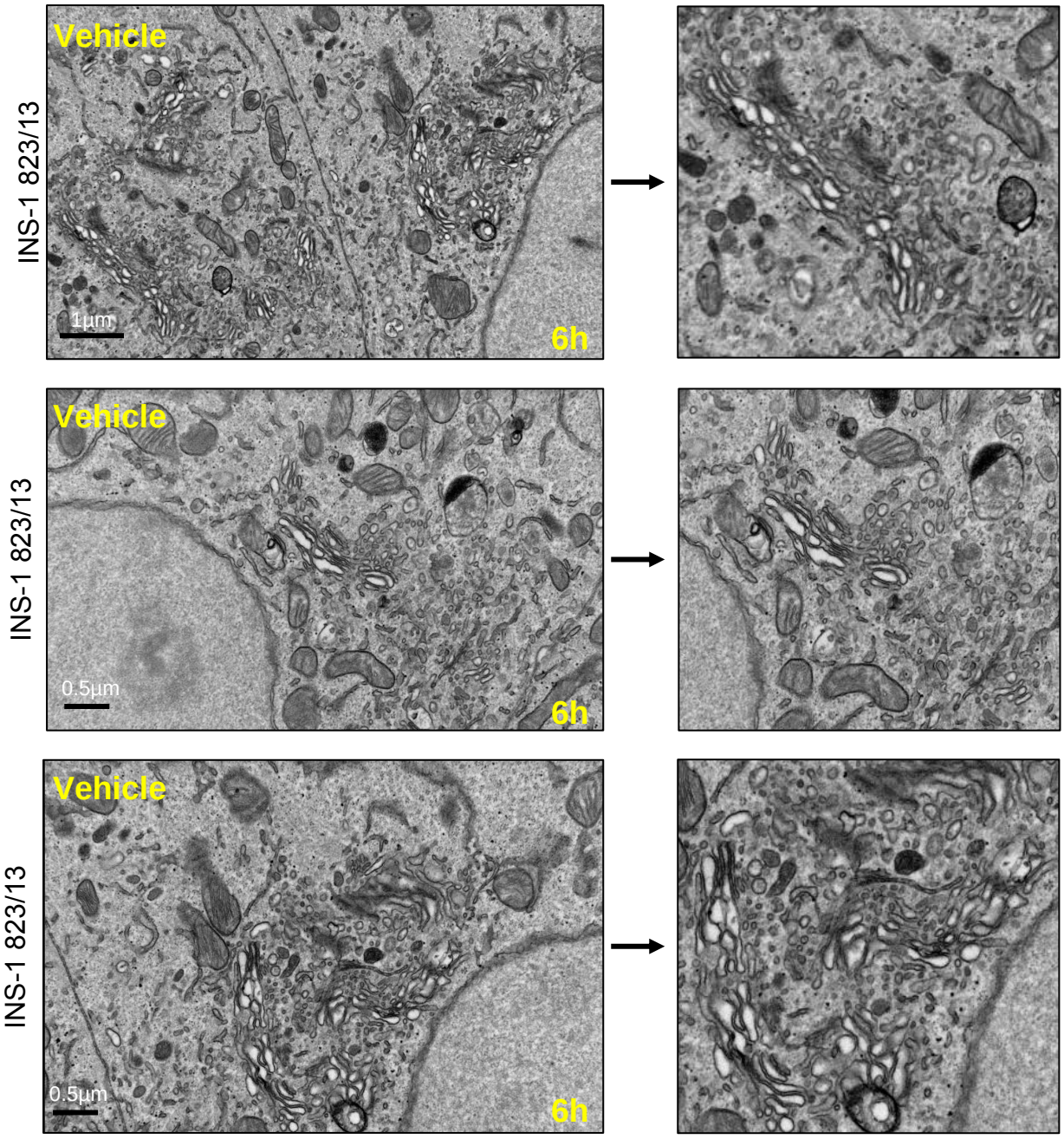

Effect of BSA vehicle control on Golgi morphology in INS-1 823/13 cells. INS-1 823/13 cells were treated for 6hrs with BSA vehicle only. INS-1 823/13 cells were then fixed in an osmium tetroxide fixative before being imaged with TEM.

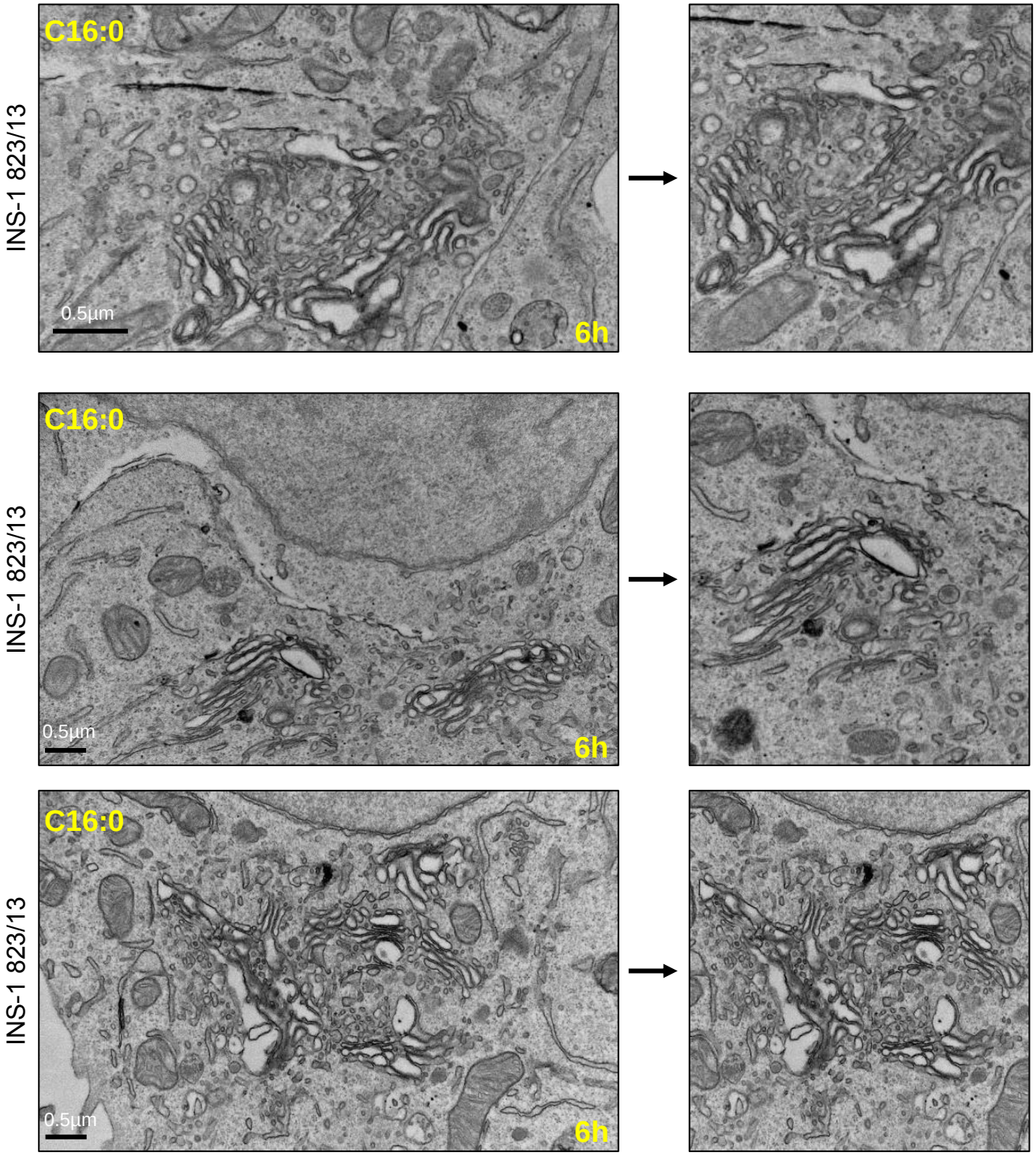
INS-1 823/13
C16:0
0.5µm
6h
INS-1 823/13
C16:0
0.5µm
6h
INS-1 823/13
C16:0
0.5µm
6h

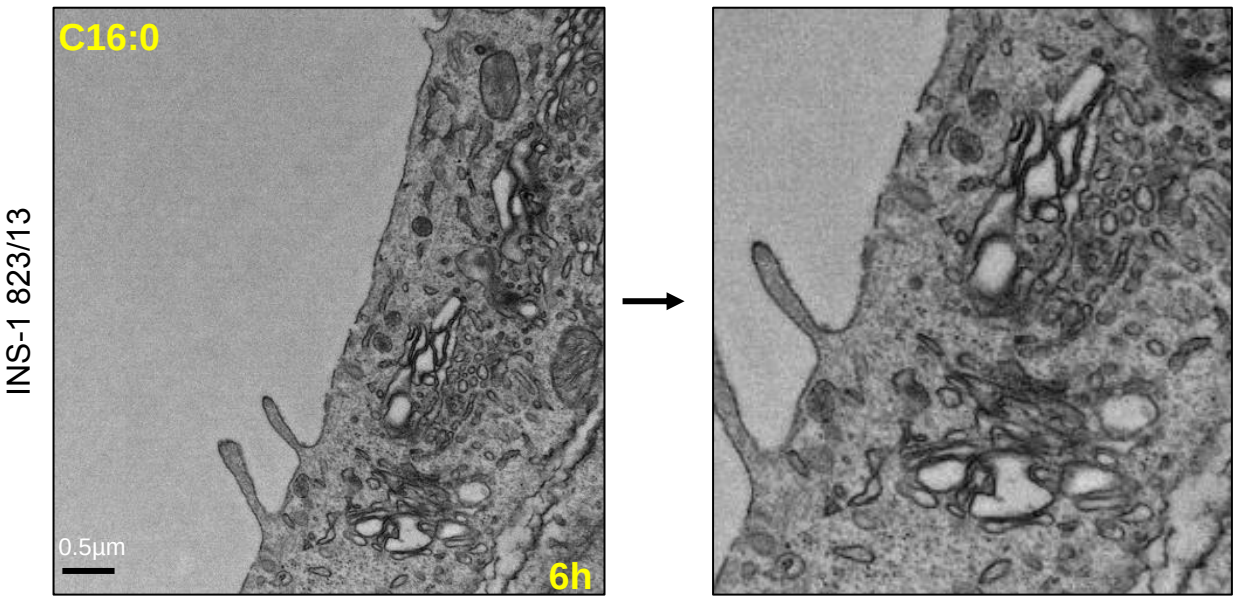

Effect of C16:0 on Golgi morphology in INS-1 823/13 cells. INS-1 823/13 cells were treated for 6hrs with 250µM C16:0. INS-1 823/13 cells were then fixed in an osmium tetroxide fixative before being imaged with TEM.

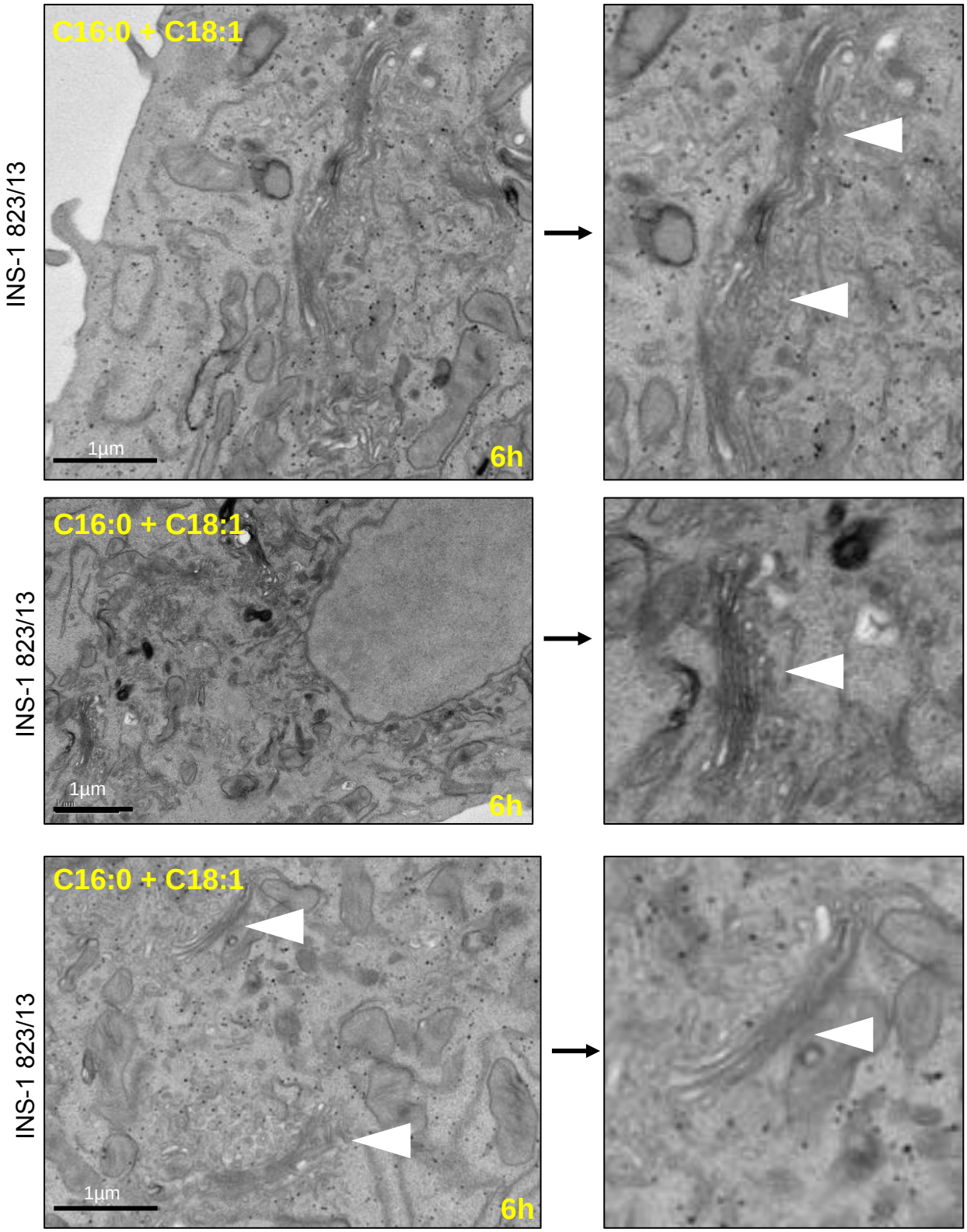

Effect of C16:0 with C18:1 on Golgi apparatus morphology in INS-1 823/13 cells. INS-1 823/13 cells were treated for 6hrs with 250µM C16:0 and 250µM C18:1. INS-1 823/13 cells were then fixed in an osmium tetroxide fixative before being imaged with TEM.

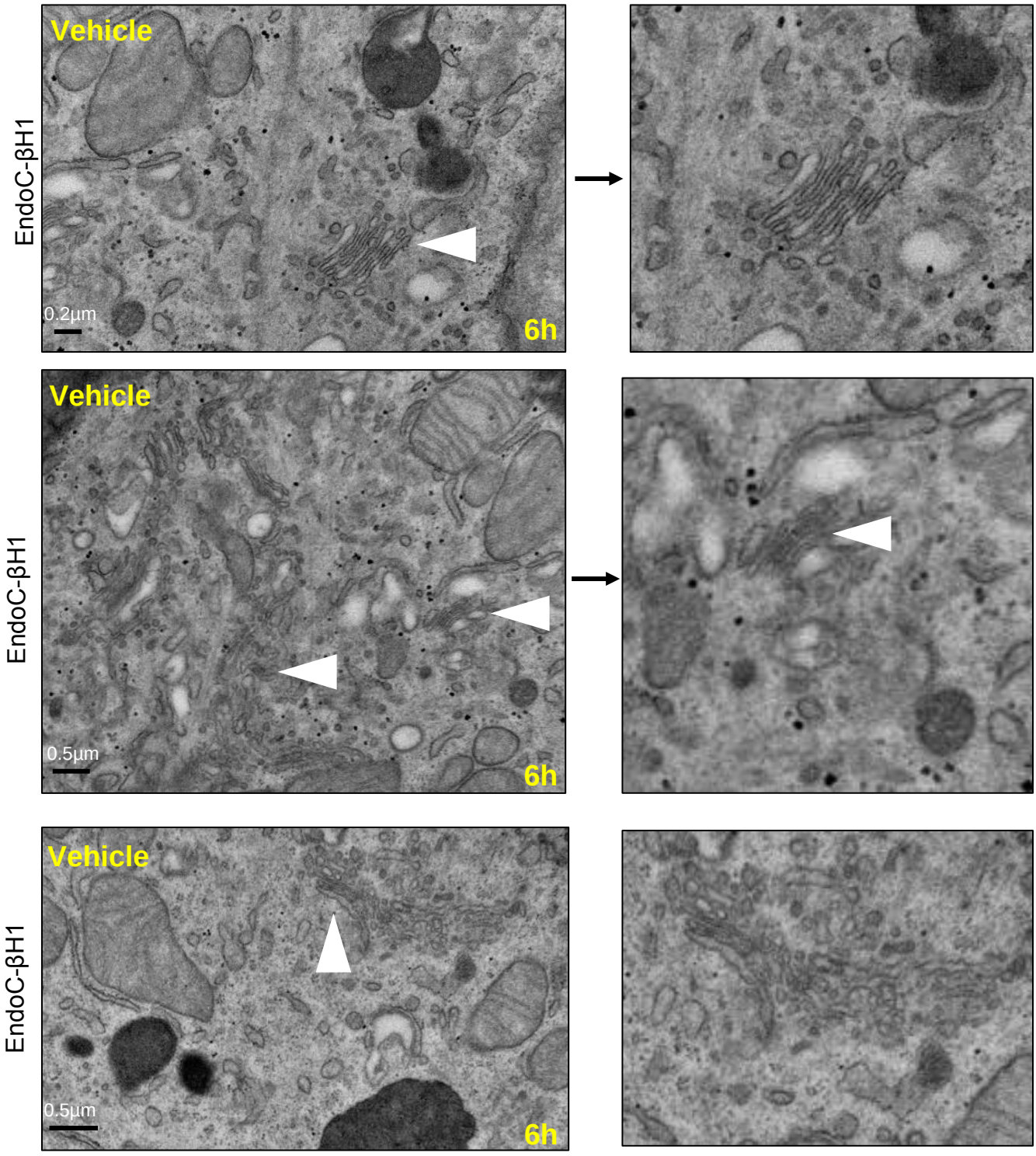

Effect of BSA vehicle control on Golgi morphology in EndoC-βH1 cells. EndoC-βH1 cells were treated for 6hrs with BSA vehicle only. EndoC-βH1 cells were then fixed in an osmium tetroxide fixative before being imaged with TEM.

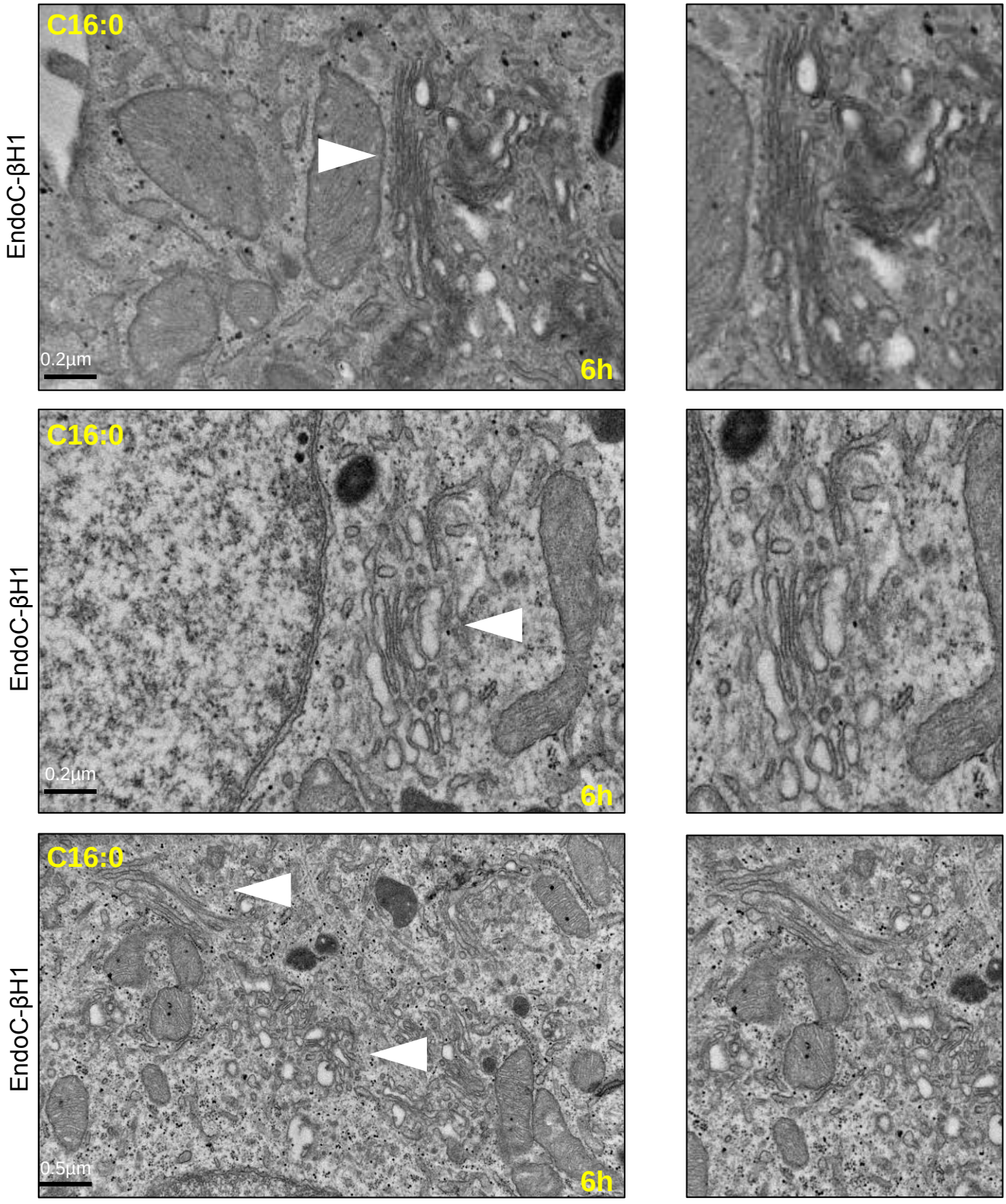

Effect of C16:0 on Golgi morphology in EndoC-βH1. EndoC-βH1 cells were treated for 6hrs with 250µM C16:0. EndoC-βH1 cells were then fixed in an osmium tetroxide fixative before being imaged with TEM.

Appendix 3

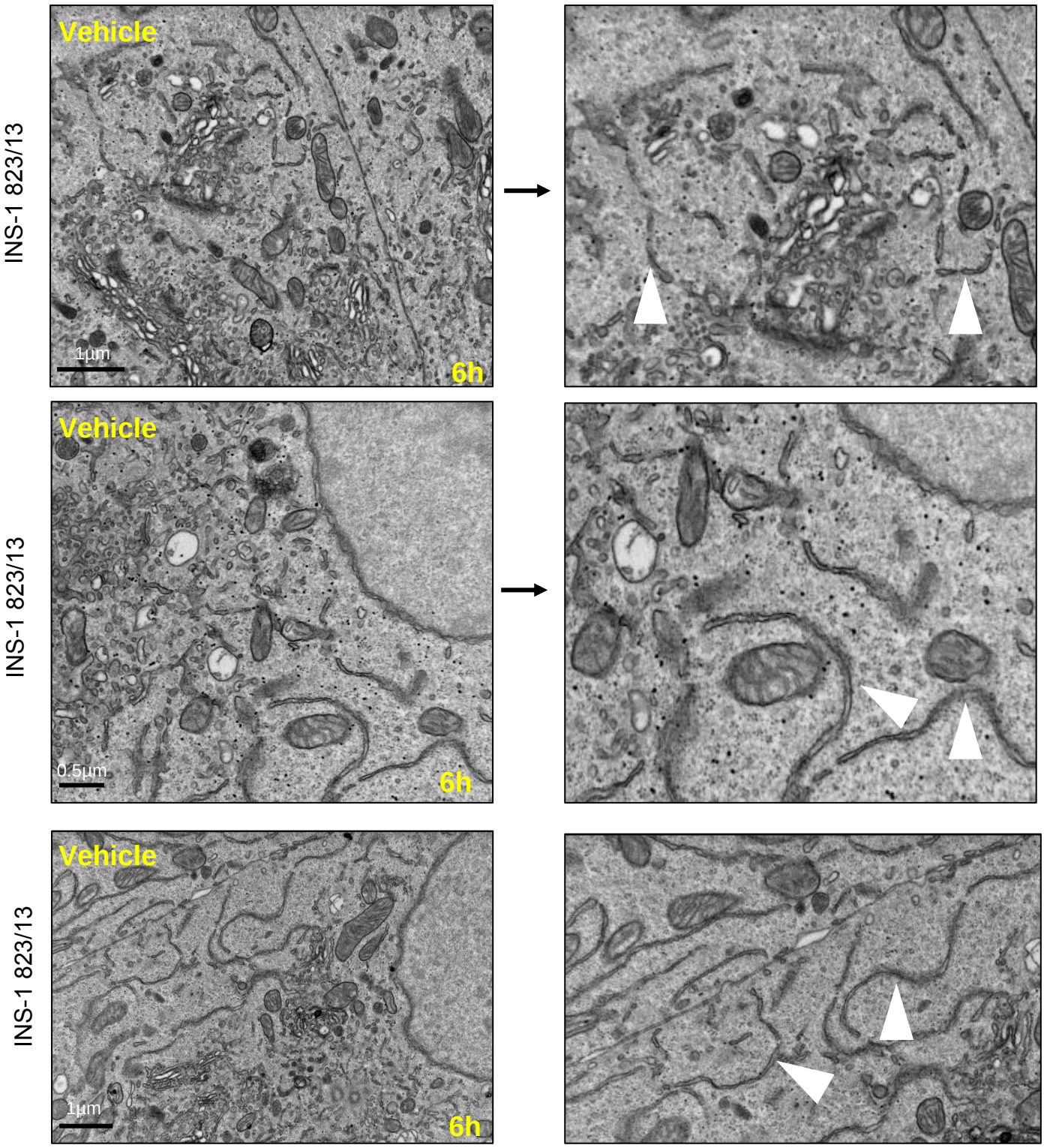

Effect of BSA vehicle control on ER morphology in INS-1 823/13 cells. INS-1 823/13 cells were treated for 6hrs with BSA vehicle only. INS-1 823/13 cells were then fixed in an osmium tetroxide fixative before being imaged with TEM.

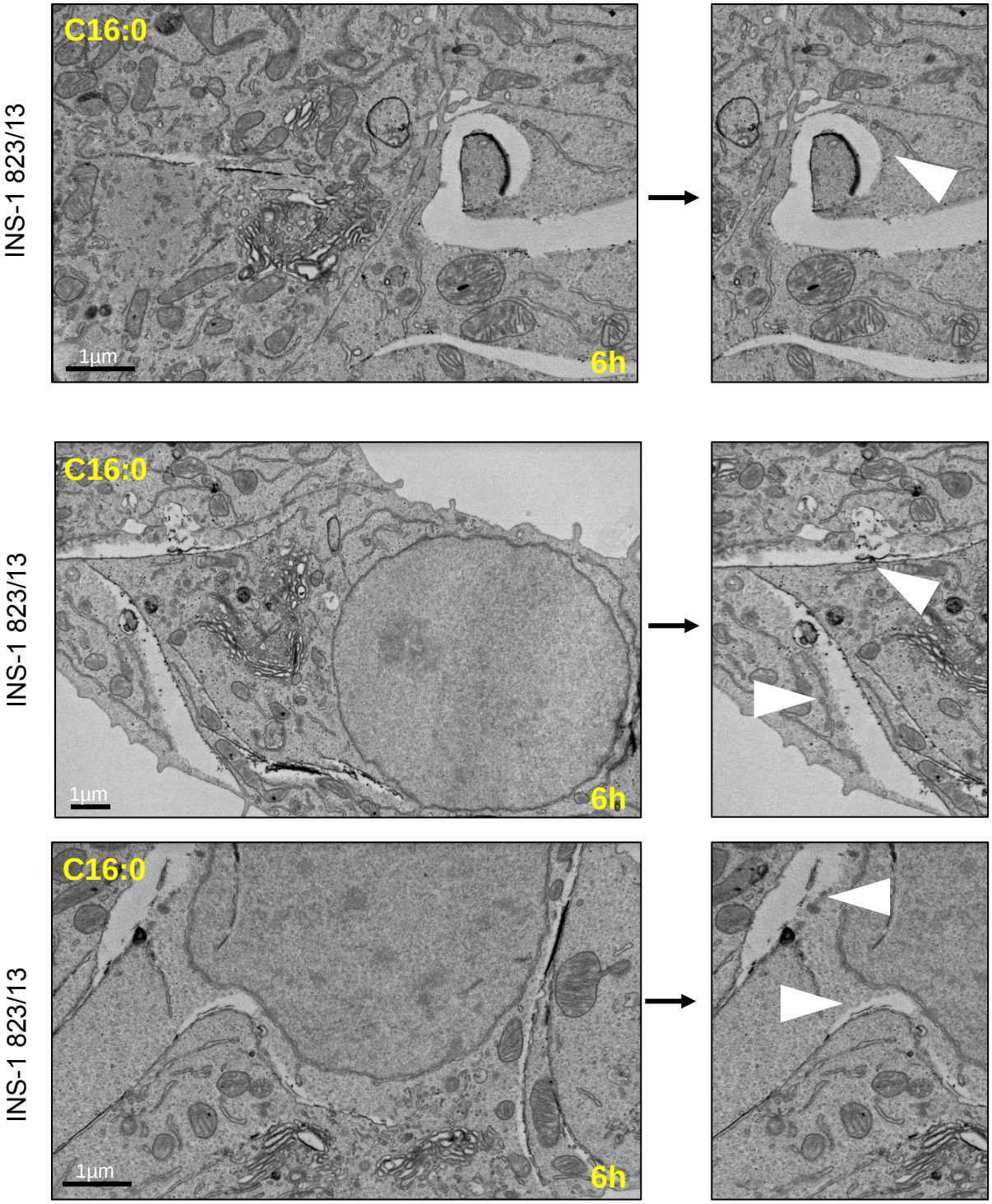
INS-1 823/13
C16:0
1µm
6h
INS-1 823/13
C16:0
1µm
6h
INS-1 823/13
C16:0
1µm
6h

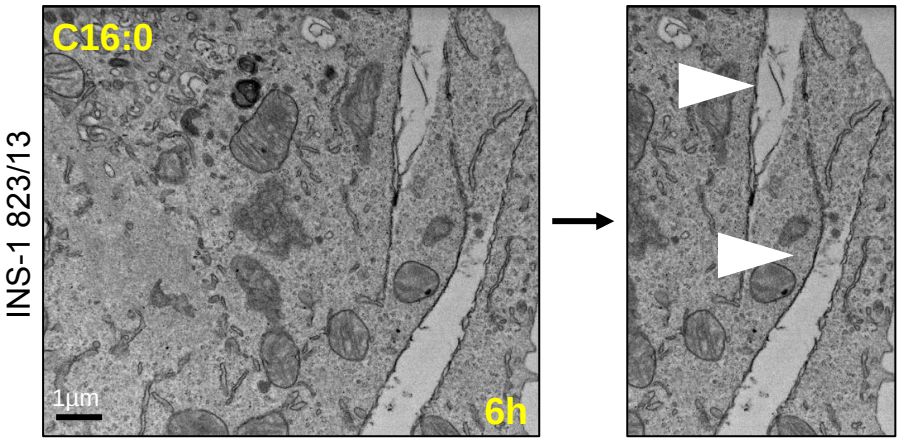

Effect of C16:0 on ER morphology in INS-1 823/13 cells. INS-1 823/13 cells were treated for 6hrs with 250µM C16:0. INS-1 823/13 cells were then fixed in an osmium tetroxide fixative before being imaged with TEM.

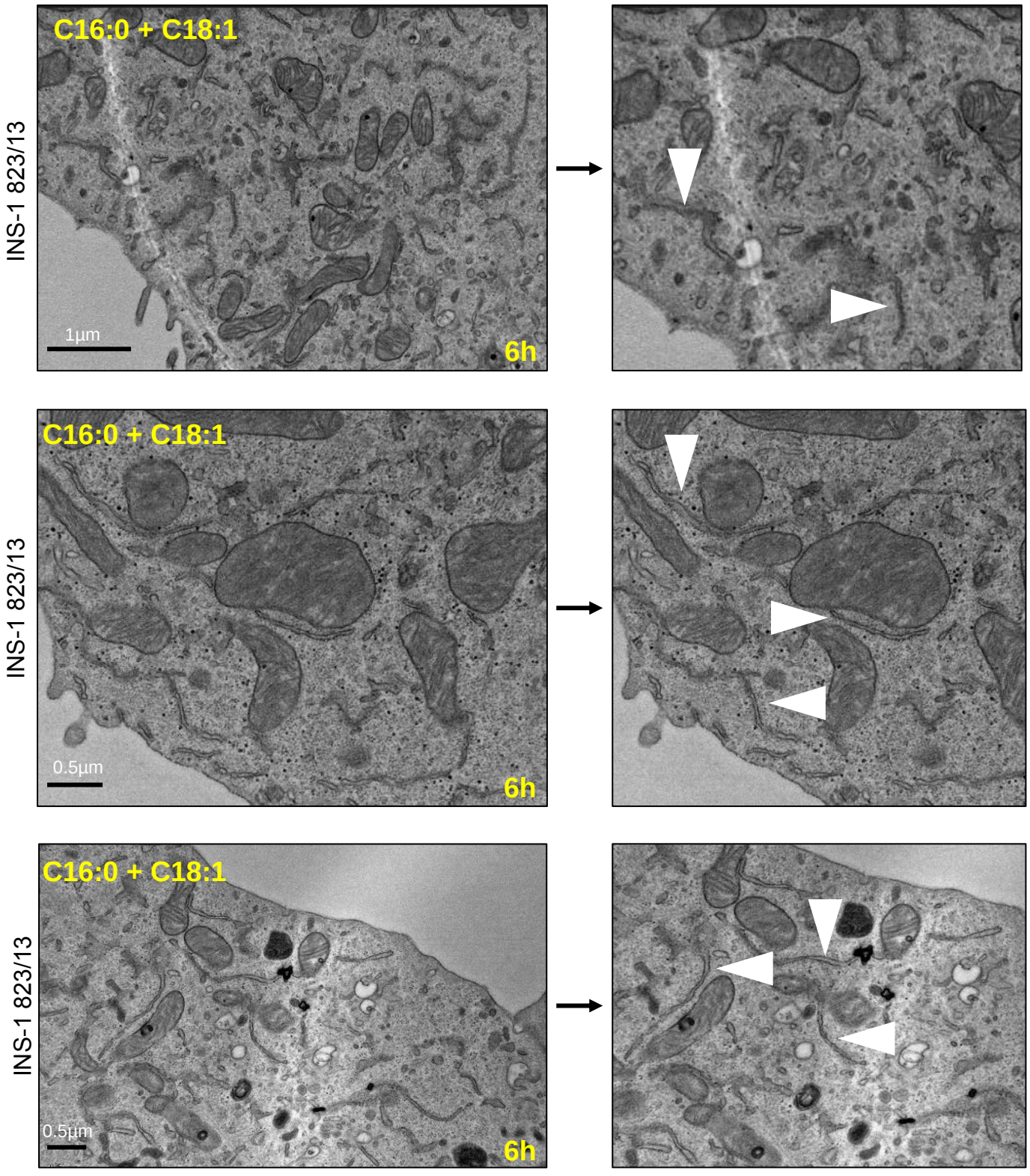

Effect of C16:0 with C18:1 on ER morphology in INS-1 823/13 cells. INS-1 823/13 cells were treated for 6hrs with 250µM C16:0 and 250µM C18:1. INS-1 823/13 cells were then fixed in an osmium tetroxide fixative before being imaged with TEM.

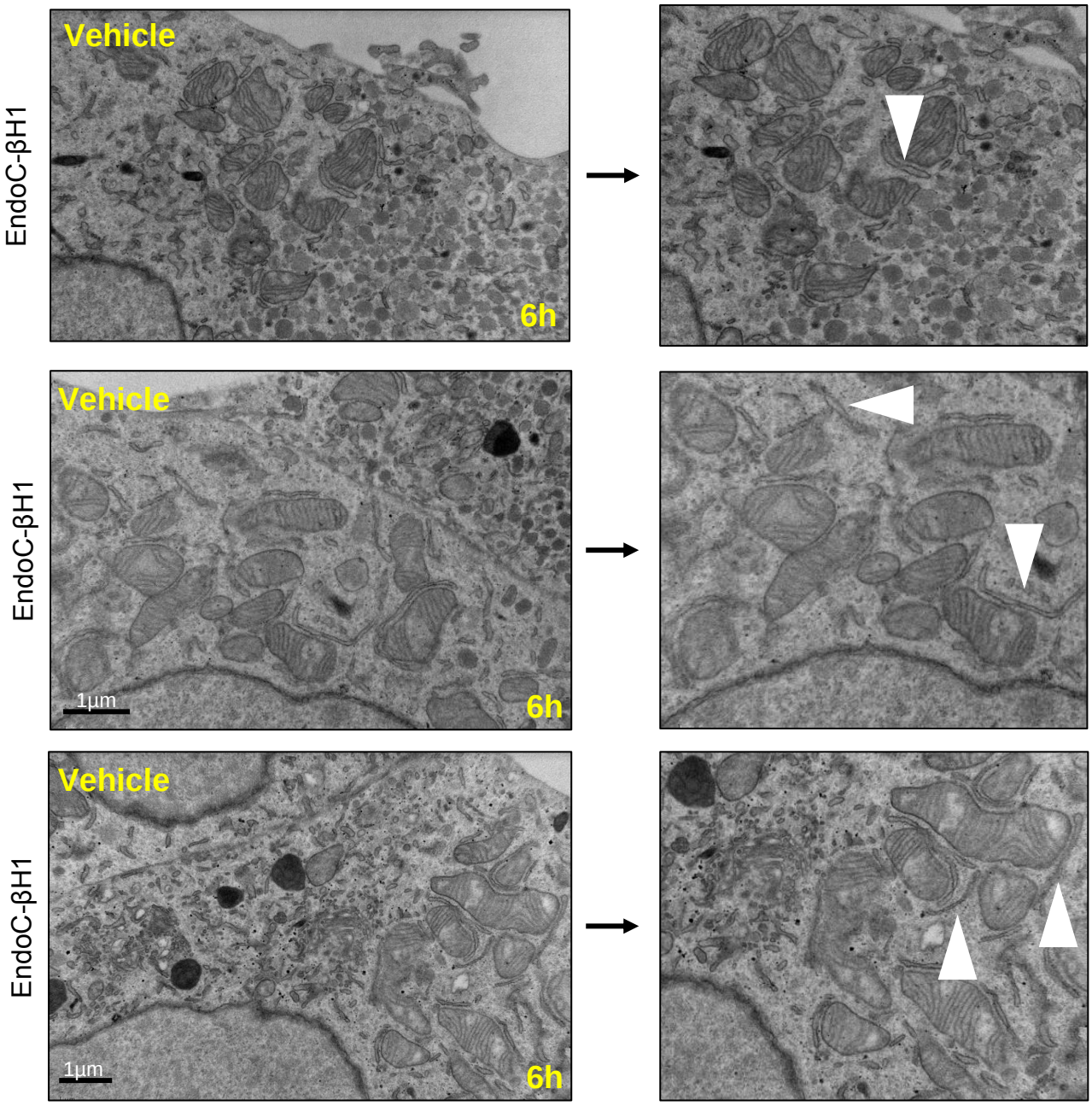

Effect of BSA vehicle control on ER morphology in EndoC-βH1 cells. EndoC-βH1 cells were treated for 6hrs with BSA vehicle only. EndoC-βH1 cells were then fixed in an osmium tetroxide fixative before being imaged with TEM.

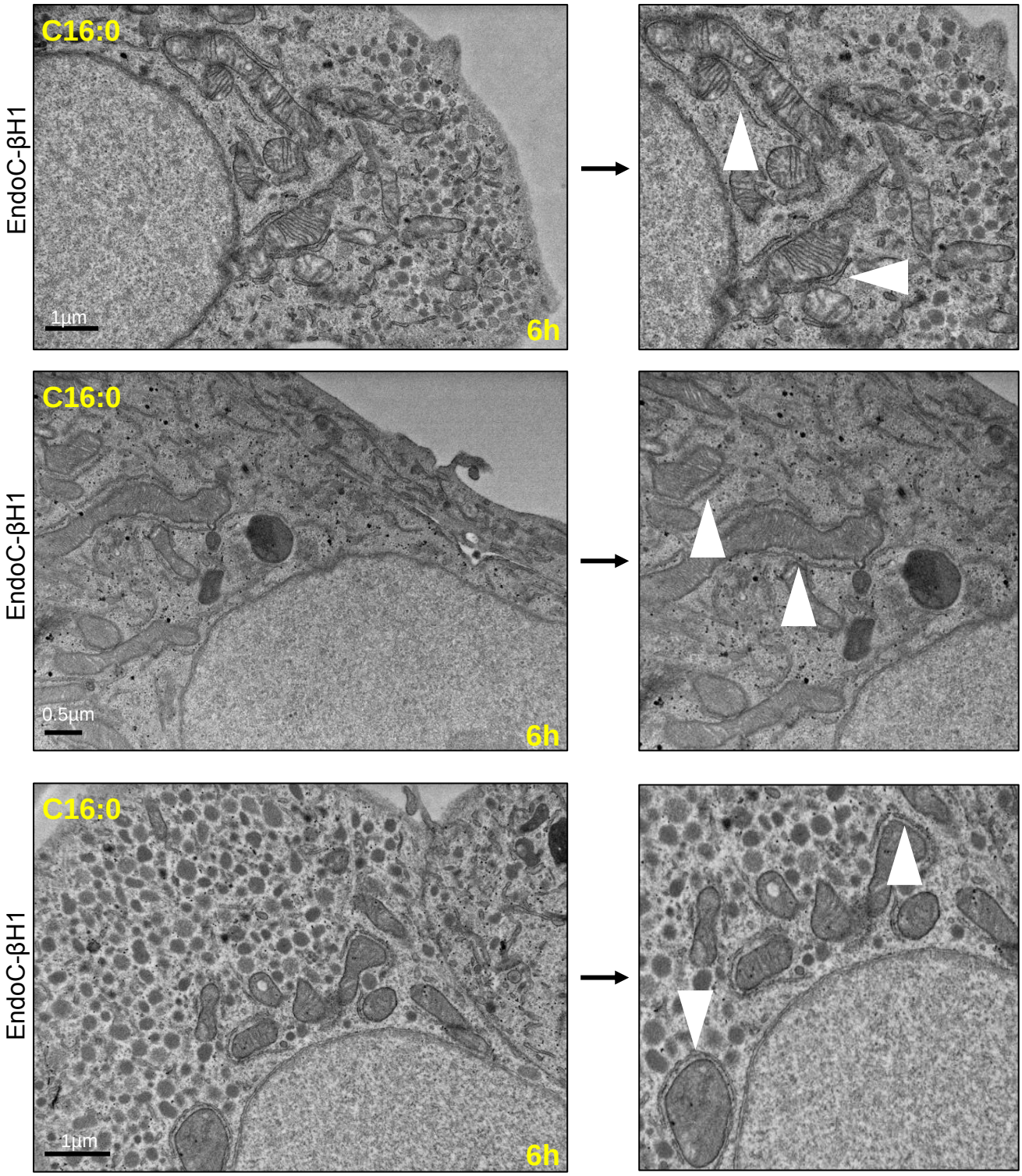

Effect of C16:0 on ER morphology in EndoC-βH1 cells. EndoC-βH1 cells were treated for 6hrs with 250µM C16:0. EndoC-βH1 cells were then fixed in an osmium tetroxide fixative before being imaged with TEM.